

**FUNCTIONAL TRANSFER OF THE
PAPAVER SI SYSTEM INTO
SELF-COMPATIBLE *A. THALIANA* AND
INVESTIGATING THE ROLE OF THE
PROTEASOME IN THE *PAPAVER* SI
RESPONSE**

by

ZONGCHENG LIN

A thesis submitted to
the University of Birmingham
for the degree of
DOCTOR OF PHILOSOPHY

School of Biosciences
The University of Birmingham
January 2015

UNIVERSITY OF
BIRMINGHAM

University of Birmingham Research Archive

e-theses repository

This unpublished thesis/dissertation is copyright of the author and/or third parties. The intellectual property rights of the author or third parties in respect of this work are as defined by The Copyright Designs and Patents Act 1988 or as modified by any successor legislation.

Any use made of information contained in this thesis/dissertation must be in accordance with that legislation and must be properly acknowledged. Further distribution or reproduction in any format is prohibited without the permission of the copyright holder.

ABSTRACT

Self-incompatibility is adopted by many flowering plants to prevent inbreeding. In *Papaver rhoeas*, it is controlled by a multi-allelic *S*-locus. The pistil *S*-determinant is PrsS (a small secreted protein); the pollen *S*-determinant is PrpS (a novel transmembrane protein). Cognate PrpS-PrsS interaction induces DEVDase-mediated programmed cell death of incompatible pollen. Here, we examined the role of proteasome during the *Papaver* SI response and showed that the proteasome is a target of the *Papaver* SI response, and is distinct from the SI-induced DEVDase activity.

Our main focus here is translational work, attempting to move the *Papaver* SI system into *A. thaliana*. We previously demonstrated that PrpS:GFP expressed in *A. thaliana* pollen was functional *in vitro*. Here, we expressed the female *S*-determinant, PrsS, in *A. thaliana* and investigated function *in vivo*. We present data demonstrating that transgenic *A. thaliana* stigmas expressing PrsS pollinated with *A. thaliana* pollen expressing PrpS:GFP inhibited pollen tube growth in an *S*-specific manner, and virtually no seed was set. Transformation of both *PrpS:GFP* and *PrsS* into *A. thaliana* generated self-incompatible plants that set no self-seed. This demonstrates that transfer of the *Papaver* SI system into a highly diverged self-compatible species can result in a fully functional SI system.

I dedicate this thesis to my wonderful family:

Dad, Yaoxuan Lin, Mum, Fengmei Lan & younger sister, Wen Lin.

ACKNOWLEDGEMENTS

First and foremost, a HUGE thanks to my supervisors, Professors Noni Franklin-Tong and Chris Franklin, not only for offering me an exciting project. Noni has been really supportive and patient in guiding me through the project, and encouraging me to present myself and meet great scientist from all over the world in the past three years, which I do really appreciate a lot. I am also very grateful to Chris for his critical advices and insightful discussions. Talking science with him is always enjoyable to me.

I'd like to thank all the lab members and PIs in the second floor, past and present, for their kindness and support. In particular, I thank Deborah Eaves for her instrumental comments and suggestions on my thesis. I'd like to thank Kim Osman, Ruth Perry, Lisa Burke and Steve Price for their technical suggestions and help. I also thank Karen Staples and Andi Breckles for their horticultural assistance. Special thanks go to Carlos Flores, Tamanna Haque, Andrew Beacham, Javier Andrés Juárez Díaz, Nianjun Teng, and Lijun Chai for being so fantastic colleagues.

I acknowledge Prof. Daphne Goring, University of Toronto, for providing pORE O3-*SLR1* vectors, and Prof. Ikuko Hara-Nishimura, Kyoto University, for providing *ipba1* transgenic lines.

I'd also like to thank the University of Birmingham and the China Scholarship Council for funding this project.

Finally, warm thanks to all my friends and families. They have been a great support throughout my PhD study.

TABLE OF CONTENTS

CHAPTER 1 INTRODUCTION	1
1.1 Plant reproduction and breeding	2
1.1.1 Plant reproduction.....	2
1.1.1.1 Pollen-pistil interactions	3
1.1.1.2 Pollen tube reception for double fertilization	4
1.1.1.3 Seed development.....	5
1.1.2 Plant breeding	6
1.1.2.1 Cytoplasmic male sterility for hybrid breeding.....	6
1.1.2.2 Self-incompatibility for hybrid breeding.....	8
1.2 Ubiquitin-proteasome system	9
1.2.1 Ubiquitin (Ub) and ubiquitination	9
1.2.2 Structure of the proteasome	12
1.3 Programmed cell death (PCD) and caspases	13
1.3.1 Plant programmed cell death and caspase-like activities	13
1.3.2 Involvement of UPS in the regulation of PCD	15
1.3.3 Involvement of proteasome in PCD as DEVDase.....	16
1.4 Self-incompatibility (SI).....	17
1.4.1 Brassicaceae SI.....	20
1.4.1.1 Brassicaceae SI <i>S</i> -determinants: SRK and SCR.....	21
1.4.1.2 The UPS is involved in the Brassicaceae SI.....	21
1.4.2 <i>S</i> -RNase-based SI	24
1.4.2.1 Stigma and pollen <i>S</i> -determinants: <i>S</i> -RNase and SLF	24
1.4.2.2 Models for pollen recognition and rejection for <i>S</i> -RNase-based SI.....	26
1.4.3 <i>Papaver</i> SI.....	29
1.4.3.1 <i>Papaver</i> SI pistil and pollen <i>S</i> -determinants: PrsS and PrpS	30
1.4.3.2 Mechanisms involved in <i>Papaver</i> SI.....	31
1.5 Transfer of SI system between different species	38
1.5.1 Transfer of the Brassicaceae SI system between different species.....	39
1.5.2 Transfer of the <i>Papaver</i> SI system into <i>A. thaliana</i>	41
1.6 Project aims.....	42
CHAPTER 2 MATERIALS AND METHODS.....	44
2.1 Development of an improved <i>Arabidopsis</i> pollen <i>in vitro</i> germination/growth system and functional analysis of <i>PrpS</i> in <i>A. thaliana in vitro</i> using this system	45
2.1.1 Plant materials: BG16 transgenic lines.....	45

2.1.2	<i>A. thaliana</i> pollen <i>in vitro</i> germination assay	45
2.1.3	<i>A. thaliana</i> pollen SI assays <i>in vitro</i>	47
2.1.4	Screening of improved BG16 lines	48
2.1.5	Construction of <i>At-ntp303::PrpS</i> transgenic lines.....	48
2.2	Constitutive expression and functional analysis of <i>PrsS</i> in <i>A. thaliana</i> using an <i>in vitro</i> SI assay	52
2.2.1	Construction of <i>At-35S::PrsS</i> transgenic lines	52
2.2.2	Construction of <i>At-35S::PrsS::GFP</i> transgenic lines	54
2.2.3	Screening of transgenic seeds.....	56
2.2.4	Analysis of <i>PrsS</i> mRNA expression in <i>A. thaliana</i> transgenic lines	57
2.2.5	Analysis of constitutively expressed <i>PrsS</i> protein expression in <i>A. thaliana</i> transgenic lines	59
2.2.5.1	MG132 treatment of transgenic seedlings.....	59
2.2.5.2	Detection of constitutively expressed <i>PrsS₁::GFP</i> using western blot	60
2.2.5.3	Analysis of <i>PrsS₁::GFP</i> using GFP fluorescence microscopy	61
2.2.6	<i>In vitro</i> SI assay using transgenic seedling extracts	61
2.2.7	<i>PrsS::GFP</i> protein enrichment using ammonium sulphate precipitation.....	62
2.3	Functional analysis of <i>PrpS</i> and <i>PrsS</i> in <i>A. thaliana in vivo</i> and generation of self-incompatible <i>A. thaliana</i> by transfer of <i>Papaver</i> SI system.....	62
2.3.1	Construction of <i>At-SLR1::GFP</i> , <i>At-SLR1::PrsS</i> and <i>At-SLR1::PrsS::GFP</i> transgenic lines	62
2.3.2	Analysis of <i>SLR1</i> promoter expression pattern using GFP fluorescence microscopy.....	65
2.3.3	Analysis of <i>SLR1</i> promoter expression pattern using RT-PCR	65
2.3.4	Semi- <i>in-vivo</i> pollination assay.....	65
2.3.5	Analysis of the <i>PrsS₁</i> mRNA expression in <i>At-SLR1::PrsS₁</i> transgenic lines	68
2.3.6	Analysis of the <i>PrsS₁</i> protein expression in <i>At-SLR1::PrsS₁</i> transgenic lines	68
2.3.7	Generation of self-incompatible <i>A. thaliana</i>	70
2.4	Investigating the role of the proteasome in the <i>Papaver</i> SI response.....	71
2.4.1	Poppy pollen germination/growth <i>in vitro</i> , SI assay <i>in vitro</i> and MG132 treatment	71
2.4.2	Poppy pollen protein extraction.....	72
2.4.3	Proteasome activity assay using fluorogenic peptide substrates	72
2.4.4	Caspase activity assays	73
2.4.5	Proteasome activity profiling with MV151	73
2.4.6	DNA fragmentation assay.....	74
2.4.7	Fluorescein diacetate (FDA) staining	75
2.4.8	Biotin-DEVD pull down assay	76

CHAPTER 3	DEVELOPMENT OF AN IMPROVED ARABIDOPSIS POLLEN IN VITRO GERMINATION/GROWTH SYSTEM AND FUNCTIONAL ANALYSIS OF PRPS IN A. THALIANA IN VITRO USING THIS SYSTEM.....	78
3.1	Introduction	79
3.2	Results.....	83
3.2.1	Optimization of <i>A. thaliana</i> pollen germination <i>in vitro</i>	83
3.2.2	<i>In vitro</i> SI assay revealed the S-specific inhibition of <i>At-PrpS:GFP</i> pollen ..	88
3.2.3	Comparison between <i>At-PrpS:GFP</i> pollen and <i>Papaver</i> pollen, and screening of improved <i>At-ntp303::PrpS:GFP</i> transgenic lines.....	95
3.2.4	Construction of <i>At-ntp303::PrpS</i> transgenic lines.....	99
3.3	Discussion	100
3.3.1	Development of an improved <i>A. thaliana</i> pollen germination/growth assay	100
3.3.2	Development of an improved <i>A. thaliana</i> pollen SI assay	101
3.3.3	Screening of improved <i>At-PrpS</i> transgenic lines.....	103
3.3.4	Summary.....	103
CHAPTER 4	CONSTITUTIVE EXPRESSION AND FUNCTIONAL ANALYSIS OF PRSS IN A. THALIANA USING AN IN VITRO SI ASSAY.....	105
4.1	Introduction	106
4.1.1	The establishment of <i>in vitro</i> SI bioassay.....	106
4.1.2	Previous analysis of <i>A. thaliana</i> expressed PrsS protein using the <i>in vitro</i> SI assay.....	107
4.1.3	Aims of this chapter.....	110
4.2	Results.....	110
4.2.1	Construction of transgenic <i>A. thaliana</i> lines constitutively expressing <i>PrsS</i> or <i>PrsS:GFP</i>	110
4.2.2	Analysis <i>PrsS</i> expression in <i>A. thaliana</i> transgenic lines.....	112
4.2.2.1	Analysis of <i>PrsS₁</i> mRNA expression in transgenic <i>A. thaliana</i> lines.....	112
4.2.2.2	Analysis of expression of PrsS ₁ protein in transgenic lines using western blotting.....	115
4.2.2.3	Analysis of PrsS ₁ :GFP protein expression using GFP fluorescence microscopy	118
4.2.3	Functional analysis of <i>A. thaliana</i> constitutively-expressed PrsS protein using the <i>in vitro</i> SI assay.....	122
4.2.3.1	Testing the SI activities of transgenic seedling extracts on <i>At-PrpS₁:GFP</i> pollen	122
4.2.3.2	Testing the SI activities of <i>At-35S::PrsS:GFP</i> transgenic seedling extracts on poppy pollen	127
4.2.4	Enrichment of PrsS ₁ :GFP protein by (NH ₄) ₂ SO ₄ precipitation	129

4.3	Discussion	134
4.3.1	The constitutive expression of <i>PrsS</i> mRNA in transgenic lines	135
4.3.2	The expression of PrsS protein in <i>A. thaliana</i> transgenic lines	136
4.3.3	Functional analysis of constitutively expressed PrsS protein in <i>A. thaliana in vitro</i>	139
4.3.3.1	Is it possible that <i>A. thaliana</i> -expressed PrsS proteins have no biological activity?	140
4.3.3.2	It is more likely due to the low expression level of constitutively-expressed PrsS protein in <i>A. thaliana</i>	141
4.3.4	Summary	143
CHAPTER 5	FUNCTIONAL ANALYSIS OF <i>PRSS</i> AND <i>PRPS</i> IN <i>A. THALIANA IN VIVO</i> AND GENERATION OF SELF-INCOMPATIBLE <i>A. THALIANA</i> BY TRANSFER OF THE <i>PAPAVER</i> SI SYSTEM.....	144
5.1	Introduction	145
5.2	Results.....	148
5.2.1	Construction of transgenic lines expressing stigma specific <i>PrsS</i> driven by the <i>SLR1</i> promoter	148
5.2.2	Analysis of the <i>SLR1</i> promoter expression pattern in <i>A. thaliana</i>	150
5.2.3	Set up of a <i>semi-in-vivo</i> pollination assay: germination and growth of <i>A. thaliana</i> Col-0 pollen on Col-0 pistil.....	153
5.2.4	Functional analysis of <i>At-SLR1::PrsS:GFP</i> transgenic lines <i>in vivo</i>	156
5.2.4.1	Analysis of PrsS:GFP protein expression in <i>At-SLR1::PrsS:GFP</i> transgenic lines.....	156
5.2.4.2	Functional analysis of <i>A. thaliana</i> expressed PrsS:GFP protein using <i>semi-in-vivo</i> pollination assay	160
5.2.5	Functional analysis of <i>PrsS</i> in <i>A. thaliana in vivo</i>	163
5.2.5.1	Analysis of <i>PrsS</i> mRNA expression in <i>At-SLR1::PrsS</i> transgenic lines	163
5.2.5.2	Analysis of PrsS ₁ protein expression in <i>At-SLR1::PrsS₁</i> transgenic lines....	165
5.2.5.3	Functional analysis of <i>A. thaliana</i> expressed PrsS protein using the <i>semi-in-vivo</i> pollination assay	166
5.2.5.4	Inhibition of <i>At-PrpS.GFP</i> pollen in PrsS-expressing stigmas is developmentally controlled	173
5.2.5.5	PrpS-PrsS triggered pollen growth inhibition in <i>A. thaliana</i> was <i>S</i> -allele specific.....	175
5.2.5.6	PrpS-PrsS triggered SI responses in transgenic <i>A. thaliana</i> results in shorter siliques and no seeds	178
5.2.6	Generation of self-incompatible <i>A. thaliana</i> by co-transformation of <i>PrpS</i> and <i>PrsS</i>	182
5.3	Discussion	185

5.3.1	PrsS protein expressed in different organisms.....	186
5.3.2	GFP fusion might affect the proper function of PrsS	188
5.3.3	Functional transfer of <i>Papaver</i> SI system into <i>A. thaliana</i>	190

**CHAPTER 6 INVESTIGATING THE ROLE OF THE PROTEASOME IN THE
PAPAVER RHOEAS SI RESPONSE..... 194**

6.1	Introduction	195
6.1.1	Tools to study the proteasome: proteasome-specific inhibitors.....	196
6.1.2	Measuring proteasome activities	197
6.1.3	Project aims	200
6.2	Results.....	201
6.2.1	Characterization of proteasomal activities during the poppy SI response....	201
6.2.2	Investigating the effects of proteasomal inhibition on pollen tube growth ..	205
6.2.2.1	MG132 inhibits poppy proteasome activity <i>in vitro</i>	205
6.2.2.2	MG132 inhibits poppy proteasome activity <i>in vivo</i>	208
6.2.2.3	Proteasome inhibition affected the germination and elongation of poppy pollen tubes.....	210
6.2.3	Investigating the effects of proteasome inhibition on poppy SI response	212
6.2.3.1	Effects of proteasome inhibition on SI-triggered pollen growth inhibition .	212
6.2.3.2	Effects of proteasome inhibition on SI stimulated viability decrease	214
6.2.3.3	Effects of proteasome inhibition on SI triggered DNA fragmentation.....	216
6.2.4	Characterization of SI-triggered proteasome and DEVDase activity.....	220
6.2.4.1	Identification of proteasome subunits in a biotin-DEVD pull down assay ..	221
6.2.4.2	Effects of DEVDase inhibitors on proteasome activities <i>in vitro</i>	224
6.2.4.3	Effects of proteasome inhibitors on DEVDase activities <i>in vitro</i>	225
6.2.4.4	Characterization of proteasome and DEVDase activities in buffers with different pHs	230
6.3	Discussion	232
6.3.1	The proteasome is required for the normal poppy pollen germination and pollen tube growth.....	233
6.3.2	SI induces an increase in proteasome activity in incompatible pollen	234
6.3.3	SI-induced proteasome activity increase and acidification	237
6.3.4	Role of proteasome in SI-induced pollen tube growth inhibition, viability decrease and DNA fragmentation.....	239
6.3.5	Which protease is responsible for SI-induced DEVDase activity?	241
6.3.6	SI signalling model and summary	243

CHAPTER 7 GENERAL DISCUSSION 246

7.1	Introduction	247
------------	---------------------------	------------

7.2	PrpS-PrsS interaction triggers signals not only in <i>P. rhoeas</i>	247
7.2.1	PrpS-PrsS interaction triggers pollen tube growth inhibition in both <i>A. thaliana</i> and <i>N. tabacum</i> -implication in the evolution of SI signalling across the higher plants?.....	248
7.2.2	PrpS-PrsS might function in <i>A. thaliana</i> protoplast and mammalian cells, which has implication in elucidating mechanisms involved in the PrpS-PrsS interaction	250
7.3	How far can we go? Possible application of <i>Papaver</i> SI system in F1 hybrids breeding	252
7.3.1	Brassicaceae SI and <i>Papaver</i> SI in F1 hybrid breeding	254
7.3.2	Comparison between CMS and the <i>Papaver</i> SI in hybrids breeding.....	258
7.4	Functional transfer of the <i>Papaver</i> SI system into <i>A. thaliana</i>: implications in the SI molecular mechanism research	261
7.4.1	Experimental design and preliminary work in investigating the <i>Papaver</i> SI molecular mechanism using transgenic <i>A. thaliana</i>	263
7.5	Summary	266
REFERENCE LIST		268
APPENDIX I-PUBLISHED PAPER		292

LIST OF FIGURES AND TABLES

CHAPTER 1 INTRODUCTION	1
Figure 1-1 Cartoon of plant sexual reproduction	3
Figure 1-2 Three-line hybridization system in rice	7
Figure 1-3 Organization and structure of Ub/26S proteasome system	10
Figure 1-4 Cartoon of SCF complex	11
Figure 1-5 Illustration of the genetic basis of sporophytic and gametophytic SI	19
Table 1-1 Male and female <i>S</i> -determinants identified in the representative SI systems.	20
Figure 1-6 Model for the molecular mechanism underlying Brassicaceae SI	23
Figure 1-7 Model for the recognition between pollen and pistil <i>S</i> -determinants in <i>S</i> -RNase-based SI	25
Figure 1-8 Sequestration/compartimentalization model for the <i>S</i> -RNase-based SI.....	26
Figure 1-9 Ubiquitination/degradation model for <i>S</i> -RNase-based SI.....	29
Figure 1-10 A cartoon showing the signalling network in an incompatible pollen in <i>Papaver rhoeas</i>	32
CHAPTER 2 MATERIALS AND METHODS.....	44
Figure 2-1 Cartoon of BG16 transgenic line.....	45
Table 2-1 Recipe for <i>AtGM</i>	46
Table 2-2 Screening of improved BG16 lines.....	48
Figure 2-2 Construction of pORE O3- <i>ntp303::PrpS</i>	49
Table 2-3 Primers for the construction of pGreen0029- <i>ntp303::PrpS</i> vectors	50
Table 2-4 Double digestion reaction system	51
Table 2-5 T4 DNA ligase-mediated ligation system	51
Figure 2-3 Construction of binary Ti vectors pEG205-35S:: <i>PrsS</i>	53
Table 2-6 Primers for the construction of pENTR- <i>PrsS</i> vectors.....	54
Table 2-7 Vectors constructed for constitutively expressing <i>PrsS</i> in <i>A. thaliana</i>	54
Figure 2-4 Construction of binary Ti vectors pEG103-35S:: <i>PrsS:GFP</i>	55
Table 2-8 Primers for the construction of pENTR- <i>PrsS(NS)</i> vectors	56
Table 2-9 Vectors constructed for constitutively expressing <i>PrsS:GFP</i> in <i>A. thaliana</i> ..	56
Table 2-10 One-step RT-PCR reaction system.....	58
Table 2-11 One-step RT-PCR setting	59
Table 2-12 Primers for detection of <i>PrsS</i> mRNA transcripts.....	59
Table 2-13 Antibody probing details for the detection of PrsS ₁ :GFP	60
Table 2-14 Ammonium sulphate precipitation	62
Figure 2-5 Cloning of target DNA fragments into binary Ti vector pORE O3.....	63
Table 2-15 Primers for the construction of pEG103-35S:: <i>PrsS:GFP</i> vectors	64

Figure 2-6 <i>Semi-in-vivo</i> pollination settings	66
Table 2-16 Primers for the detection of <i>PrsS₁</i> mRNA transcript	68
Table 2-17 Antibody probing details for the detection of PrsS ₁	69

CHAPTER 3 DEVELOPMENT OF AN IMPROVED ARABIDOPSIS POLLEN IN VITRO GERMINATION/GROWTH SYSTEM AND FUNCTIONAL ANALYSIS OF PRPS IN A. THALIANA IN VITRO USING THIS SYSTEM.....78

Figure 3-1 <i>Arabidopsis thaliana</i> pollen germinates on solidified <i>AtGM</i> with high germination rate	85
Figure 3-2 Time course of <i>A. thaliana</i> pollen tube growths <i>in vitro</i>	86
Figure 3-3 <i>A. thaliana</i> pollen tube lengths distribution	87
Figure 3-4 PrpS ₁ :GFP is expressed in transgenic <i>A. thaliana</i> pollen.....	91
Figure 3-5 The growth of <i>At-PrpS₁:GFP</i> pollen is inhibited by PrsS ₁ protein <i>in vitro</i> ..	92
Figure 3-6 <i>At-PrpS₁:GFP</i> pollen tube growth is inhibited by PrsS ₁ protein in an S-specific manner	94
Figure 3-7 BG16.25 pollen is not as sensitive as <i>Papaver</i> pollen to PrsS protein treatment	96
Figure 3-8 BG16 lines exhibit varied strength of SI response	98
Table 3-1 Construction of <i>At-ntp303::PrpS</i> transgenic lines.....	99

CHAPTER 4 CONSTITUTIVE EXPRESSION AND FUNCTIONAL ANALYSIS OF PRSS IN A. THALIANA USING AN IN VITRO SI ASSAY..... 105

Table 4-1 Transgenic <i>A. thaliana</i> lines built for functional analysis of constitutively expressed <i>PrsS in vitro</i>	111
Figure 4-1 <i>PrsS₁</i> mRNA is expressed in <i>At-35S::PrsS₁:GFP</i> transgenic lines.....	113
Figure 4-2 <i>PrsS₁</i> mRNA is expressed in <i>At-35S::PrsS₁</i> transgenic lines.....	114
Figure 4-3 PrsS ₁ :GFP protein is detected in transgenic <i>A. thaliana</i>	116
Figure 4-4 Characterization of PrsS ₁ antibody sensitivities.....	117
Figure 4-5 GFP signal was observed in <i>At-35S::PrsS₁:GFP</i> seedling tissue sample ...	119
Figure 4-6 PrsS ₁ :GFP appears to be subject to proteasomal degradation <i>in vivo</i>	120
Figure 4-7 Western blot confirms <i>in vivo</i> degradation of PrsS ₁ :GFP	121
Figure 4-8 Constitutively expressed PrsS ₁ in transgenic <i>A. thaliana</i> seedling extracts do not affect the growth of <i>At-PrpS₁:GFP</i> pollen	124
Figure 4-9 Constitutively expressed PrsS ₁ in transgenic <i>A. thaliana</i> seedling extracts do not affect the <i>At-PrpS₁:GFP</i> pollen tube length <i>in vitro</i>	126
Figure 4-10 <i>At-35S::PrsS:GFP</i> seedling extracts do not affect the growth of poppy pollen	128
Figure 4-11 Separation and enrichment of PrsS ₁ :GFP by (NH ₄) ₂ SO ₄ precipitation	130

Figure 4-12 PrsS ₁ :GFP is under protease degradation <i>in vitro</i>	132
--	-----

CHAPTER 5 FUNCTIONAL ANALYSIS OF PRSS AND PRPS IN A. THALIANA IN VIVO AND GENERATION OF SELF-INCOMPATIBLE A. THALIANA BY TRANSFER OF THE PAPAVER SI SYSTEM..... 144

Table 5-1 Transgenic lines built for functional analysis of stigma specific expressed PrsS in <i>A. thaliana in vivo</i>	149
Figure 5-1 SLRI is expressed in a stigma specific and developmentally regulated manner in transgenic <i>A. thaliana</i>	151
Figure 5-2 SLRI promoter directs downstream gene expressed in a developmentally controlled manner	153
Figure 5-3 Germination and growth of Col-0 pollen on Col-0 stigma <i>semi-in-vivo</i>	155
Figure 5-4 Cartoon of <i>At-SLRI::PrsS₁:GFP</i> and <i>At-SLRI::PrsS₁</i> transgenic lines.....	156
Figure 5-5 PrsS ₁ :GFP protein is expressed in <i>At-SLRI::PrsS₁:GFP</i> pistils	157
Figure 5-6 No GFP can be observed in transgenic <i>At-SLRI::PrsS₁:GFP</i> stigma using fluorescent microscopy	159
Figure 5-7 <i>At-PrpS:GFP</i> pollen grows normally on PrsS:GFP expressing pistils	161
Figure 5-8 PrsS ₁ mRNA is expressed at varying levels in <i>At-SLRI::PrsS₁</i> transgenic lines.....	164
Figure 5-9 PrsS protein is expressed in the <i>At-SLRI::PrsS</i> transgenic line.....	165
Figure 5-10 PrsS expressing stigma inhibits the growth of <i>At-PrpS:GFP</i> pollen <i>semi-in-vivo</i>	167
Figure 5-11 Different <i>At-SLRI::PrsS₁</i> lines express varied strengths of SI.....	170
Figure 5-12 Inhibition of <i>At-PrpS:GFP</i> pollen is correlated with the expression level of PrsS transcript in <i>At-SLRI::PrsS</i> stigma	172
Figure 5-13 The expression of SI response in transgenic <i>A. thaliana</i> is developmentally regulated	174
Figure 5-14 Cartoon of the <i>At-SLRI::PrsS</i> and <i>At-ntp303::PrpS:GFP</i> lines	176
Figure 5-15 PrpS-PrsS triggered pollen tube growth inhibition in <i>A. thaliana</i> is S-allele specific.....	177
Figure 5-16 PrpS-PrsS triggered SI response in <i>A. thaliana</i> results in shorter siliques and no seed	179
Table 5-2 Summary of the lengths of siliques and the number of seeds.....	180
Figure 5-17 Self-incompatible <i>A. thaliana</i> is generated through transforming BG16 with PrsS ₁	183
Figure 5-18 Self-incompatible <i>A. thaliana</i> forms shorter siliques and sets no seed	184

CHAPTER 6 INVESTIGATING THE ROLE OF THE PROTEASOME IN THE PAPAVER RHOEAS SI RESPONSE..... 194

Table 6-1 Fluorogenic substrates to assay proteasome activities.....	198
Figure 6-1 Structure of MV151.....	200
Figure 6-2 No significant alteration in proteasomal activity is observed in the early phase of poppy SI response	202
Figure 6-3 Poppy SI response triggers an increase of proteasomal activity 5h after SI induction in the incompatible pollen	204
Figure 6-4 MG132 inhibits proteasome activity <i>in vitro</i>	206
Figure 6-5 MV151 labelling revealed MG132 inhibited proteasome activities <i>in vivo</i>	209
Figure 6-6 Proteasome inhibition slightly reduces poppy pollen germination	211
Figure 6-7 Effects of proteasome inhibition on poppy pollen tube elongation.....	211
Figure 6-8 Proteasome inhibition does not alleviate SI-induced poppy pollen tube growth inhibition	213
Figure 6-9 Proteasome inhibition does not alleviate SI-induced poppy pollen viability decrease	215
Figure 6-10 MG132 does not trigger DNA fragmentation in poppy pollen	217
Figure 6-11 Proteasome inhibitors do not alleviate SI-triggered DNA fragmentation .	219
Figure 6-12 Cartoon of the biotin-DEVD pull down assay	222
Table 6-2 20S proteasome subunits were identified in Biotin-DEVD pull down assay	223
Figure 6-13 DEVDase inhibitor does not inhibit proteasome activities <i>in vitro</i>	225
Figure 6-14 MG132 has no obvious inhibition on DEVDase activity <i>in vitro</i>	226
Figure 6-15 Epoximicin does not inhibit DEVDase activity <i>in vitro</i>	228
Figure 6-16 Poppy pollen proteasome and DEVDase activities are pH-dependent	231
Figure 6-17 Signalling model for the <i>Papaver</i> SI response.....	244

CHAPTER 7 GENERAL DISCUSSION246

Figure 7-1 Comparison between the Brassicaceae SI system and <i>Papaver</i> SI system in hybrid breeding.....	257
Figure 7-2 Comparison between CMS and the <i>Papaver</i> SI system in hybrid breeding	259
Figure 7-3 Investigating the <i>Papaver</i> SI response using omics-based approaches in <i>A. thaliana</i>	264
Figure 7-4 Characterizing the role of a target gene during the <i>Papaver</i> SI response in <i>A. thaliana</i>	266

ABBREVIATIONS

- 2Pi:** Inorganic orthophosphate
- ABA:** Abscisic Acid
- ABI4:** ABA-INTENSIVE 4
- ARC1:** Arm-Repeat Containing 1
- As-OND:** Antisense Oligonucleotide
- ATP:** Adenosine Triphosphate
- BSA:** Bovine Serum Albumin
- Caspase:** CysteinyI aspartate-specific protease
- CMS:** Cytoplasmic Male Sterility
- CP:** Core Particle
- DEPC:** Diethylpyrocarbonate
- EC1:** Egg Cell 1
- ECL:** Enhanced chemiluminescence
- ECM:** Extracellular Matrix
- F-actin:** Filamentous actin
- FragEL:** Fragment End Labelling
- GAPC:** Glyceraldehyde-3-phosphate dehydrogenase C
- GFP:** Green Fluorescence Protein
- GSI:** Gametophytic SI
- HR:** Hypersensitive Response
- HRP:** Horseradish Peroxidase
- IEF:** Isoelectric Focusing
- Kan:** Kanamycin
- MAP:** Minutes After Pollination
- MAPK:** Mitogen-activated Protein Kinase
- MLPK:** *M*-Locus Protein Kinase
- MYA:** Million Years Ago
- MS:** Murashige and Skoog

NO: Nitric Oxide

ORF: Open Reading Frame

PAGE: Polyacrylamide gel electrophoresis

PARP: Poly ADP Ribose Polymerase

PCD: Programmed Cell Death

PCPs: Pollen Coat Proteins

PCR: Polymerase Chain Reaction

PFA: Paraformaldehyde

PLCP: Papain-Like Cysteine Protease

PPi: inorganic Pyrophosphate

PrpS: *Papaver rhoeas* pollen *S*

PrsS: *Papaver rhoeas* stigma *S*

ROS: Reactive Oxygen Species

RP: Regulatory Particle

RT-PCR: Reverse Transcription PCR

SBP: *S*-protein Binding Protein

SBP1: *S*-RNase Binding Protein 1

SCF: Skp1/Cullin/F-box

SCR: *S*-locus Cysteine-Rich protein

SDW: sterile distilled water

SLF: *S*-Locus F-box

SI: Self Incompatibility

SLG: *S*-Locus Glycoprotein

SLR1: *S*-Locus-Related gene 1

SP11: *S*-locus Protein 11

SPH: *S*-Protein Homologues

sPPase: soluble inorganic pyrophosphatase

SRK: *S*-locus Receptor Kinase

SSI: Sporophytic SI

THL1: Thioredoxin H-Like 1

Ti: Tumor inducing

TMV: Tobacco Mosaic Virus

TT: Transmitting Tract

TUNEL: Terminal deoxynucleotidyl transferase mediated dUTP nick end labelling

UPS: Ubiquitin-Proteasome System

VPE: Vacuolar Processing Enzyme

VS: Vinyl Sulfone

Z-LLL-al: Carbobenzoxy-leucinyl-leuciny-leucinal-H

CHAPTER 1 INTRODUCTION

1.1 Plant reproduction and breeding

Plant reproduction and breeding has long played a prominent role in human civilization by providing a food supply, seeds and fruits. Understanding plant reproduction is of fundamental importance and has significant practical value for plant breeding.

1.1.1 Plant reproduction

The success of plant sexual reproduction requires the formation of the plant gametophytes, comprising male pollen and female embryo sac. A pollen grain comprises a vegetative cell nucleus and two sperm cells. See reviews by Ma (2005) and Zhang and Yang (2014) for more details about male gametophyte development. The female gametophyte is surrounded by the nucellus tissue and maternal integument, with the egg cell and central cell embedded in the middle. See reviews Cucinotta et al. (2014) and Drews et al. (1998) for more details.

Next, the establishment of pollen-pistil interaction, successful germination of the pollen grain and pollen tube growth, facilitates subsequent fertilization, and eventually embryogenesis and seed formation (Figure 1-1), which will be described briefly below. A series of complex regulatory mechanisms are used by plants to control sexual reproduction.

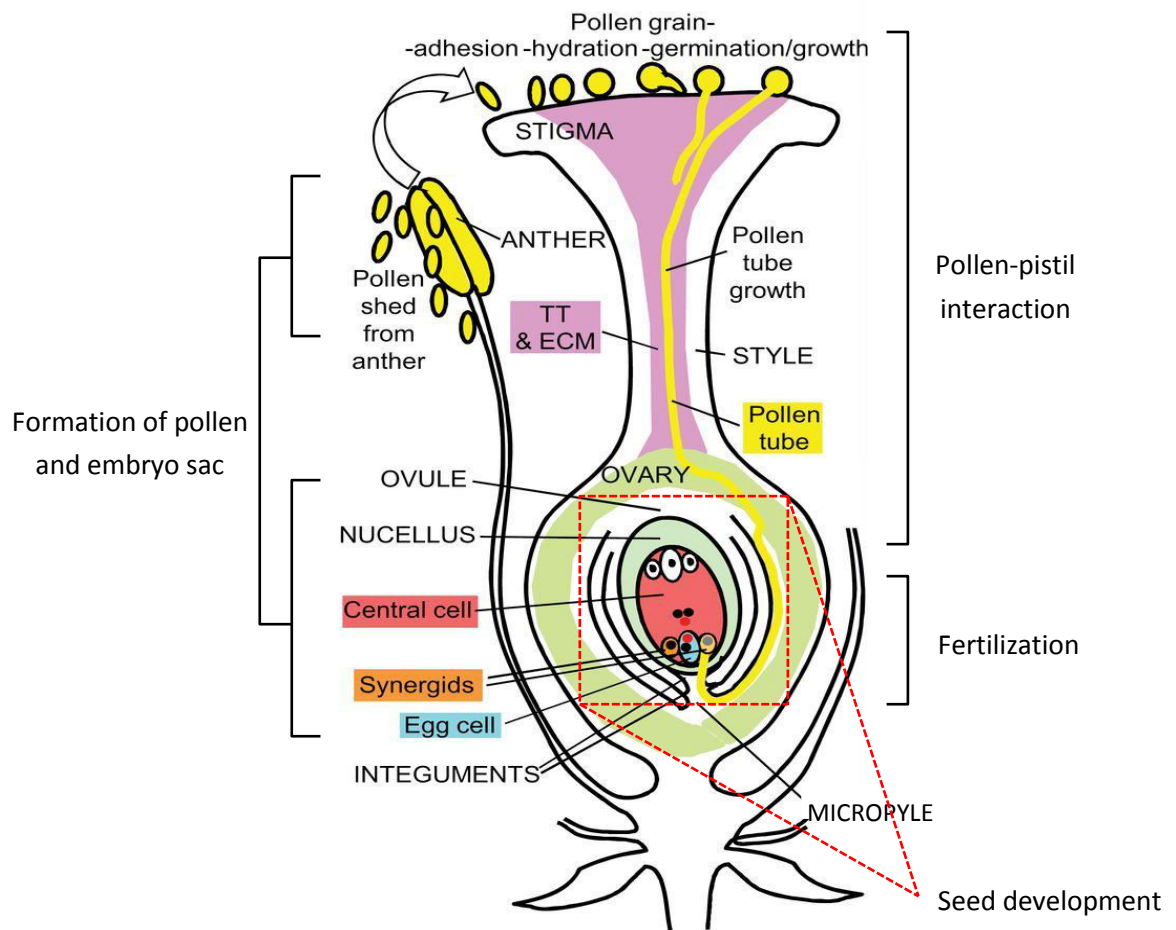


Figure 1-1 Cartoon of plant sexual reproduction

Plant sexual reproduction initiates from the formation of the gametophytes, pollen and embryo sac. During a compatible pollination, when a mature pollen grain lands on the stigma, proper interaction between pollen and the stigmatic papillae allows the successful adhesion, hydration, germination and subsequent penetration of the pollen tube into the pistil style. Pollen tube is guided to the embryo sac, and ruptures to release the two sperm cells for double fertilization. The last step of plant sexual reproduction is the development of seed, which comprises embryo, endosperm and seed coat. TT: transmitting tract; ECM: extracellular matrix. Image adapted from Dresselhaus and Franklin-Tong (2013)

1.1.1.1 Pollen-pistil interactions

A complex series of pollen-pistil interactions begins when a pollen grain lands on the stigma. A compatible pollination (see a detailed description about the incompatible

pollination in section 1.4) comprises two major stages: (1) pollen-pistil interaction allows the adherence and germination of the pollen on the stigmatic surface of the pistil in the initial stage, and later (2) pollen tube guidance to the ovary for release of sperm cells (Figure 1-1).

Despite long interest in the recognition between pollen and stigmatic papilla, only a little is known about this. In Brassicaceae, two stigma-specific secreted proteins, the *S*-Locus Related protein 1 (SLR1) and the *S*-Locus glycoprotein (SLG), have been identified as mediating pollen adhesion through interaction with pollen coat proteins (Doughty et al., 1998; Luu et al., 1999, 1997). Recently, another stigmatic factor, Exo70A1, has also been shown to be involved in the exocytosis of the stigmatic papillae cells, which is crucial for the pollen grain hydration and pollen tube penetration by tethering secretory vesicles containing various enzymes to the stigmatic papilla membrane (Safavian and Goring, 2013; Samuel et al., 2009). For pollen tube guidance, the diffusible defensin-like polypeptides, LUREs (EA1 in maize), have been identified as pollen tube attractants secreted from synergids (Márton et al., 2005; Okuda et al., 2009). See reviews by Leydon et al. (2014) and Takeuchi and Higashiyama (2011) for more details.

1.1.1.2 Pollen tube reception for double fertilization

After pollen tube arrival, intercellular interactions between the pollen tube and the

synergid cells of the embryo sac are required for the rupture of the pollen tube to release the two sperm cells, one of which fertilises the egg cell to form the embryo and the other one combines with the two polar nuclei to form the endosperm, leading to the subsequent programmed cell death (PCD) of the pollen tube and one synergid. A number of synergid expressed genes, such *LORELEI* and *FERONIA*, have been demonstrated to be involved in this pollen tube reception process (Capron et al., 2008; Escobar-Restrepo et al., 2007). Recently, a Ca^{2+} dialogue between the pollen tube and synergids has been observed to play a role in initiating the pollen tube reception procedure by mediating the *FERONIA* signalling pathway (Ngo et al., 2014). See reviews by Dresselhaus and Franklin-Tong (2013) and Kessler and Grossniklaus (2011) for more details.

1.1.1.3 Seed development

Successful double fertilization results in the formation of the embryo, and the endosperm, which is a nurturing tissue destined to support the development of the embryo. This will develop into the seed. As seed is one of the main components of plant yields in agriculture, seed formation has been intensively investigated. It has been demonstrated that development of the seed is a coordinated process between the seed coat, embryo and endosperm. In *A. thaliana*, this involves flavonoids as a fundamental role (Doughty et al., 2014; Figueiredo and Köhler, 2014). See reviews by Doughty et al. (2014) and Figueiredo and Köhler (2014) for more details.

1.1.2 Plant breeding

With the increase in the world population and food demands, in the meantime, shrinkage in the environmental resources and changes in climate, a substantial increase in agricultural production is an urgent requirement. Robust breeding technologies need to be developed to sustainably increase crop yields without enlarging the farmland area or adding the environmental impacts to provide food for the future (Godfray et al., 2010; Whitford et al., 2013). Hybrid breeding, by systematically exploiting heterosis (hybrid vigour), represents one of the most superior and popular breeding technologies in increasing crop yields, especially for cereal crops which are inbreeding species. For autogamous plants, heterosis can offer 20% to 50%, and sometimes >100% increases in seed yields compared with the parental lines (Tester and Langridge, 2010; Yamagishi and Bhat, 2014). In an effective hybrid breeding system, a robust system is required to block inbreeding and force outcrossing. Cytoplasmic male sterility (CMS) and self-incompatibility (SI) are two of the most often utilized systems in hybrid breeding.

1.1.2.1 Cytoplasmic male sterility for hybrid breeding

CMS is the most often used system to avoid self-pollination in cereal hybrid breeding. Hybrid breeding in rice represents a remarkable successful story in increasing production. One of the classic examples of CMS-based hybrid breeding system is the three-line hybridization system (Wang et al., 2013). It comprises a CMS line, a restorer line and a maintainer line (Figure 1-2). F1 hybrid seeds are produced through cross

between the CMS line and restorer line. As CMS line is sterile, it is maintained by crossing with a specific maintainer line. See Figure 1-2 for full details.

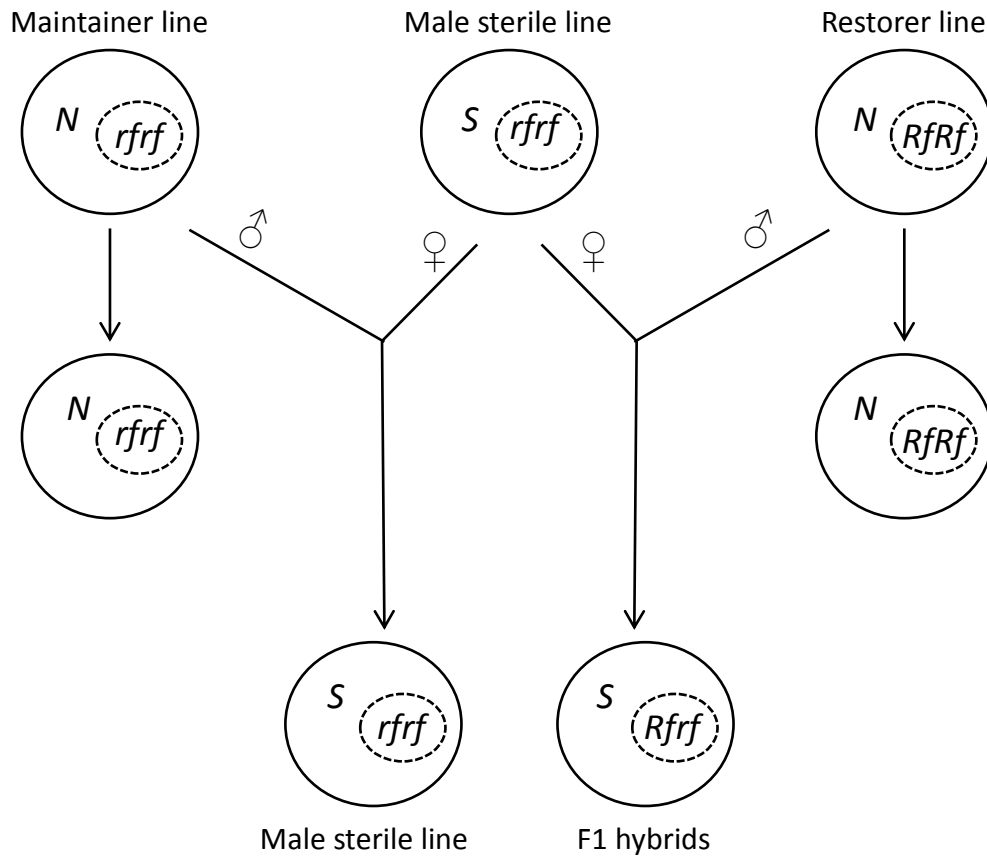


Figure 1-2 Three-line hybridization system in rice

The three-line hybridization system comprises the male sterile line, restorer line and maintainer line. *N*: cytoplasmic male fertile gene; *S*: cytoplasmic male sterile gene; *Rf*: restorer of fertility gene, dominant; *rf*: restorer of fertility gene, recessive. Only if the genotype of a certain line is $S(rfrf)$, it is male sterile. Sterility in the male sterile line results from the detrimental interaction between the cytoplasmic *S* gene and nuclear *rf* gene (Luo et al., 2013). The maintenance of male sterile line and the restoration of self-fertility phenotype in F1 offspring plants are two of the most crucial steps in establishing a hybrid breeding system. In this three-line hybridization system, the male sterile line is maintained through crossing to a maintainer line, whose genotype is $N(rfrf)$. F1 hybrid seeds are produced through crossing the male sterile line with the restorer line. The expression of the cytoplasmic male sterile gene in the F1 offspring plants can be masked by the expression of *Rf* gene derived from the restorer line, thus self-fertility phenotype in F1 is restored.

1.1.2.2 Self-incompatibility for hybrid breeding

SI is a genetically controlled mechanism to regulate the rejection of self-pollen (see section 1.4 for more details). It represents an alternative method for hybrid breeding as it prevents self-pollination (Whitford et al., 2013).

SI in the Brassicaceae has long been an important agricultural trait for hybrid breeding. For plants, such as turnip and cabbage, which are self-incompatible, a combination of honey bee pollination and CO₂ treatment to break down SI has been well established as a practical hybrid breeding system for commercial F1-hybrid seed production (Watanabe et al., 2008). *B. napus*, the oilseed rape, which is self-compatible, is one of the most important economic crops in the world. CMS has been successfully applied in oilseed rape hybrid breeding. See Yamagishi and Bhat (2014) for more details about the application of CMS in the hybrid breeding of Brassicaceae crops. Utilisation of SI in the Brassicaceae crop hybrid seed breeding is currently under investigation (Ma et al., 2009; Tochigi et al., 2011). Self-incompatible *B. napus* has been generated through interspecific hybridization by introgressing a *B. rapa* *S* haplotype into *B. napus*. A two-line hybrid breeding system has been developed, in which the self-incompatible line is maintained through triggering the SI breakdown by spraying salt solution (Ma et al., 2009). However, this hybrid breeding system remains at the experimental stage, and has not been involved in practical use.

In the grasses, the SI molecular mechanism is still not very clear and *S*-determinants have not been identified (Klaas et al., 2011). This constrains the application of the SI system in cereal crop hybrid breeding.

Before introducing SI, the ubiquitin-proteasome system (UPS) and programmed cell death (PCD), which are two important molecular mechanisms involved in the regulation of SI, are briefly introduced.

1.2 Ubiquitin-proteasome system

The regulation of most, if not all, cellular processes includes the balance between synthesis of new polypeptides and degradation of pre-existing proteins (Smalle and Vierstra, 2004). In eukaryotes, proteolysis including the turnover of misfolded and damaged proteins as well as numerous regulatory proteins is mainly carried out by the ubiquitin-proteasome system (UPS), in which proteasome recognize and degrade ubiquitinated proteins. The significance of the UPS has been demonstrated in diverse plant physiological events, such as growth and development (Sheng et al., 2006), abiotic environment responses (van Ooijen et al., 2011), PCD (Bader and Steller, 2009) and the SI response (Entani et al., 2014; Indriolo et al., 2014). The involvement of UPS in SI will be described in more detail in section 1.4.

1.2.1 Ubiquitin (Ub) and ubiquitination

Ub is a 76-amino acid protein, containing seven lysine residues. It is highly conserved

structurally and is ubiquitously expressed across all eukaryotic organisms. Ub can be covalently attached to target proteins by an ATP-dependent E1-E2-E3 conjugation cascade (referred to as ubiquitination; Figure 1-3), resulting in the recognition and degradation of ubiquitinated proteins by the 26S proteasome, releasing Ub moieties for reuse (Hicke, 2001; Smalle and Vierstra, 2004).

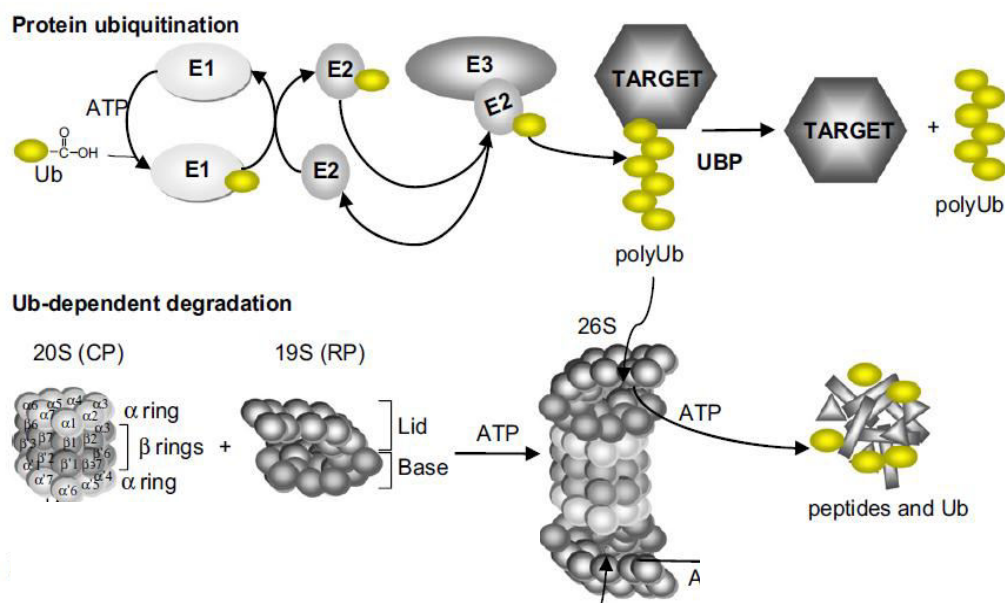


Figure 1-3 Organization and structure of Ub/26S proteasome system

Target protein ubiquitination starts from the activation of an Ub protein by binding to an Ub-activating enzyme (E1). This activated Ub is then transferred to an Ub-conjugating enzyme (E2) through transesterification. With an Ub-protein ligase (E3) as the recognition element, Ub is delivered to target substrate protein (Kurepa and Smalle, 2008; Orłowski and Wilk, 2003). PolyUb can be catalyzed to detach from the target protein by Ub-specific proteases to prevent its proteasomal degradation. The 26S proteasome contains a 20S core particle (CP) and a 19S regulatory particle (RP). Ubiquitinated protein can be degraded by the 26S proteasome in an ATP-dependent manner. Generally, the RP is responsible for substrate recognition and unfolding, removing the Ubs, opening the α -ring gate, and subsequently directing the unfolded substrates into the CP lumen for degradation. Images adapted from Kurepa and Smalle (2008)

The involvement of ubiquitination pathways in differentially modifying a variety of substrate proteins is determined by the diverse nature of E3 Ub-protein ligases. Bioinformatic analysis of *A. thaliana* genome identified more than 1400 genes (more than 5% of the *A. thaliana* proteome) encoding UPS related components (Gagne et al., 2002), most of which are putative E3s or E3 complex subunits (Hua and Vierstra, 2011; Kraft et al., 2005; Stone et al., 2005). In general, E3 serves as the scaffold to bring together E2 and substrate protein to promote conjugation during ubiquitination. Of the three major types of E3s, RING containing E3 Ub ligase has been most intensively studied. RING containing E3 Ub ligases can occur as monomeric E3s or multi-subunit E3 complexes, which is typified by Skp1/CUL1/F-box/Rbx1 (SCF) complex (Figure 1-4). It is the largest family of E3 ligase.

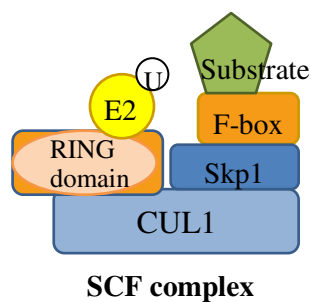


Figure 1-4 Cartoon of SCF complex

As the largest family of E3 Ub-protein ligase, SCF E3 complex consists of at least four subunits: Skp1, CUL1, F-box and Rbx1. CUL1 functions as a platform upon which all the other subunits assemble. The Skp1/CUL1/Rbx1 sub-complex confers the Ub-transferase activity, while a multitude of F-box proteins function to determine substrate specificity (Deshaies, 1999; Smalle and Vierstra, 2004).

1.2.2 Structure of the proteasome

The 26S proteasome is a multisubunit, multicatalytic protease localized in the cytosol and nucleus, whose structure is highly conserved in eukaryotes. It consists of two subparticles (Figure 1-3): the 20S core particle (CP), which is an ATP- and Ub-independent, broad-spectrum protease responsible for the degradation of ubiquitinated proteins and the 19S regulatory particle (RP), which confers ATP- and Ub-dependence to the protease (Hanna and Finley, 2007). See reviews by Kurepa and Smalle (2008) and Smalle and Vierstra (2004) for more structural details. Structural characterization using X-ray crystallography revealed a large central chamber which harbours the protease active sites provided by the PBA, PBB and PBE subunits. They have peptidyl glutamyl-peptide hydrolase activities (caspase-like activities), trypsin-like activities and chymotrypsin-like activities, respectively (Groll et al., 1997; Hanna and Finley, 2007; Unno et al., 2002). The CP is very sensitive to proteasome-specific inhibitors specifically designed to inhibit the active threonine site of the catalytic β subunit (Bogyo et al., 1997; Lee and Goldberg, 1998). Proteasome-specific inhibitors represent a useful tool in studying the role of proteasome during various cellular procedures. See Chapter 6 for detailed description about these inhibitors.

As mentioned earlier, UPS has been demonstrated to be involved in the regulation of PCD. Before we describe the involvement of UPS in PCD, PCD is introduced.

1.3 Programmed cell death (PCD) and caspases

PCD is a mechanism adopted by most organisms to remove unwanted cells in a precisely controlled way (Raff, 1998). As an integral part of the life cycle in both plants and animals, PCD is central to growth, development, and homeostasis, as well as the adaptation to a variety of extrinsic stresses, like injury and infection (Jacobson et al., 1997; Pennell and Lamb, 1997). It is a genetically defined process associated with distinctive morphological and biochemical hallmarks, such as mitochondrial cytochrome *c* leakage and DNA fragmentation, involving caspases (termed cysteinyl aspartate-specific proteases) as the central components of the PCD signalling network (Alnemri et al., 1996; Nicholson and Thornberry, 1997; Shi, 2002). Since the first identification of caspase (caspase-1) in humans (Cerretti et al., 1992), large numbers of caspase family members were isolated and characterized in animals (Riedl and Shi, 2004). They are generally divided into two classes: the initiator caspases, including caspase-2, -8, -9 and -10; and the effector/executioner caspases, including caspase-3, -6 and -7. During the PCD signalling cascade, the auto-activated initiator caspases activate the effector caspases by cleavage at specific internal Asp residues, which leads to the subsequent proteolytic cleavage of a broad spectrum of cellular targets, committing the cell to death (Nicholson and Thornberry, 1997; Riedl and Shi, 2004; Steller, 1995).

1.3.1 Plant programmed cell death and caspase-like activities

Though the signalling networks and molecular mechanisms of plant PCD are far less

studied and understood, it has been increasingly documented in the last decade and has been established as playing an important role in plant growth and survival, such as senescence (Bleecker and Patterson, 1997), xylem tracheary element differentiation (Fukuda and Komamine, 1983), seed development (Pennell and Lamb, 1997), as well as plant-pathogen interaction (Greenberg, 1997) and SI (Thomas and Franklin-Tong, 2004).

As plants and animals are evolutionarily distinct from each other and have distinctive cellular architectures, while they share some common features, many different biochemical and cytological signatures have been observed between plant PCD and animal PCD (van Doorn et al., 2011). Caspase enzymes represent one example of this.

Caspase activities have been identified as playing essential roles in both plant and animal PCD. Use of tetrapeptide-based fluorogenic substrates and inhibitors has allowed the identification and functional analysis of at least eight different caspase-like activities involved in plant PCD, such as YVADase (caspase-1-like) (Bosch et al., 2010; Hatsugai et al., 2004), DEVDase (caspase-3-like) (Bosch and Franklin-Tong, 2007; Korthout et al., 2000) and VEIDase (caspase-6-like) (Borén et al., 2006; Bosch and Franklin-Tong, 2007). However, no caspase homologue gene has been identified in the plant genome. Therefore, it is of considerable interest to know which protease enzymes are responsible for the caspase-like activities during the plant PCD and what their

identities are.

1.3.2 Involvement of UPS in the regulation of PCD

Over the past few years, it has become increasingly clear that the UPS is involved in the regulation of animal PCD by directly targeting key cell death proteins. Whether the UPS functions as an accelerator or retarder of PCD depends on whether caspases or Inhibitors of Apoptosis Proteins (IAPs) are targeted for ubiquitination and proteasome degradation (Bader and Steller, 2009; Broemer and Meier, 2009).

The role of Ub/proteasome pathway in plant PCD has also been investigated, though less extensively. Similar to animal PCD, apparently contradictory results were obtained in different studies (Beers et al., 2000). In *N. benthamiana* leaves, virus-induced gene silencing of the 20S proteasome subunit $\alpha 6$ and the 19S regulatory complex subunit RPN9 not only resulted in down-regulation of the proteasome activity, but also PCD of the leaf cells (Kim et al., 2003). In contrast, in some other plant PCD models, both activation of proteasomal activities and Ub/proteasome related gene expression were observed. For example, in the heat shock-induced PCD of tobacco Bright-Yellow 2 cells, increased proteasomal activities were observed, and MG132 treatment resulted in the block of PCD (Vacca et al., 2007). Similar phenomena have also been reported in acetic acid-induced PCD of *Saccharomyces cerevisiae* (Valenti et al., 2008), which also lacks caspase homologous genes. Taken together, these indicate the indispensable role of

proteasomal proteolysis in plant PCD. Recently, there has been further characterization of how the proteasome might be involved in plant PCD. Emerging evidence shows that the proteasome is involved in plant PCD by being responsible for the caspase-3-like activity (Han et al., 2012; Hatsugai et al., 2009; Pajerowska-Mukhtar and Dong, 2009).

1.3.3 Involvement of proteasome in PCD as DEVDase

Bacterial pathogen-induced hypersensitive cell death adopts a membrane fusion mechanism to discharge the vacuolar defence proteins into the extracellular space to stop bacteria proliferation (Hara-Nishimura and Hatsugai, 2011). This novel membrane fusion mechanism was triggered in a proteasome- and caspase-3-like activity-dependent manner (Hara-Nishimura and Hatsugai, 2011). Both proteasome inhibitors (Ac-APnLD-CHO and β -Lactone) and caspase-3 inhibitor (Ac-DEVD-CHO), as well as gene silencing of proteasome β subunits *PBA1*, *PBB* or *PBE*, prevented this pathogen-induced membrane fusion and the subsequent PCD (Hatsugai et al., 2009). Most importantly, a biotin-DEVD-fmk pull-down followed by an anti-PBA1 antibody immunoblot analysis demonstrated that PBA1 was responsible for the DEVDase activity. In addition, the correlation between DEVDase activity and PBA1 activity was verified in *A. thaliana* *PBA1* RNAi lines, revealing PBA1 involved in the regulation of plant PCD as the caspase-3-like enzyme (Hatsugai et al., 2009; Pajerowska-Mukhtar and Dong, 2009).

A similar role for proteasome was also identified during xylem development, which involves PCD (Fukuda, 1996; Han et al., 2012). Caspase-3-like activities were identified during the xylem differentiation in *Populus tomentosa*, and both caspase-3 inhibitor (Ac-DEVD-CHO) and proteasome inhibitor (β -Lactone) suppressed the xylem differentiation in *A. thaliana* (Han et al., 2012). An assay using chromatography and mass spectrometry showed that the 20S proteasome was responsible for the caspase-3-like activity in the xylem development of *P. tomentosa* (Han et al., 2012). Thus, these are two examples of the proteasome being identified as the DEVDase enzyme during the plant PCD.

1.4 Self-incompatibility (SI)

Self-incompatibility (SI) is an important mechanism that genetically regulates the acceptance or rejection of pollen that land on the stigma of the same species. It is developed by angiosperms to prevent inbreeding and promote outcrossing to generate genetic diversity. The SI phenomenon is widespread in higher plants, and has been identified in at least 71 families as well as 250 of the 600 genera (Allen and Hiscock, 2008). Even major selfing species are thought to have evolved through the loss of SI, which has been partly revealed by recent molecular approaches combined with evolutionary analysis (Chantha et al., 2013; Sherman-Broyles and Nasrallah, 2008; Tang et al., 2007). Generally, in most of the angiosperms where SI exists, it is genetically controlled by a multi-allelic *S*-locus. It is known that each *S*-haplotype

encodes at least two proteins, which are designated as *S*-determinants, responsible for the male and female specificity, respectively. The ability of stigma to discriminate between “self” and “non-self” pollen is based on the allele-specific interactions between these two highly polymorphic *S*-determinants.

Considerable knowledge relating to the distribution, physiology and genetics of SI in flowering plants has been accumulated since Darwinian times. From classical genetic studies, SI in homomorphic plants is classified into two main types, sporophytic SI (SSI) and gametophytic SI (GSI), depending on whether the SI phenotype of the pollen is determined by the *S*-genotype in the diploid pollen donor or the *S*-haplotype in the haploid pollen (Figure 1-5). Although SSI has been found in Brassicaceae, Asteraceae and Convolvulaceae, it is still relatively limited in its distribution compared to GSI. GSI species, which are widespread and found in many more families, can be further divided into two categories: (1) *S*-RNase based GSI in the Solanaceae, Plantaginaceae, Scrophulariaceae and Rosaceae, and (2) PrpS/PrsS mediated GSI in Papaveraceae.

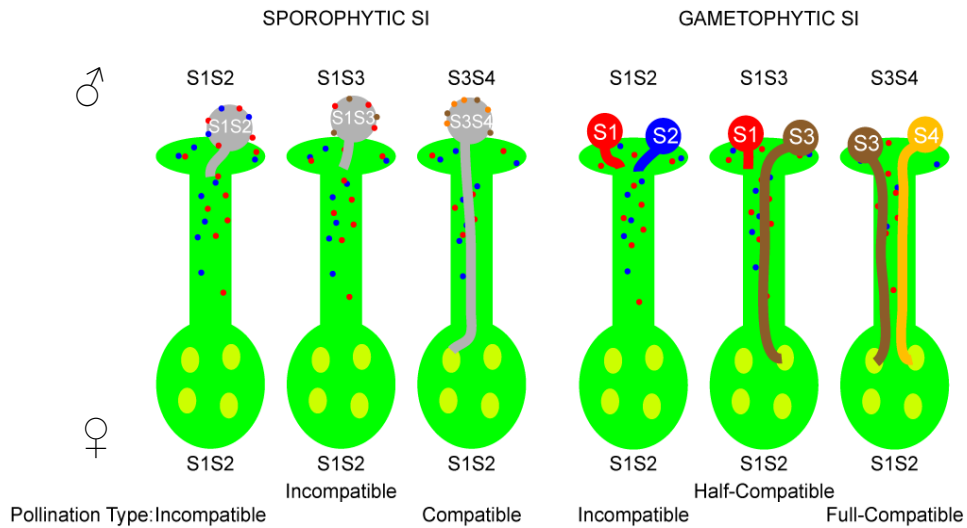


Figure 1-5 Illustration of the genetic basis of sporophytic and gametophytic SI

For sporophytic SI, the SI phenotype of the pollen is determined by the *S*-genotype in the diploid maternal tissue. Pollen from sporophytic species carries the products of both two *S*-genotypes from parents. So, when an *S*₁*S*₂ stigma is pollinated with *S*₁*S*₂ or *S*₁*S*₃ pollen, the outcomes are both incompatible reactions. Only pollen without any of the parents' *S*-genotype products, in this case, such as *S*₃*S*₄, can germinate and fertilize normally. In term of gametophytic SI, the SI phenotype of the pollen is determined by the *S*-haplotype in the haploid pollen. Pollen from gametophytic species only carries one of the *S*-gene products from parents. So, incompatible interaction on the *S*₁*S*₂ stigma can only be observed when it is pollinated with *S*₁*S*₂ pollen. Besides full compatible and incompatible interactions, a phenomenon called half-compatibility can also be observed in gametophytic species. For example, when pollen from *S*₁*S*₃ plants land on the *S*₁*S*₂ stigma, *S*₁ pollen is rejected and *S*₃ pollen grows normally.

Early efforts to identify the biochemical basis of SI started in the second half of last century. Since the first detection and characterization of SI proteins by Nasrallah and Wallace in 1967 (Nasrallah and Wallace, 1967; Nasrallah et al., 1970), world-wide efforts to identify the *S*-determinants were followed. In recent decades, understanding of the molecular mechanisms underlying the SI phenomenon has increased greatly, marked by the identification of the *S*-determinants in the representative SI species (Table 1-1). Three different SI systems and their components will be briefly described below.

Table 1-1 Male and female S-determinants identified in the representative SI systems

Plant family	Plant species	SI type	Male S-gene	Female S-gene	References
Brassicaceae	<i>Brassica rapa</i> (syn. <i>campestris</i>)	SSI	<i>SCR/SP11</i>	<i>SRK</i>	(Schopfer et al., 1999; Shiba et al., 2001; Takasaki et al., 2000; Takayama et al., 2000)
	<i>Brassica oleracea</i>				(Stein et al., 1991)
	<i>Arabidopsis lyrata</i>				(Kusaba et al., 2001)
Solanaceae	<i>Petunia inflata</i>	GSI	<i>SLF/SFB</i>	<i>S-RNase</i>	(Lee et al., 1994; Sijacic et al., 2004)
	<i>Nicotiana glauca</i>				(McClure et al., 1989; Murfett et al., 1994)
	<i>Lycopersicon peruvianum</i>				(Royo et al., 1994)
Scrophulariaceae	<i>Antirrhinum hispanicum</i>	GSI	<i>SLF/SFB</i>	<i>S-RNase</i>	(Lai et al., 2002; Xue et al., 1996)
Papaveraceae	<i>Papaver rhoeas</i>	GSI	<i>PrpS</i>	<i>PrsS</i>	(Foote et al., 1994; Wheeler et al., 2009)

1.4.1 Brassicaceae SI

Of the three families utilising SSI, Brassicaceae SI has been studied extensively at the molecular level. The ability for Brassicaceae SI species to discriminate between self and non-self-pollen relies on two highly polymorphic and genetically-linked proteins derived from the S-locus. They are the stigma S-locus Receptor Kinase (SRK) (Takasaki et al., 2000) and the pollen S-locus Cysteine-Rich protein (SCR, or S-locus protein 11, SP11) (Schopfer et al., 1999; Takayama et al., 2000). They control the SI specificity of Brassicaceae through S-allele-specific receptor-ligand interactions (Kachroo et al., 2001;

Takayama et al., 2001).

1.4.1.1 Brassicaceae SI S-determinants: SRK and SCR

SRK is a membrane-spanning Ser/Thr receptor kinase (Goring and Rothstein, 1992; Watanabe et al., 1994), which was identified to be a tightly linked polymorphic *S*-locus gene, temporally and spatially-expressed in the papillar cells of the stigma specifically (Goring et al., 1993; Nasrallah et al., 1994; Stein et al., 1991). SRK as the role to determine *S*-haplotype specificity was not finally established until 2000, when Takasaki et al. showed that SRK conferred the ability to reject cognate pollen on the transgenic plants (Takasaki et al., 2000).

SCR is a small secreted hydrophilic protein (~8.6 kD), acting as a ligand for the stigmatic receptor SRK during SI interaction expressed on the pollen coat (Kachroo et al., 2001; Takayama et al., 2001). It was identified during the sequence analysis of the region between *SRK* and *SLG* in *B. rapa* (Schopfer et al., 1999; Suzuki et al., 1999). Further transgenic gain and loss of function studies demonstrated its pollen SI specificity (Schopfer et al., 1999; Takayama et al., 2000); see Franklin-Tong and Franklin (2000) for a review.

1.4.1.2 The UPS is involved in the Brassicaceae SI

Great advances in understanding the Brassicaceae SI response have been achieved in recent years, marked by the molecular characterization of several important components,

especially the identification of UPS related factors, within the SI signalling network. Arm-Repeat Containing 1 (ARC1) has been demonstrated to play an important role in Brassicaceae SI (Goring et al., 2014; Indriolo et al., 2012, 2014). It is a novel U-box protein with E3 ubiquitin ligase activity (Stone et al., 2003), identified to interact with the kinase domain of SRK in a phosphorylation dependent manner. RNAi-mediated down-regulation of ARC1 resulted in a partial breakdown of SI in the transgenic plants (Gu et al., 1998; Stone et al., 1999). In addition, no alteration in the ubiquitination level was detected in the ARC1 knockdown pistil, while increased ubiquitinated protein levels were observed in the pistil upon incompatible pollination. Moreover, inhibition of the proteasomal proteolytic activity of the stigma using proteasome-specific inhibitors disrupted the SI response (Stone et al., 2003). These suggest that ARC1 is involved in the Brassicaceae SI by mediating the protein ubiquitination in incompatible pollination pistil. Exo70A1 is a putative substrate of ARC1, identified in a screening for ARC1-interacting proteins. It is a putative component of the exocytosis complex and functions in polarized secretion (Hsu et al., 2004). Transgenic studies showed that Exo70A1 over-expression resulted in partial breakdown of SI in the transgenic plants, whereas its reduced expression disrupted compatible pollen tube growth (Samuel et al., 2009). This suggests that Exo70A1 is involved in the Brassicaceae SI by inhibiting the polarized secretion in the stigmatic papillae which is crucial for pollen hydration and pollen tube penetration (Safavian and Goring, 2013).

Based on these findings, a hypothesis proposing involvement of the UPS in Brassicaceae SI has been raised. As shown in Figure 1-6, it is proposed that Exo70A1 functions as a positive regulator for pollen grain hydration by facilitating specialized secretion of stigmatic factors following compatible pollination. In contrast, during the SI response, cognate SRK and SCR interaction activates ARC1, which would lead to the ubiquitination and proteasomal degradation of Exo70A1, resulting in the failure of stigmatic factors secretion, and then culminating in self-pollen rejection (Goring et al., 2014; Zhang et al., 2009).

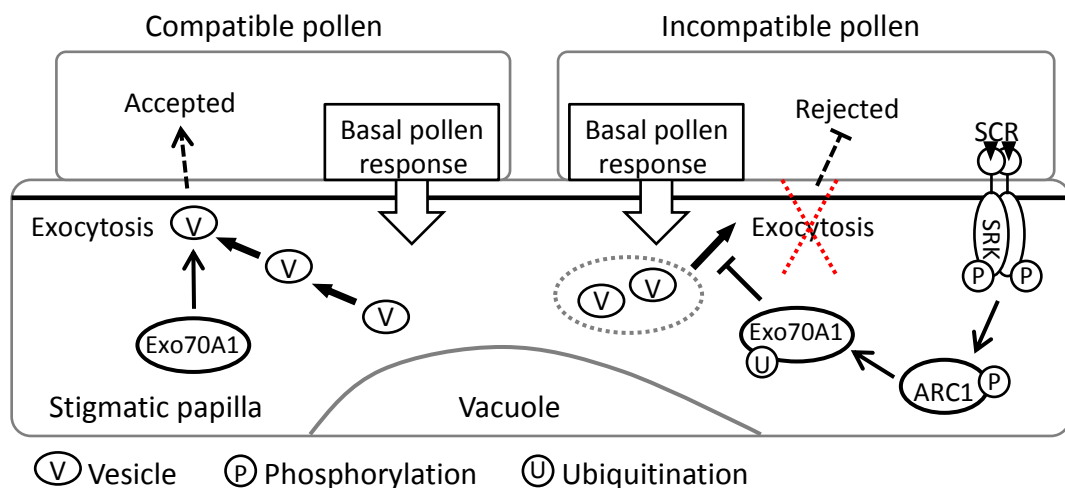


Figure 1-6 Model for the molecular mechanism underlying Brassicaceae SI

During compatible pollination, Exo70A1 functions as a positive regulator for pollen hydration and pollen tube penetration by facilitating specialized secretion of stigmatic factors. Upon self-pollination, SRK recognizes and binds with its cognate SCR ligand, which causes the phosphorylation of SRK itself, followed by the recruitment of ARC1, resulting in the phosphorylation and activation of ARC1 subsequently. As a substrate for ARC1, Exo70A1 is ubiquitinated by the activated ARC1 and relocated to the proteasome for degradation. This leads to the failure of exocytosis, thus resulting in the rejection of self-pollen by inhibiting the polarized secretion. Images adapted from Indriolo et al. (2014).

Other cellular components such as *M*-Locus Protein Kinase (MLPK), Thioredoxin H-Like 1 (THL1) and actin cytoskeleton have also been shown to be involved in the Brassicaceae SI (Bower et al., 1996; Iwano et al., 2007; Murase et al., 2004); see reviews Ivanov et al. (2010) and Tantikanjana et al. (2010) for more details.

1.4.2 *S*-RNase-based SI

The ability of SI plants in the Solanaceae to selectively inhibit the growth of self-pollen is determined by a pair of *S*-locus-encoded proteins: a ribonuclease known as the *S*-RNase in the style, and a large number of pollen specific F-box proteins, named *S*-locus F-box (SLF) (Kao and Tsukamoto, 2004; Kubo et al., 2010).

1.4.2.1 Stigma and pollen *S*-determinants: *S*-RNase and SLF

The stigma *S*-determinant for the *S*-RNase-based SI system is a ribonuclease gene, *S*-RNase, which encodes a ~30 kD glycoprotein. It was identified in the search for pistil-specific expressed and *S*-allele-associated genes (Ai et al., 1990; Bredemeijer and Blaas, 1981; Sassa et al., 1993). The ribonuclease activity of *S*-RNase was demonstrated to be crucial for self-pollen rejection (McClure et al., 1989; Royo et al., 1994). The role of *S*-RNase as the female *S*-determinant was established in 1994 via transgenic experiments (Lee et al., 1994; Murfett et al., 1994). Immunolocalization studies demonstrated that *S*-RNases could be imported into pollen tubes while the pollen tubes were growing in pistils regardless of whether they were compatible or incompatible

(Goldraij et al., 2006; Luu et al., 2000).

The pollen *S*-gene must be tightly linked to the *S*-RNase gene. Based on this assumption, sequencing analysis of the *S*-locus identified several pollen expressed F-box genes, *S*-locus F-box gene (*SLF*), with *S*-allelic diversity (Entani et al., 2003; Lai et al., 2002; Ushijima et al., 2003). *SLF* encodes F-box-containing protein, whose N-terminal F-box domain can be recognized by E3 ubiquitin ligase (Cardozo and Pagano, 2004). Further transgenic analysis confirmed the role of SLF protein as the male *S*-determinant (Sijacic et al., 2004). A collaborative non-self-recognition model was raised to explain how SLF functions as the pollen *S*-determinant with much lower *S*-allelic diversity than *S*-RNase (Figure 1-7); see Iwano and Takayama (2012) for more details.

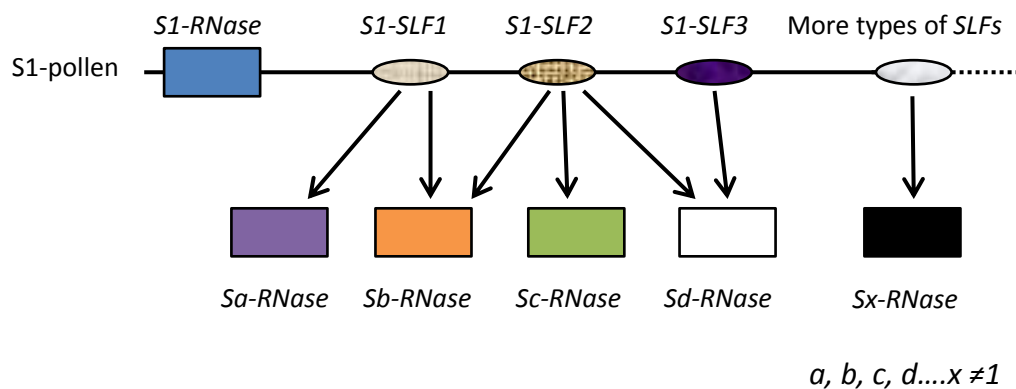


Figure 1-7 Model for the recognition between pollen and pistil *S*-determinants in *S*-RNase-based SI

In this model, an as yet unknown number of divergent SLF proteins are encoded by each *S*-allele. Each SLF protein recognizes a subset of non-self *S*-RNases, thus all the SLF proteins encoded from each *S*-allele function together to recognize all the non-self *S*-RNases to mediate their detoxification (Iwano and Takayama, 2012; Kubo et al., 2010; Sawada et al., 2014; Sun and Kao, 2013; Williams et al., 2014a, 2014b). Images adapted from Wang and Kao (2012).

1.4.2.2 Models for pollen recognition and rejection for *S*-RNase-based SI

A consensus has been reached that during the *S*-RNase-based incompatible response: upon self-pollination, self-*S*-RNases degrade cytoplasmic RNA, resulting in the growth inhibition of incompatible pollen tubes, whereas in the compatible reaction, non-self *S*-RNases are somehow detoxified. However, it is still controversial how the cytotoxic effects of non-self *S*-RNases are counteracted. Currently, two independent models have been developed to explain the molecular mechanism underlying the recognition and detoxification of non-self-*S*-RNase in this SI system: the compartmentalization model (Figure 1-8) and the ubiquitination/degradation model. See Goldraij et al. (2006) and McClure et al. (2011) for more details about the compartmentalization model. Here, we only focus the ubiquitination/degradation model in more detail.

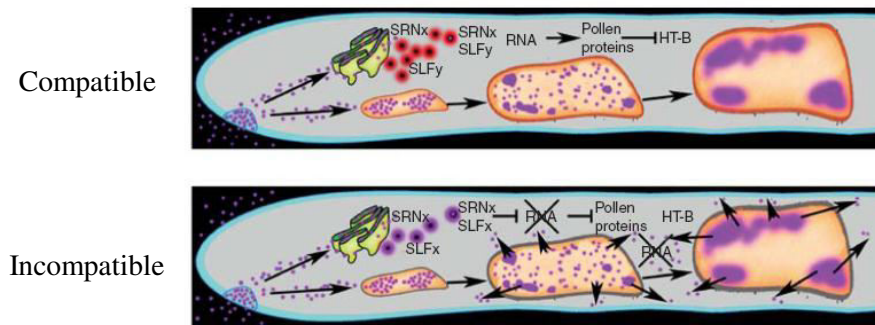


Figure 1-8 Sequestration/compartmentalization model for the *S*-RNase-based SI

In the compartmentalization model, it is proposed that in the compatible response, non-self-*S*-RNase enters the pollen tube and is compartmentalized into vacuoles (Goldraij et al., 2006). While in the incompatible response, compartmented self-*S*-RNase is released into cytoplasm due to the signalling cascade caused by self-*S*-RNase-SLF interaction, which results in pollen RNA degradation and consequent pollen tube growth inhibition (Goldraij et al., 2006). Image adopted from McClure et al. (2011)

A variety of ubiquitin/proteasome related proteins have been identified in the investigations for the protein-protein interaction between the *S*-determinants (*S*-RNase and SLF) and other pollen cellular components, suggesting the involvement of ubiquitin/proteasome pathway in the *S*-RNase-based SI. Yeast two-hybrid screening using the N-terminal region of *S*-RNase as the bait identified *S*-RNase-binding protein 1 (SBP1). SBP1 corresponds to a RING finger protein, and is a putative E3 ubiquitin ligase (O'Brien et al., 2004; Sims and Ordanic, 2001).

Skp1/CUL1/F-box/Rbx1 (SCF) ubiquitin ligase complex is the largest family of E3 ubiquitin ligase mediating the ubiquitination of a variety of regulatory proteins (Zheng et al., 2002; section 1.2.1). Several studies have demonstrated the involvement of SCF complex subunits in the *S*-RNase-based SI. SLF-interacting SKP1-like1 (SSK1) was isolated through a yeast two-hybrid screening using SLF as the bait (Huang et al., 2006; Xu et al., 2013). The interaction between SSK1 and SLF was further confirmed by GST pull-down assays. It was observed that SSK1 could be the adaptor for SLF and CUL1-like protein (Huang et al., 2006). It has also been demonstrated that SSK1 was required for cross-pollen compatibility in *S*-RNase-based SI (Zhao et al., 2010). The rigid scaffold of SCF complex, CUL1 was also identified in pollen (Hua and Kao, 2006). The functional role of pollen-expressed CUL1 in *S*-RNase-based SI has been verified by RNAi studies (Li and Chetelat, 2014). Involvement of SCF complex in *S*-RNase-based SI was further confirmed by the identification of a complex consisting SLF, CUL1,

SSK1 and Rbx1 using co-immunoprecipitation followed by mass spectrometry analysis (Li et al., 2014).

Recently, further evidence indicating the involvement of Ub/proteasome system in *S*-RNase-based SI has been obtained. Treatment of pollen with proteasome inhibitors MG115 or MG132 blocked the compatible pollination both *in vitro* and *in vivo*, but little effect was observed in incompatible pollination (Qiao et al., 2004). Degradation of non-self-*S*-RNase could be observed in compatible pollen tubes *in vivo* (Boivin et al., 2014). Moreover, SCF^{SLF} complex mediated the polyubiquitination and cytosolic degradation of non-self *S*-RNase, and this could be attenuated by proteasome inhibitor treatment (Entani et al., 2014; Liu et al., 2014). In addition, target-site mutation of *S*-RNase lysine residues reduced both polyubiquitination and degradation of the mutant *S*-RNase *in vitro* (Hua and Kao, 2008). All these observations fit well with the hypothesis proposing a role for the UPS in *S*-RNase-based SI. Figure 1-9 outlines a model for how this might operate. In a compatible reaction, non-self-*S*-RNase is recognized and ubiquitinated by SLF containing E3 ligase complex, resulting in its degradation. While in an incompatible reaction, *S*-RNase is left intact, leading to the inhibition of pollen tube growth due to its cytotoxic activity (McClure et al., 2011; Zhang et al., 2009).

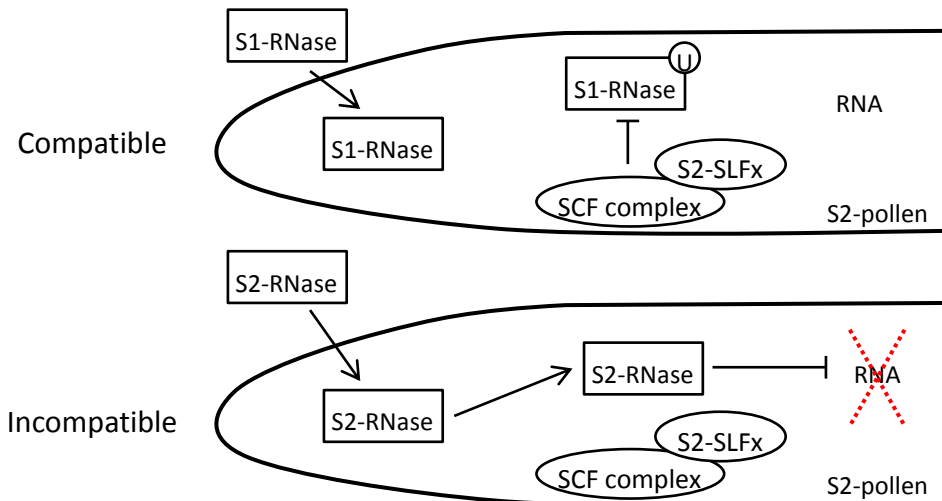


Figure 1-9 Ubiquitination/degradation model for *S*-RNase-based SI

SLF, SBP1 and SSK1 are recruited together with E2 ligase and CUL1 to form a SCF-like ubiquitin ligase complex, in which SLF serves as the adaptor to determine the specificity of substrates. Upon compatible pollination, SCF^{SLF} complex recognizes and polyubiquitinates non-self *S*-RNases, resulting in the proteasomal degradation of non-self *S*-RNase, thus preventing the degradation of pollen RNA. During the incompatible reaction, SLF complex cannot recognize self-*S*-RNase, which results in the degradation of pollen RNA and subsequently self-pollen rejection.

Taken with what has been described in section 1.4.1, good evidence has been provided that the UPS is involved in both Brassicaceae SI and the *S*-RNase-based SI. Therefore, it is of considerable interest to know whether the UPS is a universal mechanism involved in the pollen rejection across different SI systems.

1.4.3 *Papaver* SI

Papaver SI involves a completely different SI molecular mechanism compared with Brassicaceae SI and *S*-RNase-based SI. It is also genetically controlled by a single polymorphic *S*-locus. The female and male *S*-determinants are *Papaver rhoeas* Stigma *S*-determinant (PrsS) and *Papaver rhoeas* Pollen *S*-determinant (PrpS), respectively.

Cognate PrpS-PrsS interaction triggers PCD in incompatible pollen, resulting in the rejection of incompatible pollen.

1.4.3.1 *Papaver* SI pistil and pollen S-determinants: PrsS and PrpS

PrsS is a small secreted protein (~14 kD) specifically expressed in the stigma papilla cells. It was cloned by using an oligonucleotide probe based on the N-terminal amino acid sequence from stigmatic proteins that showed complete linkage with the *S* gene on isoelectric focusing gels (Foote et al., 1994; Walker et al., 1996). Sequence alignment analysis showed that *PrsS* did not fall into either of the two *S*-genes families in *S*-RNase-based SI and Brassicaceae SI systems, revealing a different SI mechanism adopted by field poppy (Foote et al., 1994).

To confirm that the putative *S* gene was genuinely a biologically active and functional *S*-determinant, the nucleotide sequences encoding the predicted mature polypeptide were cloned and expressed in *E. coli*. Although the recombinant *S*-proteins were not post-translationally processed in the same way as the protein would be in plants, and there was an additional methionine residue at the N-terminal, they did exhibit *S*-specific *in vitro* pollen inhibitory activities as expected (Foote et al., 1994; Kurup et al., 1998; Walker et al., 1996).

PrpS is a novel transmembrane protein (~20 kD). It was identified through sequencing analysis of a cosmid clone comprising the *S*-locus (Wheeler et al., 2009). Expression

analysis demonstrated that PrpS has a pollen-specific and developmental-regulated expression pattern, which is spatially and temporally correlated well with the appearance of SI. Segregation and polymorphic analysis between different *S* alleles, as well as evolutionary analysis of *PrsS* and *PrpS* further confirmed *PrpS* as the role of *Papaver* pollen *S* gene (Wheeler et al., 2009).

Functional evidence for the role of *PrpS* in SI has been obtained. Knockdown expression of *PrpS* by antisense oligonucleotide (as-OND) resulted in the alleviation of pollen tube growth inhibition in an *S*-specific manner. Additionally, SI-mediated pollen inhibition was rescued by adding peptides of the putative PrpS extracellular domain in an *in vitro* SI bioassay (Wheeler et al., 2009). With the observation of PrsS binding to the predicted extracellular loop of PrpS, a hypothesis that PrsS and PrpS mediate the SI response through a ligand-receptor-type interaction was raised (Wheeler et al., 2009, 2010).

1.4.3.2 Mechanisms involved in *Papaver* SI

A considerable number of cellular components have been identified to be involved in the regulation of the *Papaver* SI response. A model has been developed: the binding of PrsS to the extracellular domain of its cognate PrpS protein triggers a Ca²⁺-dependent signalling network within the pollen, resulting in the inhibition of subsequent pollen tube growth and PCD in compatible pollen (Figure 1-10).

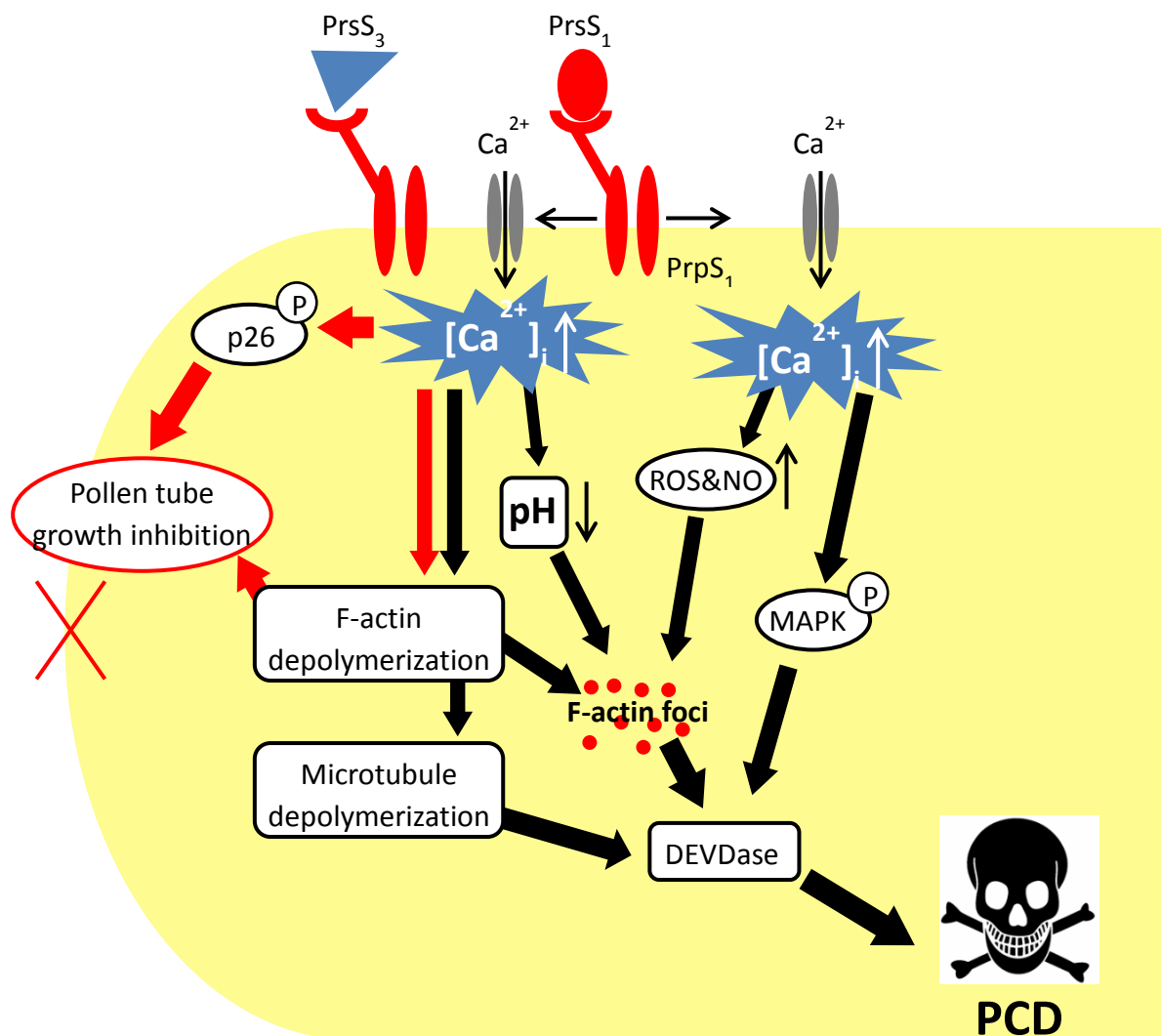


Figure 1-10 A cartoon showing the signalling network in an incompatible pollen in *Papaver rhoeas*

Cognate PrpS and PrsS interaction triggers a Ca^{2+} -dependent signalling network, comprising two inter-related signalling cascade: pollen tube growth inhibition signalling cascade and pollen death signalling cascade. Pollen tube growth inhibition signalling cascade (red arrows): increase in cytosolic Ca^{2+} triggers the phosphorylation and inactivation of p26, a soluble inorganic pyrophosphatase, and dramatic alteration in the F-actin cytoskeleton. As a result, pollen tube growth is inhibited. Pollen death signalling cascade: increases in cytosolic Ca^{2+} also triggers microtubule depolymerization, cytosolic acidification, increases in ROS and NO levels, F-actin foci formation, activation of p56-MAPK and DEVDase activation which commits the pollen to death.

1.4.3.2.1 Pollen tube growth inhibition signalling cascade

SI induction triggers a rapid pollen tube growth inhibition in incompatible pollen. So far, Ca^{2+} , actin cytoskeleton and soluble inorganic pyrophosphatases (sPPases) have been found to be involved in the pollen tube growth inhibition signalling (Figure 1-10). Ca^{2+} is a well characterized second messenger, and plays a key role in a multitude of biological cellular processes (Bibikova et al., 1997; Malho et al., 1994). Involvement of Ca^{2+} in mediating intracellular signalling of poppy SI response is well established. An *S*-specific transient increase of cytosolic free calcium ($[\text{Ca}^{2+}]_i$) in the sub-apical/shank regions of the pollen tube was induced in an incompatible reaction (Figure 1-10), within a few seconds of incompatible *S*-protein challenge (Franklin-Tong et al., 1993, 1995, 1997). The role of $[\text{Ca}^{2+}]_i$ in the *Papaver* SI response was further confirmed by the observation that artificially elevated $[\text{Ca}^{2+}]_i$ resulted in the cessation of pollen tube growth (Franklin-Tong et al., 1993).

An *S*-specific and rapid F-actin depolymerisation and re-arrangement has been observed downstream of cytosolic Ca^{2+} increase in incompatible pollen in response to cognate PrsS protein treatment (Geitmann et al., 2000; Poulter et al., 2010; Snowman et al., 2002). Functioning cytoskeletal apparatus is vital to normal pollen tube growth (Cai et al., 1997). Therefore, it was proposed that the Ca^{2+} -mediated F-actin depolymerisation was an important mechanism adopted by the *Papaver* SI system to achieve pollen tip growth inhibition.

sPPases are responsible for the hydrolytic conversion of inorganic pyrophosphate (PPi) to inorganic orthophosphate (2Pi) and play an important role in biosynthesis and metabolism stability (Cooperman et al., 1992). p26-sPPases were identified in a differentiated protein phosphorylation analysis (Rudd et al., 1996). They were found to be rapidly phosphorylated after SI induction in a Ca^{2+} - and calmodulin-dependent manner (Rudd et al., 1996). It has been well established that both Ca^{2+} and phosphorylation inhibited the p26-sPPases activity (de Graaf et al., 2006; Rudd et al., 1996). In addition, it was observed that down-regulation of p26-sPPases using the as-OND resulted in a significant reduction of pollen tube length (de Graaf et al., 2006). Based on these data, a model was proposed to explain the role of p26-sPPases during the *Papaver* SI response: upon incompatible pollination, increased phosphorylation of p26-sPPases results in the inhibition of sPPases activity, and subsequent reduction in the metabolic activity thus contributing to the pollen tube growth inhibition (Bosch and Franklin-Tong, 2008; de Graaf et al., 2006).

1.4.3.2.2 Pollen PCD signalling cascade

PCD, which has been introduced in section 1.2, is an effective mechanism adopted by many organisms to remove unwanted cells in a precisely controlled manner (Raff, 1998). It has been established that PCD is involved in the *Papaver* SI response (Thomas and Franklin-Tong, 2004), revealing a novel mechanism to prevent self-fertilization.

DNA fragmentation is considered to be one of the reliable diagnostic features of PCD. It has been demonstrated that SI triggers DNA fragmentation in incompatible pollen in a Ca^{2+} -dependent and *S*-specific manner (Jordan et al., 2000). The SI-induced DNA fragmentation could be inhibited by the DEVDase inhibitor, indicating the involvement of DEVDase, which is another PCD hallmark, as an event upstream of DNA fragmentation in the *Papaver* SI response (Thomas and Franklin-Tong, 2004). The detection of an increase in DEVDase activity in SI pollen provided direct evidence that DEVDase is involved in the *Papaver* SI signalling cascade (Bosch and Franklin-Tong, 2007; Thomas and Franklin-Tong, 2004). Furthermore, pre-treatment of pollen with DEVDase inhibitor, but not other caspase inhibitors, significantly alleviated the SI-induced pollen tube growth inhibition (Thomas and Franklin-Tong, 2004). Moreover, biochemical characterization of SI-induced DEVDase activities demonstrated that it had an acidic pH optimum (Bosch and Franklin-Tong, 2007), suggesting cytosolic acidification triggered by SI for the activation of DEVDase (this will be described in more detail below). However, despite detailed characterisation (Bosch and Franklin-Tong, 2007), the identity of the DEVDase gene so far remains unknown. Taken together, PCD has been demonstrated as a novel mechanism for the irreversible inhibition and final rejection of incompatible pollen in the *Papaver* SI system (Figure 1-10).

Several cellular components, such as F-actin cytoskeleton, p56-Mitogen-activated

protein kinases (MAPKs), F-actin, and cytosolic acidification have also been identified as the targets of the *Papaver* SI response, and demonstrated to be involved in the SI-induced PCD (Figure 1-10).

A role for the cytoskeleton in regulating stimuli response and PCD has been studied extensively (Franklin-Tong and Gourlay, 2008; Nick, 1999; Staiger, 2000). As described above, SI induces rapid F-actin depolymerisation resulting in the cessation of pollen tube growth (Figure 1-10). Furthermore, evidence has also been obtained that F-actin dynamics is involved in the SI-induced PCD in incompatible pollen (Thomas et al., 2006). It has been demonstrated that drug-induced actin depolymerisation is sufficient to initiate PCD in poppy pollen mediated by a DEVDase activity (Figure 1-10). Moreover, drug-induced stabilization of F-actin significantly alleviated SI-induced PCD (Thomas et al., 2006). These demonstrate that F-actin cytoskeleton plays a crucial role in initiating PCD in incompatible pollen upon SI induction.

MAPKs have been well characterized in yeast and mammals as a signalling molecule downstream of receptor-ligand interactions (Widmann et al., 1999). Evidence implicating the involvement of protein kinases in poppy SI has also been obtained. The activation of p56-MAPK has been observed in incompatible pollen in an *S*-specific and Ca^{2+} -dependent manner (Rudd et al., 2003). Suppressed activation of p56-MAPK by MAPK cascade inhibitor resulted in a reduction in SI-induced DEVDase activity and

DNA fragmentation in incompatible pollen, and also alleviated SI-induced pollen viability decrease (Li et al., 2007). These demonstrate that p56-MAPK is involved in the initiation phase of PCD in incompatible pollen (Figure 1-10). It is proposed by Li and Franklin-Tong (2008) that “p56 signalling represents the ‘gateway’ through which incompatible pollen must pass to become irreversibly inhibited”.

A substantial decrease of cytosolic pH has been shown in SI-induced poppy pollen, which coincided well with the observation that DEVDase had highest activity in an acidic environment (Bosch and Franklin-Tong, 2007). Cytosolic acidification during the SI response was investigated. Cytosolic pH decreases could be observed as early as 5 min after SI induction, and the pH decrease lasted around 1h, resulting in the cytosolic pH drop from ~7.0 to ~5.5 (Wilkins et al., submitted). No significant pH changes were seen in untreated or compatible pollen. It has been demonstrated that Ca^{2+} increases were upstream of cytosolic acidification, and artificial acidification of poppy pollen tubes using propionic acid triggered formation of F-actin foci and induced caspase-3-like activities (Wilkins et al., submitted), demonstrating the involvement of cytosolic acidification in SI-induced PCD (Figure 1-10).

Other cellular components and signals such as microtubules, reactive oxygen species and nitric oxide have also been identified in the SI signalling network involving in the SI-induced PCD (Figure 1-10). See Poulter et al. (2008) and Wilkins et al. (2011) for

more details. Taken together, the *Papaver* SI induces a Ca^{2+} -dependent signalling network involving F-actin alteration, p56-MAPK activation, cytosolic acidification and subsequent DEVDase activation, culminating in the PCD in incompatible pollen (Figure 1-10). Thus, significant progress has been made in our understanding of the mechanisms involved in *Papaver* SI.

1.5 Transfer of SI system between different species

Self-incompatibility (SI) in flowering plants presents many intriguing opportunities and challenges for the study of plant reproductive diversity, evolution and adaptation, polymorphism population genetics, cell-to-cell recognition and interaction, and potential application in agriculture. Understanding the evolutionary, genetic and molecular mechanisms involved in SI has been an enduring source of curiosity since the discovery of the SI phenomenon by Charles Darwin. Undoubtedly, considerable knowledge on the distribution, genetics, physiological and biochemical bases of SI has been accumulated in the last century. However, it is difficult to carry out molecular genetic studies in non-model self-incompatible species. Moreover, as described in section 1.1.2, SI represents a potentially useful system for building an effective hybrid-breeding system by preventing self-pollination. To establish a self-incompatible line is the first step towards the construction of an SI-based hybrid breeding system. Therefore, much effort has been devoted to the identification of the *S*-determinants so that functional transfer of the SI system into related self-compatible species might be

made possible. There are important biological reasons why the successful interspecies SI transfer is of particular interest to biologists. Not only will it facilitate the investigation of SI molecular mechanisms by making full use of the array of the genetic tools available in model plants, but it will also help to address some of the long-standing issues that remain about the evolution of SI in flowering plants. It is also worthy of our attention that successful interspecies transfer of the SI system is of immense practical importance for agricultural biotechnology, because it has implications for solving food security issues by allowing breeding of superior F1 hybrid plants more easily and cheaply.

So far, there are no reports regarding the functional transfer of the *S*-RNase-based SI system between different species. For the Brassicaceae SI, the *SCR/SRK* gene pair isolated from self-incompatible *A. lyrata* has been demonstrated to be functional in *A. thaliana* (Nasrallah et al., 2002, 2004). However, attempts to restore SI in *A. thaliana* utilising the *Brassica* *S*-locus failed (Bi et al., 2000; Boggs et al., 2009a). In terms of the *Papaver* SI, the male *S*-determinant, PrpS, has been successfully transferred into *A. thaliana*, and demonstrated to be functional (de Graaf et al., 2012). These studies will be briefly described below.

1.5.1 Transfer of the Brassicaceae SI system between different species

It has been demonstrated that transfer of the *SRK-SCR* gene pairs derived from

out-crosser crucifer *A. lyrata* or *Capsella grandiflora* is sufficient to impart the SI phenotype in self-fertile *A. thaliana* C24 (Boggs et al., 2009a; Nasrallah et al., 2004). Aniline blue staining showed a robust pollen inhibition in the transgenic *A. thaliana* C24. Seed set analysis showed that only 54 ± 7 seeds (~10,000 seeds in a normal *A. thaliana* plant) were produced per plant. These demonstrate that *A. thaliana* C24 express a strong and developmentally stable SI upon transformation with the *S*-locus genes. However, variation in the expression of SI in different *A. thaliana* ecotypes has been observed (Nasrallah et al., 2004). Transgenic *A. thaliana* Col-0 which has been transformed with the *SCR-SRK* gene pair can set seeds normally as with untransformed plants. Aniline blue staining demonstrated that even though young flowers could recognize and inhibit self-pollen, older flowers failed to express SI and regained the capacity to accept self-pollen (Nasrallah et al., 2002). This suggests that the *A. lyrata* *S*-locus is conditionally functional in *A. thaliana*, only if it is transformed into a certain genetic background.

In addition to the *A. lyrata* and *C. grandiflora* *S*-locus, the *Brassica* *S*-locus has also been transformed into *A. thaliana* attempting to restore SI in *A. thaliana*, but this failed (Bi et al., 2000; Boggs et al., 2009a). The reason might be that the *Brassica* SRK cannot interact effectively with the SI signalling components in *A. thaliana* due to the larger evolutionary distance between *Brassica* and *Arabidopsis* (Boggs et al., 2009a). *A. thaliana* is evolutionarily diverged with *A. lyrata* and *C. grandiflora* ~5 MYA and

~6.2-9.8 MYA, respectively, while *Arabidopsis* and *Brassica* separated ~14-20 MYA (Acarcan et al., 2000; Koch et al., 2000). This indicates that the Brassicaceae SI can only be functionally transferred into evolutionarily close related species, which constrains the application of Brassicaceae SI in self-compatible Brassicaceae crops hybrid seeds breeding (see more discussion about this in Chapter 7).

The establishment of self-incompatible *A. thaliana* has already been developed as a model for the molecular mechanistic studies of the Brassicaceae SI (Indriolo et al., 2014; Kitashiba et al., 2011; Rea et al., 2010). This also has an important implication for the evolutionary analysis of the switch from SI to selfing in the crucifer family (Boggs et al., 2009b; Nasrallah et al., 2004).

1.5.2 Transfer of the *Papaver* SI system into *A. thaliana*

P. rhoeas has an evolutionary distance ~144 MYA with *A. thaliana*. It is of considerable interest to establish whether the *Papaver* SI system can be functionally transferred into *A. thaliana*, because this will provide important insights into the evolution of SI systems across the flowering plant families, and may have implications for the breeding of hybrid seeds. As a first step, the *P. rhoeas* pollen *S*-determinant, *PrpS*, was transformed into *A. thaliana*. *PrpS:GFP* could be successfully expressed in *A. thaliana* pollen directed by a pollen specific promoter, *ntp303* (de Graaf et al., 2012; Weterings et al., 1995). When the *At-PrpS:GFP* pollen was exposed to cognate recombinant PrsS protein,

S-specific pollen tube growth inhibition and death were observed. Moreover, a “*Papaver* SI-like” signalling cascade was demonstrated to be involved in the death of transgenic pollen. SI induction in *At-PrpS:GFP* pollen triggered dramatic shifts in the structure of the F-actin cytoskeleton. Pre-treatment with DEVDase inhibitor significantly alleviated the SI-induced pollen death (de Graaf et al., 2012). This demonstrates the involvement of F-actin and DEVDase, which are major hallmarks of the *Papaver* SI response, in the death of transgenic *A. thaliana* pollen. These data also provide good evidence that *PrpS* is functional in *A. thaliana* pollen, possibly by recruiting the cellular components to form a new signalling network for an SI-induced PCD response which does not normally operate in *A. thaliana* (de Graaf et al., 2012; Vatovec, 2011). The demonstration that *PrpS* is functional in *A. thaliana in vitro* marked an important step toward establishing whether the *Papaver* SI system, comprising *PrpS* and *PrsS*, can be functionally transferred into *A. thaliana in vivo*.

1.6 Project aims

The work presented here comprises two main parts: functional transfer of *Papaver* SI system into self-compatible *A. thaliana* (Chapters 3, 4 and 5), and investigating the role of Ub/proteasome system during the *Papaver* SI-induced PCD (Chapter 6). As mentioned earlier, hybrid breeding is one of the most important plant breeding technologies. SI provides an improved method for plant hybrid breeding. Here, we focus on initiating translational work to attempt to utilise the *Papaver* SI system for

hybrid breeding. As a first step, this project has focused on the functional transfer of the *Papaver* SI system into self-compatible *A. thaliana*. It has been previously demonstrated that PrpS:GFP expressed in transgenic *A. thaliana* pollen was functional in the *in vitro* SI assay. Here, we have focused on attempting to functionally transfer the *Papaver* female *S*-determinant, *PrsS*, into *A. thaliana* to establish whether it is possible to obtain an SI response in *A. thaliana in vivo*. Moreover, we also transferred both *PrpS:GFP* and *PrsS* into *A. thaliana* to establish whether the *Papaver* *S*-determinants are functional enough to generate self-incompatible *A. thaliana*.

The Ub/proteasome system has been demonstrated to play an important role in both Brassicaceae SI and *S*-RNase-based SI systems. In addition, the proteasome has also been observed to be involved in the plant PCD conferring DEVDase activities. Whether the UPS has a role in the *Papaver* SI response remains unknown. Moreover, the *Papaver* SI response triggers a DEVDase-dependent PCD in incompatible pollen, and the identity of DEVDase in the *Papaver* SI-induced PCD is still unclear. Therefore, we examined the role of UPS during the *Papaver* SI response in this study, and also investigated the relationship between proteasome and SI-induced DEVDase activity.

CHAPTER 2 MATERIALS AND METHODS

2.1 Development of an improved *Arabidopsis* pollen *in vitro* germination/growth system and functional analysis of *PrpS* in *A. thaliana in vitro* using this system

2.1.1 Plant materials: BG16 transgenic lines

In this study, *Col-0 A. thaliana* plants and BG16 transgenic lines were used. BG16 was generated by Barend de Graaf in the Franklin-Tong lab by introducing *PrpS₁:GFP* fusion gene into *A. thaliana* (Figure 2-1; de Graaf et al., 2012). The expression of *PrpS₁:GFP* in *A. thaliana* is driven by a *N. tobacco* pollen specific promoter, *ntp303* (Weterings et al., 1995). Thirty-five independent BG16 lines (BG16.[1-35]) were obtained, and only BG16.25 was functionally analysed. It has been demonstrated by Sabina Vatovec that the T₃ plant BG16.25.1.1 was homozygous (Vatovec, 2011). Therefore, seeds derived from plant BG16.25.1.1 were used in this study to grow *PrpS₁:GFP* homozygous plants.

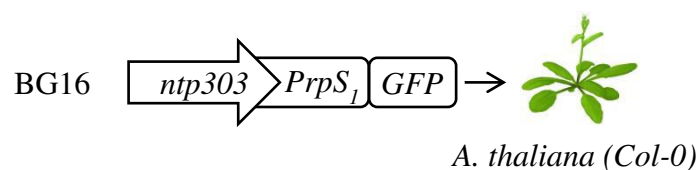


Figure 2-1 Cartoon of BG16 transgenic line

Vectors containing *ntp303::PrpS₁:GFP* were transformed into *Col-0 A. thaliana*. The resulting transgenic line was named BG16.

2.1.2 *A. thaliana* pollen *in vitro* germination assay

Arabidopsis pollen *in vitro* germination assays were carried out based on the protocol

published by Boavida and McCormick (Boavida and McCormick, 2007). Individual salt stock solutions (1% (w/v) H_3BO_3 ; 0.5 M KCl; 0.1 M $MgSO_4$; 0.5 M $CaCl_2$) were made before preparation of *A. thaliana* germination medium (*AtGM*). It is worthy to note that, unlike poppy GM, it is not applicable to make a concentrated *AtGM* stock solution by mixing different components of *AtGM* together, which would result in precipitation when stored in the cold room. *AtGM* was prepared according to the recipe shown in Table 2-1.

Table 2-1 Recipe for *AtGM*

<i>AtGM</i>
<hr/>
<i>0.01% (w/v) H_3BO_3</i>
<i>5 mM KCl</i>
<i>1 mM $MgSO_4$</i>
<i>5 mM $CaCl_2$</i>
<i>10% (w/v) Sucrose</i>
<i>pH adjusted to 7.5 using 1M NaOH</i>

AtGM was filter sterilized (Pall Corporation, 0.2 μm) and kept in the cold room. This could last for 1 week. Solidified *AtGM* was always freshly prepared before use by dissolving 1% (w/v) ultrapure agarose (Invitrogen) in liquid *AtGM*. Ultra low melting temperature agarose from Sigma (PCode: 1001494829) were also tried and it did not work as well as Invitrogen's ultrapure agarose. Agarose was dissolved using microwave, and to compensate for the loss of H_2O caused by the evaporation during microwave

heating process, MilliQ water was always added post-heating. Flasks were labelled before microwave heating so that how much MilliQ water was needed after heating could be known. Boiled *AtGM* was poured into tissue culture dish (35mm, Becton Dickinson Labware), and it was ready for use after solidified.

A. thaliana flowers were always collected at stage 14 (Smyth et al., 1990). For each individual *in vitro* pollen germination experiment, one flower, which was able to supply enough pollen for this, was used. Pollen was spread on the surface of the agarose by inverting the flower using forceps under dissecting microscope. Pollen was incubated at 22 °C with a tissue culture plate lid on to keep a moist germination environment. The pollen germination and pollen tube growth were visualised using light microscopy. Pollen tube lengths were measured using Nikon Element Software.

2.1.3 *A. thaliana* pollen SI assays *in vitro*

For the *Arabidopsis* pollen *in vitro* SI assay, recombinant PrsS protein was dialysed against *AtGM* overnight, and the concentration was determined using Bradford assay (Bio-Rad). *AtGM* with 1.5% agarose was prepared (the final concentration of agarose was 1% after addition of recombinant PrsS proteins). After the boiled *AtGM* had cooled, but before it had completely solidified (approximately 3 min), recombinant PrsS protein was mixed with *AtGM* quickly and poured into tissue culture dish. Pollen was collected, spread on the surface of solidified *AtGM*, and cultured as described above for *in vitro*

pollen germination.

2.1.4 Screening of improved BG16 lines

Seeds derived from different BG16 lines were sterilized and sowed on Murashige and Skoog (MS) plates containing 20 $\mu\text{g mL}^{-1}$ kanamycin (Kan) as described in Vatovec (2011). Surviving seedlings were transplanted into soil pots in the greenhouse. Pollen derived from these plants was checked for PrpS₁:GFP expression using GFP fluorescence microscopy. Only those plants who were demonstrated to be *PrpS₁:GFP* homozygous were further analysed. See table 2-2 for the detail information.

Table 2-2 Screening of improved BG16 lines

<i>Seeds</i>	<i>No. of surviving seedlings/ No. of seeds sowed</i>	<i>No. of homozygous obtained</i>
<i>T₁: BG16.1</i>	<i>6/75</i>	<i>2</i>
<i>T₂: BG16.3.6</i>	<i>10/75</i>	<i>2</i>
<i>T₁: BG16.4</i>	<i>3/75</i>	<i>1</i>
<i>T₂: BG16.6.1</i>	<i>4/75</i>	<i>2</i>
<i>T₂: BG16.7.2</i>	<i>6/75</i>	<i>0</i>
<i>T₂: BG16.8.3</i>	<i>5/75</i>	<i>5</i>
<i>T₁: BG16.10</i>	<i>1/75</i>	<i>0</i>
<i>T₁: BG16.12</i>	<i>7/75</i>	<i>5</i>

2.1.5 Construction of *At-ntp303::PrpS* transgenic lines

At-ntp303::PrpS transgenic lines were generated by transform *Col-0 A. thaliana* with tumor inducing (Ti) vectors pORE O3-*ntp303::PrpS* based on the protocols published

by Davis et al. (2009) and Zhang et al. (2006). The procedure of pORE O3-*ntp303::PrpS* vectors construction is shown in Figure 2-2.

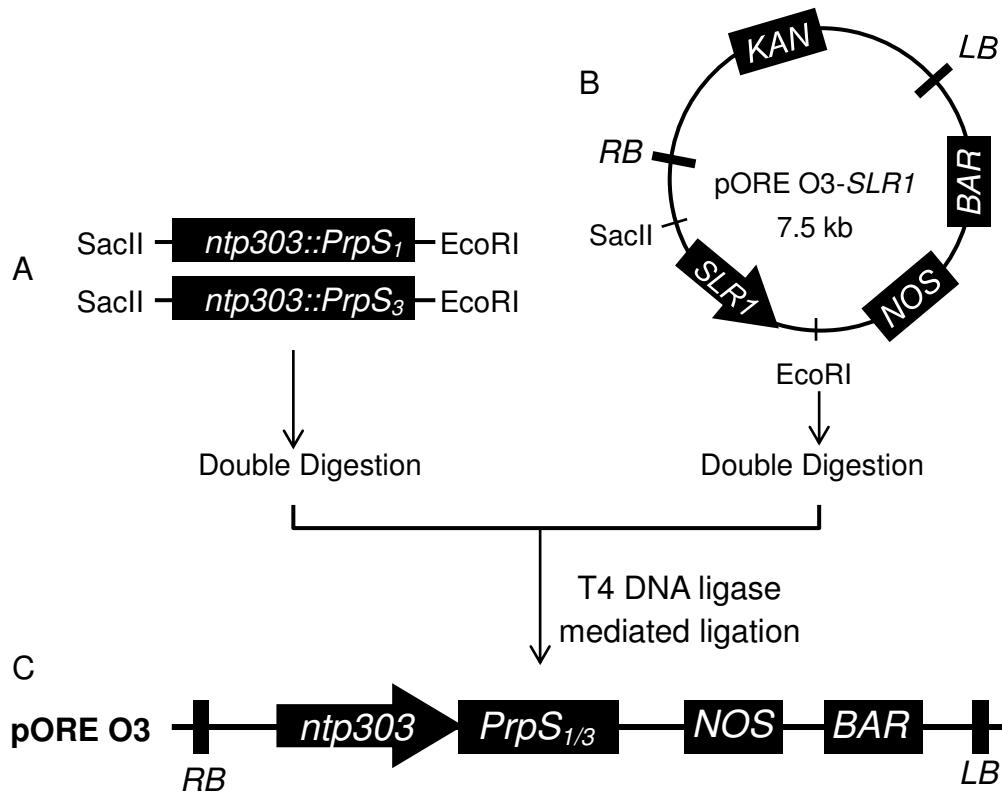


Figure 2-2 Construction of pORE O3-*ntp303::PrpS*

pORE O3-*ntp303::PrpS* vectors were constructed through T4 DNA ligase mediated ligation. A: DNA fragments *ntp303::PrpS* were amplified, purified and double digested using restriction enzymes SacII and EcoRI. B: binary vectors pORE O3 were double digested using restriction enzymes SacII and EcoRI. C: integration of *ntp303::PrpS* into pORE O3 through T4 DNA ligase mediated ligation.

Target DNA fragments (*ntp303::PrpS₁* and *ntp303::PrsS₃*) were amplified using template vectors pGreen0029-*ntp303::PrpS_{1/3}:GFP* (de Graaf et al., 2012) and primers with SacII and EcoRI restriction sites flanked in the 5' and 3' ends respectively (Table 2-3; Figure 2-2-A).

Table 2-3 Primers for the construction of pGreen0029-ntp303::PrpS vectors

<i>DNA fragment</i>	<i>Primer name</i>	<i>Sequence (5'-3')</i>
<i>ntp303::PrpS₁</i>	<i>F-SacII-ntp303</i>	aaaaaaaa ccg cgggatacactcgcaacg
	<i>R-EcoRI-PrpS₁</i>	cgg aat cttaagcttgagtataagatgagg
<i>ntp303::PrpS₃</i>	<i>F-SacII-ntp303</i>	aaaaaaaa ccg cgggatacactcgcaacg
	<i>R-EcoRI-PrpS₃</i>	cgg aat ctcaagcctcattaggacatg

PCR products were purified using Gel Purification kit (QIAGEN) according to the manufacturer's instruction and double digested using restriction enzymes SacII and EcoRI in 37 °C incubator overnight.

pORE is a series of binary vectors suitable for *Agrobacterium*-mediated transformation of both monocot and dicot plants. pORE O3, which belongs to the Open Series, is a 6.3 kb plasmid with multiple cloning sites suitable for general plant transformation (Coutu et al., 2007). pORE O3 vector containing *SLR1* promoter within the multiple cloning sites was nicely provided by Prof. Daphne Goring's group in Toronto University. In order to obtain a reasonable amount of vectors, vectors were transformed into *E. coli* DH5 α cells, and single colony was picked and cultured in liquid LB containing Kan (50 $\mu\text{g mL}^{-1}$), followed by plasmids extraction using PureYield™ Plasmid Miniprep System (Promega). pORE O3-SLR1 vectors were linearized through double digestion using SacII and EcoRI (Figure 2-2-B). Double digestion reaction systems were set as shown in Table 2-4.

Table 2-4 Double digestion reaction system

Double digestion mix

2 μg DNA

5 μL 10× CutSmart Buffer (NEB)

2 μL EcoRI (NEB)

2 μL SacII (NEB)

Water make up to 50 μL

Double digestions were checked by DNA gel electrophoresis and target bands were cut and purified using Gel Purification kit (QIAGEN), followed by concentration determination using Nanodrop (Thermo). Target DNA fragments were cloned into linearized pORE O3 vectors through T4 DNA ligase mediated ligation (Figure 2-2-C). Ligation mixtures (Table 2-5) were incubated 1 h at 22 °C before proceeding to *E. coli* transformation. Sequencing was performed using both *F-SacII-ntp303* and *R-EcoRI-PrpS* (Table 2-3) primers to ensure that there is no mutation in the target DNA fragment.

Table 2-5 T4 DNA ligase-mediated ligation system

Ligation mix

100 ng Purified linear pORE O3 vectors DNA

50 ng Purified ntp303::PrpS DNA fragment

2 μL 10× T4 DNA Ligase Buffer

1 μL T4 DNA ligase

Water to make 20 μL

2.2 Constitutive expression and functional analysis of *PrsS* in *A. thaliana* using an *in vitro* SI assay

2.2.1 Construction of *At-35S::PrsS* transgenic lines

At-35S::PrsS transgenic lines were generated by transform *Col-0 A. thaliana* with Ti vectors pEG205-35S::*PrsS* based on the protocols published by Davis et al. (2009) and Zhang et al. (2006). The procedure of pEG205-35S::*PrsS* vectors construction is shown in Figure 2-3. *PrsS* was cloned into binary Ti vector pEG205 using the Gateway Cloning Technology (www.lifetechnologies.com/support). *PrsS* was amplified and cloned into the entry vector pENTRTM/D-TOPO (Invitrogen; pENTR) mediated by topoisomerase, and then cloned into destination Ti vector pEG205 through LR clonase mediated recombination (Figure 2-3).

pENTR is a 2.6 kb plasmid with a TOPO recognition site for capturing of PCR product of interest. CACC was added on the 5' end of the forward primer for directional cloning (see Table 2-6 for the primers information). *PrsS* was amplified using poppy genome DNA as the template and purified using gel purification kit (QIAGEN). Purified PCR product was cloned into the pENTR vector according to the manufacturer's instruction (Figure 2-3-B). Sequencing was carried out to confirm that there were no mutations generated during the cloning procedure.

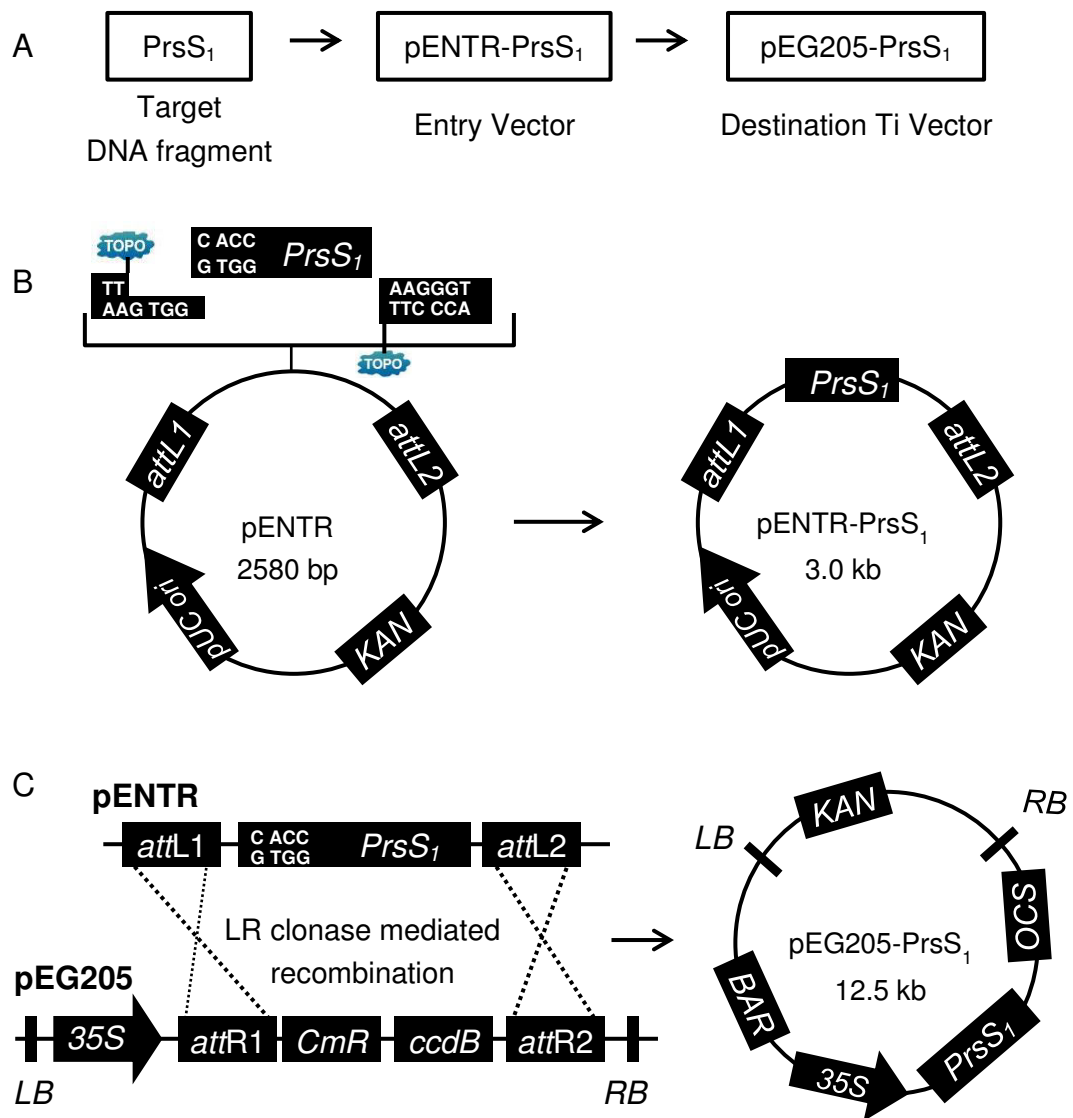


Figure 2-3 Construction of binary Ti vectors pEG205-35S::PrsS

A: flowchart of the Ti vectors pEG205-35S::PrsS construction. B: cloning of *PrsS* into pENTR mediated by topoisomerase. C: *PrsS* was cloned into destination Ti vector pEG205 following LR clonase mediated recombination between the corresponding recombination sites on pENTR and pEG205. *attL1/2* and *attR1/2*: gateway specific recombination sites from entry vector and destination vector, respectively. *KAN*: kanamycin resistance gene. pUC ori: origin of replication. *LB* and *RB*: the left border and right border of T-DNA. *BAR*: the BASTA herbicide resistance gene for selection of transgenic plants. *35S*: the cauliflower mosaic virus 35S promoter. *CmR*: chloramphenicol resistance gene. *ccdB*: control of cell death gene B, which is a killer gene to the bacterial. *OCS*: the 3' sequence of the octopine synthase gene, including polyadenylation and presumptive transcription termination sequences.

Table 2-6 Primers for the construction of pENTR-PrsS vectors

<i>Vectors</i>	<i>Primer name</i>	<i>Sequence (5'-3')</i>
<i>pENTR-PrsS₁</i>	<i>F-cacc-PrsS₁</i>	<i>cacc</i> atgaacatatatttatgttattgtgctgctatgg
	<i>R-PrsS₁</i>	<i>tcagg</i> ttcgaccttccttcctttctttctttatc
<i>pENTR-PrsS₃</i>	<i>F-cacc-PrsS₃</i>	<i>cacc</i> atgaagatattgtgcgttattgtgcttc
	<i>R-PrsS₃</i>	<i>tcagact</i> tccttctcaccattcctggtaaac

pEG205 is a gateway-compatible destination binary Ti vector. It contains the 35S promoter and is designed to constitutively express transgene in plant biology research (Earley et al., 2006). PrsS was captured into pEG205 from pENTR through LR clonase mediated recombination according to the manufacturer's instruction. Table 2-7 details the information related to the pEG205-35S::*PrsS* vectors. Sequencing was performed using both *F-cacc-PrsS* and *R-PrsS* primers (Table 2-6) to ensure that there was no mutation in the target DNA fragment.

Table 2-7 Vectors constructed for constitutively expressing *PrsS* in *A. thaliana*

<i>Vector</i>	<i>DNA fragment inserted</i>	<i>Resulting DNA chimera</i>	<i>Resistance</i>
<i>pEG205-35S::<i>PrsS</i>₁</i>	<i>PrsS₁</i>	<i>35S::<i>PrsS</i>₁</i>	<i>Kan (Baterial)/BASTA (Plant)</i>
<i>pEG205-35S::<i>PrsS</i>₃</i>	<i>PrsS₃</i>	<i>35S::<i>PrsS</i>₃</i>	<i>Kan (Baterial)/BASTA (Plant)</i>

2.2.2 Construction of *At-35S::*PrsS*:GFP* transgenic lines

*At-35S::*PrsS*:GFP* transgenic lines were generated by transformation of *Col-0 A. thaliana* with Ti vectors pEG103-35S::*PrsS*:GFP based on the protocols published by Davis et al. (2009) and Zhang et al. (2006). An outline of the procedure of

pEG103-35S::*PrsS*:*GFP* vector construction is shown in Figure 2-4.

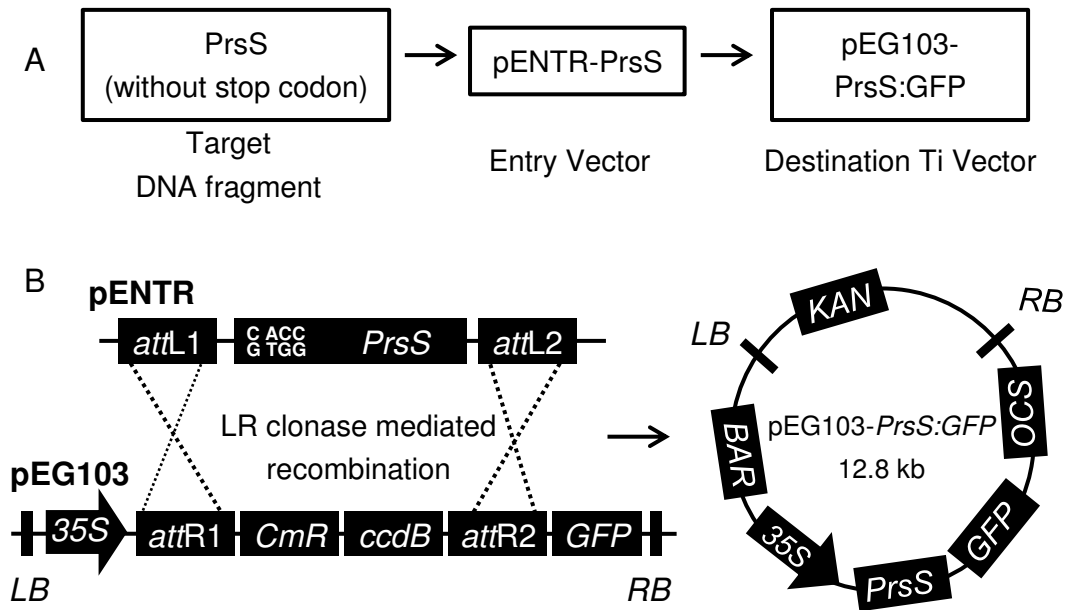


Figure 2-4 Construction of binary Ti vectors pEG103-35S::*PrsS*:*GFP*

A: flowchart of the Ti vectors pEG103-35S::*PrsS*:*GFP* construction. B: *PrsS* (without stop codon) was cloned into destination Ti vector pEG103 following LR clonase mediated recombination.

PrsS (without stop condon) was amplified and cloned into the entry vector pENTR as described previously (section 2.2.1; see Table 2-8 for the primers details), and then cloned into destination Ti vector pEG103 through LR clonase mediated recombination (Figure 2-4-A). pEG103 is also a Gateway-compatible destination binary Ti vector, which contains the 35S promoter and is designed to constitutively expressed transgene in plant biology research (Earley et al., 2006). In addition, pEG103 translationally fuses GFP that allows the affinity purification, immunolocalization or immunoprecipitation of recombinant proteins expressed *in vivo* (Earley et al., 2006). *PrsS* was captured into

pEG103 without stop codon so that GFP could be translationally fused to the C-terminus of PrsS when expressed in the transgenic plants (Figure 2-4-B). Table 2-9 details the information related to the pEG103-35S::*PrsS*:*GFP* vectors. Sequencing was performed using both *F-cacc-PrsS* and *R-NS-PrsS* primers (Table 2-8) to ensure that there was no mutation in the target DNA fragment.

Table 2-8 Primers for the construction of pENTR-*PrsS*(NS) vectors

<i>Vectors</i>	<i>Primer name</i>	<i>Sequence (5'-3')</i>
<i>pENTR-PrsS₁</i>	<i>F-cacc-PrsS₁</i>	<i>cacc</i> atgaacatattttatgttattgtgctgctatgg
(without stop codon)	<i>R-NS-PrpS₁</i>	ggttcgaccttccttcctttctttctttatc
<i>pENTR-PrsS₃</i>	<i>F-cacc-PrsS₃</i>	<i>cacc</i> atgaagatattgtgcgttattgtgcttc
(without stop codon)	<i>R-NS-PrpS₃</i>	gacttcctctcaccattcctggtaaac

Table 2-9 Vectors constructed for constitutively expressing *PrsS*:*GFP* in *A. thaliana*

<i>Vector</i>	<i>DNA fragment inserted</i>	<i>Resulting DNA chimera</i>	<i>Resistance</i>
<i>pEG103-35S::<i>PrsS₁</i>:<i>GFP</i></i>	<i>PrsS₁</i> (no stop codon)	35S:: <i>PrsS₁</i> : <i>GFP</i>	<i>Kan</i> (Baterial)/ <i>BASTA</i> (Plant)
<i>pEG103-35S::<i>PrsS₃</i>:<i>GFP</i></i>	<i>PrsS₃</i> (no stop codon)	35S:: <i>PrsS₃</i> : <i>GFP</i>	<i>Kan</i> (Baterial)/ <i>BASTA</i> (Plant)

2.2.3 Screening of transgenic seeds

T₀ *A. thaliana* transgenic seeds were sterilized and sowed on Murashige and Skoog (MS) plates containing BASTA (20 µg mL⁻¹) as described in Vatovec (2011). Plates with seeds were incubated at 4 °C for two days to vernalize before germination at 22 °C room. Surviving seedlings were transplanted to the soil pots in the greenhouse (20-22 °C, under 16/8 h photoperiod condition) two weeks later.

To further confirm the integration of *PrsS* in the *A. thaliana* genome, PCR genotyping was carried out. To extract DNA, leaf samples from transgenic plants were collected and 50 μ L extraction buffer (0.1 M Tris-HCl pH 9.5; 0.25 M KCl; 0.01 M EDTA) was added. The leaf disk was ground with a sterile yellow pipette tip until the solution turned green followed by incubation at 95 °C for 10 min and cooled on ice for 2 min. 50 μ L dilution buffer [3% (w/v) BSA] was added and the mixtures were vortexed vigorously and centrifuged at 13200 rpm for 1 min. Supernatants were collected and subjected to PCR analysis using ReddyMix PCR Master Mix (Thermo) according to manufacturer's instruction. For each PCR analysis, 1 μ L of DNA extraction was used as the template in a 25 μ L PCR reaction system.

Plants which were demonstrated to be transgenic were protected by plant sleeves to stop the pollen spreading when flowering. When plants were completely dry around 6 weeks after flowering, seeds were collected and stored at the 16 °C room.

2.2.4 Analysis of *PrsS* mRNA expression in *A. thaliana* transgenic lines

The expression of *PrsS* mRNA in *A. thaliana* transgenic lines was checked on the T₂ transgenic seedlings. T₁ seeds were screened on MS plates as described in section 2.2.3 and two-week-old surviving T₂ seedlings were collected and subjected to RNA extraction. Total RNA was extracted according to the protocol provided by RNeasy Mini Kit (Qiagen). RNA was checked using agarose gel electrophoresis with a

RNase-free electrophoresis tank. 1% (w/v) agarose gel was prepared using DEPC treated TBE buffer (45 mM H₃BO₃; 45 mM Tris, 1.25 mM EDTA). 4 µL RNA sample was mixed with 8 µL RNA loading buffer (Sigma), denatured at 65 °C for 10 min and chilled in ice before loading into the agarose gel. RNA concentrations were determined using NanoDrop (ND-1000, Labtech).

The *PrsS* mRNA expression level was analysed using One-step RT-PCR kit (Qiagen). *Glyceraldehyde-3-phosphate dehydrogenase C (GAPC)* was chosen as the internal reference. One-step RT-PCR reaction system and primers details are shown in Table 2-10, Table 2-11 and Table 2-12.

RT-PCR results were analysed using agarose gel electrophoresis and gels were scanned using Gel DocTM XR Imaging System (Bio-Rad). The Quantity One software was used for the analysis of band intensities.

Table 2-10 One-step RT-PCR reaction system

One-step RT-PCR mix

100 ng RNA

10 µL 5× buffer

2 µL dNTP (400 µM of each dNTP)

3 µL forward primer (10 mM)

3 µL reverse primer (10 mM)

2 µL enzyme mix

RNase-free water make up to 50 µL

Table 2-11 One-step RT-PCR setting

<i>One-step RT-PCR setting</i>		
Step 1: 50 °C	30 min	
Step 2: 95 °C	15 min	
Step 3: 94 °C	45 s	
Step 4: 57 °C	45 s	
Step 5: 72 °C	1 min	Go to step 3 27 cycles
Step 6: 72 °C	10 min	

Table 2-12 Primers for detection of *PrsS* mRNA transcripts

<i>Genes</i>	<i>Primer name</i>	<i>Sequence (5'-3')</i>
<i>PrsS₁</i>	<i>RT-PCR-PrsS₁-F</i>	<i>ggagcattggcatccattgccg</i>
	<i>RT-PCR-PrsS₁-R</i>	<i>ccattatcttccagaggcactggg</i>
<i>PrsS₃</i>	<i>RT-PCR-PrsS₃-F</i>	<i>cgatccactgccaatcagaagacg</i>
	<i>RT-PCR-PrsS₃-R</i>	<i>tggagcaccttccgccgtcg</i>
<i>GAPC</i>	<i>GAPC-F</i>	<i>cactgacaaagacaaggctgcagc</i>
	<i>GAPC-R</i>	<i>cctgttgcgccaacgaagtcag</i>

2.2.5 Analysis of constitutively expressed *PrsS* protein expression in *A. thaliana* transgenic lines

2.2.5.1 MG132 treatment of transgenic seedlings

T₁ transgenic seeds of line A31 (*At-35S::PrsS₁:GFP*) were sowed on selective MS plate containing BASTA (20 µg mL⁻¹). MS plate was incubated at 22 °C for 5 day to allow the seeds to germinate. Surviving and healthy seedlings were transferred onto another MS plate containing MG132 (50 µM) in a sterile fume cupboard. DMSO was used as

the controls. Seedlings were subjected to microscopic visualisation or western blot analysis 24 h after MG132 treatment.

2.2.5.2 Detection of constitutively expressed PrsS₁:GFP using western blot

Line A31 seedling samples were collected. Root and leaf tissues were separated using forceps. Root tissue protein and leaf tissue protein were extracted separately. Proteins were extracted by grinding liquid nitrogen frozen-tissue samples in protein extraction buffers (50 mM Tris-HCl, pH=7.5; 100 mM NaCl; 5 mM DTT; 2 mM EDTA) using blue pestle. Rough lysates were centrifuged at 13,200 rpm at 4 °C for 20 min. Supernatants were subjected to protein concentration analysis using the Bradford assays (Bio-Rad) and the following western blot analysis.

SDS-polyacrylamide gel (12.5%) was prepared according to the Bio-Rad self-assembly kits protocol. 20 µg protein from leaf tissue and 10 µg protein from root tissue were subjected to SDS-PAGE analysis. Two identical SDS-PAGEs were prepared, one for coomassie blue staining and the other one for western blot. Western blot was carried out as described in Vatovec (2011) using enhanced chemiluminescence (ECL) detection kit (Amersham). Antibody details are shown in Table 2-13.

Table 2-13 Antibody probing details for the detection of PrsS₁:GFP

<i>Antibody probing</i>	
<hr/>	
<i>Detection of PrsS₁:GFP</i>	<i>1st: anti-GFP (B-2 monoclonal, Santa Cruz Biotechnology), 1:250</i>
	<i>2nd: anti-Mouse-HRP, 1:1000</i>

2.2.5.3 Analysis of PrsS₁:GFP using GFP fluorescence microscopy

Seedling root tissues were collected and transferred to a microscopic slide using forceps. Samples were visualised using Nikon TE300 microscopy with GFP setting (excitation 395 nm/emission 475 nm). In order to compare the strength of GFP signals between Col-0 and transgenic samples, microscopic visualisation settings were kept the same for all the samples (objective lens: 10×; analog gain: 4×; exposure time: 500 ms).

2.2.6 *In vitro* SI assay using transgenic seedling extracts

Two-week-old transgenic seedling (line A31: *At-35S::PrsS₁:GFP*) samples were collected in a 1.5 ml microtube and snap frozen using liquid nitrogen. Samples were roughly ground using disposable mini-pestle. Pre-chilled poppy GM was added to the ground seedling samples and kept on ice for 20 min, followed by centrifugation at 13,200 rpm at 4 °C for 20 min. Protein concentration in the supernatants was determined using the Bradford assay.

Solidified *At*GM was prepared as described in section 2.1.3. Two pieces of Whatman filter papers (5 mm × 20 mm) were placed parallel (5 mm apart from each other) on the solidified *At*GM plate. Seedling extracts were loaded to the filter papers, the same amount for each of the filter paper. *At*GM plates were air dried in a laminar flow cabinet (~15 min). Subsequently, pollen was sowed between the two pieces of filter papers and incubated under optimized conditions as described in section 2.1.3.

2.2.7 PrsS:GFP protein enrichment using ammonium sulphate precipitation

Line A31 (*At-35S::PrsS₁:GFP*) seeding extracts were obtained as described in section 2.2.6. (NH₄)₂SO₄ precipitation was started with 500 μL protein extracts (1μg μL⁻¹). Fractionates with different (NH₄)₂SO₄ saturation were achieved by adding saturated (NH₄)₂SO₄ solution to the protein extracts according to Table 2-14.

Table 2-14 Ammonium sulphate precipitation

<i>(NH₄)₂SO₄</i> <i>Saturation</i>	0%	20%	30%	40%	50%	60%	70%
<i>Total Volume (μL)</i>	500	625	714	833	1000	1250	1667
<i>Saturated (NH₄)₂SO₄</i> <i>added (μL)</i>	0	125	89	119	167	250	417

After saturated (NH₄)₂SO₄ solution was added to the extracts, samples were incubated on ice for 20 min before centrifugation (13,200 rpm, 4 °C, 20 min). Supernatants were taken for the next precipitation. Fractionates were obtained by dissolving the pellets using poppy pollen GM.

2.3 Functional analysis of *PrpS* and *PrsS* in *A. thaliana* *in vivo* and generation of self-incompatible *A. thaliana* by transfer of *Papaver* SI system

2.3.1 Construction of *At-SLRI::GFP*, *At-SLRI::PrsS* and *At-SLRI::PrsS:GFP* transgenic lines

At-SLRI::GFP, *At-SLRI::PrsS* and *At-SLRI::PrsS:GFP* transgenic lines were generated

by transform *Col-0 A. thaliana* with corresponding Ti vectors based on the protocols published by Davis et al. (2009) and Zhang et al. (2006). The procedure of pORE O3-*SLR1::GFP*, pORE O3-*SLR1::PrsS* and pORE O3-*SLR1::PrsS::GFP* vectors construction is shown in Figure 2-5.

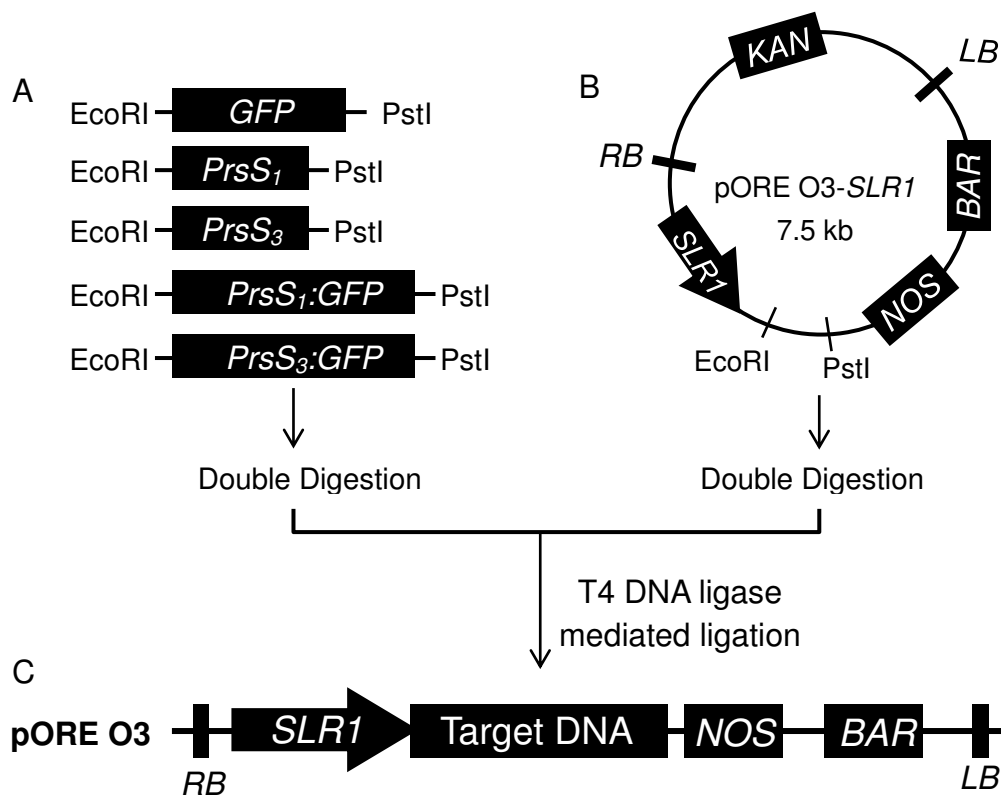


Figure 2-5 Cloning of target DNA fragments into binary Ti vector pORE O3

Ti vectors containing target DNA fragments were constructed through T4 DNA ligase mediated ligation. A: target DNA fragments (*GFP* or *PrsS₁*, *PrsS₃*, *PrsS₁:GFP*, *PrsS₃:GFP*) were PCR amplified with EcoRI and PstI restriction sites flanked in the 5' and 3' ends respectively. B: binary vectors pORE O3 were double digested using restriction enzymes EcoRI and PstI. C: integration of target DNA fragments into pORE O3 through T4 DNA ligase mediated ligation.

Target DNA fragments (*GFP* or *PrsS₁*, *PrsS₃*, *PrsS₁:GFP*, *PrsS₃:GFP*) were amplified from template vectors pEG103-35S::*PrsS_{1/3}:GFP* with primers shown in Table 2-15

(Figure 2-5-A).

Table 2-15 Primers for the construction of pEG103-35S::*PrsS*:*GFP* vectors

<i>DNA fragment</i>	<i>Primer name</i>	<i>Sequence (5'-3')</i>
<i>GFP</i>	<i>F-EcoRI-GFP</i>	<i>cggaattc</i> atggtagatctgactagtaaag
	<i>R-PstI-GFP</i>	<i>aactgcagt</i> cacacgtggtggtg
<i>PrsS₁</i>	<i>F-EcoRI-PrsS₁</i>	<i>cggaattc</i> atgaacatattttatattattgtgctg
	<i>R-PstI-PrsS₁</i>	<i>aactgcagt</i> caggttcgaccttc
<i>PrsS₃</i>	<i>F-EcoRI-PrsS₃</i>	<i>cggaattc</i> atgaagatattgtgcgttattg
	<i>R-PstI-PrsS₃</i>	<i>aactgcagt</i> cagacttcctctcac
<i>PrsS₁:GFP</i>	<i>F-EcoRI-PrsS₁</i>	<i>cggaattc</i> atgaacatattttatattattgtgctg
	<i>R-PstI-GFP</i>	<i>aactgcagt</i> cacacgtggtggtg
<i>PrpS₃:GFP</i>	<i>F-EcoRI-PrsS₃</i>	<i>cggaattc</i> atgaagatattgtgcgttattg
	<i>R-PstI-GFP</i>	<i>aactgcagt</i> cacacgtggtggtg

PCR products were purified using Gel Purification kit (QIAGEN) according to the manufacturer's instruction and double digested using restriction enzymes EcoRI and PstI in 37 °C overnight. pORE O3-SLR1 vectors were linearized by EcoRI and PstI enzymes (Figure 2-5-B). Target DNA fragments were ligated into linearized pORE O3 vectors through T4 DNA ligase mediated ligation (Figure 2-5-C) followed by *E. coli* (DH 5 α) transformation. Sequencing was performed using corresponding forward and reverse primers (Table 2-15) to ensure that there was no mutation in the target DNA fragment.

2.3.2 Analysis of *SLRI* promoter expression pattern using GFP fluorescence microscopy

The *SLRI* promoter expression pattern in *A. thaliana* was analysed in *At-SLRI::GFP* transgenic lines using GFP fluorescence microscopy (Nikon TE300; excitation 395 nm/emission 475 nm). All 22 T₁ independent *At-SLRI::GFP* transformants were analysed. Pistils from staged flowers were collected, placed on a slide and visualised without cover slide. Col-0 pistil controls were also visualised. Microscopic visualisation settings were identical for all samples (objective lens: 4×; analog gain: 4×; exposure time: 500 ms).

2.3.3 Analysis of *SLRI* promoter expression pattern using RT-PCR

Line *At-SLRI::GFP.19* exhibited the strongest GFP expression using GFP fluorescence microscopy. Therefore, this line was chosen for RT-PCR analysis. Staged pistils (10 in each independent experiment) were collected and total RNA was extracted using RNeasy Mini Kit (Qiagen). The *GFP* mRNA expression was analysed using One-step RT-PCR kit (Qiagen) as described in section 2.2.4.

2.3.4 Semi-*in-vivo* pollination assay

Pollen-free pistils were collected using forceps with very fine points between 8:00-12:00 am. The developmental stage of stigma was dependent on the requirements of the experiments. Pollen-free pistils were collected at the stage 13 (Figure 2-6), when

stigmas were receptive but before the pollen grains were mature. At the same time, mature pollen (stage 14) was also collected.

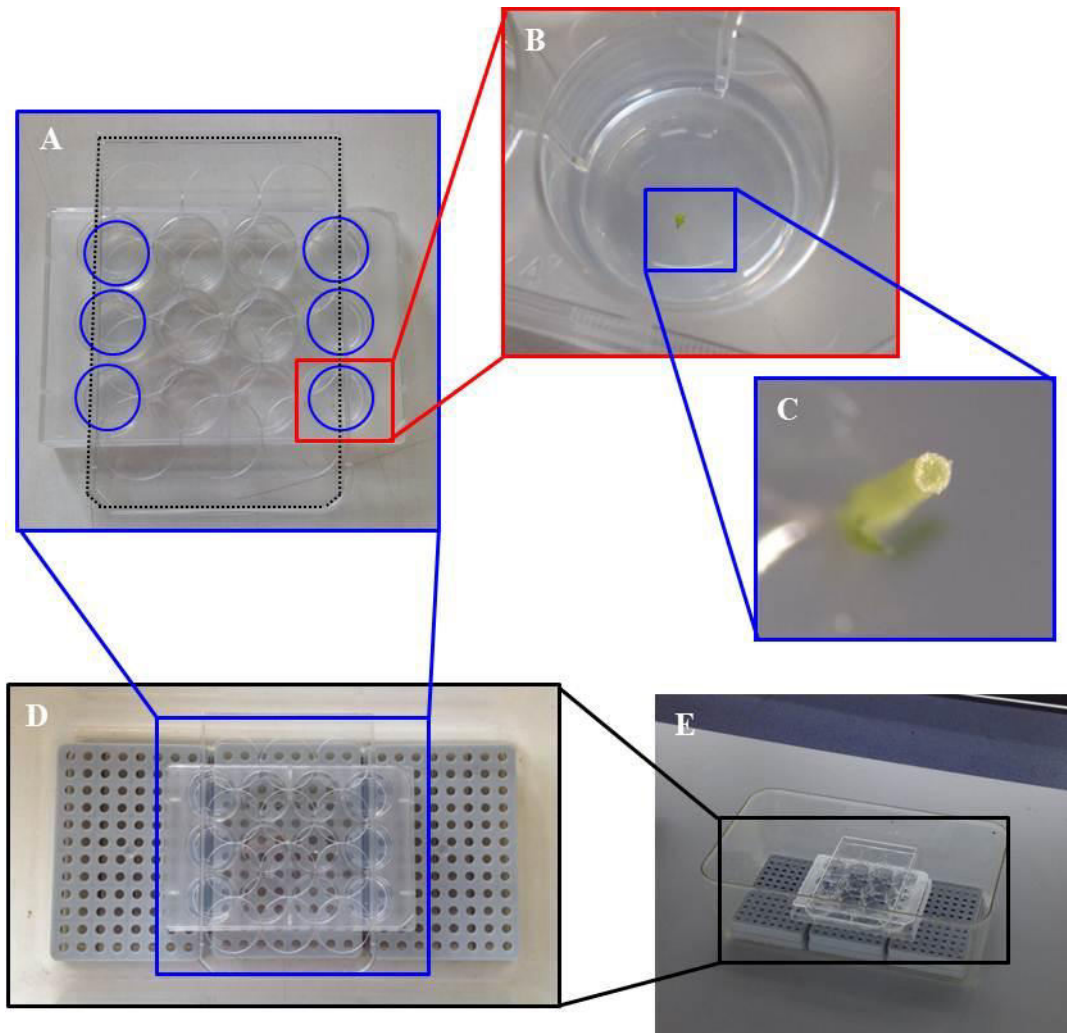


Figure 2-6 *Semi-in-vivo* pollination settings

12-well tissue culture plate was used for *semi-in-vivo* pollination. A: 1% agarose was poured into the side wells, indicated by the blue circles. Only those 6 well positions were used. The lid is indicated by the black dotted lines. B and C: a pistil was emasculated and placed vertically in the well with the stalk part inserted into the 1% agarose. D and E: plate was placed in a sandwich box (height: 10 cm) to avoid strong air flow from the conditioner, and incubated in the constant degree room (22 °C).

Before pollination assay, 1% agarose was prepared and poured into a 12-well tissue

culture plate (Figure 2-6-A). Pistils were excised from the flower with the stalk and emasculated under a dissecting scope. Emasculated pistils were placed vertically on the well of the tissue culture plate with the stalk part inserting into the 1% agarose (Figure 2-6 B and C). Pollinations were carried out immediately after emasculation using freshly collected pollen. Tissue culture plates were covered with its lid rotated at 90° angle (Figure 2-6-A; this was important because covering the plates completely with the lid resulted in abnormal pollen tube growth presumably due to excess humidity), placed in a sandwich box (height: 10 cm) to avoid strong air flow from the conditioner, and allowed for incubation at 22-25 °C (Figure 2-3 D and E). It was also important that plate should not be exposed under direct light, as this resulted in antigravity pollen tube growth. The length of incubation time was dependent on the experiments. 4N NaOH solution was added to the well directly to fix and soften the pistils overnight. Pistils were washed for 5 min with MilliQ H₂O twice, before aniline blue staining [0.01% (w/v) aniline blue in KPO₄ buffer, pH=7.5; 5% (v/v) glycerol].

Pistil samples were ready for UV fluorescent microscopy checking 12 h after staining (Nikon TE300; excitation 360 nm/emission 460 nm). The sample was carefully taken out from the tissue culture plate, placed on a slide, and a drop of 65% (v/v) glycerol was added to the pistil sample to protect it from damage. The sample was gently covered with a coverslip. As the sample was very soft, squashing with gentle thumb pressure was not necessary.

2.3.5 Analysis of the *PrsS₁* mRNA expression in *At-SLR1::PrsS₁* transgenic lines

Ten independent T₁ *At-SLR1::PrsS₁* transgenic lines were subjected to *PrsS₁* mRNA expression analysis. Pistils (stage 13) were collected and total RNA was purified using the RNeasy Mini Kit (Qiagen). RNA concentration was determined using NanoDrop (Thermo). 100 ng of RNA was subjected to cDNA synthesis in a 20 µl reaction system using SuperScript II Reverse Transcriptase (Invitrogen) according to manufacturer's instructions. The expression of *PrsS₁* mRNA was analysed using PCR (ReddyMix PCR Master Mix; Thermo) with 1 µl cDNA as the template in a 25 µl PCR system. See Table 2-16 for primer details.

Table 2-16 Primers for the detection of *PrsS₁* mRNA transcript

<i>DNA fragment</i>	<i>Primer name</i>	<i>Sequence (5'-3')</i>
<i>PrsS₁</i>	<i>F-EcoRI-PrsS₁</i>	<i>cggaattc</i> atgaacatattttatattattgtgctg
	<i>R-PstI-PrsS₁</i>	<i>aactgcag</i> tcaggttcgacctcc
<i>GAPC</i>	<i>GAPC-F</i>	<i>cactgacaaagacaaggctgcagc</i>
	<i>GAPC-R</i>	<i>cctgttgc</i> ccaacgaagtcag

Agarose gel was scanned using Gel Doc XR Imaging System (Bio-Rad) and the band intensity was quantified using the Quantity One Software.

2.3.6 Analysis of the PrsS₁ protein expression in *At-SLR1::PrsS₁* transgenic lines

At-SLR1::PrsS₁.9 exhibited the highest *PrsS₁* mRNA expression level. Therefore, T₂ plants derived from this line was chosen for PrsS₁ protein expression analysis. As PrsS₁

protein was tissue-specifically expressed in the stigma (Chapter 5), only the stigmatic part of *At-SLR1::PrsS₁* transgenic plant was collected. Around 400 stage 13 stigmas were collected in 40 µl 2× SDS loading buffer. Stigmas from Col-0 plants were collected as controls. Protein was extracted by roughly pipetting the stigma samples in the loading buffer up and down with a cut tip. Samples were boiled for 10 min followed by centrifugation at 13,200 at room temperature for 1 min. Supernatant was subjected to western blot analysis for the detection of PrsS₁ protein as described in section 2.2.5.2 using 15% SDS-PAGE and ECL detection.

Anti-PrsS₁ serum (raised in Rabbit) was purified using Immobilized *E. coli* Lysate kit (Pierce Biotechnology) to remove the non-specific binding caused by the unremoved *E. coli* proteins left in the recombinant PrsS₁ proteins. Melon Gel IgG Purification Kit (Pierce Biotechnology) was applied to remove albumin and transferrin in the anti-PrsS₁ serum. Antibody probing details are shown in Table 2-17.

Table 2-17 Antibody probing details for the detection of PrsS₁

<i>Antibody probing</i>	
<i>Detection of PrsS₁</i>	<i>1st: anti-PrsS₁, 1:100</i>
	<i>2nd: anti-Rabbit-HRP, 1:1000</i>
<i>Detection of Actin</i>	<i>1st: anti-Actin (CP01, CALBIOCHEM), 1:2000</i>
	<i>2nd: anti-Mouse-HRP, 1:5000</i>

In order to show equal loadings, membrane was stripped for actin reprobing. Membrane was stripped by incubating with stripping buffer [1.5% (w/v) glycine; 0.1% (w/v) SDS;

1% (v/v) Tween-20; pH=2.2] for 10 min at room temperature twice, followed by PBS (10 min ×2) and TBST (5 min ×2) washes. Membrane after stripping was subjected to western blot analysis as described in section 2.2.5.2 using actin antibodies. Antibody probing details are shown in Table 2-17.

2.3.7 Generation of self-incompatible *A. thaliana*

Self-incompatible *A. thaliana* were generated by transformation of homozygous *At-ntp303::PrpS₁:GFP* (BG16) transgenic plants with the Ti vector pORE O3-*SLR1::PrsS₁* based on the protocols published by Davis et al. (2009) and Zhang et al. (2006). pORE O3-*SLR1::PrsS₃* was also transformed as the controls. See section 2.1.1 and section 2.3.1 for the details about BG16 transgenic lines and the construction of pORE O3-*SLR1::PrsS_{1/3}* vectors, respectively. T₀ transgenic seeds were screened on selective MS plates containing BASTA (20 μg mL⁻¹). Surviving seedlings were transplanted to soil pots in the greenhouse. Genotyping was carried out as described in section 2.2.3 to confirm the integration of both *PrsS* and *PrpS:GFP* in the *A. thaliana* genome. Transgenic plants containing both *PrpS:GFP* and *PrsS* were left to grow and produce seed set naturally.

2.4 Investigating the role of the proteasome in the *Papaver* SI response

2.4.1 Poppy pollen germination/growth *in vitro*, SI assay *in vitro* and MG132 treatment

Poppy pollen was hydrated for 45 min in a moist chamber at 22 °C. After hydration, pollen was re-suspended in liquid germination medium [GM: 13.5% (w/v) sucrose; 0.1% (w/v) H₃BO₃; 0.1% (w/v) KNO₃; 0.1% (w/v) Mg(NO₃)₂; 3.6% (w/v) CaCl₂] and spread on solid GM (1% agarose). Usually, for 10 mg of pollen, around 1 mL GM was required. Pollen was pre-germinated at 22 °C for 1 h before treated as required for different experiments.

For the *in vitro* SI assay, recombinant PrsS protein was dialysed against poppy pollen GM overnight in 4 °C. Protein concentration was determined using the Bradford assay. PrsS protein was added to poppy pollen which had already been pre-germinated for 1 h so that the final concentration of PrsS protein was 7.5 µg ml⁻¹. Pollen sample was incubated at 22 °C for certain period of time as required by different experiments.

When MG132 treatment was needed, MG132 was added to the poppy pollen GM from the beginning. DMSO treatment was employed as the solvent control. When SI was induced, MG132 was also added to avoid the concentration changes caused by adding PrsS protein.

2.4.2 Poppy pollen protein extraction

Pollen was collected and snap-frozen in liquid nitrogen. Samples were ground thoroughly using glass homogenizer with appropriate extraction buffer. Crude lysates were sonicated at 10 000 amp for 2×5 s. Samples were kept on ice for at least 1 min between sonication step and incubated on ice for 20 min after sonication. Centrifuge at 13,200 rpm in cold room for 20 min, then supernatant was removed into a new microtube and protein concentration was determined by the Bradford assay. Protein extracts were aliquoted and stored at -20 °C.

2.4.3 Proteasome activity assay using fluorogenic peptide substrates

Protein samples for proteasome activity assay were extracted using proteasome assay buffer [50 mM Tris-HCl, pH=7.5; 5 mM MgCl₂; 250 mM sucrose; 1 mM DTT; 0.05 mg mL⁻¹ bovine serum albumin (BSA)]. ATP was freshly added to the buffer to make a final concentration of 5 mM before use (Kisselev and Goldberg, 2005). Each activity assay (100 µL) contained 10 µg protein lysates and 100 µM fluorogenic probes. Z-GGL-amc and 100 µM Ac-nLPnLD-amc were applied in PBE and PBA1 activity measurements respectively. Technical duplicates were performed for each sample. Assays were carried out on a flat-bottom, black fluorescence 96-well plate using a time-resolved fluorescence plate reader (FLUOstar OPTIMA; BMA LABTECH). Fluorescence was monitored with the excitation at 380 nm and emission at 460 nm every 10 mins over a period of 4 h (22 cycles). The activity was calculated by subtracting the fluorescence

reading to the second cycle from the final (22nd) cycle reading.

For proteasome activity assay in buffers at different pH, 50 mM Tris-HCl buffer was replaced with 50 mM Citrate-phosphate buffer.

2.4.4 Caspase activity assays

Protein samples for caspase activity assay were extracted using caspase extraction buffer (50 mM Na-Acetate; 10 mM L-Cysteine; 10% (v/v) Glycerol; 0.1% (w/v) CHAPS; pH=6.0). Caspase activity was assayed in caspase activity assay buffer (50 mM Na-Acetate; 10 mM L-Cysteine; 10% (v/v) Glycerol; 0.1% (w/v) CHAPS; pH=5.0). Each activity assay (100 μ L) contained 10 μ g protein lysates and 100 μ M fluorogenic probes Ac-DEVD-amc. Caspase activity was monitored in the plate reader as described in section 2.4.3.

For caspase activity assay in buffers at different pH, 50 mM Na-Acetate buffer was replaced with 50 mM Citrate-phosphate buffer.

2.4.5 Proteasome activity profiling with MV151

Proteasome activity profiling probe MV151 was kindly provided by Dr. Renier van der Hoorn. The proteasome activity profiling protocol described here is adapted from Gu et al. (2010) published by Dr. Renier van der Hoorn's lab. Samples for proteasome activity assay were extracted using proteasome assay buffer (50 mM Tris-HCl, pH=7.5; 5 mM

MgCl₂; 250 mM Sucrose; 1 mM DTT; 0.05 mg mL⁻¹ BSA). 50 µg of lysates were transferred to a fresh microtube and the volume was adjusted to 49.5 µL with proteasome activity assay buffer. 0.5 µL of 100 µM MV151 stock solution was added to the sample to obtain a final concentration of 1 µM proteasome probe. Samples were gently vortexed and incubated at 27 °C for 2 h. 10 µL of 6× protein loading buffer was added and boiled for 10 min. Proteins were separated by SDS-PAGE (12.5%) and the wet gel slab was imaged using fluorescence imager FX (Bio-Rad) with filter set excitation at 530 nm, emission at 580nm (Gu et al., 2010; de Jong et al., 2012).

2.4.6 DNA fragmentation assay

Terminal deoxynucleotidyl transferase mediated dUTP nick end labelling (TUNEL) is a commonly used technology for the detection of fragmented DNA resulting from programmed cell death (Gavrieli et al., 1992; Zhang and Galileo, 1997). In this study, The DeadEnd™ Fluorometric TUNEL System (Promega) was used to measure the DNA fragmentation in incompatible poppy pollen. The principle involved in this system is that recombinant terminal deoxynucleotidyl transferase catalyses the incorporation of fluorescein-12-dUTP at the 3'-OH ends of DNA, thus fragmented DNA incorporates more fluorescein-12-dUTP than intact DNA. This can be visually distinguished using FITC fluorescence microscopy.

Poppy pollen was grown *in vitro* for 10 h, followed by 2% (w/v) paraformaldehyde

(PFA) fixation at room temperature for 45 min. Pollen samples were washed with 1×TBS buffer (3×5 min) before being kept at 4 °C overnight or proceeding to the next step directly. Pollen samples were loaded on slides (SuperFrost Plus, VWR) followed by 1h incubation at 60 °C on a hotplate. Permeabilisation of pollen tube samples were carried out at room temperature by dipping slide in 1×TBS buffer [0.1% (v/v) Triton-100 in 1×TBS buffer] for 10 min at room temperature. Samples were washed twice with 1×TBS buffer, 5 min each time, and pre-equilibrated in 100 µl equilibration buffer for 10 min at room temperature. Labelling of DNA strand breaks was carried out at 37 °C for 1 h by incubating samples with 50 µl labelling buffer (mix of 44 µl equilibration buffer, 5 µl nucleotide mix and 1 µl rTdT enzyme). Samples were covered with plastic coverslip during incubation. Light exposure was also avoided. The labelling reaction was stopped by dipping samples in 2×SSC solution for 15 min followed by 1×TBS buffer washing (3×5 min). 20 µl vectashield DAPI was added for nucleotide DNA staining. Samples were analysed using fluorescence microscopy with UV and FITC (Nikon 90i).

2.4.7 Fluorescein diacetate (FDA) staining

Pollen sample was collected into a microtube using pipette with a cut tip. FDA was added to the pollen sample with final concentration at 5 µg mL⁻¹. Sample was incubated at room temperature in dark for 5 min before microscopic visualisation (Nikon TE300; excitation 395 nm/emission 475 nm). Pollen that showed strong green fluorescence

signal was classified as viable, and those showed faint green fluorescence signals were classified as dead pollen.

2.4.8 Biotin-DEVD pull down assay

Pollen was grown in liquid GM layered on GM solidified with 1.2% (w/v) agarose. Pollen protein was extracted with DEVDase extraction buffer (50 mM Na-Acetate; 10 mM L-Cysteine; 10% (v/v) Glycerol; 0.1% (w/v) CHAPS; pH=6.0) 4 h after SI treatment (GM treatment as control). Protein concentration was determined by Bradford assay and adjusted to $1\mu\text{g } \mu\text{L}^{-1}$ with DEVDase extraction buffer, 500 μL in total. Biotin-DEVD (final concentration 100 μM) was incubated with pollen protein extracts for 4 h in room temperature. 500 μL of sedimented CaptAvidinTM Agarose beads (Invitrogen) was equilibrated with 500 μL Pull-Down buffer 1 (50 mM Na-Acetate; 10 mM L-Cysteine; pH=4.5) at the same time. The protein extraction/Biotin-DEVD-CHO mixture was added to the equilibrated Agarose beads (500 μL protein extractions, 500 μL Pull-Down buffer 1 and 500 μL CaptAvidin Agarose beads) and incubated on a rotor overnight at 4 °C. Samples were centrifuged at 4 °C for 15 min at 3,000 g, and supernatant was removed. Beads were washed once with Pull-Down buffer 1. To elute the protein bound to the agarose beads, 250 μL Pull-Down buffer 2 (50 mM NaCO₃; pH adjusted to 10.0 with HCl) was added to the sample and incubated on a rotor at room temperature for 30 min followed by centrifugation at room temperature for 15 min at 3,000 g. The supernatant was divided and electrophoresed on two identical

SDS-polyacrylamide gels, one of which was stained by Coomassie Blue. The protein in the other gel was electro-transferred onto the nitrocellulose membrane for western blot analysis with Neutravidin-HRP. Biotinylated proteins were detected using the chemoluminescence detection kit. Protein bands corresponding to the biotinylated spots detected on the membrane in the Coomassie Blue stained gel were excised from the gel, digested with trypsin and sent for identification by Mass-Spectrometry (Bosch et al., 2010).

**CHAPTER 3 DEVELOPMENT OF AN
IMPROVED *ARABIDOPSIS* POLLEN *IN*
VITRO GERMINATION/GROWTH SYSTEM
AND FUNCTIONAL ANALYSIS OF *PRPS* *IN A.*
THALIANA IN VITRO USING THIS SYSTEM**

3.1 Introduction

Self-incompatibility (SI) in flowering plants represents many intriguing opportunities for the study of plant reproductive diversity, evolution, population genetics, cell-to-cell recognition, as well as potential application in agriculture. However, it is difficult to carry out molecular genetic studies in non-model self-incompatible species, such as *Papaver rhoeas*. Therefore, it is of considerable interest to establish whether the *Papaver* SI system can be functionally transferred into self-compatible model plant, *A. thaliana*, as success in achieving this not only facilitate the *Papaver* SI molecular mechanism investigation, but also has important implication for plant F1 hybrid breeding.

Prior to the establishment that whether the *Papaver* SI system, comprising PrpS and PrsS, is functional *in vivo* in *A. thaliana*, the *Papaver* SI male *S*-determinant, *PrpS*, was transferred and tested in *A. thaliana* as a first step (de Graaf et al., 2012; Vatovec, 2011). De Graaf et al. (2012) reported that PrpS:GFP could be specifically expressed in transgenic *A. thaliana* pollen. When *At-PrpS:GFP* pollen was exposed to cognate recombinant PrsS protein *in vitro*, a “*Papaver-SI*” like signalling cascade was elicited resulting in the pollen tube growth inhibition and PCD in incompatible pollen (de Graaf et al., 2012). Even though this was an important demonstration, it was noticed that the transgenic *At-PrpS:GFP* pollen used in Barend de Graaf’s studies did not exhibit as strong SI response as that observed in *Papaver* pollen. Therefore, to ultimately establish

the functionality of PrpS and PrsS in *A. thaliana in vivo*, it was necessary to carry out screening for an improved *At-PrpS:GFP* transgenic line with optimized expression of PrpS:GFP and expressing comparable strength of SI response as *Papaver* pollen. It was also noticed that the *A. thaliana* pollen *in vitro* SI assay, which was employed to demonstrate the functionality of PrpS:GFP in transgenic *A. thaliana*, performed in Barend de Graaf and Sabina Vatovec's study was time consuming and difficult to repeat. Therefore, a robust and reliable *A. thaliana* pollen SI assay was needed to be developed for the screening of improved *At-PrpS:GFP* transgenic line more conveniently.

For functional analysis of *PrpS* in *A. thaliana in vitro*, one of the most critical techniques involved is *in vitro* pollen germination and growth. Pollen from many species, e.g. lily and field poppy, can germinate and grow easily *in vitro* in a simple growth medium consisting sucrose, calcium and boric acid (Taylor and Hepler, 1997). For *in vitro* poppy pollen tube growth and SI bioassays, it has already been well established in the late 1980s by Franklin-Tong et al (Franklin-Tong et al., 1988, 1989). It has been shown that poppy pollen can germinate and sustain reasonable pollen tube growth on an artificial and quite simple growth medium with precisely controlled temperature and humidity. Moreover, by treating poppy pollen with cognate stigma extracts or recombinant PrsS proteins, a quantitatively indistinguishable S-specific inhibition of pollen tube growth could be observed as with *in vivo* pollinations (Foote et al., 1994; Franklin-Tong et al., 1988, 1989). This well established *in vitro* poppy pollen

growth and SI assay provided a very good platform for investigating the poppy SI response.

For *in vitro* germination of *Arabidopsis* pollen, with world-wide effort in the past decades, a robust, efficient and reproducible protocol has also been pursued by several labs. *A. thaliana* pollen belongs to the trinucleate type of pollen, which are thought to be much more difficult to grow *in vitro*, and was observed barely germinate in an artificial growth medium (Taylor and Hepler, 1997). The first well established *in vitro* *Arabidopsis* pollen germination protocol was reported by Li et al. in 1999, in which pollen tube growth showed a Ca^{2+} dependent manner, and pollen tube length could reach around 300 μm on average after 6h incubation. However, no information regarding to the germination rate is available in this report. In 2007, by establishing temperature and pollen density as two of the main factors important for *A. thaliana* pollen germination and growth, Boavida and McCormick were able to achieve *Arabidopsis* pollen germination rates above 80%, with pollen tube length reaching several hundred micrometers, using either solidified or liquid growth medium (Boavida and McCormick, 2007). Recently, by the incorporation of the spermidine into the germination medium and introducing a synthetic cellulosic membrane as the germination substrate, Rodriguez-Enriquez et al. further increased the pollen germination rate to 90% (Rodriguez-Enriquez et al., 2013). The only drawback was the pollen tube length could only reach around 200 μm , even after 24h incubation

(Rodriguez-Enriquez et al., 2013), making it unsuitable for the purposes of an SI bioassay. Despite these well-developed protocols involving a very widely used model plant, researchers still face the problem of reproducibility, and even the same protocol may work differently in different labs. Thus, for those studies in which the *A. thaliana* pollen *in vitro* germination assay is employed, it is necessary to build a stable, reliable and robust *in vitro* pollen germination system first.

The work described in this chapter aimed to perform functional analyses of *PrpS* in *A. thaliana* using the *in vitro* SI assay. An improved protocol for *Arabidopsis* pollen germination was developed by refining the protocols introduced above. In addition, by incorporation of recombinant PrsS protein into the solidified *AtGM* plate, an improved *in vitro* *A. thaliana* pollen SI assay was also developed. Prior to further studies establishing whether PrpS and PrsS function *in vivo* in *A. thaliana*, it was considered necessary to screen more *At-ntp303::PrpS:GFP* lines so that a line with optimal expression of PrpS:GFP that provided a more distinct SI response could be identified. Therefore, the screening of new *At-ntp303::PrpS:GFP* lines using the *in vitro* *A. thaliana* pollen SI assay was undertaken and will also be described in this chapter. As study progressed, it became more and more evident that GFP tagging might affect the proper function of *PrpS* in *A. thaliana* pollen, new transgenic lines (*At-ntp303::PrpS*) without GFP tag were constructed.

3.2 Results

3.2.1 Optimization of *A. thaliana* pollen germination *in vitro*

In the functional analysis of *PrpS* in *A. thaliana* carried out by Dr. Sabina Vatovec, *Arabidopsis* pollen was grown in liquid GM based on a protocol from Prof. Zhenbiao Yang's lab (Li et al., 1999; Vatovec, 2011). For each individual germination assay experiment, at least 20 newly opened flowers were needed, which introduced variability, and it also involved a time consuming pollen collection procedure based on centrifugation (Vatovec, 2011). In addition, this liquid pollen germination protocol did not yield stable or high pollen germination rates, which made it difficult to distinguish whether the low pollen germination rate was due to the drawback of protocol itself or the SI induction by recombinant PrsS protein treatment. Therefore, for the current studies aimed at using an *in vitro* system for analysing transgenic *A. thaliana* pollen, a simple but robust pollen germination protocol for *A. thaliana* was needed. The development of this protocol is described here.

To improve the protocol, several changes were made. As a first step, solidified *AtGM* plates were employed to grow pollen instead of liquid *AtGM*. Moreover, pollen derived from only one flower, instead of 20, was proved sufficient for an individual pollen germination assay in this new set-up. This saved the pollen collection time, removed some of the variability within a sample, and reduced the potentially deleterious effects of centrifugation and vortexing brought to the pollen grains during pollen collection

procedures. Pollen grains derived from a stage 14 flower (day 1) were placed onto solidified *AtGM* plate by inverting the flower or the stamens with the help of a pair of forceps, and incubated at 22 °C (see section 2.1.2 for more details). The *AtGM* plate was checked every 2h using microscopy in order to observe the germination and growth of *A. thaliana* pollen.

Only a few pollen grains were observed to germinate in the first 2h, but after incubation for 4-6 h, a relatively high proportion of pollen grains germinated. Figure 3-1 A and B show the representative images of pollen germination and pollen tube growth under optimized conditions for 6 h, in which a germination rate of 50-70% could be observed. When the pollen was left to incubate overnight at 22 °C, 80% germination on average, and sometimes up to 95% germination, was observed. Figure 3-1-C shows a typical pollen tube grown on solidified *AtGM* for 4h.

It is worth mentioning here that though the overall germination rate after overnight incubation was observed to be quite high (~80%) and reproducible, it was noticed that the germination rates in the first 4-6 h were less consistent and varied from 20% to 70%, in different experiments carried out in different days.

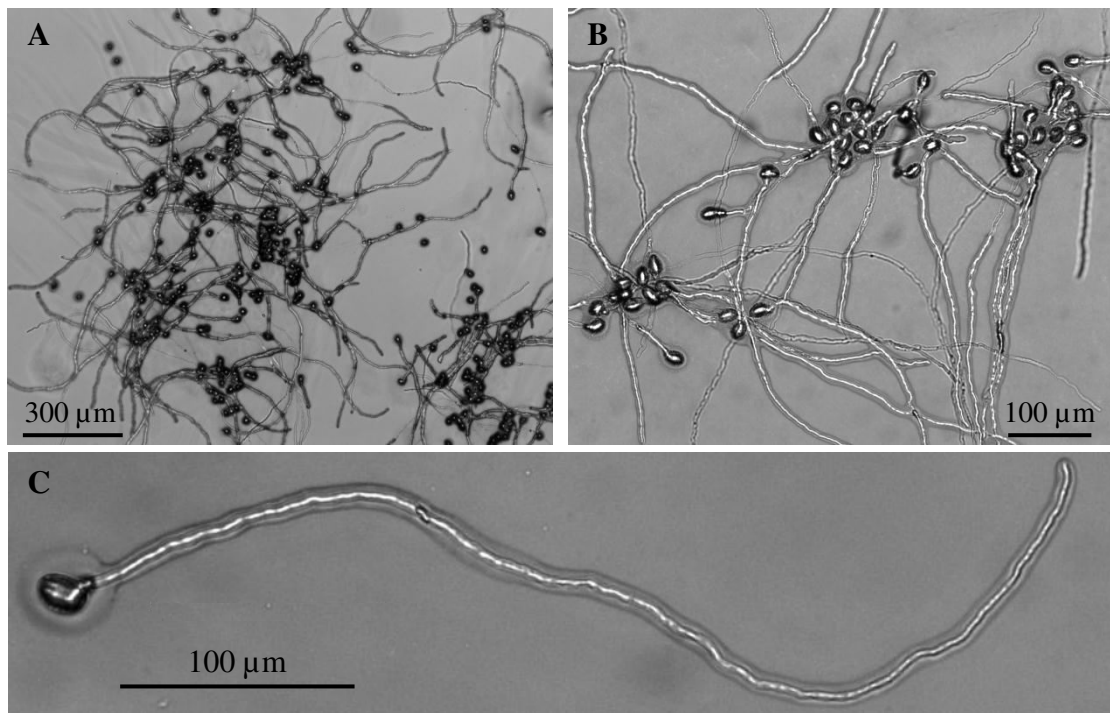


Figure 3-1 *A. thaliana* pollen germinates on solidified *AtGM* with high germination rate

A and B: visualization of *Arabidopsis* pollen germination and pollen tube growth 6 h after being incubated under optimized conditions. C: representative image of a pollen tube after 4h germination on solidified *AtGM*.

In addition to the pollen grain germination rate, the growth of *A. thaliana* pollen was also investigated by measuring the lengths of pollen tubes every 2 h (n=100) after pollen was deposited on the solidified *AtGM* plate. The mean pollen tube lengths at different time points are shown in Figure 3-2, as well as the length of a single representative pollen tube. The *in vitro* growth of *A. thaliana* pollen tubes shows a time dependent manner. The average length of *Arabidopsis* pollen tubes at t=2h, 4h, 6h, was observed to be $187 \pm 71 \mu\text{m}$ (mean \pm SD), $299 \pm 154 \mu\text{m}$ and $441 \pm 233 \mu\text{m}$, respectively (Figure 3-2), showing a mean elongation rate of $\sim 74 \mu\text{m h}^{-1}$. The pollen tube lengths obtained in this study are much longer than those were reported in Vatovec (2011), Li et

al. (1999) and Rodriguez-Enriquez et al. (2013), and are comparable with those were reported in Boavida and McCormick (2007). This demonstrates that the conditions were optimized for *A. thaliana* pollen tube growth in this study.

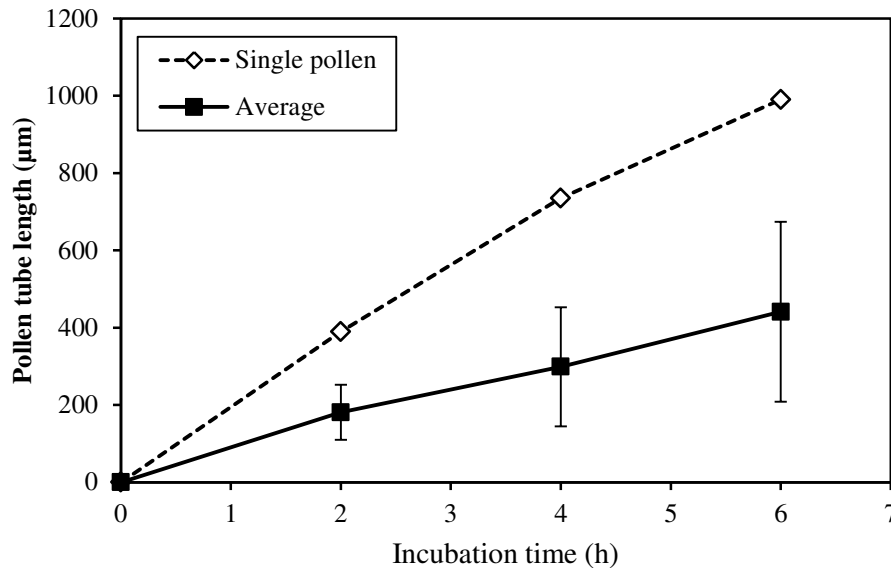


Figure 3-2 Time course of *A. thaliana* pollen tube growths *in vitro*

Dashed line: the growth of a single representative pollen tube, which germinated immediately after deposited on the growth medium. Solid line: mean pollen tube length at different time points (result =mean ±SD; n=100).

The growth of a single representative pollen tube, which germinated immediately after deposited on the growth medium, is also shown in Figure 3-2. This pollen showed a rapid pollen tube growth rate after germination, and the length reached nearly 1000 µm by incubating for 6 h, revealing an average elongation rate of 165 µm h⁻¹. It was noticed that the growth rate of a single pollen tube is much more rapid than that of the mean pollen tube lengths. It was also noticed that the standard deviations of the pollen tube lengths are large. The reason for these observations was thought to be mainly due to the

unsynchronized germination of *A. thaliana* pollen, in which some pollen had already grown to several hundred micro-meters, while others were just starting to germinate. To investigate this possibility, the distribution of pollen tube lengths at $t=4\text{h}$ was studied (Figure 3-3-A), and the germination and growth of 6 individual pollen grains were monitored for 9 h (Figure 3-3-B).

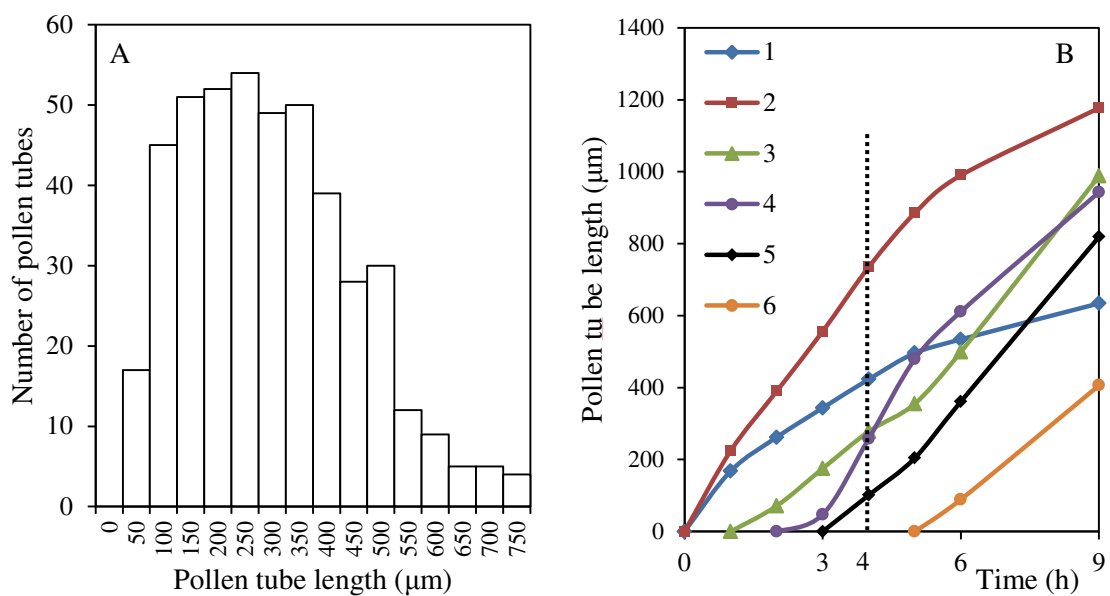


Figure 3-3 A. *thaliana* pollen tube lengths distribution

A: the distribution of 450 *A. thaliana* pollen tube lengths after incubation for 4 h. B: germination of 6 individual pollen grains was monitored using microscopy for 9 h, and pollen tube lengths were measured every one hour.

Figure 3-3-A shows the distribution of the lengths of 450 pollen tubes after 4 h incubation. At $t=4\text{h}$, pollen tube lengths over 750 μm were observed. However, these only accounted for less than 1% (4/450), and the lengths of nearly 70% of the pollen tubes fell in the maximal range between 100-400 μm . This explains the large standard deviation of the pollen tube lengths observed. Unsynchronized germination of *A.*

thaliana pollen is shown in Figure 3-3-B. Of the six pollen grains which were monitored, only two pollen grains were observed to germinate at $t=1\text{h}$, and the other 4 pollen grains were observed to germinate at different time points 1-5 h after incubation on the *AtGM*. This unsynchronized germination of *A. thaliana* pollen resulted in the finding that some pollen tubes had already grown to more than 700 μm , while others were just starting to germinate (Figure 3-3-B). This resulted in the large standard deviation, and also explains why the average growth rate of 100 pollen tubes was slower than that of a single pollen tube.

It has been demonstrated in this section that, under optimized conditions, *A. thaliana* pollen can germinate with a high rate and grow with a rapid growth rate, which are comparable to the very best results which have been reported previously. Moreover, using one flower per assay is a major improvement because it is time saving, removes some of the variability within a sample, and reduces the pollen grain damages during pollen collection procedures. The development of this improved *A. thaliana* pollen *in vitro* germination made it possible to develop a better *A. thaliana* pollen *in vitro* SI assay.

3.2.2 *In vitro* SI assay revealed the S-specific inhibition of *At-PrpS:GFP* pollen

An *in vitro* SI assay for *A. thaliana* pollen needed to be developed to test whether recombinant PrpS protein treatment can result in the *At-PrpS:GFP* pollen tube growth

inhibition to determine whether PrpS:GFP protein expressed in *A. thaliana* pollen is functional. Having established an improved *A. thaliana* pollen *in vitro* germination/growth assay, it was necessary to adapt the SI set-up for the *in vitro* SI assay, as this required the addition of recombinant PrsS proteins to the growth medium. An earlier method described by Franklin-Tong et al. (1988) employed filter paper wicks to fix the PrsS protein. Vatovec (2011) added the PrsS proteins directly to the liquid growth medium. After preliminary experiments, incorporation of recombinant PrsS protein into the AtGM [1% (w/v) agarose] directly was proved to be most reliable for this study. Thus, an *A. thaliana* pollen *in vitro* SI assay was further developed by incorporating recombinant PrsS protein into the solid AtGM (section 2.1.3).

For the measurement of SI in *A. thaliana* pollen *in vitro* SI assay, either pollen germination rate or pollen tube lengths can potentially be used as the measurement criterion. As mentioned in the last section, the germination rates at t=4-6h were quite variable. If the germination rate was used as the measurement criterion, it would be difficult to tell whether the low germination rate observed was caused by the experiment itself or due to the S-specific SI inhibition. Therefore, it was decided that pollen tube length measured between 4-6 h after incubation might be a better parameter to assess the SI response during *A. thaliana* pollen *in vitro* SI assay.

It has been previously demonstrated that the growth of pollen derived from BG16.25

(the only *At-PrpS₁:GFP* line characterized previously) could be specifically inhibited by recombinant PrsS₁ protein treatment (de Graaf et al., 2012; Vatovec, 2011). Therefore, BG16.25 pollen was used as a starting point to test whether the newly developed *A. thaliana* pollen *in vitro* SI assay worked or not.

Genotyping of the BG16.25 transgenic plants (Figure 3-4-A) was always performed using leaf DNA to confirm the integration of *PrpS₁:GFP* into the Col-0 plant genome, before carrying out the newly developed *in vitro* SI assays with BG16.25 pollen. Furthermore, BG16.25 pollen was always checked using GFP fluorescence microscopy to ensure that 100% of the pollen showed GFP signals, i.e., that the pollen was homozygous for PrpS₁:GFP. Weak GFP signals, due to the auto-fluorescence of the pollen coat, were observed from untransformed Col-0 pollen (Figure 3-4 B and C). In contrast, much stronger GFP signals were observed from BG16.25 pollen (Figure 3-4 D and E). Moreover, all the BG16.25 pollen showed strong GFP signals, and no auto-fluorescence was seen. This demonstrates that 100% BG16.25 pollen shows GFP signals.

For the *in vitro* SI bioassay, BG16.25 pollen was placed onto solidified *At*GM plates with or without incorporation of recombinant PrsS₁ proteins (15 µg mL⁻¹). Col-0 pollen controls were identically treated. After incubation at 22 °C for 6h, pollen samples were visualised using microscopy. Representative results are shown in Figure 3-5.

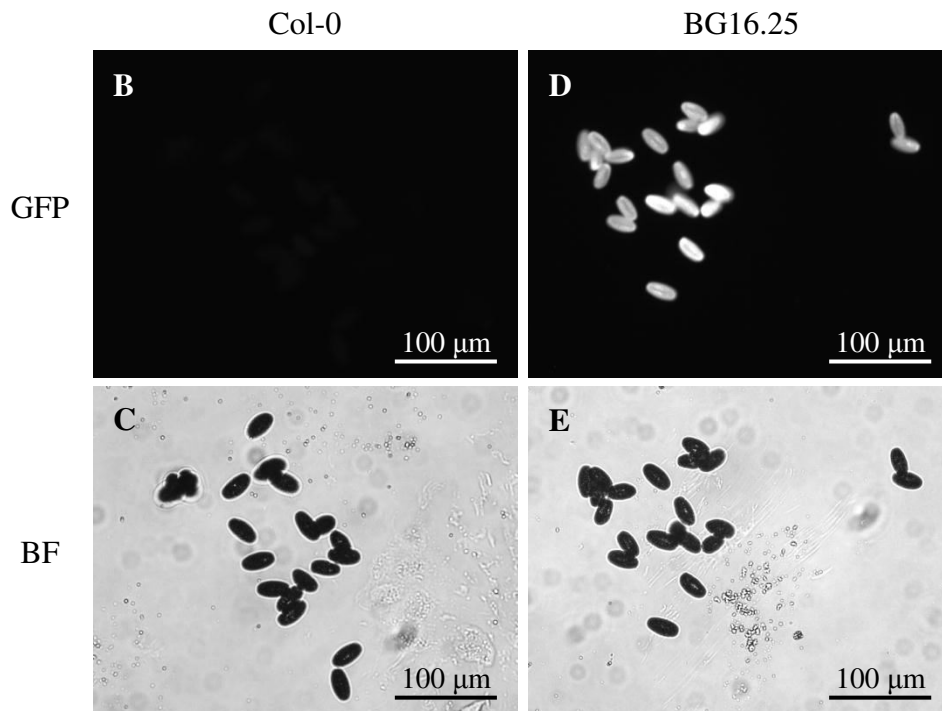
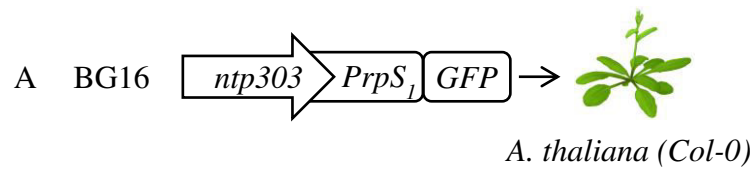


Figure 3-4 PrpS₁:GFP is expressed in transgenic *A. thaliana* pollen

Col-0 and BG16.25 pollen were visualized using GFP fluorescence microscopy. A: cartoon of BG16 transgenic line. Auto-fluorescence from Col-0 pollen (B) and this Col-0 pollen sample was visualized with bright field (C). Strong GFP signals were observed from BG16.25 pollen (D), and this BG16.25 pollen sample was visualized with bright field (E). BF: bright field.

Col-0 pollen germinated normally on *AtGM* plates (Figure 3-5-A) and the majority of the pollen tubes were observed to grow to more than 400 µm by 6 h. The incorporation of 15 µg mL⁻¹ recombinant PrsS₁ protein did not affect the growth of Col-0 pollen tubes (Figure 3-5-B), and no major difference regarding to the pollen tube lengths was observed compared with those grown on *AtGM* plate. For BG16.25 pollen, normal pollen tube growths were observed on the control *AtGM* plate without PrsS₁ protein

treatment (Figure 3-5 C), and the pollen tube lengths were comparable with those of Col-0 pollen. This demonstrates that the expression of PrpS₁:GFP in *A. thaliana* pollen does not affect the normal pollen tube growth. However, when BG16.25 pollen was grown on *At*GM plate with recombinant PrsS₁ protein included, a significant decrease of pollen tube lengths was observed (Figure 3-5 D).

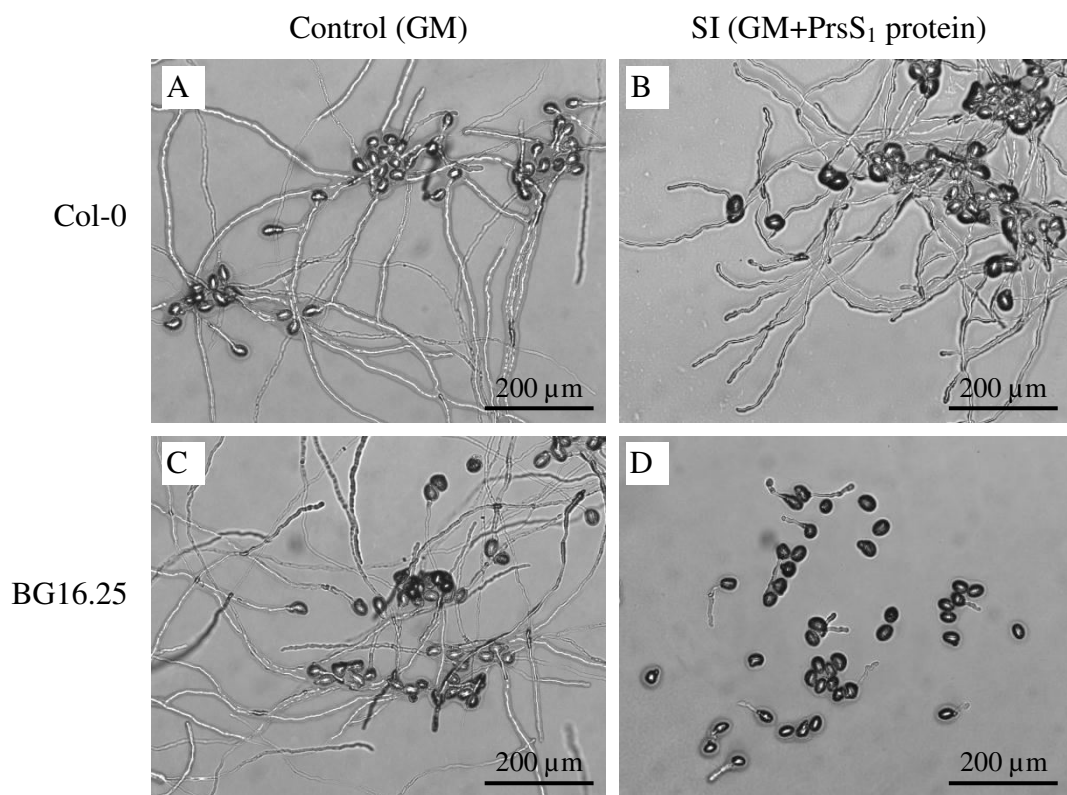


Figure 3-5 The growth of *At-PrpS₁:GFP* pollen is inhibited by PrsS₁ protein *in vitro*

Col-0 and BG16.25 pollen were grown on solidified *At*GM plate for 6 h under optimized conditions with or without adding of recombinant PrsS₁ protein (15 μg mL⁻¹). A: Col-0 pollen germinated normally on solidified *At*GM plate. B: incorporation of recombinant PrsS₁ protein in the *At*GM plate did not affect the growth of Col-0 pollen. C: introduce of *PrpS₁:GFP* to *A. thaliana* did not affect pollen germination on GM plate. D: the growth of pollen expressing *PrpS₁:GFP* was inhibited by recombinant PrsS₁ protein treatment. Experiments were carried out independently for three times. Scale bar indicates 200 μm.

The observation of strong GFP signals from BG16.25 pollen, and inhibition of BG16.25 pollen tube growth when treated with PrsS₁ protein demonstrate that *PrpS₁:GFP* is expressed and functional in *A. thaliana* pollen to trigger an SI response. This also demonstrated that it was possible to perform the *in vitro* *A. thaliana* pollen SI assay using the improved methodology by incorporation of recombinant PrsS₁ protein into the solidified *AtGM* plate in the *A. thaliana* pollen *in vitro* germination assay.

Next, to determine whether the pollen inhibition observed in Figure 3-5 was an authentic SI response, we tested if pollen tube growth inhibition was *S*-specific. BG16.25 pollen was treated with either PrsS₁ or PrsS₃ protein at different concentrations and pollen tube lengths (n=100) were measured after 4 h incubation (Figure 3-6). Col-0 pollen was grown as the control. The lengths of Col-0 pollen tubes were not affected by increasing amounts of recombinant PrsS₁ protein (Figure 3-6), and no significant differences could be observed when they were treated with up to 30 µg mL⁻¹ PrsS₁ proteins (p=0.751, One-way ANOVA). However, the lengths of BG16.25 pollen tubes were strongly inhibited by recombinant PrsS₁ protein, and this inhibition was observed to be both concentration dependent and *S*-specific (Figure 3-6). It can be clearly observed from Figure 3-6 that pollen tube lengths decreased dramatically with the increase of PrsS₁ protein concentrations (p<0.001, One-Way ANOVA). Addition of a 3.75 µg mL⁻¹ dose of PrsS₁ protein treatment was sufficient to significantly reduce pollen tube mean lengths from 350 µm to 190 µm (p<0.001, student's *t*-test). The half

maximal inhibition dose was estimated to be $\sim 4.5 \mu\text{g mL}^{-1}$, and a $30.0 \mu\text{g mL}^{-1}$ dose of PrsS₁ protein resulted in almost complete inhibition of BG16.25 pollen tube growth. In contrast, PrsS₃ proteins treatment (up to $30.0 \mu\text{g mL}^{-1}$) had no significant effect on the BG16.25 pollen tube length ($p=0.694$, One-way ANOVA; Figure 3-6). This demonstrates that *PrpS* is functional in *A.thaliana* pollen *in vitro*, as recombinant PrsS protein can trigger pollen tube growth inhibition, and the inhibition is *S*-specific.

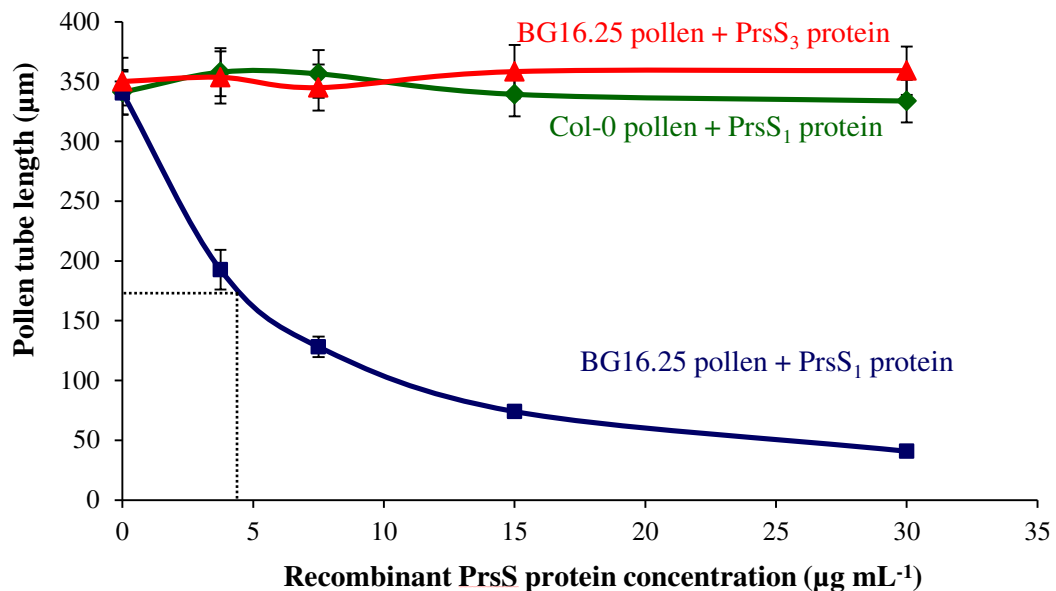


Figure 3-6 *At-PrpS₁:GFP* pollen tube growth is inhibited by PrsS₁ protein in an *S*-specific manner

Col-0 and BG16.25 pollen were allowed to germinate on solidified *AtGM* incorporated with PrsS₁ or PrsS₃ proteins at different concentrations for 4 h. 100 pollen tubes from 3 independent experiments were measured in each individual germination sample. Result = mean \pm SE. Green line: Col-0 pollen germinated on *AtGM*-PrsS₁ plate. Red line: BG16.25 pollen germinated on *AtGM*-PrsS₃ plate. Blue line: BG16.25 pollen germinated on *AtGM*-PrsS₁ plate.

It has been shown in this section that *A. thaliana* pollen *in vitro* SI assay has been successfully developed. This was achieved by developing an *A. thaliana* pollen *in vitro*

germination/growth assay by incorporating the recombinant PrsS protein into the solidified *AtGM*. Moreover, it was also demonstrated that the growth of *At-PrpS:GFP* pollen tubes can be *S*-specifically inhibited by recombinant PrsS protein during the *A. thaliana* pollen *in vitro* SI assay. The successful establishment of an improved *A. thaliana* pollen *in vitro* SI assay made it possible to carry out screening for improved *At-ntp303::PrpS:GFP* transgenic lines, which will be presented in the next section.

3.2.3 Comparison between *At-PrpS:GFP* pollen and *Papaver* pollen, and screening of improved *At-ntp303::PrpS:GFP* transgenic lines

Despite it having been demonstrated that the introduction of *PrpS:GFP* into the *A. thaliana* pollen results in the *S*-specific growth inhibition of *At-PrpS:GFP* pollen when treated with cognate PrsS protein, it was noticed that the transgenic *A. thaliana* BG16.25 pollen was less sensitive than *Papaver* pollen to PrsS protein treatment (Figure 3-7). As demonstrated previously, 7.5 $\mu\text{g mL}^{-1}$ recombinant PrsS protein treatment resulted in the significant reduction of BG16.25 pollen tube lengths from ~350 μm to ~140 μm (Figure 3-6; Figure 3-7-A). However, when *Papaver* pollen was treated with the same concentration of PrsS protein, few pollen tubes longer than 50 μm were observed (Figure 3-7-B). This clearly demonstrates that BG16.25 pollen is much less sensitive to PrsS protein than *Papaver* pollen.

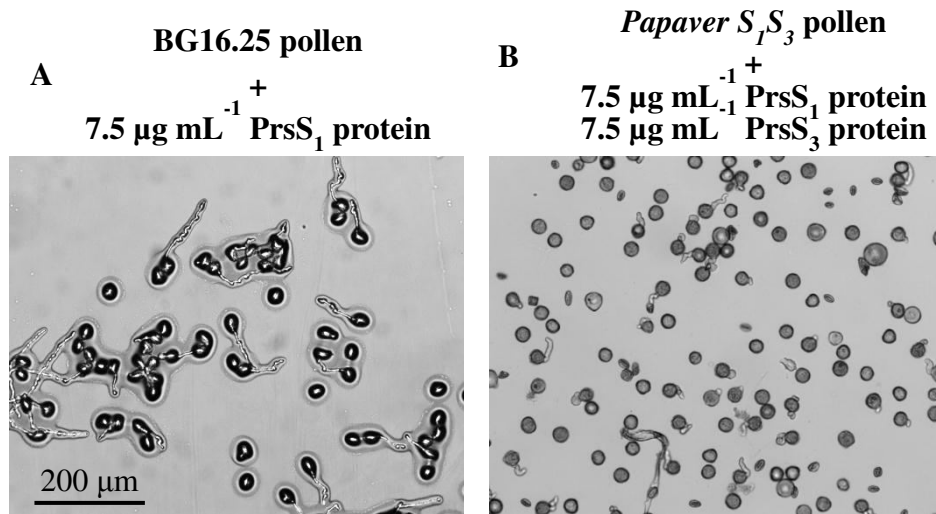


Figure 3-7 BG16.25 pollen is not as sensitive as *Papaver* pollen to PrsS protein treatment

BG16.25 pollen (A) and *Papaver S₁S₃* pollen (B) were treated with the same concentration of cognate recombinant PrsS proteins.

Prior to studies attempting establishing whether *PrpS* and *PrsS* are fully functional *in vivo* in *A. thaliana*, it was considered necessary to identify an *At-ntp303::PrpS:GFP* line which exhibited a similar strength of SI response as *Papaver* pollen. Therefore, more BG16 lines were screened so that a line with optimal expression of PrpS:GFP that provided a more distinct SI response could be identified.

Pollen derived from different homozygous *At-PrpS₁:GFP* transgenic lines (see section 2.1.4 for the full details about the screening of homozygous plants) were collected and subjected to *in vitro* SI assays in which $7.5 \mu\text{g mL}^{-1}$ recombinant PrsS₁ proteins were used. Non-transformed Col-0 pollen was also treated with the same concentration of PrsS₁ proteins as the controls. To compare the strength of SI response between different BG16 lines, pollen tube lengths (n=100) were measured 4 h after incubation and

subjected to one-way ANOVA analysis followed by Multiple Comparisons.

In addition to the original BG16.25 line, homozygous *At-ntp303::PrpS₁:GFP* plants were screened from six other BG16 lines (BG16.1/3/4/6/8/12; section 2.1.4). Preliminary experiments showed that pollen derived from these BG16 lines (including BG16.25) grew normally on the *AtGM in vitro*, and the pollen tube lengths were comparable with that of Col-0 pollen (data not shown). Thus, the expression of PrpS₁:GFP in the pollen of these BG16 lines did not affect the normal pollen tube growth. When pollen derived from these BG16 lines were treated with recombinant PrpS₁ protein, significant pollen tube length reductions were observed for all the 7 BG16 lines compared to the Col-0 pollen tube lengths (Figure 3-8).

Significant variation in pollen tube lengths was observed between different BG16 lines. Of the 6 new BG16 lines screened, 4 of them (BG16.4/6/8/12) showed comparable pollen tube lengths with that of BG16.25, whereas BG16.1 pollen tube lengths were significantly longer, and BG16.3 pollen tube lengths were significantly shorter (Figure 3-8). This demonstrates that the PrpS₁:GFP expressed in transgenic *Arabidopsis* pollen is functional to trigger an SI response resulting in the pollen tube growth inhibition, but the extent of SI response expressed in different BG16 lines varies. Whether the strength of SI expression in different BG16 lines is correlated with the expression PrpS₁:GFP protein remains to be further investigated.

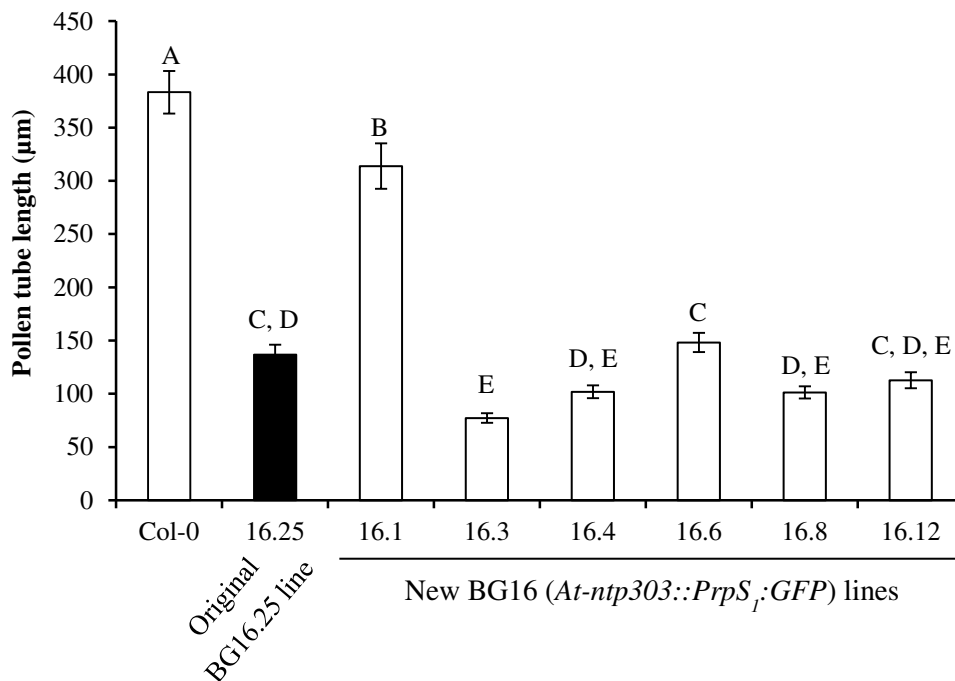


Figure 3-8 BG16 lines exhibit varied strength of SI response

Pollen obtained from different homozygous *At-PrpS_i:GFP* transgenic lines [six new BG16 lines (dashed bars) as well as the original BG16.25 line (black bar)] were subjected to *A. thaliana* pollen *in vitro* SI assays in which 7.5 µg mL⁻¹ recombinant PrsS₁ proteins were used. Non-transformed Col-0 pollen was also treated with the same concentration of PrsS₁ proteins as the controls (white bar). Pollen tube lengths were measured 4 h after incubation (n=100) and subjected to one-way ANOVA analysis. Letters above the bars indicate statistically significant difference (p<0.05). There is no significant difference between those samples which share a same letter. Result = mean ± SE.

In summary, BG16.3 was demonstrated to express the strongest SI response among the 7 BG16 lines characterized so far. A 7.5 µg mL⁻¹ dose of PrsS₁ protein treatment resulted in BG16.3 pollen tube growth reduced from 383 µm to only 77 µm (Figure 3-8). Compared with the BG16.25 pollen tube lengths (136 µm), a further 43% reduction in pollen tube lengths was observed. This demonstrates that BG16.3 represents an improved BG16 line exhibiting a significantly stronger SI response than BG16.25.

However, the SI response observed in BG16.3 pollen was still not as strong as that observed in *Papaver* pollen. Thus, efforts are still needed to identify the best possible *Arabidopsis PrpS* transgenic line to obtain a fully optimized maximal SI response in *A. thaliana*.

3.2.4 Construction of *At-ntp303::PrpS* transgenic lines

BG16.3 represents the best SI-responsive *At-ntp303::PrpS₁:GFP* transgenic line so far. Despite the significant pollen tube growth inhibition observed when BG16.3 pollen was treated with recombinant PrsS₁ protein, the SI response was still obviously weaker than in *Papaver* pollen. It was considered that the GFP fusion at the C-terminus of PrpS might prevent the PrpS being fully functional in *A. thaliana* pollen, as GFP is a large protein compared to PrpS, and may interfere with protein interaction (Rappoport and Simon, 2008). Therefore, new Ti vectors were made for the construction of new *A. thaliana PrpS* transgenic lines without the GFP fusion (section 2.1.5) in order to test this hypothesis, and to obtain a *PrpS* transgenic line which was able to express comparable strength of SI response as *Papaver* pollen. Table 3-1 details the information related to the Ti vectors for the construction of *At-ntp303::PrpS* transgenic lines.

Table 3-1 Construction of *At-ntp303::PrpS* transgenic lines

<i>Vector Backbone</i>	<i>Promoter::DNA fragment</i>	<i>Resistance</i>
<i>pORE O3</i>	<i>ntp303::PrsS₁</i>	<i>BASTA</i>
<i>pORE O3</i>	<i>ntp303::PrsS₃</i>	<i>BASTA</i>

Further experiments are still needed for the construction of transgenic lines and screening of transgenic seeds and functional analysis *PrpS* in *Arabidopsis* pollen. This lays the foundation for future studies to optimize the transgenic SI system in *A. thaliana*.

3.3 Discussion

3.3.1 Development of an improved *A. thaliana* pollen germination/growth assay

A. thaliana pollen belongs to the trinucleate type of pollen and was observed to barely germinate *in vitro* (Taylor and Hepler, 1997). Li et al. reported the first well established *in vitro* *A. thaliana* pollen germination protocol in 1999, in which pollen tube length could reach around 300 μm on average after 6h incubation. In 2001, Fan refined the germination protocol and achieved nearly 75% germination rate (Fan et al., 2001). However, the pollen tube lengths only reached 135 μm on average after 6h incubation (Fan et al., 2001). In 2007, by using either solidified or liquid growth medium, Boavida and McCormick were able to achieve *Arabidopsis* pollen germination rates above 80%, with pollen tube length reaching several hundred micrometers (Boavida and McCormick, 2007). They also established temperature and pollen density as two of the main factors important for *A. thaliana* pollen germination and growth in their study. Recently, the *A. thaliana* pollen germination rate was further increased to 90% by Rodriguez-Enriquez et al. through the introduction of a synthetic cellulosic membrane as the germination substrate and incorporation of spermidine into the germination

medium (Rodriguez-Enriquez et al., 2013). The only drawback of this study was that long pollen tube length could not be achieved. It only reached around 200 μm , even after 24h incubation (Rodriguez-Enriquez et al., 2013). This makes it unsuitable for the purposes of an SI bioassay.

In order to develop a simple and robust SI assay for the functional analysis of *PrpS* in transgenic *A. thaliana* pollen *in vitro*, an improved *A. thaliana* pollen *in vitro* germination/growth assay was developed for this study, based on the protocol published by Boavida and McCormick. In this study, the pollen tube lengths could reach nearly 1 mm, which were much longer than those reported in Vatovec (2011), Li et al. (1999) and Rodriguez-Enriquez et al. (2013), and were comparable with those were reported in Boavida and McCormick (2007). In terms of germination rate, overnight incubation yielded more than 80% germination, sometimes up to 95%. This demonstrates that the conditions had been further optimized for *A. thaliana* pollen tube germination/growth in this study, and makes it possible for the development of a more reproducible and reliable *A. thaliana* pollen *in vitro* SI assay.

3.3.2 Development of an improved *A. thaliana* pollen SI assay

The establishment of poppy pollen *in vitro* SI assay made it possible for the investigation of molecular mechanisms underlying poppy pollen SI response *in vitro*, and facilitated the identification of SI signalling components such as Ca^{2+} , actin,

DEVDase, making poppy SI one of the best characterized SI systems (Franklin-Tong et al., 1988, 1995; Geitmann et al., 2000; Thomas and Franklin-Tong, 2004). Therefore, in order to screen for improved *At-PrpS* transgenic lines and facilitate poppy SI mechanism research in transgenic *A. thaliana* pollen, the development of a simple but robust *A. thaliana* pollen *in vitro* SI assay was necessary.

The first *A. thaliana* pollen *in vitro* SI assay was described by Vatovec (2011), in which liquid *AtGM* was used, and 20 flowers were needed for an individual SI assay. This was time consuming and pollen viability was seriously affected during the pollen collection procedure through vortexing and centrifugation. The establishment of improved *A. thaliana* pollen germination/growth assay made it possible to develop a better *A. thaliana* pollen *in vitro* SI system. A major improvement for the *A. thaliana* pollen germination/growth assay described in this study is that one flower is sufficient for an individual germination experiment by using solidified *AtGM*. By incorporating recombinant PrsS protein into the solid *AtGM* directly, a better *A. thaliana* pollen *in vitro* SI assay was achieved. Moreover, by using this *A. thaliana* pollen *in vitro* SI assay, it has been demonstrated that the growth of *At-PrpS:GFP* pollen tube can be S-specifically inhibited by recombinant PrsS protein. The successful establishment of the *A. thaliana* pollen *in vitro* SI assay made it possible to carry out screening of improved *At-ntp303::PrpS:GFP* transgenic lines, though this needs to be followed up in future studies.

3.3.3 Screening of improved *At-PrpS* transgenic lines

It has been demonstrated that PrpS:GFP is functionally expressed in *A. thaliana* pollen by using the improved *A. thaliana* pollen SI assay. Strong and *S*-specific pollen tube growth inhibition was observed when the *At-PrpS:GFP* pollen was treated with recombinant PrpS protein. In addition to the original BG16.25 line, which was screened by Barend de Graaf and Sabina Vatovec, six more BG16 transgenic lines were screened. They all showed significant pollen tube growth inhibition when SI was induced by adding recombinant PrpS, and line BG16.3 exhibited the best SI response. However, it is noticed that when poppy pollen and *At-PrpS:GFP* pollen was treated with the same concentration of recombinant PrpS protein, poppy pollen tube lengths were significantly shorter than *At-PrpS:GFP* pollen tube lengths. This suggests that PrpS:GFP is not fully functional in triggering SI response in transgenic *A. thaliana* pollen. It was considered that it might be due to the GFP tag at the C-terminus of PrpS, as several reports had pointed out that GFP fusions altered the proper function of target proteins (Rappoport and Simon, 2008). Therefore, in order to obtain a fully functional transgenic line expressing PrpS, new transgenic lines *At-ntp303::PrpS* without GFP fusion were constructed. Further experiments to screen these transgenic lines are in progress.

3.3.4 Summary

In summary, an improved *A. thaliana* pollen *in vitro* germination/growth assay has been developed. This improved assay has facilitated the development of a better *A. thaliana*

pollen *in vitro* SI assay. Functional analysis of the transgenic BG16 line expressing PrpS:GFP using this *A. thaliana* pollen *in vitro* SI assay has demonstrated that PrpS:GFP is functionally expressed in *A. thaliana* pollen. Further experiments are in progress to screen *At-ntp303::PrpS* transgenic lines to obtain an improved *A. thaliana* transgenic lines with fully optimized expression of PrpS and exhibit as strong SI response as *Papaver* pollen. Moreover, this improved methodology laid the foundation for studies described in the next chapter (Chapter 4), which aimed to constitutively express PrsS in *A. thaliana* and test its functionality. Thus, the work described in this chapter marks a very important first step towards establishing the functionality of the *Papaver* SI system in transgenic *A. thaliana*.

**CHAPTER 4 CONSTITUTIVE EXPRESSION
AND FUNCTIONAL ANALYSIS OF *PRSS* IN *A.
THALIANA* USING AN *IN VITRO* SI ASSAY**

4.1 Introduction

So far, the focus has been on functional transfer of the *Papaver* male *S*-determinant, *PrpS*. *PrpS* has been demonstrated to be functional in transgenic *A. thaliana* revealed by the application of an *in vitro* SI bioassay in which *At-PrpS:GFP* pollen was treated with cognate recombinant *PrsS* protein (de Graaf et al., 2012; Vatovec, 2011; Chapter 3 of this thesis). However, of course, there remains the female *S*-determinant, *PrsS*, and it has not yet been established whether *PrsS* can also be functionally transformed into *A. thaliana*. The work in this chapter aimed to initiate studies to express *PrsS* constitutively in *A. thaliana* and test the activity of constitutively expressed *PrsS in vitro* as a first step towards establishing whether *PrsS* can also be functionally transformed into *A. thaliana*.

4.1.1 The establishment of *in vitro* SI bioassay

The first obvious step to establish if *PrsS* can be functionally expressed in *A. thaliana* is to use an *in vitro* SI system. The first poppy pollen *in vitro* SI assay was developed around 30 years ago. Poppy pollen could be germinated and give a sustained reasonable pollen tube growth on a simple growth medium with precisely controlled temperature and humidity (Franklin-Tong et al., 1988). By treating poppy pollen with cognate stigma extracts, a quantitatively indistinguishable inhibition of pollen tube growth was observed as with *in vivo* pollinations (Franklin-Tong et al., 1988). The establishment of the *in vitro* SI assay provided a very good *in vitro* platform for the investigations of the molecular mechanisms involved in the poppy SI response. This has also allowed us to

test whether PrsS proteins produced by organisms other than *P. rhoeas* were biologically active. The demonstration that both *E. coli* produced PrsS proteins were functional in inhibiting cognate poppy pollen was benefited from this *in vitro* SI bioassay (Foote et al., 1994).

Based on the well-established poppy pollen *in vitro* SI assay and an improved *A. thaliana* pollen *in vitro* germination/growth assay, an *A. thaliana* pollen *in vitro* SI system has been developed (Chapter 3). The establishment of *A. thaliana* pollen *in vitro* SI assay has successfully demonstrated that *PrpS:GFP* was functionally expressed in *A. thaliana* pollen (de Graaf et al., 2012; Vatovec 2011; Chapter 3). Moreover, this *A. thaliana* pollen *in vitro* SI assay has also proved useful for the screening of improved *At-ntp303::PrpS:GFP* transgenic lines (Chapter 3). Therefore, it was considered that it might be also be possible to apply the *in vitro* SI system to test the biological activity of PrsS protein expressed in *A. thaliana*, using *At-PrpS:GFP* pollen or *Papaver* pollen. This could be an important step towards assessing if, in principle, it was possible to express PrsS successfully in *A. thaliana* prior to more *in vivo* laborious testing.

4.1.2 Previous analysis of *A. thaliana* expressed PrsS protein using the *in vitro* SI assay

For the *in vitro* SI assays carried out in this study, one of the key issues was to obtain sufficient *A. thaliana* expressed PrsS protein to use, instead of recombinant *E. coli* PrsS protein, for functional testing. There were two possible approaches to express PrsS in *A.*

thaliana: (1) stigma-specifically expressed PrsS driven by a stigma specific promoter or, (2) constitutively expressed PrsS driven by the 35S promoter.

Some functional analysis of *A. thaliana* expressed PrsS driven by the stigma specific promoter, *Stig1*, had already been carried out by Sabina Vatovec. In that study, RT-PCR showed the presence of *PrsS* mRNA transcript in the stigma of transgenic *A. thaliana* flowers, but western blots failed to detect any PrsS protein (Vatovec, 2011). This suggested either an extremely low level of PrsS protein expression, or that it was not properly translated or secreted in transgenic *A. thaliana*. This was consistent with the observation that crosses between *A. thaliana PrsS* lines and their cognate *PrpS* lines resulted in pollen tubes growing through the style, resulting in normal seed set (Vatovec, 2011). Confusingly, a modified *in vitro* SI assay, in which *Papaver* pollen tube growth was monitored in the presence of stigmatic extracts from transgenic *At-Stig1::PrsS*, showed *S*-specific pollen inhibition, together with some morphological changes, like pollen tube tip swelling. These observations suggested possible functional expression of PrsS protein driven by the stigma specific *Stig1* promoter (Vatovec, 2011). Thus it appeared possible that lack of biological functionality in this study might have been due to the low level of PrsS protein expressed in the transgenic *A. thaliana* stigma. Therefore, although it had been suggested by Vatovec (2011) that PrsS might be functional in *A. thaliana*, it was still unclear whether PrsS protein was functionally expressed in the *At-Stig1::PrsS* transgenic plants. In addition, as the expression of *PrsS*

was directed by the stigma-specific promoter in the transgenic *A. thaliana*, it was time consuming and labour intensive to collect enough tissue materials for the *in vitro* SI assay, as compared with poppy stigmas, *A. thaliana* stigmas are much smaller.

An alternative approach is to use a constitutive promoter. This would make it possible to perform expression and functional analysis for *PrsS* more quickly and easily, using extracts from transgenic seedling material (eg. leaves), rather than having to wait until the flowering stage to collect only stigmas.

Functional analysis of constitutively expressed *PrsS* can be traced back to early 1990s, when Humphrey Foote tried to obtain biologically active *PrsS* protein from transgenic tobacco plants (Foote, 1993). *PrsS* driven by the Cauliflower Mosaic Virus RNA gene promoter (CaMV 35S, hereafter 35S) was introduced into *N. tabacum* (Guilley et al., 1982). The 35S promoter, which is generally considered as a very strong constitutive promoter, leading to the high levels expression of transgene in both dicot and monocot plants, is widely used in plant transgenic engineering to drive target gene expression (Odell et al., 1985). Northern hybridization analysis showed the expression of *PrsS* mRNA transcripts in the leaf samples (Foote, 1993). Preliminary functional analysis using *in vitro* SI assay with tobacco leaf washes was also carried out, which suggested active *PrsS* proteins eluted from tobacco leaves (personal communication, Noni Franklin-Tong and Chris Franklin). These preliminary results suggested that it might be

possible to carry out functional analysis of constitutively expressed PrsS in *A. thaliana* using the 35S promoter to drive the expression of *PrsS*.

4.1.3 Aims of this chapter

To establish whether *PrsS* can be functional *in vivo* in *A. thaliana*, in the studies described in this chapter, transgenic *A. thaliana* plants, in which the 35S promoter was used to drive the constitutive expression of *PrsS* or *PrsS:GFP*, were constructed. To investigate whether *A. thaliana* produced PrsS proteins were biologically active and capable of triggering the SI response, *in vitro* SI assays were carried out in which poppy pollen or *At-PrpS:GFP* pollen was grown in the presence of protein extracts derived from transgenic seedlings.

4.2 Results

4.2.1 Construction of transgenic *A. thaliana* lines constitutively expressing *PrsS* or *PrsS:GFP*

Previous studies have demonstrated that *PrpS* can be functionally transferred from *P. rhoeas* to *A. thaliana*. However, whether *PrsS* can be functionally expressed in *A. thaliana* remained to be elucidated. It was decided to use the *in vitro* SI bioassays described in Chapter 3 to investigate whether *A. thaliana* produced PrsS protein is biologically active and capable of triggering the SI response *in vitro*. For the *in vitro* SI bioassay, sufficient plant material extracts containing PrsS protein was needed.

Therefore, for these studies, instead of the stigma specific promoter, the strong, constitutive 35S promoter, was chosen to drive the expression of *PrsS* in transgenic *A. thaliana*. This would have the advantage of shortening the experimental period, because transgenic plants could be analysed when they are young seedlings rather than waiting until the flowering stage. Moreover, it would also make the analysis more easily and convenient, because much more plant material would potentially be available, and it is much quicker and easier to collect vegetative seedling tissue than stigmas. To facilitate the analysis of expression of *PrsS* in transgenic *A. thaliana*, *At-35S::PrsS:GFP* transgenic lines were also constructed, so that a GFP antibody could be used for detection of recombinant protein. Table 4-1 details the transgenic lines constructed for the *in vitro* analysis of constitutively expressed *PrsS* in *A. thaliana* (details relating to vector construction, *Agrobacterium*-mediated transformation and transgenic seed screening are described in Materials and Methods, sections 2.2.1, 2.2.2 and 2.2.3).

Table 4-1 Transgenic *A. thaliana* lines built for functional analysis of constitutively expressed *PrsS* *in vitro*

<i>Name</i>	<i>Promoter::DNA fragment</i>	<i>Resistance</i>	<i>Independent T₁ lines generated</i>
<i>A</i>	<i>35S::PrsS₁:GFP</i>	<i>BASTA</i>	<i>69</i>
<i>B</i>	<i>35S::PrsS₃:GFP</i>	<i>BASTA</i>	<i>17</i>
<i>E</i>	<i>35S::PrsS₁</i>	<i>BASTA</i>	<i>38</i>
<i>F</i>	<i>35S::PrsS₃</i>	<i>BASTA</i>	<i>36</i>

4.2.2 Analysis *PrsS* expression in *A. thaliana* transgenic lines

4.2.2.1 Analysis of *PrsS₁* mRNA expression in transgenic *A. thaliana* lines

As the first step for the screening of transgenic plants, RT-PCR was carried out to detect the expression of *PrsS₁* mRNA in transgenic *A. thaliana* lines (section 2.2.4). RT-PCR demonstrated that *PrsS₁* mRNA was expressed in all the *At-35S::PrsS₁:GFP* and *At-35S::PrsS₁* transgenic lines analysed (Figure 4-1; Figure 4-2). *GAPC* was chosen as an internal reference gene as it is a housekeeping gene and it has a relatively stable and strong expression comparing with other endogenous genes. As there is no intron in *PrsS* gene, specific care needed to be taken to make sure that there was no genomic DNA contamination in mRNA. Therefore, *GAPC* primers were designed across two different exons, resulting in the size of PCR product from cDNA and genomic DNA differed at 568 bp and 955 bp respectively, thus RNA contaminated by the genomic DNA could be determined.

The expression of *PrsS₁* mRNA was analysed in two-week-old T₂ transgenic seedlings. Thirty-three independent *At-35S::PrsS₁:GFP* lines were analysed using RT-PCR, of which representative results of 11 of them are shown in Figure 4-1-A. For *At-35S::PrsS₁:GFP* lines, *PrsS₁* mRNA was found to be expressed in all of the transgenic lines analysed (Figure 4-1-A). *GAPC* and *PrsS₁* were both amplified for 27 cycles during the RT-PCR amplification step. Col-0 RNA and water were used as negative controls (data not shown). As shown in Figure 4-1-A, only the 568 bp *GAPC*

PCR products could be observed from RT-PCR. In addition, PCR was also carried out with the same RT-PCR kit using RNA as template directly; no DNA products could be identified in the agarose gels (data not shown). This demonstrates that there was no genomic DNA contamination in the RNA. In order to confirm the integrity of full length *PrsS₁:GFP* in transgenic plants, full length *PrsS₁:GFP* was amplified using cDNA as the template followed by sequencing. In addition, it was also confirmed by the sequencing that there was no mutation within *PrsS₁:GFP* cDNA.

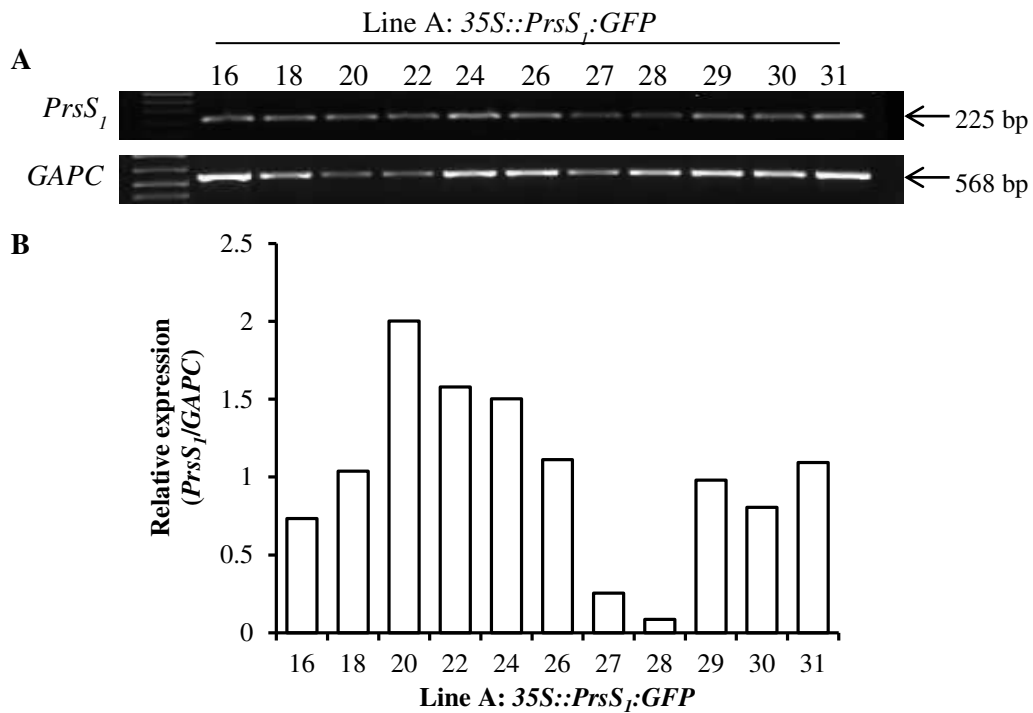


Figure 4-1 *PrsS₁* mRNA is expressed in *At-35S::PrsS₁:GFP* transgenic lines

A: agarose gel electrophoresis shows the RT-PCR results of 11 independent *At-35S::PrsS₁:GFP* transgenic lines. B: semi-quantification of the expression of *PrsS₁* relative to that of *GAPC*. Expression level of *GAPC* was normalized as 100%.

Moreover, *PrsS₁* mRNA was expressed at high levels under the direction of the 35S

promoter, because quantification of the band intensity showed that the *PrsS₁* mRNA expression level in 7 of the 11 lines (A18, A20, A22, A24, A26, A29 and A31) was higher than that of *GAPC* (Figure 4-1-B), which is a strongly expressed housekeeping gene. As RT-PCR experiment was only performed once, therefore, no solid conclusion could be addressed regarding to quantification of the relative expression level of *PrsS₁*/*GAPC* between different transgenic lines.

The expression of *PrsS₁* mRNA in 16 independent *At-35S::PrsS* transgenic lines (Line E) was analysed, of which eight representative results are shown in Figure 4-2. The expression of *PrsS₁* mRNA was observed in all the *At-35S::PrsS₁* lines analysed. During the RT-PCR amplification step, different amplification cycles were applied for *PrsS₁* (32 cycles) and *GAPC* (27 cycles). For this reason, the relative mRNA expression levels of *PrsS₁*/*GAPC* of *At-35S::PrsS₁* lines could not be properly quantified for this RT-PCR experiment.

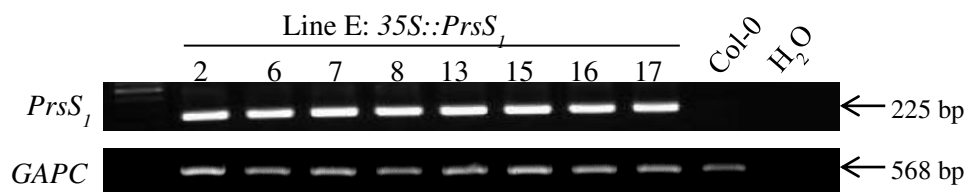


Figure 4-2 *PrsS₁* mRNA is expressed in *At-35S::PrsS₁* transgenic lines

The expression of *PrsS₁* mRNA was analyzed using RT-PCR. Col-0 RNA and water were used as negative controls. Agarose gel electrophoresis shows the RT-PCR results of 8 independent *At-35S::PrsS₁* transgenic lines.

4.2.2.2 Analysis of expression of PrsS₁ protein in transgenic lines using western blotting

As expression of the PrsS mRNA was clearly obtained, the next step was to investigate whether the PrsS protein was produced in transgenic *A. thaliana*. Western blots were employed to detect the expression of the PrsS protein (section 2.2.5). The expression PrsS₁:GFP in *At-35S::PrsS₁:GFP* lines was analysed using GFP antibodies, and the expression of PrsS₁ protein in *At-35S::PrsS₁* lines was checked using PrsS₁ antibodies.

4.2.2.2.1 Detection of PrsS₁:GFP protein in *At-35S::PrsS₁:GFP* lines

The expression of PrsS₁:GFP protein was analysed in two-week-old transgenic seedlings using GFP antibodies (Figure 4-3). Seven independent *At-35S::PrsS₁:GFP* lines, which had a wide range of *PrsS₁* mRNA expression levels, were chosen for further characterization of PrsS₁:GFP protein expression. Clear GFP signals were detected at 45 kD, while there is no corresponding GFP signal observed in the Col-0 control (Figure 4-3-A). As the molecular weight of PrsS₁:GFP protein was predicted to be 44.6 kD (PrsS₁: 14.0 kD; linker: 2.2 kD; GFP: 28.4 kD), therefore, it was considered that the GFP signals detected in the transgenic seeding samples represented PrsS₁:GFP. Thus, fusion protein PrsS₁:GFP was detected in all the seven different *At-35S::PrsS₁:GFP* lines analysed. Coomassie blue staining shows the equal loading of total proteins in each lane (Figure 4-3-B). Figure 4-3-C shows the quantification of relative PrsS₁:GFP expression level in different lines, in which the expression level of

A31 was normalised as 100%. Considerable variation of PrsS₁:GFP protein signals in different lines could be clearly observed. It can be seen from Figure 4-3-C that lines A18 and A22 had the lowest PrsS₁:GFP signals, while A27 and A30 showed moderate PrsS₁:GFP expression, A24, A29 as well as A31 were among the highest. It is noticed that there is not any obvious correlation between the expression of *PrsS₁:GFP* mRNA and protein in *At-PrsS₁:GFP* transgenic lines (data not shown).

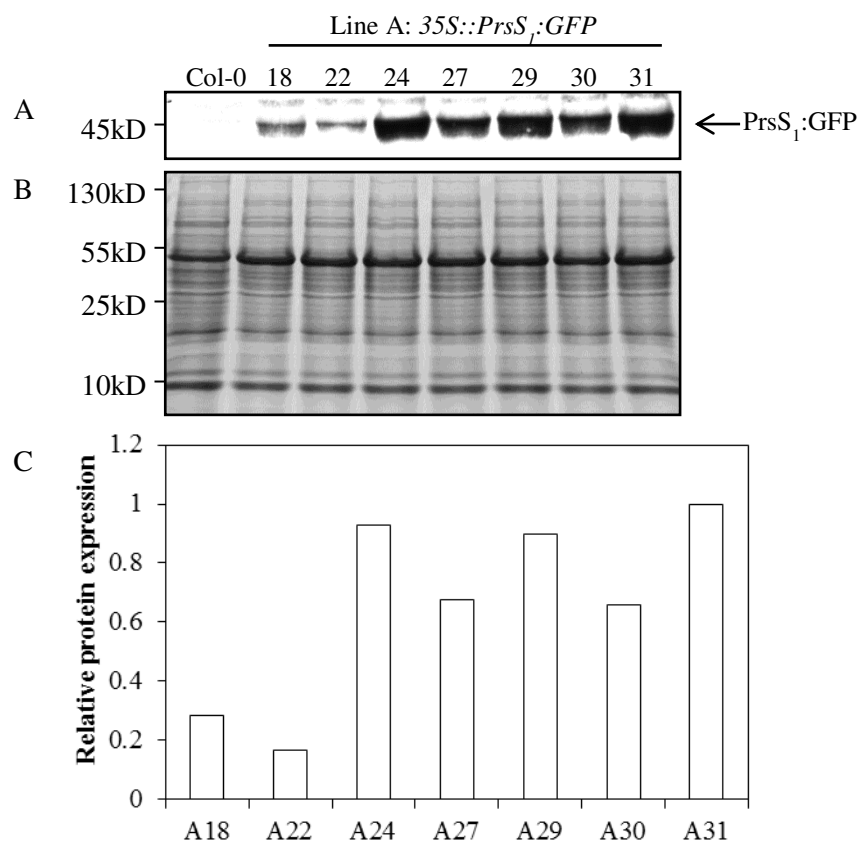


Figure 4-3 PrsS₁:GFP protein is detected in transgenic *A. thaliana*

The expression of PrsS₁:GFP protein were checked on two-week-old transgenic seedlings by western blot using GFP antibody. A: western blotting of *At-35S::PrsS₁:GFP* lines and Col-0 control are shown. The arrow indicates PrsS₁:GFP signal. B: coomassie blue staining shows the equal loading. C: quantification of the relative expression of PrsS₁:GFP protein in different *At-35S::PrsS₁:GFP* lines. The expression level in line A31 was normalized as 100%.

In order to confirm the signals detected on the western blot shown in Figure 4-3 were PrsS₁:GFP signals, PrsS₁ antibodies were also used to analyze the expression of PrsS₁:GFP protein in *At-35S::PrsS₁:GFP* transgenic lines, in which the expression of PrsS₁:GFP protein had been demonstrated (Figure 4-3). Prior to the western blot using PrsS₁ antibodies, PrsS₁ antibodies were first tested on *E. coli* recombinant PrsS₁ proteins to check the antibody sensitivity (Figure 4-4). PrsS₁ antibodies could detect as low as 25 ng recombinant PrsS₁ proteins, while no visible band could be observed in the lane with 10 ng recombinant PrsS₁ proteins (Figure 4-4).

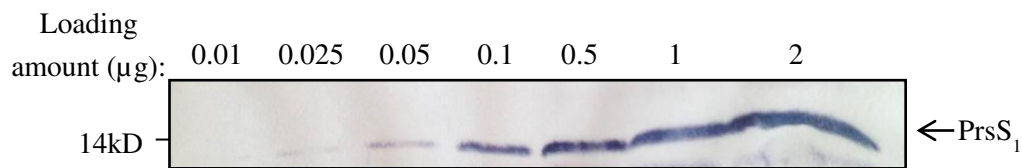


Figure 4-4 Characterization of PrsS₁ antibody sensitivities

PrsS₁ antibody sensitivities were checked using recombinant PrsS₁ proteins. Different amounts of recombinant PrsS₁ proteins were loaded on SDS-PAGE followed by western blot using PrsS₁ antibodies. PrsS₁ antibodies were able to detect recombinant PrsS₁ proteins as low as 25 ng. 10 ng recombinant PrsS₁ proteins showed no visible band.

Western blot using the PrsS₁ antibodies showed that no obvious signal corresponding to the 45 kD band could be observed, when up to 50 µg of transgenic *At-35S::PrsS₁:GFP* seedling extracts were loaded. This suggested that PrsS₁ antibodies were not as sensitive as GFP antibodies in detecting PrsS₁:GFP fusion protein. In addition, this also indicated that the expression level of PrsS₁:GFP protein was less than 0.05% in *At-35S::PrsS₁:GFP* seedling extracts.

4.2.2.2.2 Detection of PrsS₁ protein in *At-35S::PrsS₁* lines

An attempt to detect the PrsS₁ protein in *At-35S::PrsS₁* transgenic seedlings using PrsS₁ antibodies was also carried out. However, no visible signal on western blot was detected using the PrsS₁ antibodies, when up to 50 µg of seedling extracts were loaded, suggesting a very low expression level (less than 0.05%) of PrsS₁ protein in the *At-35S::PrsS₁* transgenic lines. The expression level of PrsS₁ protein in poppy stigma has not been detected using this PrsS₁ antibody, therefore, no information is available regarding to the relative expression levels of PrsS₁ protein in *At-35S::PrsS₁* transgenic plants compared with that of poppy stigma.

4.2.2.3 Analysis of PrsS₁:GFP protein expression using GFP fluorescence microscopy

4.2.2.3.1 GFP signals could be observed from transgenic *At-35S::PrsS₁:GFP* seedling tissue sample

The transgenic *At-35S::PrsS₁:GFP* plants were also analyzed for the expression of PrsS₁:GFP protein using microscopy to attempt to detect GFP fluorescence. Five-day-old A31 seedlings were checked. No GFP signal could be detected in the Col-0 controls (Figure 4-5-A), but surprisingly, no GFP signals could be detected in stems and leaves from A31, and only very weak signals could be observed in the vasculature of roots (Figure 4-5-B), although it had already been demonstrated by western blot that PrsS₁:GFP proteins did express in both leaves and roots in this line.

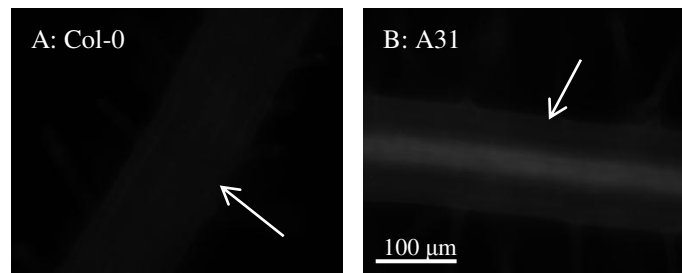


Figure 4-5 GFP signal was observed in *At-35S::PrsS₁:GFP* seedling tissue sample

The expression of PrsS₁:GFP protein in *At-35S::PrsS₁:GFP* transgenic lines were analyzed using GFP fluorescence microscopy using five-day-old A31 (*At-35S::PrsS₁:GFP.31*) seedlings. A: there is no GFP signal detected in the Col-0 control. B: weak GFP signal could be observed in the vasculature of A31 root. Bar indicates 100 μm.

4.2.2.3.2 PrsS₁:GFP appeared to be under proteasomal degradation *in vivo*

One possible hypothesis to explain this unexpected observation was that PrsS₁:GFP might be under certain degradation mechanisms in *A. thaliana in vivo*. Due to protein turnover, very low level of PrsS₁:GFP proteins may be maintained in the cells. If this was the case, blocking proteasomal degradation should result in the increase of PrsS₁:GFP abundance, therefore increased GFP fluorescent signals should be observed. To test this hypothesis, the proteasome specific inhibitor MG132 was employed to investigate PrsS₁:GFP protein turnover in these transgenic *A. thaliana* plants *in vivo*.

Both Col-0 and line A31 5-day old seedlings were transferred onto new MS plates with or without the incorporation of 50 μM MG132 and incubated for 24 hours before they were visualized for PrsS₁:GFP expression using GFP fluorescent microscopy. As shown in Figure 4-6, no GFP signal was found in Col-0 roots (Figure 4-6-A) and there was still

no GFP signal after MG132 treatment (Figure 4-6-B). Weak GFP signals, which were restricted in the vasculature part of roots, were observed in line A31 (Figure 4-6-C). MG132 treatment significantly increased the GFP signals observed in the roots of line A31 (Figure 4-6-D). This provided good evidence that PrsS₁:GFP is under proteasomal degradation *in vivo*, as assumed inhibition of proteasomal activity using MG132 significantly increased the abundance of PrsS₁:GFP proteins.

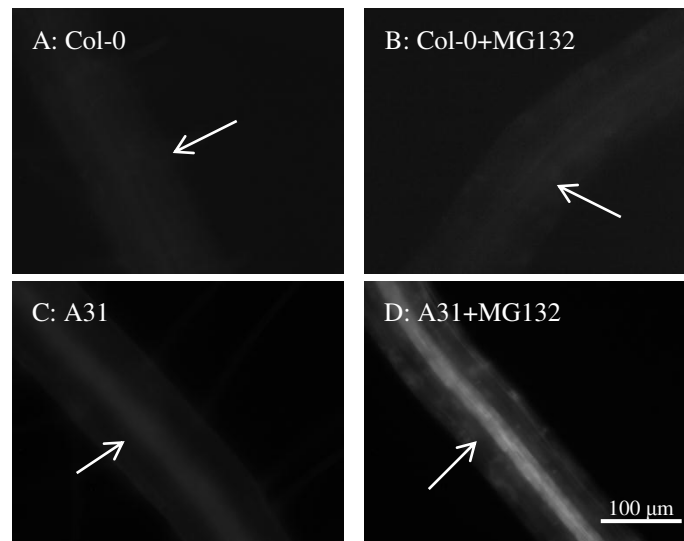


Figure 4-6 PrsS₁:GFP appears to be subject to proteasomal degradation *in vivo*

Five-day-old A31 (*At-35S::PrsS₁:GFP.31*) seedlings with or without MG132 (50 μM) treatment were visualized using GFP fluorescence microscopy. Representative images for the zone of cell differentiation of the roots are shown above. A: no GFP signal was observed in the Col-0 root. B: faint GFP signals were observed in the vasculature of A31 root. C: MG132 treatment made no difference to the GFP signal in Col-0 root. D: the GFP signals were clearly increased after MG132 treatment in the roots of live A31. White arrows indicate the vasculature of roots. Scale bar indicates 100 μm. At least 5 seedlings were analyzed in each treatment.

Western blots were also carried out to confirm the GFP signal changes observed before and after MG132 treatment (Figure 4-7). As GFP signals could only be observed in

roots and no GFP signal was detected in leaves, the roots and leaves were separated from seedling samples, extracted and subjected to western blot analysis using GFP antibodies. As shown in Figure 4-7-A, GFP signal representing PrsS₁:GFP, was detected in both leaf and root extracts from the seedlings, although no GFP signal had been seen in leaf tissue using GFP fluorescence microscopy. Although only 10 µg of root protein samples were loaded compared to 20 µg for leaf sample, the assumed PrsS₁:GFP protein signals observed in root was obviously higher than that in leaf. This demonstrated that roots had much higher PrsS₁:GFP protein expression level than leaf tissue.

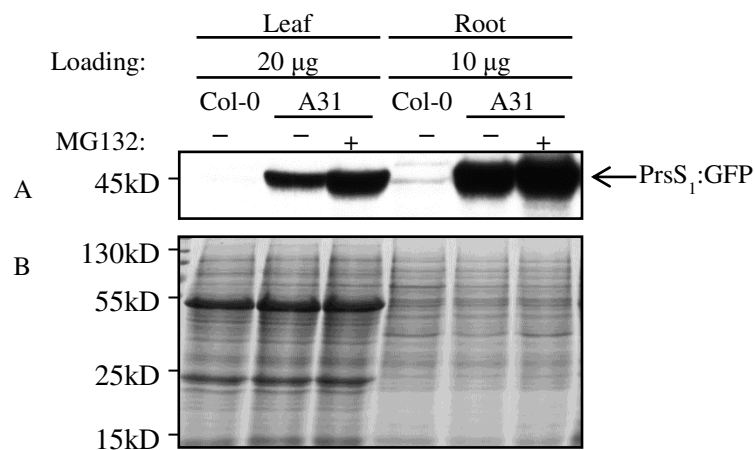


Figure 4-7 Western blot confirms *in vivo* degradation of PrsS₁:GFP

Five-day-old A31 seedlings grown with and without MG132 treatment were subjected to PrsS₁:GFP detection using western blot using GFP antibodies. A: PrsS₁:GFP was detected in both leaf and root tissue of A31, while no PrsS₁:GFP signal was observed in the Col-0 control. MG132 treatment increased the abundance of PrsS₁:GFP in both leaf and root tissue. Black arrow indicates GFP signals. B: coomassie blue staining shows the equal loadings. 20 µg of leaf protein extractions and 10 µg of root protein extractions were loaded respectively.

After MG132 treatment, a significant increase in PrsS₁:GFP signal was detected in both

leaves and roots (Figure 4-7-A). Figure 4-7-B shows the equal loading of each sample. This clearly demonstrated that PrsS₁:GFP was expressed in both leaf and root tissues in *At-35S::PrsS₁:GFP* transgenic seedlings but at very different levels. In addition, the observation that MG132 treatment significantly increased PrsS₁:GFP abundance provided strong evidence that the proteasome was involved in the degradation of PrsS₁:GFP protein in both leaf and root tissues *in vivo*.

4.2.3 Functional analysis of *A. thaliana* constitutively-expressed PrsS protein using the *in vitro* SI assay

So far, it has been demonstrated that both PrsS₁:GFP mRNA transcript and protein are expressed in *At-35S::PrsS₁:GFP* transgenic seedling leaves and roots. However, whether *A. thaliana* produced PrsS₁:GFP protein was biologically active remained to be elucidated. Therefore, *in vitro* SI assays using transgenic seedling extracts, from both leaf and root tissues, were carried out to investigate whether the *A. thaliana* expressed *PrsS₁:GFP* protein was sufficient and functional in inhibiting the growth of *At-PrpS₁:GFP* pollen or poppy pollen *in vitro*. In addition, even though no direct evidence had been obtained to show the expression of PrsS₁ protein, *in vitro* SI assays were also performed on these *At-35S::PrsS₁* transgenic lines.

4.2.3.1 Testing the SI activities of transgenic seedling extracts on *At-PrpS₁:GFP* pollen

The ability of *At-35S::PrsS₁:GFP*.31 (line A31, which had the highest PrsS₁:GFP

protein expression among all the *At-35S::PrsS₁:GFP* transgenic lines analyzed; see Figure 4-3) and *At-35S::PrsS_{1.8}* (line E8, which had the highest *PrsS₁* mRNA expression of all the *At-35S::PrsS₁* transgenic lines analyzed; see Figure 4-2) seedling extracts to inhibit transgenic *A. thaliana* pollen expressing PrpS₁:GFP in the *in vitro* SI assay was tested (section 2.2.6). Protein extracts obtained from two-week-old seedlings from line A31 or E8 were incorporated into solidified *AtGM* plates. *At-PrpS₁:GFP* (BG16.25, hereafter referred to as BG16) pollen, which had been demonstrated to express functional PrpS₁:GFP and which was inhibited by recombinant PrsS₁ protein (de Graaf et al., 2012), was grown on these *AtGM* plates. Whether the growth of BG16 pollen could be inhibited by transgenic seedling extracts was assessed 5 h after incubation at 22 °C. Preliminary experiments had demonstrated that *A. thaliana* pollen could germinate normally and was not inhibited by up to 250 µg of Col-0 seedling extract treatment. So, in the *in vitro* SI assay, 250 µg transgenic seedling (line A31 or E8) extracts were applied in each *AtGM* plate, and recombinant PrsS₁ proteins were employed as positive controls. The results are shown in Figure 4-8.

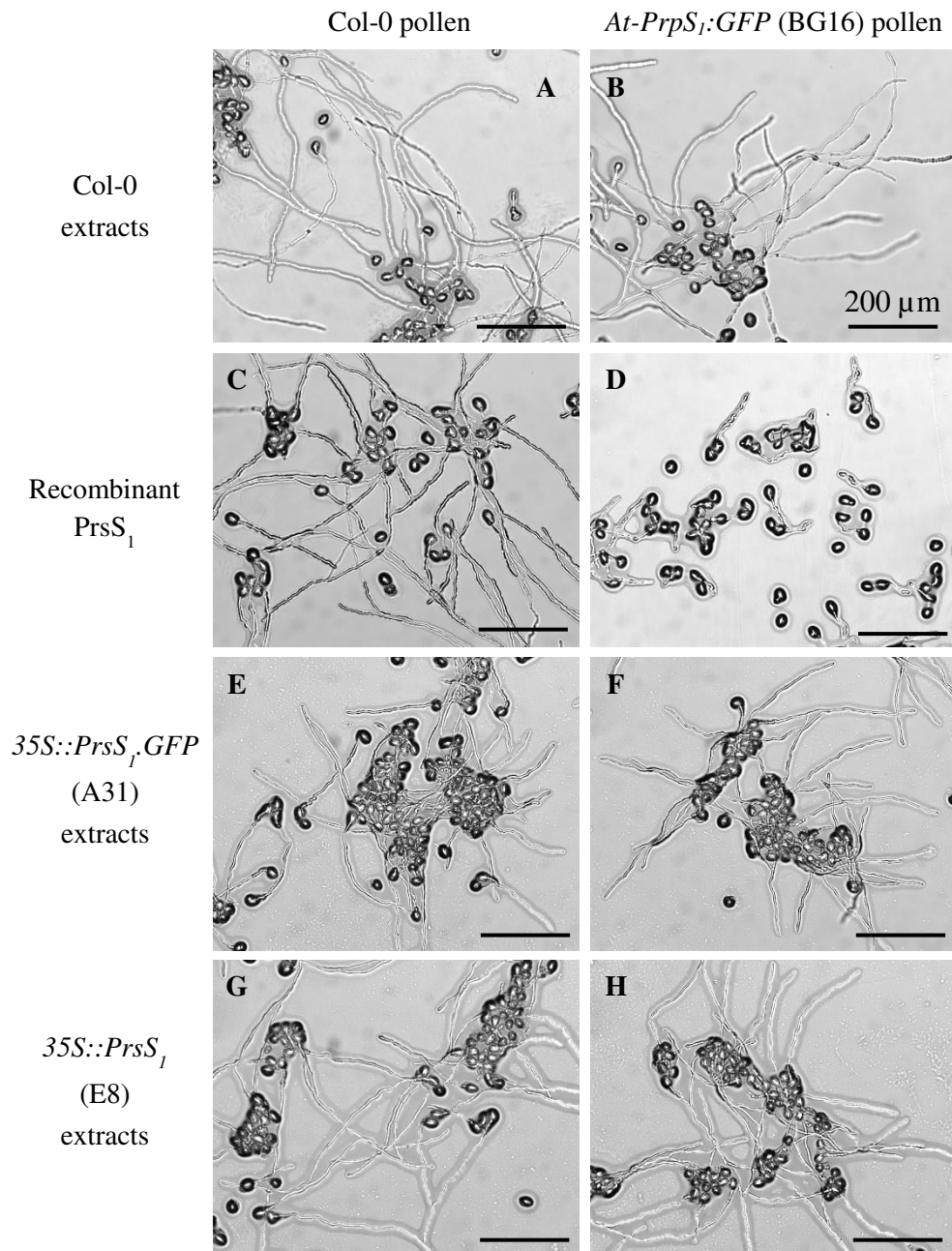


Figure 4-8 Constitutively expressed PrsS₁ in transgenic *A. thaliana* seedling extracts do not affect the growth of *At-PrpS₁:GFP* pollen

In vitro SI assays were carried out using *At-35S::PrsS₁:GFP.31* (A31) and *At-35S::PrpS₁.8* (E8) seedling extracts. Growth of Col-0 pollen on *AtGM* with Col-0 extracts (A), recombinant PrsS₁ protein (C), A31 extracts (E), and E8 extracts (G). Growth of BG16 pollen on solidified *AtGM* with Col-0 extracts (B), recombinant PrsS₁ protein (D), A31 extracts (F), and E1 extracts (H). Scale bars indicate 200 μm. Experiments were performed independently for three times.

As shown in Figure 4-8, both Col-0 and BG16 pollen germinated successfully on plates containing Col-0 extracts (Figure 4-8 A and B). Recombinant PrsS₁ protein did not affect the growth of Col-0 pollen (Figure 4-8-C), while the germination of BG16 pollen was almost completely blocked by recombinant PrsS₁ proteins treatment (Figure 4-8-D). These controls indicated that the *in vitro* SI assay system was technically working. Treatment of BG16 pollen with 250 µg seedling extracts from line A31 (Figure 4-8-E) or line E8 (Figure 4-8-G) had no obvious inhibition on the Col-0 pollen germination and growth. However, no significant differences were observed when BG16 pollen were treated with either seedling extracts from line A31 (Figure 4-8-F) or E8 (Figure 4-8-H), suggesting that constitutively expressed PrsS₁ and PrsS₁:GFP protein, even using as much as 250 µg total protein, was not functional in inhibiting the growth of BG16 pollen.

Of all of the key hallmark features of the poppy SI response, pollen tube growth inhibition is the easiest to be observed and measured. It has been described in Chapter 3 that pollen tube length had been established as the main parameter to assess the SI response in the *A. thaliana* pollen *in vitro* SI assay. Therefore, BG16 pollen tube lengths with or without addition of transgenic seedling extracts were measured 3 h after incubation, and the results are presented in Figure 4-9.

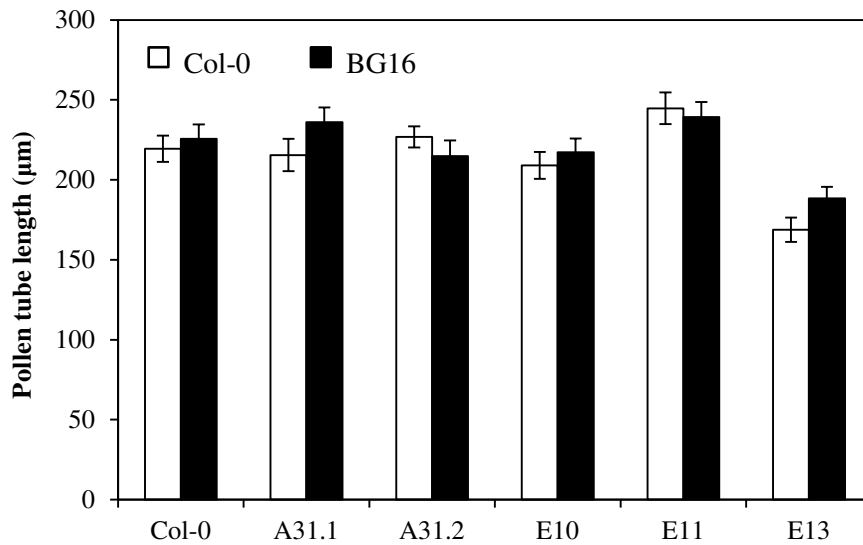


Figure 4-9 Constitutively expressed PrsS₁ in transgenic *A. thaliana* seedling extracts do not affect the *At-PrpS₁:GFP* pollen tube length *in vitro*

In vitro SI assays were carried out using transgenic seedling extracts. Pollen tube lengths were measured 3 h after incubation at 22 °C. Lengths of 100 pollen tubes from two independent experiments were recorded. White bars: Col-0 pollen. Black bars: BG16 pollen. Result= mean ±SE.

For Col-0 pollen tube lengths, one-way ANOVA analysis showed that there was no statistical difference between the Col-0 pollen tube lengths in *AtGM* containing extracts derived from Col-0, A31, or E10 seedlings ($p=0.387$). Differences in the Col-0 pollen tube lengths observed in different assays suggested the variations of the microenvironment of the *AtGM* plates. For example, pollen tube lengths in the presence of E11 extracts were significantly longer than those in the *AtGM* plate containing Col-0 extracts ($p<0.001$), while pollen tube lengths in the presence of E13 extracts were significantly shorter ($p<0.001$). As the differences of the mean pollen tube lengths grown on different plates accounted less than 10%, though they were statistically

different, the microenvironment of the plates did not seem to be too variable. In terms of BG16 pollen tube lengths, one-way ANOVA analysis showed a significantly decrease in pollen tube lengths in the presence of E13 extracts, which indicated that E13 extracts might inhibit the BG16 pollen tube growth. However, as Col-0 pollen tube length inhibition was also observed in the presence of E13, and a student's t-test showed no difference between the mean pollen tube lengths of Col-0 and BG16 pollen grown in the presence of E13 extracts. Thus the reduction in pollen tube lengths observed in the presence of E13 extracts was not due to BG16 pollen specificity. Therefore, no significant difference was observed between the Col-0 and BG16 pollen tube lengths when they were treated with Col-0 seedling extracts or transgenic seedling extracts constitutively expressing PrsS₁ and PrsS₁:GFP protein. This suggests that PrsS₁ and PrsS₁:GFP, even though they were constitutively expressed in the transgenic *A. thaliana* seedlings, were not able to inhibit the growth of *At-PrpS₁:GFP* pollen *in vitro*.

4.2.3.2 Testing the SI activities of *At-35S::PrsS:GFP* transgenic seedling extracts on poppy pollen

It had been demonstrated above that seedling extracts constitutively expressing PrsS₁ or PrsS₁:GFP had no significant inhibitory effect on the germination and growth of *At-PrpS₁:GFP* pollen. However, whether *At-35S::PrsS₁:GFP* transgenic seedling extracts could inhibit the germination and growth of poppy pollen was still not known, and this was investigated further.

Poppy pollen 442 (2013, S_1S_3) was germinated on poppy pollen GM containing A31 seedling extracts, or *At-35S::PrsS₃:GFP.8* (B8, the expression of PrsS₃:GFP protein in B8 had been demonstrated using western blot, data not shown) extracts, or A31 mixed with B8, and then pollen germination rates were recorded, as germination rate has long been established as a reliable parameter to assess the poppy pollen inhibition during the poppy pollen *in vitro* SI assay in the Franklin-Tong's lab. Results are shown in Figure 4-10.

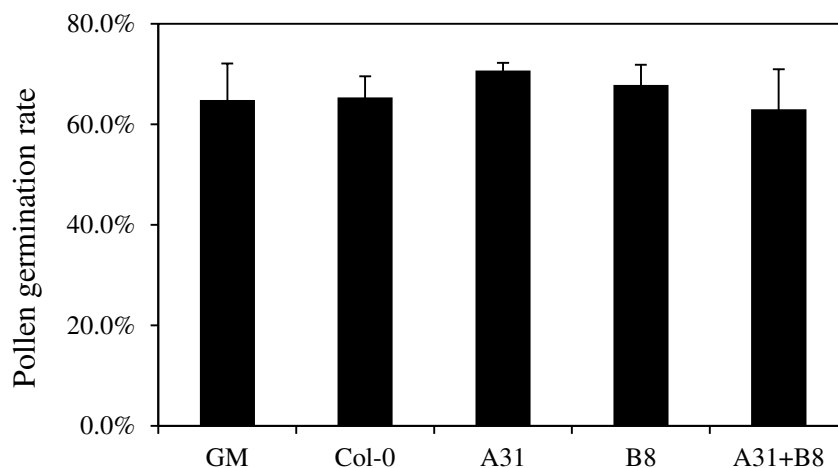


Figure 4-10 *At-35S::PrsS:GFP* seedling extracts do not affect the growth of poppy pollen

Poppy pollen (S_1S_3) *in vitro* SI assays were carried out using *At-35S::PrsS₁:GFP.31* (A31) and *At-35S::PrsS₃:GFP.8* (B8) seedling extracts. Poppy pollen germination rates were recorded 1.5 h after incubation. Result= mean \pm SD, n=3, at least 100 pollen tubes were recorded for each sample in each repeat.

As the poppy pollen is a mixture of equal amounts of two different *S*-haplotype pollen, seedling extracts from lines A31 or B8 were predicted to inhibit the germination in half of the pollen, and the combination of extracts from lines A31 and B8 was predicted to

result in the complete block of pollen germination if the *A. thaliana* expressed PrsS:GFP protein was biologically active. As shown in Figure 4-10, the pollen germination rates resulted from GM, Col-0 extracts, A31, B8, or even A31+B8 treatments were always around 60-70%, and there was no significant difference ($p=0.512$, One-way ANOVA analysis). This demonstrated that the PrsS:GFP protein expressed in A31 and B8 seedling extracts had no SI effects on poppy pollen tube growth *in vitro*.

4.2.4 Enrichment of PrsS₁:GFP protein by (NH₄)₂SO₄ precipitation

It has been demonstrated above that there was no inhibition on the growth of *At-PrpS₁:GFP* pollen or poppy pollen when they were treated with transgenic seedling extracts expressing PrsS₁ or PrsS₁:GFP protein. One of the possible reasons might be that the concentration of PrsS₁ or PrsS₁:GFP protein in the seedling extracts was not high enough to trigger SI response. Therefore, (NH₄)₂SO₄ precipitation experiments were carried out in an attempt to increase the PrsS₁:GFP protein concentration in seedlings extracts. (NH₄)₂SO₄ precipitation is widely employed in protein separation and purification, with the advantage that it does not affect the native structure and activities of proteins in most cases. As PrsS₁ antibodies were not able to detect PrsS₁ protein in the *At-35S::PrsS₁* transgenic seedlings, and without a proper method to detect the PrsS₁ protein, it was difficult to detect the enrichment. Thus, (NH₄)₂SO₄ precipitation experiments were carried out only with *At-35S::PrsS₁:GFP* seedling extracts (section 2.2.7), as a GFP antibody could be utilised to detect the PrsS₁:GFP

protein. Seedling extracts from line A31 were fractionated by increasing the concentration of $(\text{NH}_4)_2\text{SO}_4$ by adding saturated $(\text{NH}_4)_2\text{SO}_4$ (Figure 4-11-A).

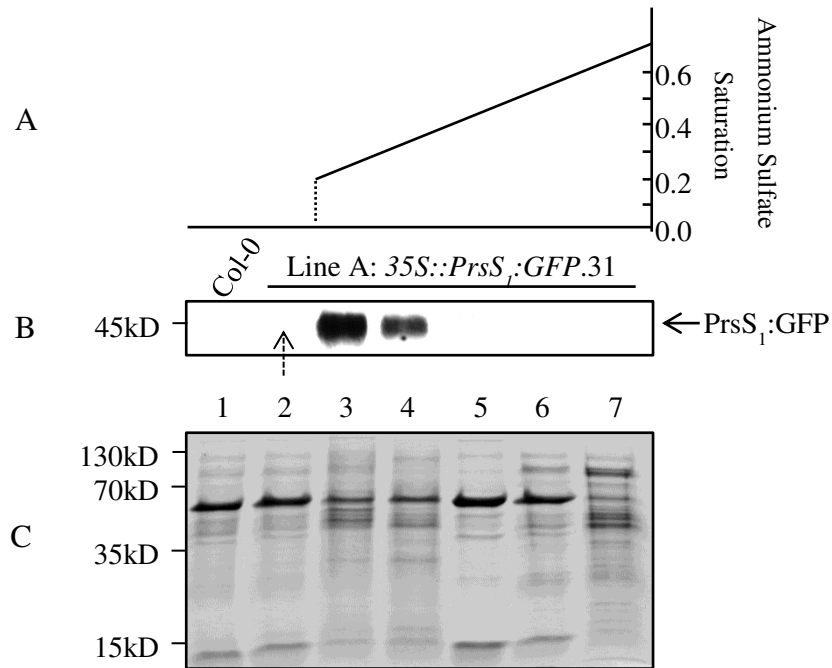


Figure 4-11 Separation and enrichment of PrsS₁:GFP by $(\text{NH}_4)_2\text{SO}_4$ precipitation

A: line A31 seedling extracts were fractionated by increasing the concentration of $(\text{NH}_4)_2\text{SO}_4$ by adding saturated $(\text{NH}_4)_2\text{SO}_4$. B: western blot was carried out with 10 μg of each fractionate using GFP antibody. C: coomassie blue staining. Signals of PrsS₁:GFP were indicated by black arrows. From left to right, the seven lanes represents: (1) Col-0 (without $(\text{NH}_4)_2\text{SO}_4$ precipitation), (2) line A31 (without $(\text{NH}_4)_2\text{SO}_4$ precipitation), (3) line A31 (20-30% $(\text{NH}_4)_2\text{SO}_4$ saturation), (4) line A31 (30-40% $(\text{NH}_4)_2\text{SO}_4$ saturation), (5) line A31 (40-50% $(\text{NH}_4)_2\text{SO}_4$ saturation), (6) line A31 (50-60% $(\text{NH}_4)_2\text{SO}_4$ saturation), (7) line A31 (60-70% $(\text{NH}_4)_2\text{SO}_4$ saturation), respectively. No Bradford assay detectable protein was found in the 0-20% $(\text{NH}_4)_2\text{SO}_4$ saturation fraction.

The fractions containing the highest concentration of PrsS₁:GFP proteins were investigated by western blotting using GFP antibodies. Figure 4-11-B shows that PrsS₁:GFP protein could only be detected in the fractions of 20-30% and 30-40% $(\text{NH}_4)_2\text{SO}_4$ saturation (lanes 3 and 4), and no PrsS₁:GFP protein was found in the

fractionates with 40-70% $(\text{NH}_4)_2\text{SO}_4$ saturation (lanes 5-7). These data indicated that PrsS₁:GFP could be enriched by ammonium sulphate precipitation. As the amount of protein in the 20-40% $(\text{NH}_4)_2\text{SO}_4$ saturated fractions (lanes 3 and 4) accounted for around 20% of total protein extractions, it was estimated that the PrsS₁:GFP was enriched nearly 5 times.

Ten μg of protein from each fraction were loaded onto SDS-PAGE gels. As shown in Figure 4-11-C, coomassie blue staining indicated that different fractions of A31 seedling extracts had different protein compositions, which demonstrated seedling extracts were separated by ammonium sulphate precipitation. Col-0 and A31 seedling extracts (without ammonium sulphate precipitation) were employed as negative and positive controls, respectively. However, unexpectedly, no PrsS₁:GFP signal was observed in the A31 seedling extracts (Figure 4-11-B), which seemed to contradict with the results shown Figure 4-3 and Figure 4-7. One possible explanation was that the A31 seedling extracts sample were placed in cold room overnight instead of -20°C before proceeding to western blot analysis. Thus it is possible that the PrsS₁:GFP protein might have degraded overnight while sitting in the cold room.

To investigate whether PrsS₁:GFP proteins were being degraded *in vitro* after being extracted, two-week old A31 seedlings were extracted using *At*GM as extraction buffer with or without adding protease inhibitor cocktail (Roche), followed by ammonium

sulphate precipitation and western blot analysis.

As shown in Figure 4-12-A, comparing the PrsS₁:GFP signals obtained from seedling extracts (Figure 4-12-A, lane 2), amounts of PrsS₁:GFP was observed to increase dramatically after ammonium sulphate precipitation in fractions with 20-40% saturation (Figure 4-12-A, lane 3), and no PrsS₁:GFP signal could be seen in fractions with 40-60% saturation (Figure 4-12-A, lane 4), regardless of whether the protease inhibitor cocktail was added or not (Figure 4-12-A, lanes 5-7). These results were consistent with what was seen in Figure 4-11.

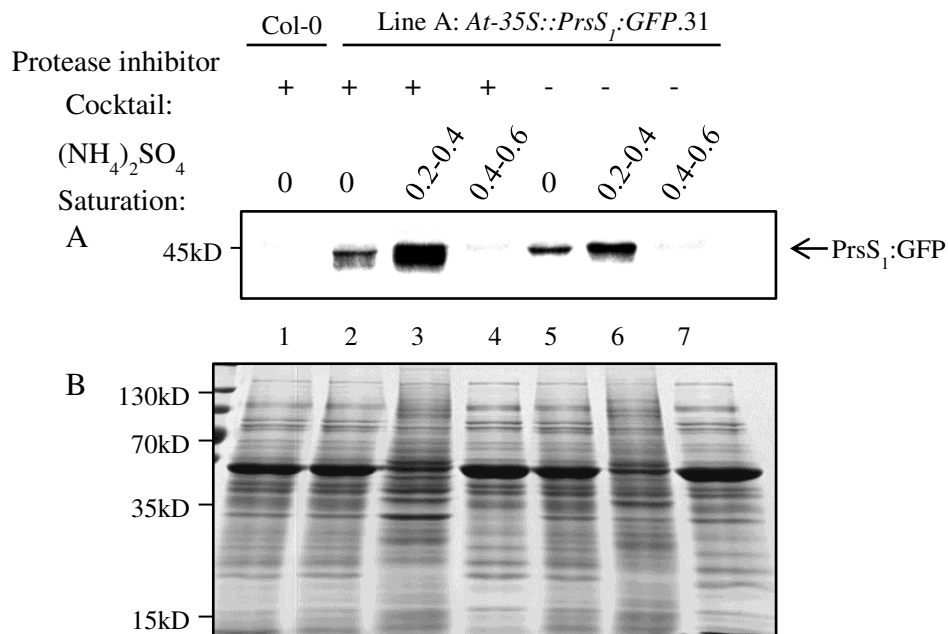


Figure 4-12 PrsS₁:GFP is under protease degradation *in vitro*

Protein extracts were obtained from A31 seedlings using extraction buffers with or without adding protease inhibitor cocktail (Roche), followed by saturated (NH₄)₂SO₄ precipitation. Western blot was performed with 10 µg of each fractionate using GFP antibody. Blot result (A) and coomassie blue staining (B) are shown above. Signals of PrsS₁:GFP are indicated by black arrows.

On the other hand, by comparing lane 2 with lane 5, lane 3 with lane 6 in Figure 4-12-A, higher PrsS₁:GFP signals were observed after adding protease inhibitor cocktail during seedling extraction and ammonium precipitation processes. This suggests that proteases are involved in the degradation of PrsS₁:GFP proteins *in vitro*, and this also potentially explains why no PrsS₁:GFP signal was observed when the whole seedling extractions were placed in cold room overnight (Figure 4-11-A).

To test the functionality of constitutively expressed PrsS₁:GFP protein from *A. thaliana* seedlings using the *in vitro* SI assay, it would be better if the PrsS₁:GFP protein could be enriched. Use of ammonium sulphate precipitation in the purification and enrichment of PrsS₁:GFP protein in seedling extracts demonstrated that the PrsS₁:GFP protein concentration was enriched nearly 5 times in the fraction of 20-40% ammonium sulphate saturation. However, for the *in vitro* SI assay, overnight dialysis against AtGM needed to be carried out after ammonium sulphate precipitation to remove the ammonium sulphate, which would inhibit pollen tube growth. But it had already been shown in this section that PrsS₁:GFP protein was under *in vitro* degradation after it was extracted from seedlings, and that leaving extracts overnight in cold room might result in the degradation of PrsS₁:GFP proteins. Thus, although (NH₄)₂SO₄ precipitation was able to improve the concentration of PrsS₁:GFP in the extracts, it was not considered feasible to be used in the *in vitro* SI assay and these experiments were not continued.

4.3 Discussion

In summary, data presented in this chapter aimed to establish whether *PrsS₁* could be expressed in *A. thaliana* and function to trigger SI response *in vitro*. *At-35S::PrsS_{1/3}:GFP* and *At-35S::PrsS_{1/3}* lines were produced and it was investigated whether constitutively expressed PrsS₁:GFP or PrsS₁ proteins by *A. thaliana* were able to inhibit the growth of *At-PrpS₁:GFP* or poppy pollen tubes was tested. It has been demonstrated in this chapter that *PrsS₁* mRNA could be successfully constitutively-expressed in *A. thaliana* under the direction of 35S promoter. Both western blot and microscopic analysis indicated the expression of PrsS₁:GFP protein in transgenic *A. thaliana* seedlings. However, the expression level of PrsS₁:GFP protein was low and was also observed undergoing proteasome degradation *in vivo*. Although there is no evidence showing the expression of PrsS₁ protein in the *At-35S::PrsS₁* transgenic seedlings, it was still considered that PrsS₁ protein was expressed. The reason why there was no PrsS₁ signal detected in the western blot using the PrsS₁ antibodies might be due to the low expression level of PrsS₁ protein, and the low sensitivity of PrsS₁ antibodies. No significant difference in the germination and growth of both *At-PrpS₁:GFP* pollen and poppy pollen was observed in the *in vitro* SI assays using either the *At-35S::PrsS₁* or *At-35S::PrsS₁:GFP* transgenic seedling extracts. Enrichment of PrsS₁:GFP proteins has been achieved by ammonium sulphate precipitation. In addition, it was demonstrated that PrsS₁:GFP protein expressed in transgenic seedlings

was apparently undergoing rapid degradation *in vitro* after being extracted. Below, various aspects of these studies are discussed.

4.3.1 The constitutive expression of *PrsS* mRNA in transgenic lines

The investigation of PrsS expression in plants other than *Papaver rhoeas* itself actually started as early as 20 years ago in the early 1990s when Foote tried to produce biologically active PrsS proteins from transgenic *N. tabacum* plants (Foote, 1993). PrsS was introduced into *N. tabacum* under the direction of 35S promoter, and Northern hybridization analysis showed the expression of *PrsS* mRNA in the leaf samples (Foote, 1993). Preliminary functional analysis using *in vitro* SI assay with tobacco leaf washes was also carried out, which suggested active PrsS proteins eluted from tobacco leaves (personal communication, Noni Franklin-Tong and Chris Franklin). The expression of *PrsS* in *A. thaliana* was also investigated. *PrsS*_{1/3} were introduced into *A. thaliana* under the direction of *Stig1*, which is a stigma specific promoter derived from *N. tabacum* (Goldman et al., 1994; Verhoeven et al., 2005), by Huawen Zou. The characterization of *At-Stig1::PrsS* transgenic lines were carried out by Sabina Vatovec (Vatovec, 2011). It was demonstrated by Sabina Vatovec that *PrsS* mRNA was specifically present in transgenic *A. thaliana* flowers, but western blots failed to detect any PrsS protein signal from 20-50 µg of flower protein extracts (Vatovec, 2011).

In order to investigate whether *A. thaliana* produced PrsS protein that was able to

trigger SI response, and thus ultimately establish in principle if PrsS was able to be function to inhibit the growth of *A. thaliana* pollen expressing PrpS, *PrsS* was introduced into *A. thaliana*. Due to the difficulties with obtaining large amounts of stigma tissue and the time taken both to get plants to flowering and to collect tissue material, the *35S* promoter, which is a constitutive promoter widely used in plant research, was chosen to direct the expression of *PrsS* in transgenic *A. thaliana*. This had the advantage of time saving and was less labour intensive by using whole transgenic seedlings, instead of stigmas, as the source of plant material for the *in vitro* SI assay. RT-PCR demonstrated the expression of *PrsS* mRNA in all the transgenic lines analysed. The observation that the expression level of *PrsS₁:GFP* mRNA in most of *At-35S::PrsS₁:GFP* lines were comparable with that of *GAPC* indicated the high expression of *PrsS* mRNA driven by *35S* promoter in transgenic plants. The detection of high *PrsS* mRNA levels in transgenic plants was a successful first step towards functional analysis of *A. thaliana* expressed *PrsS* *in vitro*.

4.3.2 The expression of PrsS protein in *A. thaliana* transgenic lines

The next step was to assess if the PrsS protein expression in transgenic *A. thaliana* was sufficiently high. The expression of PrsS/PrsS:GFP protein in both *At-35S::PrsS* and *At-35S::PrsS:GFP* transgenic lines was investigated by western blot analysis. A GFP signal band corresponding to the size of PrsS₁:GFP protein was specifically detected from the transgenic samples rather than the Col-0 control. This indicated that PrsS₁:GFP

protein was expressed in the transgenic *At-35S::PrsS₁:GFP* lines.

As it was still not known whether the GFP fusion might affect the biological activity of PrsS, *At-35S::PrsS* lines were also constructed for the functional analysis of *PrsS* in *A. thaliana in vitro*. Western blots using the anti-PrsS antibody were also carried out to characterize the expression of PrsS proteins in *At-35S::PrsS* transgenic lines. However, no PrsS protein signal was observed when up to 50 µg of total protein from transgenic seedling extracts was loaded. Preliminary experiments indicated that anti-PrsS antibody had a detection limit of 25 ng of recombinant PrsS proteins in western blot. The observation that no PrsS signal in the western blot indicated that either there was no PrsS protein expression in transgenic *At-35S::PrsS* lines, or that the expression of PrsS proteins accounted for lower than 0.05% of total seedling proteins, assuming that anti-PrsS antibody had the same affinity for recombinant PrsS proteins and *A. thaliana* produced PrsS proteins. Considering that we have obtained strong evidence (western blot and microscopic analysis) indicating the expression of PrsS:GFP protein in transgenic *At-35S::PrsS:GFP* lines, it was considered unlikely that there was no PrsS protein expression in *At-35S::PrsS* transgenic lines, but that the expression level was very low.

It was established by using the proteasome-specific inhibitor MG132 that PrsS was undergoing proteasomal degradation. PrsS:GFP protein abundance extracted from leaf

and root tissues of transgenic seedlings was significantly increased in the presence of MG132. This suggested that PrsS:GFP was under proteasomal degradation in *A. thaliana in vivo*. In addition, both western blot and microscopy indicated that PrsS:GFP protein preferentially accumulated in the roots. Thus, we have obtained good evidence suggesting PrsS:GFP protein was turned over *in vivo* in both roots and leaves, and the turnover of PrsS:GFP protein might be more rapid in leaves. These implicated that the expression of the transgene *PrsS* in *A. thaliana* was regulated, and at least part of the regulation was due to proteasomal degradation. This is the first evidence that the proteasome degradation system was involved in the PrsS expression.

The molecular mechanisms involved in mediating targeting of protein to the proteasome and the spatial distribution of PrsS:GFP proteins are still not known, but similar phenomena have been observed and reported in several studies. ABI4 (ABA-INSENSITIVE 4) is a transcription factor involved in maturing seeds and seedlings in response to ABA (Finkelstein et al., 2002). Finkelstein et al. (2011) demonstrated that ABI4:GFP fusions driven by 35S promoter were undetectable visually or immunologically in transgenic plants. Moreover, proteasomal degradation of ABI4:GUS fusion proteins and spatially preferential accumulation of ABI4:GUS in roots were also observed (Finkelstein et al., 2011). Another example comes from the expression of EC1:GFP in *A. thaliana* using 35S promoter. EC1 (EGG CELL 1) is a small cysteine-rich protein implicated in the sperm cell activation during double

fertilization in flowering plants (Sprunck et al., 2012). As with PrsS, EC1 is also a secreted protein, but secreted by the egg cell (Sprunck et al., 2012). When it is expressed as a GFP fusion in *A. thaliana* using the 35S promoter, no GFP signal could be observed visually, but MG132 treatment resulted in a dramatic accumulation of GFP signals in the vasculature part of seedling roots (personal communication, Stephanie Sprunck). These studies implicate that the expression of transgenes in *A. thaliana* was somehow regulated, and at least part of this regulation is due to proteasomal degradation. Thus, the involvement of proteasomal degradation in the constitutive transgene expression might be a more general mechanism than previously thought.

4.3.3 Functional analysis of constitutively expressed PrsS protein in *A. thaliana* *in vitro*

Functional analysis of *PrsS* in *A. thaliana* *in vitro* was firstly started by Sabina Vatovec using pistil extracts from *At-Stig1::PrsS* transgenic plants (Vatovec, 2011). Preliminary experiments showed that incubation of poppy pollen (S_1S_3) with *At-Stig1:PrsS₁* and *At-Stig1:PrsS₃* stigmatic extracts resulted in a significant reduction in pollen tube length (Vatovec, 2011). The pollen tube length inhibition suggested an inhibitory effect of PrsS₁ and PrsS₃ proteins in the stigmatic extracts on poppy pollen. However, quite a low number of pollen grains were counted during that experiment, and images provided for this experiment were not fully convincing. So, solid conclusions whether *A. thaliana* produced PrsS proteins were able to trigger SI response in poppy pollen could not be

finally made from these preliminary experiments, and further efforts were still needed. During the investigations presented in this chapter, functional analysis of PrsS in *A. thaliana in vitro* was carried out by incorporation of *At-PrsS* seedling extracts, instead of stigmatic extracts, in the SI assays *in vitro*. However, no *S*-specific inhibition of either poppy pollen or *At-PrpS:GFP* pollen was observed. Several reasons may account for this, and they are discussed below.

4.3.3.1 Is it possible that *A. thaliana*-expressed PrsS proteins have no biological activity?

Eukaryotic protein synthesis differs from prokaryotic protein synthesis in many aspects, for example, post-translational modification, which can dramatically increase the proteome diversification (Walsh et al., 2005). For the same target protein, the discrepancy between eukaryotic and prokaryotic protein biological activities is most likely due to the post-translational modification differences. A single potential N-glycosylation site is predicted at PrsS₁ (residue 51), and it has already been demonstrated at least a proportion of the mature PrsS₁ proteins are glycosylated in *Papaver rhoeas* (Foote et al., 1994). However, there is no N-glycosylation presented in the *E. coli* recombinant PrsS₁ proteins. Despite this difference, no distinguishable difference was observed between authentic PrsS₁ and *E. coli* produced PrsS₁ proteins regarding either their biological activities or specificities, which demonstrated that small modification in the N-terminus did not affect, and presumed post-translational

processing of PrsS proteins was not absolutely required for either biological activity or specificity (Foote et al., 1994). In addition, definitive evidence that *Drosophila* produced PrsS protein was able to inhibit poppy pollen growth and trigger *in vitro* SI response in an S-specific manner was obtained (Lin et al., unpublished). Therefore, the demonstration that recombinant PrsS proteins produced in both *E. coli* and *Drosophila* have biological activities suggests that it is unlikely that *A. thaliana* produced PrsS proteins are inactive.

4.3.3.2 It is more likely due to the low expression level of constitutively-expressed PrsS protein in *A. thaliana*

A more likely explanation for the failure to obtain BG16 pollen tube inhibition using constitutively expressed PrsS protein in *A. thaliana* is that the amount of protein produced was very low. Regarding the comparison between PrsS protein produced by *Papaver rhoeas* and *A. thaliana*, the abundance of PrsS protein was estimated to be around 0.5-1% of total protein in the stigmatic papillae (Foote et al., 1994). It has been estimated that the amount of PrsS protein produced constitutively in *A. thaliana* accounted for less than 0.05% of total seedling protein (section 4.3.2). This suggests that transgenic *At-PrsS* seedling-produced PrsS protein needs to be at least 10-fold more active than native PrsS produced in poppy stigmatic papillae to enable it to trigger the poppy pollen SI response *in vitro*. In the other words, assuming that PrsS protein expressed in the transgenic *A. thaliana* seedlings is as active as native PrsS proteins,

then, new transgenic lines with much higher PrsS protein expression levels would need to be screened for use in inhibition of poppy pollen growth in the *in vitro* SI assay.

Due to the low abundance of PrsS:GFP protein observed in transgenic seedling tissues, ammonium sulphate precipitation was carried out in an attempt to enrich and concentrate the PrsS:GFP protein in transgenic seedling extracts. It was observed that PrsS:GFP fusions in the 20-40% fractions of ammonium sulphate saturation were 5 times more concentrated than in un-concentrated seedling extracts. This suggested that PrsS:GFP could be partly purified by ammonium sulphate precipitation and this could potentially be employed in the *in vitro* SI assay to increase the concentration of PrsS protein in the crude seedling extracts. However, during the ammonium precipitation experiments, it was also found that PrsS:GFP fusions were subject to rapid degradation after extraction. Overnight incubation of extracts in the cold room resulted in the complete disappearance of the fusion protein. Employment of protease cocktail inhibitors during the extraction and precipitation processes significantly reduced the degradation of PrsS:GFP fusions, which implicated that endogenous proteases in the extracts played a substantial role. By demonstrating that PrsS:GFP protein was undergoing rapid degradation, the ammonium sulphate precipitation experiments partly explained why there was no inhibition on the growth of *At-PrpS₁:GFP* pollen or poppy pollen when they were treated with transgenic seedling extracts containing PrsS or PrsS:GFP protein expressed in *A. thaliana*.

Although ammonium sulphate precipitation could effectively enrich the PrsS:GFP protein, it is still not known yet whether this could be used for the *in vitro* SI assay involving overnight dialysis, as whether the proteases are co-purified with PrsS:GFP protein during ammonium sulphate precipitation has still not been investigated. Another approach which might be used to avoid PrsS:GFP protein degradation during dialysis is the rapid buffer exchanging system. This system might make it possible to employ ammonium sulphate precipitation in the *in vitro* SI assay to increase the concentration of PrsS protein in the crude seeding extracts. However, at the time these experiments were carried out, this possibility was not followed up due to limited time remaining.

4.3.4 Summary

In summary, in this chapter it has been demonstrated that *PrsS/PrsS:GFP* could be constitutively expressed in transgenic *A. thaliana* directed by the 35S promoter. Good evidences have been obtained indicating the successful expression of PrsS:GFP protein. However, it was not possible to demonstrate whether constitutively expressed PrsS:GFP in *A. thaliana* could functionally induce the SI response *in vitro*. The *in vitro* demonstration of PrsS:GFP functionality was overtaken by other studies, and in the following chapter, work which demonstrated that PrsS can be functionally expressed in *A. thaliana in vivo* will be presented.

**CHAPTER 5 FUNCTIONAL ANALYSIS OF
PRSS AND *PRPS* IN *A. THALIANA IN VIVO*
AND GENERATION OF
SELF-INCOMPATIBLE *A. THALIANA* BY
TRANSFER OF THE *PAPAVER* SI SYSTEM**

5.1 Introduction

It has been demonstrated that *PrpS:GFP* can be expressed in *A. thaliana* pollen, and *PrpS:GFP* expressed in transgenic *A. thaliana* pollen is functional enough to trigger a “*Papaver*-like” SI response in incompatible pollen, when challenged by cognate recombinant PrsS proteins, resulting in the pollen tube growth inhibition and PCD (de Graaf et al., 2012; Chapter 3). It is of considerable interest to establish whether *At-PrpS:GFP* pollen could be inhibited *in vivo* by PrsS expressed in *A. thaliana*.

Functional analysis of *PrpS* and *PrsS* in *A. thaliana in vivo* had been previously carried out by Dr. Barend de Graaf and Dr. Sabina Vatovec (Vatovec, 2011). New transgenic lines *At-Stig1::PrsS* were constructed through transformation of the *Papaver* female *S*-determinant, *PrsS*, into *A. thaliana* under the direction of a stigma-specific promoter, *Stig1*. After confirming the expression of *PrsS* transcript in the stigma of transgenic *A. thaliana*, *At-PrpS:GFP* pollen was pollinated onto *At-Stig1::PrsS* stigma followed by aniline blue staining and seed set analysis. Aniline blue staining showed that the normal growth of *At-PrpS:GFP* pollen tubes was not affected in *At-Stig1::PrsS* pistil. Seed set analysis showed that there was no significant difference in the silique length or seed number compared with that of control. This indicated that *Stig1* directed expression of PrsS in transgenic *A. thaliana* was not functional enough to inhibit the growth of *At-PrpS:GFP* pollen. One of the possible reasons involved might be due to that *Stig1* directed a low expression level of PrsS in the mature stigma.

Stig1 is a stigma specific gene first identified in tobacco (*Nicotiana tabacum*), encoding a cysteine-rich 12 kD protein, expressed in the stigma secretory region (Goldman et al., 1994; Verhoeven et al., 2005). The expression of *Stig1* is developmentally regulated at the transcriptional level. It has been demonstrated that the *Stig1* transcript is highly expressed in very young and developing flowers, but little *Stig1* mRNA can be detected in the mature flowers (Goldman et al., 1994; Verhoeven et al., 2005). The *stig1* promoter had also been demonstrated to be functional in the distantly related species *A. thaliana*, and is likely to have a similar expression pattern as it has in tobacco (Goldman et al., 1994). This suggested that the expression level of PrsS protein in the mature *At-Stig1::PrsS* stigma was very low. Thus, failure to achieve SI response in transgenic *A. thaliana* stigma was likely to be due to the low expression level of PrsS protein in the mature stigma, instead of the expression itself. Therefore, it was concluded that the *Stig1* promoter might not be a suitable promoter for *in vivo* analysis of *PrpS* and *PrsS* in *A. thaliana*.

To establish whether PrsS expressed in the transgenic *A. thaliana* is functional in inhibiting *At-PrpS:GFP* pollen *in vivo*, we then had to choose an alternative stigma-specific promoter that can drive high expression of PrsS in the mature flowers. *S-locus-related gene 1 (SLR1)* was thought to be a good choice due to its stigma-specific and developmentally regulated expression pattern. It was identified in the genetic analysis of the *Brassica S*-locus searching for genes specifically involved in

the pollen-pistil interaction (Lalonde et al., 1989; Trick, 1990; Trick and Flavell, 1989). It has been shown that it was not *S*-locus linked (Lalonde et al., 1989) and played a dispensable role in both *Brassica* SI rejection and self-compatible pollination processes (Franklin et al., 1996). However, expression analysis demonstrated that *SLRI* was temporally regulated and specifically expressed in the prominent papilla cells as other *S*-locus-specific genes like *SLG* (Lalonde et al., 1989). Its maximal expression appeared at the mature flower, which is the same stage of flower development as the onset of the SI response (Lalonde et al., 1989). In addition, transgenic analysis showed that *SLRI* promoter directed a stigma specific, high-level, and developmentally regulated expression of an exogenous gene in both tobacco (Hackett et al., 1996, 1992) and *A. thaliana* (section 5.2.2), suggesting the *SLRI* promoter might be a suitable robust stigma-specific promoter. Therefore, we chose the *SLRI* promoter in this research to drive the expression of *PrsS* in *A. thaliana* in the stigma.

In the work presented in this chapter, new transgenic lines, *At-SLRI::PrsS* and *At-SLRI::PrsS::GFP*, were generated in an attempt to obtain developmental specific and tissue specific expression of *PrsS* in the stigma of *A. thaliana* at the correct stage. Analysis of the expression of *PrsS* driven by *SLRI* promoter in *A. thaliana* and investigation into whether it was functional will also be described in this chapter. To test whether *A. thaliana* expressed PrsS protein was able to trigger the SI response, first *semi-in-vivo* pollination assays and then subsequently *in vivo* pollinations were carried

out, with analysis of pollen tube lengths, silique lengths and seed set. Finally, attempts to generate self-incompatible *A. thaliana* by transformation of homozygous *At-ntp303::PrpS:GFP* plants with *SLR1::PrsS* were also carried out and will be described here.

5.2 Results

In order to test whether *PrpS* and *PrsS* were functional enough to trigger SI response in *A. thaliana in vivo*, the *SLR1* promoter, which could direct its downstream gene expression in a stigma specific and developmentally regulated manner, was employed to drive the expression of *PrsS* in *A. thaliana*. Binary Ti vectors containing chimeric *SLR1:PrsS* or *SLR1:PrsS:GFP* gene were constructed first, followed by transgenic *A. thaliana* lines building and screening.

5.2.1 Construction of transgenic lines expressing stigma specific *PrsS* driven by the *SLR1* promoter

In contrast to the *Stig1* promoter, instead of having the peak expression at the early developmental stage of stigma, *SLR1* shows its highest expression when the stigma reaches maturity. Therefore, we constructed some new transgenic *A. thaliana* lines using the *SLR1* promoter to obtain stigma-specifically expressed *PrsS* for functional analysis of poppy SI determinants in *A. thaliana in vivo*.

Table 5-1 details the information related to the *SLR1* promoter-directed transgenic lines

generated for the *in vivo* analysis of *PrsS* in *A. thaliana* in this study. Three different categories of transgenic lines were constructed: (1) *At-SLR1::PrsS*, (2) *At-SLR1::PrsS::GFP*, and (3) *At-SLR1::GFP* (Table 5-1; see section 2.3.1 for detailed technical information related to the vector construction, *Agrobacterium*-mediated transformation and transgenic seed screening).

Table 5-1 Transgenic lines built for functional analysis of stigma specific expressed *PrsS* in *A. thaliana* *in vivo*

<i>Line name</i>	<i>Promoter::DNA fragment</i>	<i>Resistance</i>	<i>Independent T₁ transformants generated</i>
<i>M</i>	<i>SLR1::GFP</i>	<i>BASTA</i>	22
<i>L</i>	<i>SLR1::PrsS₁::GFP</i>	<i>BASTA</i>	33
<i>P</i>	<i>SLR1::PrsS₃::GFP</i>	<i>BASTA</i>	13
<i>K</i>	<i>SLR1::PrsS₁</i>	<i>BASTA</i>	12
<i>Q</i>	<i>SLR1::PrsS₃</i>	<i>BASTA</i>	13

For functional analysis of *PrsS* in *A. thaliana* *in vivo*, analysis of *PrsS* expression at the mRNA, protein level and its localization, in transgenic *A. thaliana* was a very important step. Construction of *At-PrsS::GFP* line would facilitate the characterization of *PrsS* expression by making use of the *GFP* fusion tag as this is an easy marker to detect. As knowledge related to the expression and interaction between *PrsS* and *PrpS* was limited, and whether transgenic lines comprising *GFP* fusion to the C-terminus of *PrsS* would affect the expression, targeting or interaction was still unknown, additional *At-SLR1::PrsS* transgenic lines without the *GFP* tag were also generated. The transgenic

line *At-SLR1::GFP* was also constructed to analyse the expression pattern of the *SLR1* promoter in *A. thaliana*. At least 10 independent T₁ transformants were obtained for each construct for further analysis.

5.2.2 Analysis of the *SLR1* promoter expression pattern in *A. thaliana*

SLR1 is a developmentally regulated and papilla cell-specific promoter identified in *Brassica oleracea* (Lalonde et al., 1989). Although it was thought that *SLR1* might be a suitable promoter for directing the expression of *PrsS* in *A. thaliana*, expression pattern of the *SLR1* promoter in *A. thaliana* was still unknown. Therefore, analysis was necessary to establish this. The transgenic line M (*At-SLR1::GFP*) was generated to confirm the temporal and tissue specific expression pattern of the *SLR1* promoter in *A. thaliana*. To determine the expression of the *SLR1* promoter in *A. thaliana*, RNA isolated from staged pistils, stamens, petals or leaves were subjected to RT-PCR analysis (Figure 5-1; section 2.3.3). As shown in Figure 5-1, the transcripts of *GFP* increased in the pistil tissue during flower maturation, and were sustained at a relatively high level in the mature flowers. Col-0 RNA and water were employed as negative controls, indicating the authenticity of signals detected. No amplification of *GFP* cDNA was observed in the stamen, petals, or leaves. Constant *GAPC* signals suggested equal loadings. This demonstrated the tissue specific and developmentally regulated expression pattern of *SLR1* promoter in *A. thaliana*.

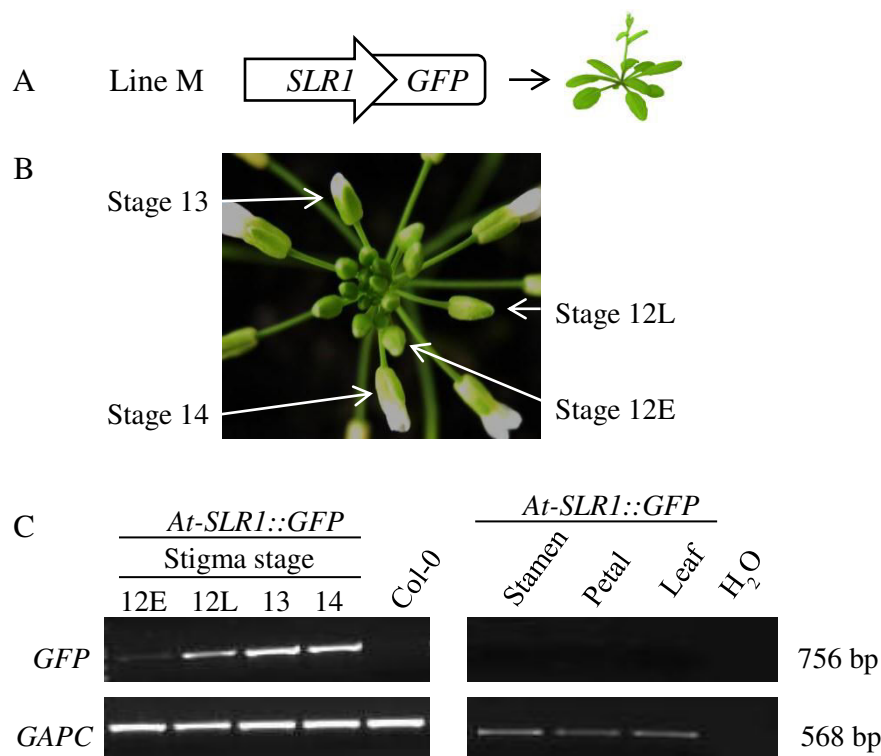


Figure 5-1 *SLRI* is expressed in a stigma specific and developmentally regulated manner in transgenic *A. thaliana*

A: cartoon of *At-SLRI::GFP* transgenic line. B: indication of bud stages of pistils (Smyth et al., 1990). C: RNA purified from staged pistils, as well as stamens, petals, or leaves were subjected to RT-PCR analysis of GFP expression. Col-0 RNA and water were negative controls. GAPC was employed as the internal reference gene. E: early. L: late.

In the younger buds (stage 12E), when the stigmas were still self-compatible, a very low level of *GFP* expression was detectable by RT-PCR (Figure 5-1-C). A significant increase of *GFP* expression was observed one day before anthesis (stage 12L; Figure 5-1). This is when buds became self-incompatible in *B. oleracea*. Sustained high levels of *GFP* expression could be detected during the periods when the buds were self-incompatible (stages 12L, 13, 14; Figure 5-1-C). Though *SLRI* has been demonstrated not to be *S*-locus linked, its expression pattern coincided exactly with the

development of SI phenomenon in *Brassica oleracea* (Lalonde et al., 1989). The expression pattern observed here in *A. thaliana* is identical to that in *B. oleracea*.

The expression of GFP protein in *At-SLR1::GFP* transgenic lines was examined using GFP fluorescence microscopy (section 2.3.2). As shown in Figure 5-2 A and B, hardly any GFP signal was observed in both early (11-E) and late phases of stage 11 stigma (11-L; 3 days before anthesis), when stigmatic papillae had just appeared (Smyth et al., 1990). Low levels of GFP signal were first observed in the stigmatic papilla cells during the early phase of stage 12 (12-E), which was around 2 days before anthesis, and no signal could be observed in the style (Figure 5-2 C). GFP signals increased dramatically during the development of papilla cells (Figure 5-2 C, D, E, F), and reached a maximum in the mature buds (stage 13, Figure 5-2 F). The development of GFP signals observed here correlated well with data from RT-PCR of *GFP* mRNA from developing pistils. Col-0 stigmas were visualised under GFP fluorescence microscopy with the same settings, and no GFP signal was observed (data not shown), indicating the GFP signals observed in Figure 5-2 were authentic.

These results demonstrated that the expression of *SLR1* promoter in *A. thaliana* occurred in the stigmatic papilla cells, and this expression was temporally controlled during the development of the stigma. This tissue specific and developmentally regulated expression pattern of *SLR1* in *A. thaliana* made it an ideal promoter to direct

the expression of *PrsS* for its functional analysis in *A. thaliana in vivo*.

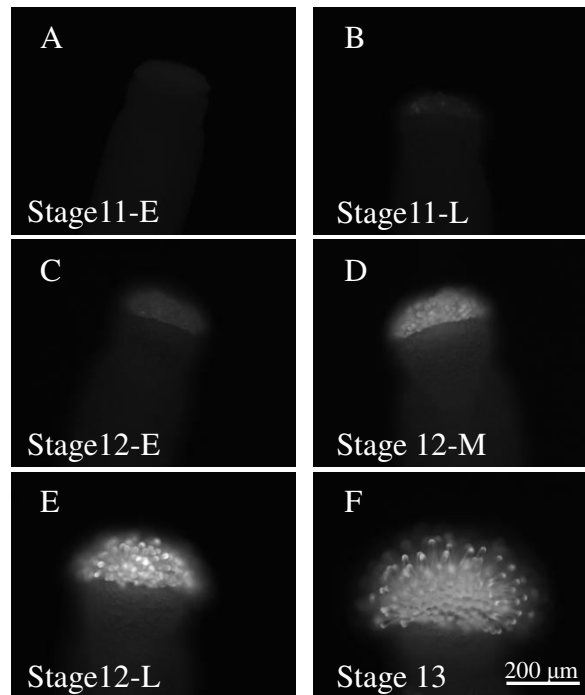


Figure 5-2 *SLRI* promoter directs downstream gene expressed in a developmentally controlled manner

Staged *At-SLRI::GFP* pistils were checked using GFP fluorescent microscopy. GFP signals were only observed in the papilla cells of stigma, and the observed GFP signals were temporally regulated during stigma development. GFP signal was hardly seen in stage 11, including both early phase (A) and late phase (B). Low level GFP signal was not observed in the stigmatic papilla cells until the early phase of stage 12 (C). GFP signals increased dramatically along with the development of papilla cells (C, D, E, F), and reached a maximum in the mature buds (stage 13, F). Scale bar indicates 200 μm. E: early. M: middle. L: late.

5.2.3 Set up of a *semi-in-vivo* pollination assay: germination and growth of *A. thaliana* Col-0 pollen on Col-0 pistil

In order to investigate whether the *A. thaliana* stigma expressing *PrsS* is functional enough to inhibit *At-PrpS::GFP* pollen *in vivo*, a *semi-in-vivo* pollination assay in which *A. thaliana* Col-0 pollen could germinate and grow normally on the Col-0 pistil was

developed. The development of a robust bio-assay that could be routinely applied for *semi-in-vivo* pollen germination and growth studies was very important. This is fully described in section 2.3.4, but briefly, pistils were collected from plants, emasculated, vertically placed in the agarose covered tissue culture plate, and pollinated with pollen for germination and pollen tube growth. Key adjustments comprised controlled temperature, humidity, light intensity and airflow for pollen germination and pollen tube growth *semi-in-vivo*. Specimen fixation and staining for microscopic visualization were also optimized to improve the assessment of the *semi-in-vivo* *A. thaliana* pollination. A time-series of *semi-in-vivo* germination and growth of Col-0 pollen on Col-0 stigmas under the optimized conditions are shown in Figure 5-3.

Pollen tubes could be observed as early as 30 minutes after pollination (Figure 5-3 A), indicating the rapid germination of pollen grains after landing on the stigma. A higher pollen germination rate and longer pollen tube lengths were observed 50 minutes after pollination (Figure 5-3 B). Figure 5-3 C-F shows that the longer pollen was left on the stigma, the longer pollen tube lengths were observed. The time-dependent *semi-in-vivo* growth of pollen was even more evident when the lengths of pollen tube bundles were quantitatively evaluated (Figure 5-3 G). Pollen tubes reached lengths of around 600 μm after 130 minutes incubation under optimal conditions, with an average growth speed of 270 $\mu\text{m h}^{-1}$ in the first two hours post pollination, which was markedly faster than those *in vitro* growth speeds that have been reported (Boavida and McCormick, 2007; Fan et

al., 2001; Rodriguez-Enriquez et al., 2013).

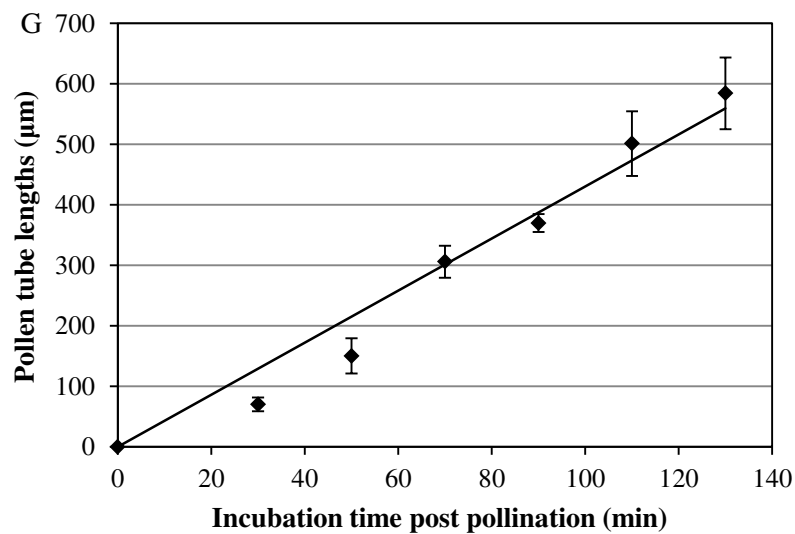
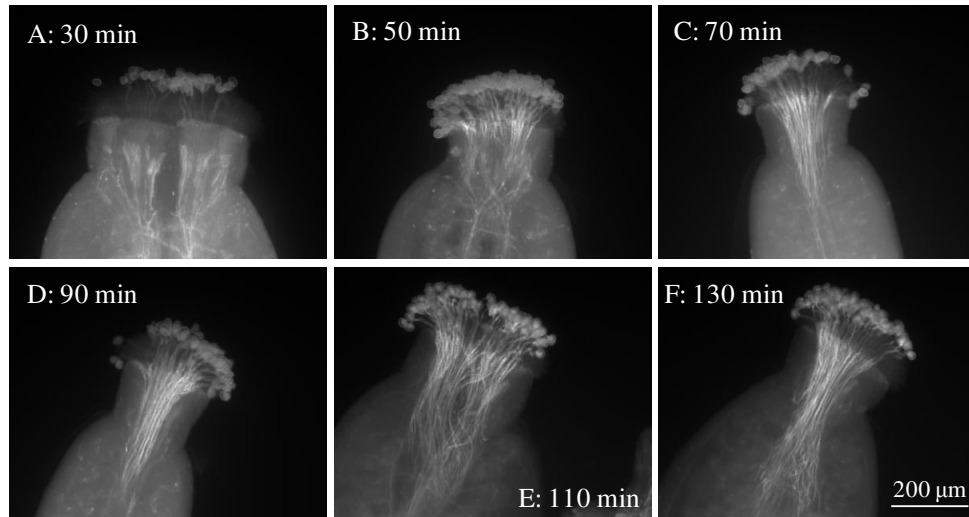


Figure 5-3 Germination and growth of Col-0 pollen on Col-0 stigma *semi-in-vivo*

Col-0 pollen showed a time-dependent semi-in-vivo germination and growth on Col-0 stigma under optimal conditions revealed by aniline blue staining and UV fluorescent microscopic analysis. Pollen germination and tube growth was first checked 30 minutes after pollination, and then every 20 minutes. A: pollen tubes could be observed as early as 30 minutes after pollination. B-F: the longer pollen was left for growth after pollination, the longer lengths of pollen tubes were observed. G: quantitative evaluation of pollen tube lengths. Result= mean \pm SD; 4 independent pollination experiments were performed. White bar indicates 200 μ m.

By optimizing various experimental conditions, the *semi-in-vivo* pollen germination and tube growth, as well as sample preparation for microscopic visualisation was substantially improved. The successful development of this experimental procedure provided a very good platform for the investigation of the interaction between *A. thaliana* stigma expressing PrsS and pollen expressing PrpS.

5.2.4 Functional analysis of *At-SLR1::PrsS:GFP* transgenic lines *in vivo*

Having established that the *SLR1* promoter was expressed exclusively in the stigmatic papilla cells in *A. thaliana* in a developmentally regulated manner, and a reliable *semi-in-vivo* pollination assay had been developed, further transgenic lines *At-SLR1::PrsS:GFP* (line L) and *At-SLR1::PrsS* (line K) (Figure 5-4) were analysed and the results are presented here.

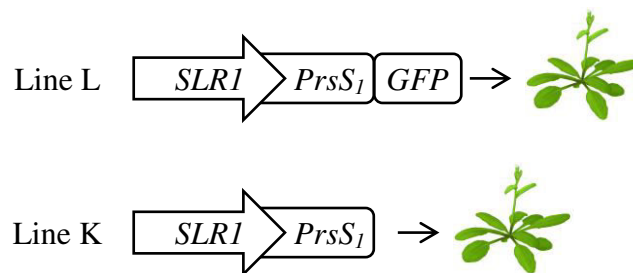


Figure 5-4 Cartoon of *At-SLR1::PrsS₁:GFP* and *At-SLR1::PrsS₁* transgenic lines

5.2.4.1 Analysis of PrsS:GFP protein expression in *At-SLR1::PrsS:GFP* transgenic lines

To analyse the expression of PrsS:GFP protein in *At-SLR1::PrsS:GFP* transgenic lines,

western blotting (Figure 5-5) and GFP fluorescence microscopic visualisation (Figure 5-6) were both employed. In order to check the expression of PrsS:GFP protein in transgenic *A. thaliana*, stage 13 pistils were collected from 5 different *At-SLRI::PrsS₁:GFP* transformants, from which proteins were extracted and subjected to western blot analysis using anti-GFP antibodies (Figure 5-5).

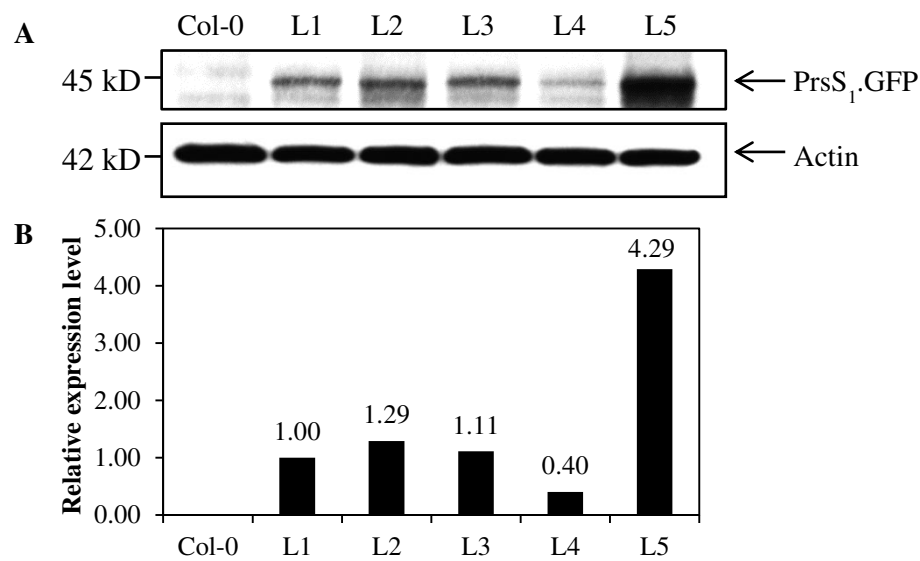


Figure 5-5 PrsS₁:GFP protein is expressed in *At-SLRI::PrsS₁:GFP* pistils

At-SLRI::PrsS₁:GFP pistils were subjected to western blot analysis using anti-GFP antibody. Col-0 was the negative control. A: PrsS₁:GFP signals were observed in all the 5 samples analysed, whereas no band was detectable for Col-0 sample. Actin was probed to show the equal loading. B: quantification of the band intensities using Quantity-One software.

As shown in Figure 5-5-A, clear GFP signals were observed in all the 5 samples analysed, whereas no band was detectable in the Col-0 sample. These GFP signals migrated to ~45 kD, which is what we would predict from a product of PrsS:GFP fusion protein [44.6 kD= 14.0 kD (PrsS₁) + 2.2 kD (linker)+ 28.4 kD (GFP)]. Therefore, these

GFP signals were considered to be derived from PrsS₁:GFP proteins. Actin was probed to show equal loading (Figure 5-5-A). The relative PrsS₁:GFP protein expression level between each transformants was evaluated by quantification of the target band intensities (Figure 5-5-B), in which the PrsS₁:GFP protein expression level in line L1 was normalized as 100%. The abundance of PrsS₁:GFP protein varied in different transformants. The highest PrsS₁:GFP protein expression was observed in lines L5. Lines L1, L2 and L3 showed similar and lower expression levels. The lowest expression was found in line L4, in which the PrsS₁:GFP protein abundance only accounted for less than 10% of that of line L5. This demonstrated that *PrsS₁:GFP* transcripts could be successfully translated into PrsS₁:GFP protein in the stigma of transgenic *A. thaliana*, and the expression level of PrsS₁:GFP protein in different transgenic lines was varied.

The expression of PrsS₁:GFP protein in *A. thaliana* was also visualised using GFP fluorescence microscopy. A representative image of *At-SLR1::PrsS₁:GFP* (L5) pistil under GFP fluorescence microscopy is shown in Figure 5-6, together with images of Col-0 and *At-SLR1::GFP* (M3) pistils, which were negative and positive controls of GFP signals respectively. As shown in Figure 5-6, no GFP signal was observed in the stigmatic papilla cells of both *At-SLR1::PrsS₁:GFP* (Figure 5-6 A) and Col-0 (Figure 5-6 B) pistils, whereas strong GFP signals were detected in the stigma of *At-SLR1::GFP* transgenic plants (Figure 5-6 C).

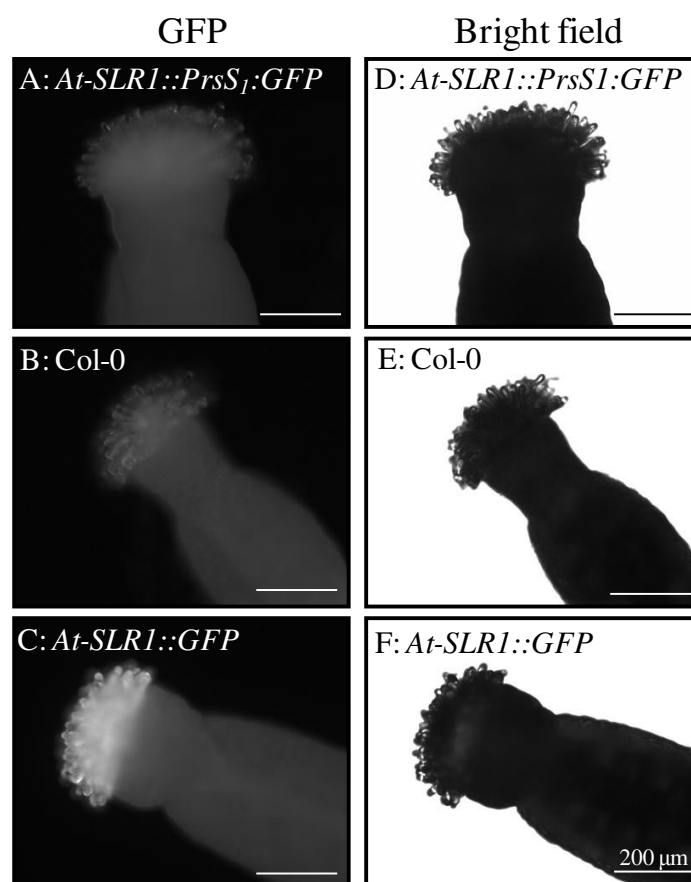


Figure 5-6 No GFP can be observed in transgenic *At-SLR1::PrsS₁:GFP* stigma using fluorescent microscopy

Stage 13 pistil samples collected from *At-SLR1::PrsS₁:GFP*, Col-0 and *At-SLR1::GFP* were checked using GFP fluorescent microscopy. A: no GFP signal was detectable in the stigma of *At-SLR1::PrsS₁:GFP* (L5) transgenic plants. B: Col-0 stigma was checked as negative controls. C: stigma of *At-SLR1::GFP* (M3) transgenic plant was employed as positive control of GFP signals. Clear GFP signals were observed in the stigmatic part of the pistil. D-F showed the bright field image of each pistil checked. Bar indicates 200 μ m.

Thirty-three independent *At-SLR1::PrsS₁:GFP* transformants were obtained (Table 6-1), and pistil samples from all the 33 transformants were checked using GFP fluorescence microscopy. However, it was found that GFP signals were absent in all the stigmas derived from those 33 independent transformants. Western blots had confirmed the expression of PrsS₁:GFP protein in the transgenic *A. thaliana* stigmas, but no GFP

signal could be observed using GFP fluorescence microscopy. One of possible reasons might be the secretion of PrsS₁:GFP protein by the stigmatic papilla cells. PrsS₁ is a small, secreted protein expressed in the poppy papilla cells (Foote et al., 1994). There is a 19-residue putative signal peptide at the N-terminal of PrsS₁ (Foote et al., 1994). So, PrsS₁:GFP expressed in the *A. thaliana* stigma would also be expected to be secreted into the extracellular matrix of papilla cells, where the low pH could result in the quenching of GFP signals (Patterson et al., 1997). So, from another perspective, the absence of GFP signals in the PrsS₁:GFP expressing stigma, which was confirmed by Western blot, indirectly suggested the proper secretion of PrsS₁:GFP in the transgenic *A. thaliana* stigma.

Having established that all the five different *At-SLR1::PrsS₁:GFP* transgenic lines expressed PrsS₁:GFP protein, but in a very variable manner, these lines were subjected to further functional analysis to investigate whether PrsS:GFP protein expressed in the stigma of *A. thaliana* was able to inhibit the growth of *At-PrpS1:GFP* pollen *in vivo*.

5.2.4.2 Functional analysis of *A. thaliana* expressed PrsS:GFP protein using *semi-in-vivo* pollination assay

Semi-in-vivo pollinations were carried out to investigate whether *PrsS₁:GFP* expressed in transgenic *Arabidopsis* was functional enough to trigger the inhibition of *At-PrpS₁:GFP.25* (BG16.25, hereafter referred to as BG16) pollen tube growth. First, the five independent *At-SLR1::PrsS₁:GFP* lines (L1-L5) were analysed by measuring

the differences of pollen tube lengths achieved by Col-0 pollen and BG16 pollen on these transgenic pistils at a set time-point, 70 min, after being pollinated onto *PrsS₁:GFP* expressing stigma. Representative images are shown in Figure 5-7 A and B.

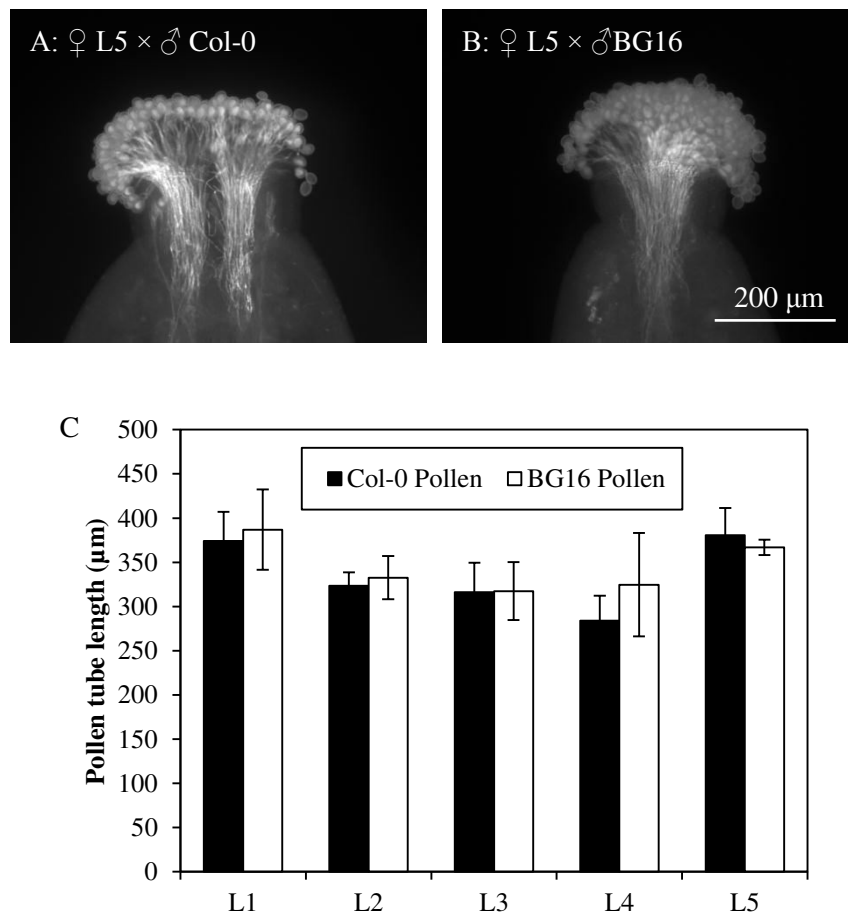


Figure 5-7 *At-PrpS:GFP* pollen grows normally on *PrsS:GFP* expressing pistils

Semi-in-vivo pollination assays were carried out in which *At-PrpS₁:GFP* pistils were pollinated with *At-PrpS₁:GFP* pollen. A and B: representative pictures showing that BG16 pollen was growing as well as Col-0 pollen in *At-PrpS₁:GFP* stigmas, and no inhibition of BG16 pollen tube growth was observed. C: Pollen tube lengths were measured and subjected to statistical analysis. All of the 5 *At-SLR1::PrsS₁:GFP* transgenic lines showed no inhibition on the growth of BG16 pollen ($p=0.666, 0.603, 0.959, 0.341, 0.494$ for L1-L5 respectively, student's t-test). Scale bar indicates 200 µm. Result =mean \pm SD, 3 independent pollination assays were performed.

There was no obvious visual difference between the growth of Col-0 pollen and BG16 pollen on the pistils expressing PrsS₁:GFP protein, which was confirmed by the quantification and statistical analysis of pollen tube lengths (Figure 5-7-C). There was no significant difference between the pollen tube lengths of Col-0 and BG16 pollen (p=0.666, 0.603, 0.959, 0.341, 0.494 for L1-L5 respectively, student's *t*-test). This demonstrated that despite the PrpS₁:GFP protein being expressed in all of the 5 *At-SLRI::PrsS₁:GFP* transgenic lines, it could not inhibit the growth of BG16 pollen *in vivo*.

In summary, it has been demonstrated in this section that PrsS:GFP protein could be specifically expressed in the stigma of transgenic *A. thaliana*. However, *semi-in-vivo* pollination assays showed that the PrsS:GFP protein expressed in the *A. thaliana* pistils was not able to inhibit the growth of *At-PrpS:GFP* pollen. This is consistent with the result shown in Chapter 4 that *A. thaliana* seedlings expressing PrsS:GFP protein could not induce the growth inhibition of *At-PrpS:GFP* pollen in the *in vitro* SI assay. Though it is still unclear whether the GFP fusion at the C-terminus of PrsS affects the proper function of PrsS as a “ligand” protein to PrpS, it is possible that the GFP fusion blocks the recognition and interaction sites of PrsS, thus resulting in the failure of PrpS-PrsS interaction. To test this hypothesis, *At-SLRI::PrsS* transgenic lines lacking the GFP fusion were constructed and analysed.

5.2.5 Functional analysis of *PrsS* in *A. thaliana* in vivo

5.2.5.1 Analysis of *PrsS* mRNA expression in *At-SLR1::PrsS* transgenic lines

As it was suspected that GFP might interfere with PrsS function, transgenic lines containing PrsS alone, under the SLR1 promoter were constructed and analysed. First, expression of *PrsS* in *A. thaliana* driven by *SLR1* promoter was investigated. Stage 13 pistils from 10 independent *At-SLR1::PrsS_I* transformants (lines K2, K4-K9, K12-K14) were collected, from which RNA was purified and subjected to RT-PCR analysis of *PrsS_I* mRNA expression (section 2.3.5).

As shown in Figure 5-8-B, *PrsS_I* transcripts were detectable in all of the 10 transformants which have been analysed, whereas only *GAPC* mRNA was detected in the Col-0 sample, indicating the authentic *PrsS_I* mRNA bands detected. Of all the 10 samples analysed, K2 had the lowest *PrsS_I* transcript abundance, and slightly higher expression was observed in K4 and K8, while all the others (K5, K6, K7, K9, K12, K13, K14) had similar high *PrsS_I* mRNA expression (Figure 5-8-B). In order to have a better idea about the relative expression level of *PrsS_I* mRNA in each of the transformant, the intensity of the gel bands shown in Figure 5-8-B was subjected to semi-quantitative analysis. As shown in Figure 5-8-C, *PrsS_I* transcripts abundance in K2 was lowest, only accounting 19% of that of *GAPC*. Higher *PrsS_I* expression was seen in K4 and K8, whose relative expressions to *GAPC* were 83% and 90%, respectively, which were still lower than the expression of *GAPC*. *PrsS_I* mRNA expression in all the other 7

At-SLR1::PrsS₁ transformants were relatively high, in which the expression level was ~150% relative to that of the *GAPC*.

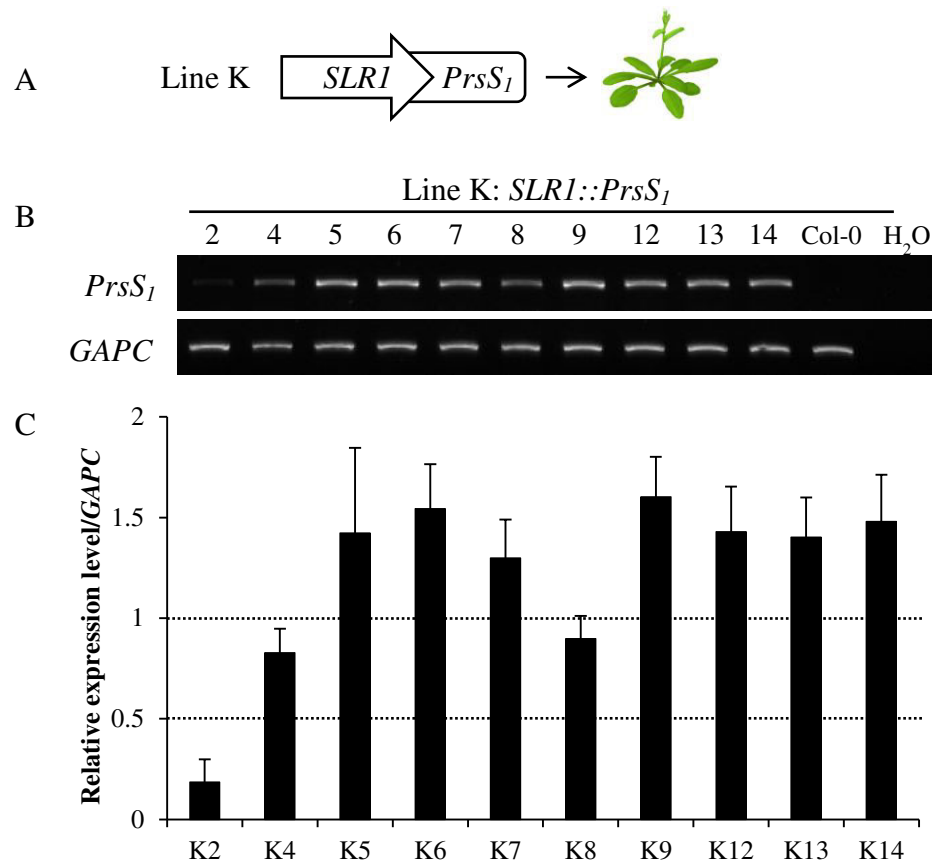


Figure 5-8 *PrsS₁* mRNA is expressed at varying levels in *At-SLR1::PrsS₁* transgenic lines

A: cartoon of *At-SLR1::PrsS₁* transgenic lines. B: Pistils derived from 10 independent transgenic *At-SLR1::PrsS₁* lines were subjected to RT-PCR analysis of *PrsS₁* mRNA expression. *GAPC* was employed as reference gene. Col-0 and water samples were used as negative controls. C: quantification of the band intensities. Results =mean ±SD, n=3.

Thus, RT-PCR showed that *PrsS₁* transcripts were detectable in all the transgenic plants of line K: *At-SLR1::PrsS₁* which have been analyzed. But there were variations in the level of expression in different transformants. The highest *PrsS₁* transcripts abundance was observed in K9, thus the K9 line was chosen for further protein expression analysis.

5.2.5.2 Analysis of PrsS₁ protein expression in *At-SLR1::PrsS₁* transgenic lines

Although the expression of PrsS₁ transcripts in *At-SLR1::PrsS₁* transgenic lines has been demonstrated by RT-PCR, whether the PrsS₁ transcripts could be successfully translated into protein remained to be investigated. As a very large amount of tissue material (~400 stigma samples) was needed to detect a band of the PrsS₁ protein on the western blot (even using ECL detection), only K9 (the highest *PrsS₁* mRNA expressing line) was used for protein expression analysis (Figure 5-9; section 2.3.6).

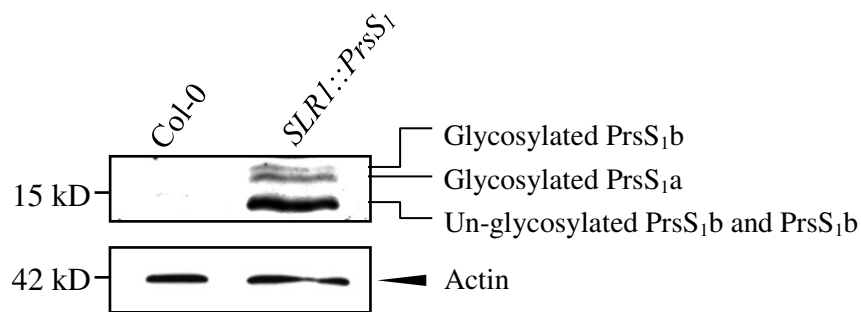


Figure 5-9 PrsS protein is expressed in the *At-SLR1::PrsS* transgenic line

K9 stigmas were subjected to western blot analysis using anti-PrsS₁ antibodies. Col-0 stigma was the negative control. Three different PrsS₁ signals were observed, including glycosylated PrsS₁b (~16.8 kD), glycosylated PrsS₁a (~16.7 kD), and un-glycosylated PrsS₁b and PrsS₁a (~14.5 kD). Un-glycosylated PrsS₁b and PrsS₁a were overlapped with each other. No band was detectable for Col-0 sample in the same position. Actin was probed to show equal loading.

The presence of PrsS₁ protein in *At-SLR1::PrsS₁* transgenic lines was confirmed by western blot analysis of the stigma protein extracts from K9, using the anti-PrsS₁ antibodies (Figure 5-9). Three bands ~15 kD were detected on the western blot. This suggested that PrsS₁ protein was expressed and subject to posttranslational modification in *A. thaliana*, which was consistent with what had been observed in *P. rhoeas* stigmas

(Foote et al., 1994). Those two bands with higher molecular weight indicated glycosylated PrsS_{1b} (~16.8 kD) and glycosylated PrsS_{1a} (~16.7 kD), respectively. The band with lowest molecular weight (~14.5 kD) contained two different isoforms, un-glycosylated PrsS_{1b} and PrsS_{1a}, which overlapped with each other.

5.2.5.3 Functional analysis of *A. thaliana* expressed PrsS protein using the *semi-in-vivo* pollination assay

To establish whether the PrsS protein expressed in *A. thaliana* was able to trigger the SI response in *At-PrpS:GFP* pollen *in vivo*, *semi-in-vivo* pollination assays were carried out in which *PrsS* expressing stigmas were pollinated with *At-PrpS:GFP* pollen and left to grow for precise lengths of time. At each time point, the pollinated pistils were subjected to aniline blue staining to assess the pollen germination and pollen tube growth (Figure 5-10). In the very early stages [30 minutes after pollination (MAP)] of pollen germination and tube growth, no major difference was observed between different pollination combinations (Figure 5-10 A1-3). However, at 50 MAP, slightly shorter and fewer pollen tubes could be observed in the ♀PrsS₁×♂PrpS₁:GFP pollination (Figure 5-10-B1), compared with those of ♀PrsS₁×♂Col-0 (Figure 5-10-B2) and ♀Col-0×♂PrpS₁:GFP (Figure 5-10-B3) controls. In the following stages of pollen tube growth (70-110 MAP), in the ♀PrsS₁×♂PrpS₁:GFP pollination, dramatically shorter pollen tubes were observed (Figure 5-10 C1-E1) compared with the lengths of pollen tubes in the controls (Figure 5-10 C2-E2 and C3-E3) at each time point.

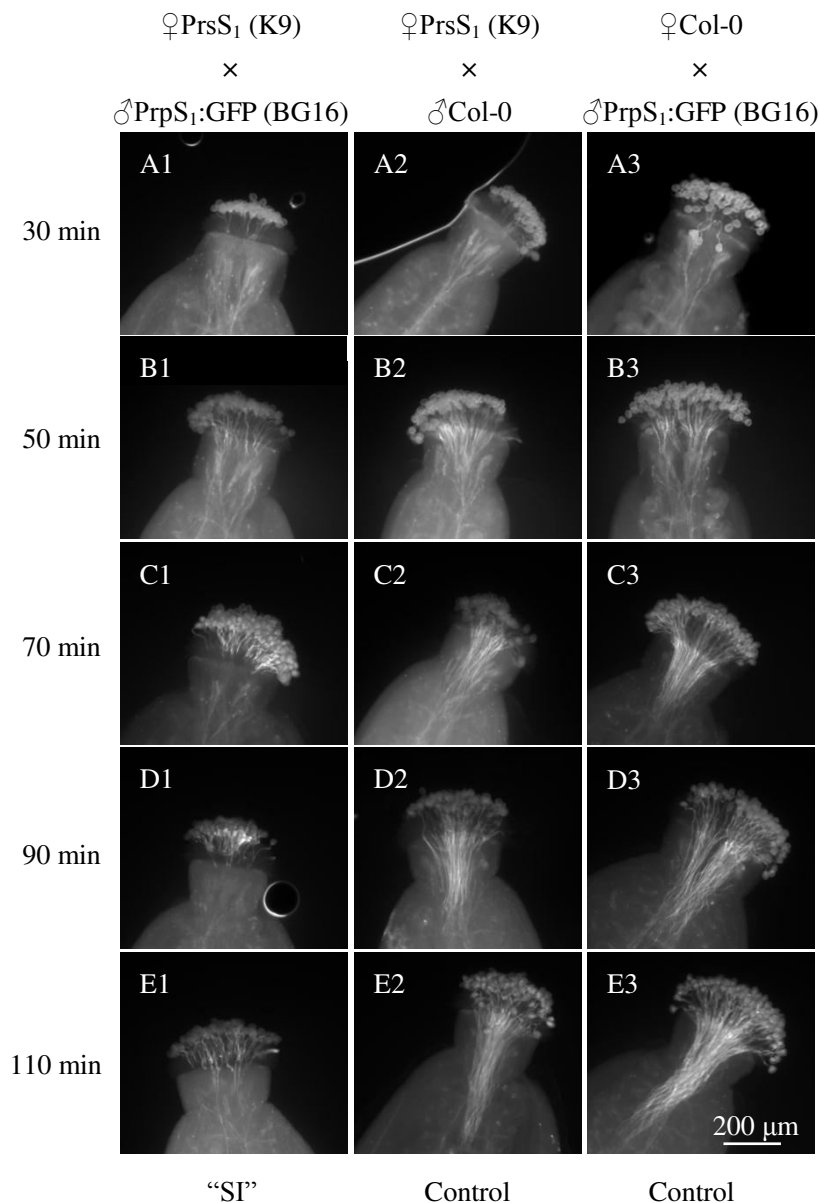


Figure 5-10 *PrsS* expressing stigma inhibits *At-PrpS*:*GFP* pollen growth *semi-in-vivo*

A1-E1: *PrsS₁* expressing stigmas (K9) were pollinated with *At-PrpS₁:GFP* (BG16) pollen, followed by aniline blue staining to monitor the pollen germination and tube growth. Pollinations between K9 stigma and Col-0 pollen (A2-E2), as well as Col-0 stigma and BG16 pollen (A3-E3) were treated as controls. No significant difference was observed between different pollination combinations in the early stages of pollen germination and tube growth (A1-3). When BG16 pollen was pollinated on K9 stigma, dramatically shorter pollen tubes were observed compared with the lengths of pollen tubes in the controls at each time point. White bar indicates 200 μ m.

The observation that Col-0 pollen could germinate and grow properly in *PrsS₁* expressing stigma (Figure 5-10 A2-E2), and germination rates and pollen tubes lengths were comparable with those observed in the Col-0 self-pollination (Figure 5-3), demonstrated that the expression of *PrsS₁* in *A. thaliana* stigma did not affect the ability of stigma to accept pollen. It could also be concluded that the expression of *PrpS₁:GFP* in *A. thaliana* pollen did not alter its capacity to germinate and grow in the Col-0 stigma (Figure 5-10 A3-E3). However, pollinating K9 stigmas with BG16 pollen resulted in marked pollen tube growth inhibition and retardation. This was the first indication that the PrsS protein expressed in the stigma of *A. thaliana* could trigger the SI response of incompatible *At-PrpS:GFP* pollen *in vivo*.

In order to confirm that inhibition of *At-PrpS₁:GFP* pollen on *PrsS₁* expressing stigmas was due to the expression of *PrsS₁*, and not caused by the T-DNA insertion in the genome, or some other unknown reasons, stigmas collected from 10 independent *At-SLRI::PrsS₁* transformants were all subjected to pollination assays using *At-PrpS₁:GFP* pollen. *At-PrpS₁:GFP* pollen tube growth inhibition were observed in all the *PrsS₁* expressing stigmas collected from the 10 independent *At-SLRI::PrsS₁* transformants, but the inhibition ability of *At-PrsS₁* stigma varied between different transformants.

In order to compare the expression of SI between different *At-SLRI::PrsS₁* lines, stage

13 pistils from 10 independent *At-SLR1::PrsS₁* lines were collected and subjected to *semi-in-vivo* pollination assays (Figure 5-11), in which *At-PrpS₁:GFP* pollen was allowed to germinate and grow under optimized conditions for 70 minutes before fixation and aniline blue staining. Col-0 pollen was also pollinated on the PrsS₁ expressing stigma as controls. There was no obvious difference between the pollen tube lengths achieved by Col-0 and BG16 pollen grown on K2 stigmas (Figure 5-11 A and D), which showed the lowest *PrsS₁* mRNA expression level (Figure 5-8). For the K4 stigmas, the growth of BG16 pollen on it was significantly inhibited, and the pollen tube lengths of BG16 pollen 70 minutes after pollination were only half of those of Col-0 pollen (Figure 5-11 B and E). The K9 stigmas also inhibited the growth of BG16 pollen (Figure 5-11 C and F). Moreover, more marked growth inhibition of BG16 pollen was observed on the K9 stigma compared with that on the K4 stigma (Figure 5-11 B and C). For K4 stigmas, after 70 minutes incubation, BG16 pollen grew across the whole stigmatic region and reached the pistil transmitting tract (Figure 5-11-B), whereas growth of BG16 pollen on K9 stigma was still restricted in the stigmatic region 70 minutes after pollination (Figure 5-11-C).

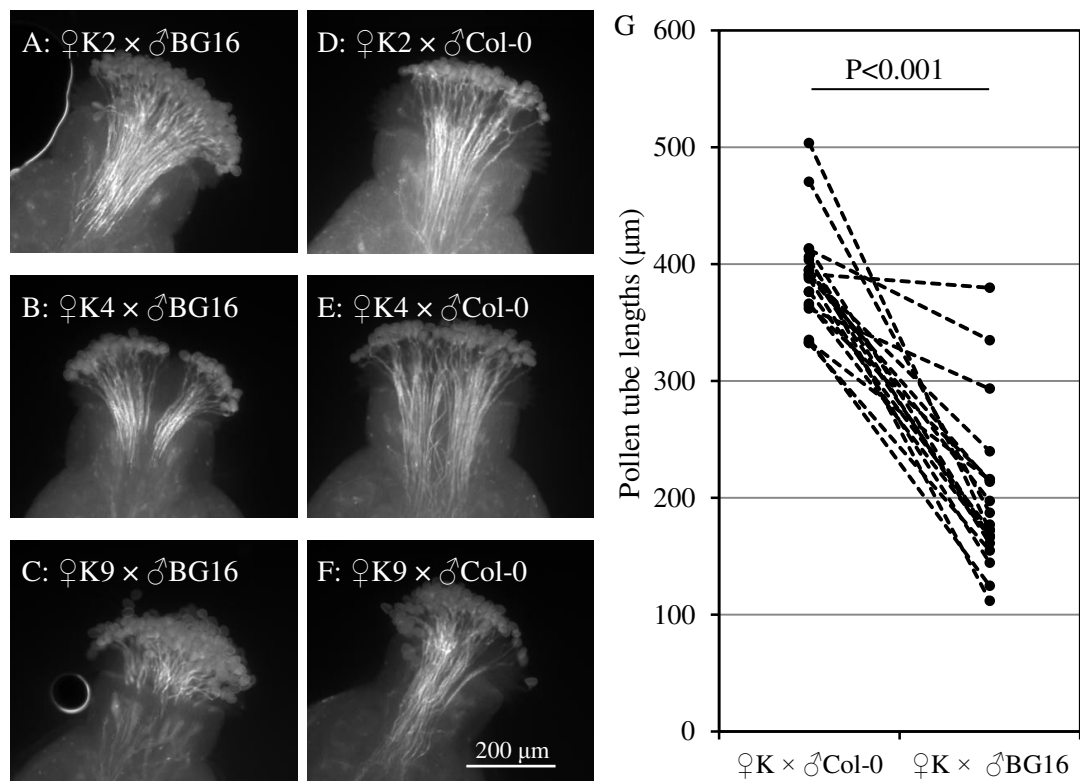


Figure 5-11 Different *At-SLR1::PrsS₁* lines express varied strengths of SI

Stage 13 pistils from 10 independent *At-SLR1::PrsS₁* lines were subjected to *semi-in-vivo* pollination assays, in which BG16 pollen was allowed to germinate and grow for 70 minutes before fixation and aniline blue staining. Col-0 pollen was also pollinated on the PrsS₁ expressing stigma as controls. A-F: representative images of BG16 pollen (A-C) and Col-0 pollen (D-F) growing on the PrsS₁ expressing stigma. G: comparison of Col-0 and BG16 pollen tube lengths 70 minutes after pollination on PrsS₁ expressing stigmas. Each dotted line segment represented a set of pollination assay in which two PrsS₁ expressing pistils collected from the same transgenic plants were pollinated with Col-0 and BG16 pollen respectively, followed by incubation in the same environmental conditions for 70 min. Black dots at the ends of each dotted line segment represented the Col-0 (left side) and BG16 (right side) pollen tube lengths. 20 stigmas from 10 independent *At-SLR1::PrsS₁* lines were analyzed, 2 stigmas from each line. White bar indicates 200 µm.

The observation of the differences between BG16 pollen tube lengths grown on different K lines stigmas expressing PrsS₁ suggested that the inhibition capacity of *At-SLR1::PrsS₁* stigmas varied between the different transgenic K lines. This became

more evident when the pollen tube lengths were measured and statistical analysis was carried out (Figure 5-11-G). Comparisons of Col-0 and BG16 pollen tube lengths after 70 minutes pollination on *PrsS₁* stigmas derived from 10 independent *At-SLRI::PrsS₁* transgenic lines showed that BG16 pollen tube lengths were significantly shorter than that of Col-0 pollen ($p < 0.001$), indicating the expression of *PrsS₁* in *A. thaliana* stigma inhibited the growth *At-PrpS₁:GFP* pollen *in vivo*. This was confirmed by the observation that the value at the left sided end (Col-0 pollen tube length) in Figure 5-11-G was larger than that at the right sided end (BG16 pollen tube lengths), indicating that Col-0 pollen grew longer than BG16 pollen on *PrsS₁* expressing stigma, named growth of BG16 could be inhibited on *At-SLRI::PrsS₁* stigma. In addition, BG16 pollen tube lengths were observed to range from ~100 μm to less than 400 μm , suggesting that different *PrsS₁* expressing stigmas had different capacities to inhibit BG16 pollen tube growth.

In order to gain insight whether the variation of BG16 pollen inhibition in *At-SLRI::PrsS₁* stigma was related to expression level of *PrsS*, the BG16 pollen tube lengths 70 min after being pollinated on the stigmas of 10 different *At-SLRI::PrsS₁* transgenic lines were plotted against the relative *PrsS₁* transcript expression level for each corresponding line (Figure 5-12). Col-0 pollen tube lengths were also measured and plotted as controls. As shown in Figure 5-12, the lengths of BG16 pollen negatively correlated with the *PrsS₁* mRNA expression in the stigma ($y = -143.75x + 390.63$,

$R^2=0.8505$), while no clear correlation could be observed between the growth of Col-0 pollen and the expression of *PrsS₁* mRNA ($y= 3.38x + 408.53$, $R^2=0.0152$). This shows that the inhibition of BG16 pollen observed in the *PrsS₁* expressing stigmas was strongly correlated with the expression of *PrsS₁*. The more *PrsS₁* that was expressed in the transgenic stigma, the stronger BG16 pollen was inhibited. Figure 5-12 further demonstrates that the *Papaver S*-determinants *PrpS* and *PrsS* are functional in *A. thaliana*, and also makes the connection between the inhibition of *At-PrpS₁:GFP* pollen and the expression level of *PrsS₁* in transgenic *Arabidopsis* stigmas.

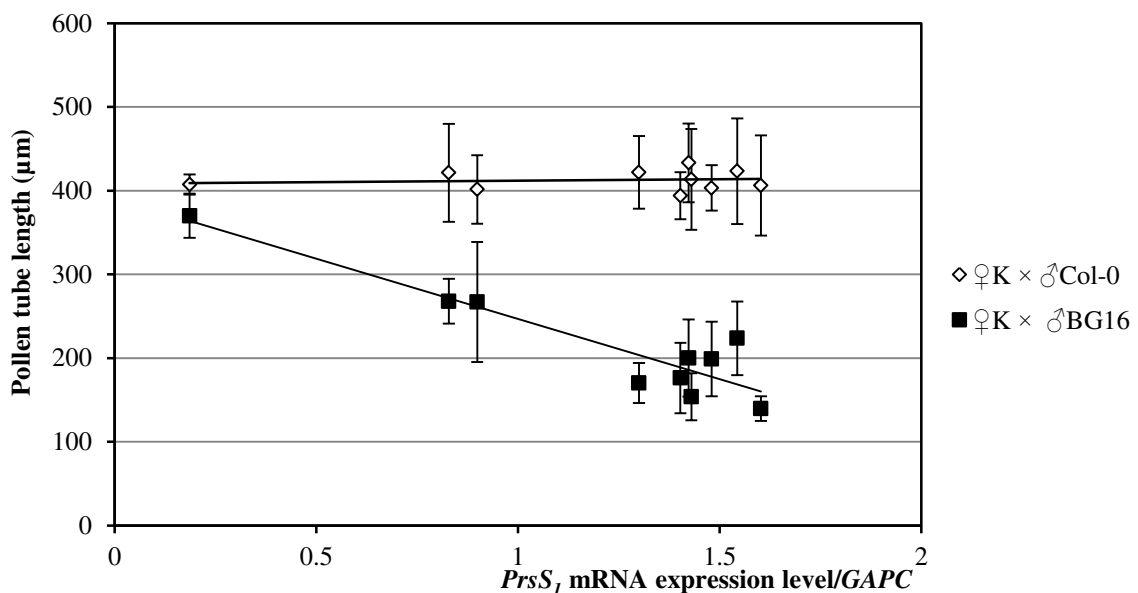


Figure 5-12 Inhibition of *At-PrpS:GFP* pollen is correlated with the expression level of *PrsS* transcript in *At-SLR1::PrsS* stigma

The inhibition of BG16 pollen in transgenic *At-SLR1::PrsS₁* stigma was closely correlated with the expression of *PrsS₁* transcripts. 10 independent *At-SLR1::PrsS₁* transgenic lines were analysed. Col-0 or BG16 pollen tube lengths were measured 70 min after pollinated in the *PrsS₁* expressing stigma. Result= mean \pm SD. K2, n=4; K7, 8, 12, n=5; K6, n=6; K4, 5, 13, 14, n=8; K9, n=10.

So far, it has been demonstrated in this section that both *PrsS* mRNA transcripts and protein were expressed in *A. thaliana* under the direction of *SLRI* promoter. The *A. thaliana*-expressed PrsS protein was likely posttranslationally modified in a similar manner to that observed in the stigmas of *P. rhoeas* as predicted from their size. *Semi-in-vivo* pollination assays showed that the expression of PrsS in the *A. thaliana* stigma inhibited the growth of *At-PrpS:GFP* pollen. This inhibition capacity was PrsS-expression dependent; the more *PrsS* mRNA was expressed in the stigma, the more *At-PrpS:GFP* pollen tube growth was inhibited. These data demonstrate that *PrsS* mRNA could be successfully translated into PrsS protein in the stigma of transgenic *A. thaliana*, and is functional to trigger an SI response in *At-PrpS:GFP* pollen *in vivo*.

5.2.5.4 Inhibition of *At-PrpS:GFP* pollen in PrsS-expressing stigmas is developmentally controlled

SI is a tightly developmentally regulated phenomenon, which is determined by the developmentally controlled expression of both pollen and stigma *S*-determinants (Franklin-Tong, 2008). Having demonstrated that PrsS expression could inhibit the growth of *At-PrpS:GFP* pollen, the next step was to investigate whether the developmental regulation was maintained in transgenic *A. thaliana* lines. Staged pistils from K9 (stage 12E, 12L, 13, 14) were collected and subject to *semi-in-vivo* pollination assays with BG16 pollen (Figure 5-13).

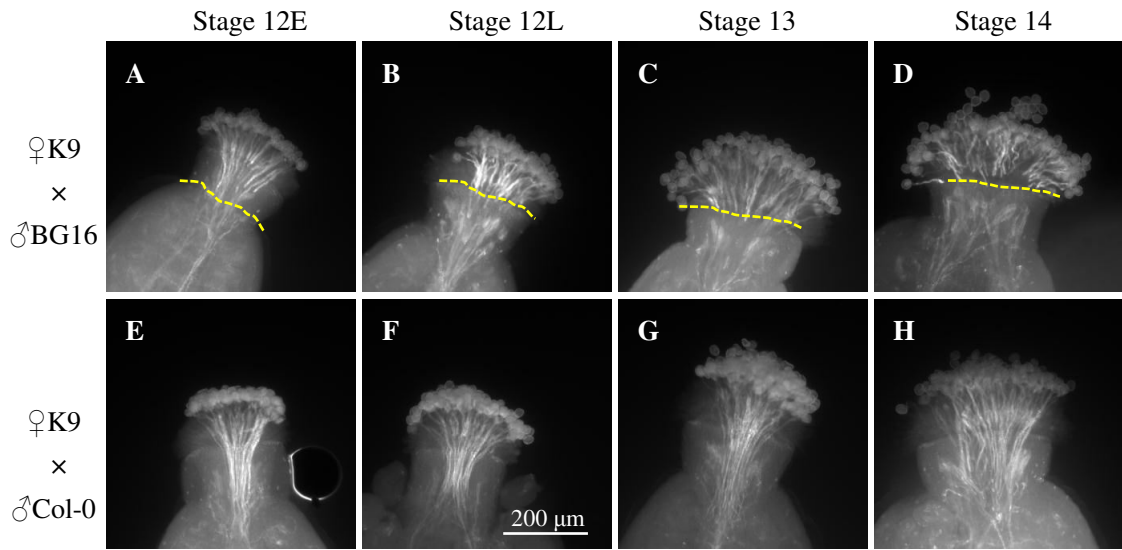


Figure 5-13 The expression of SI response in transgenic *A. thaliana* is developmentally regulated

Staged pistils (stage 12 E, 12L, 13, 14) were collected from K9 and subject to semi-in-vivo pollination assays with BG16 pollen. Col-0 pollen was also pollinated as the controls. Samples were fixed and stained 70 min after pollination. A-D: the growth of BG16 pollen was inhibited in the K9 stigmas of different developmental stages with different extents. E-H: Col-0 pollen grew normally in the K9 stigmas and the growths of Col-0 pollen in the stigmas of different developmental stages were comparable with each other. White bar indicates 200 μm, n=3.

The growth of BG16 pollen was inhibited in all the different developmental stages K9 stigmas when BG16 pollen tube lengths (Figure 5-13 A-D) were compared with those from Col-0 pollen (Figure 5-13 E-H). However, the extent of inhibition of BG16 pollen in the stigmas of different stages was observed to be different. In stage 12E K9 stigmas, 70 min incubation after pollination allowed the BG16 pollen tubes to grow all through the stigmatic papillae region and reach the transmitting tract (Figure 5-13-A). For the stigmas of stage 12L, 13 and 14, the growth of BG16 pollen were all restricted in the stigmatic papillae region and few pollen tubes were observed in the transmitting tract (Figure 5-13 B-D). This was consistent with the observations in Figure 5-1, which

showed that a low level of *SLRI* expression could already be observed at stage 12E; the expression was dramatically increased to a relatively high level at stage 12L; and this high expression level was maintained at stage 13 and 14. Figure 5-13 demonstrated that the expression of the SI response in *At-SLRI::PrsS* transgenic lines was developmentally regulated in the manner expected from use of the *SLRI* promoter.

5.2.5.5 PrpS-PrsS triggered pollen growth inhibition in *A. thaliana* was *S*-allele specific

S-allele specific inhibition is one of the key hallmarks of SI response. It has been demonstrated above that the growth of *At-PrpS₁:GFP* pollen could be inhibited by the PrsS₁ protein expressed in the *A. thaliana* stigma. However, it was still unknown that whether this inhibition was *S*-allele specific. Having established that PrsS₁ expressed in transgenic *A. thaliana* lines could inhibit the *At-PrpS₁:GFP* pollen tube growth in a developmentally regulated manner, the next step was to investigate whether the inhibition was *S*-allele specific. For this, *At-SLRI::PrsS₃* transgenic lines were analysed using the same strategy described for the screening of *At-SLRI::PrsS₁* transgenic lines. *At-SLRI::PrsS_{3.8}* (Q8) was identified to show the strongest inhibition on the growth of *At-PrpS₃:GFP* pollen among the 13 independent Q lines which have been screened (data not shown). As it has been shown in previous sections that K9 showed the strongest inhibition of the BG16 pollen tube growth amongst the 10 independent *At-SLRI::PrsS₁* transgenic lines analysed. Therefore, K9 and Q8 were chosen for the

analysis of *S*-allele specific inhibition (Figure 5-14).

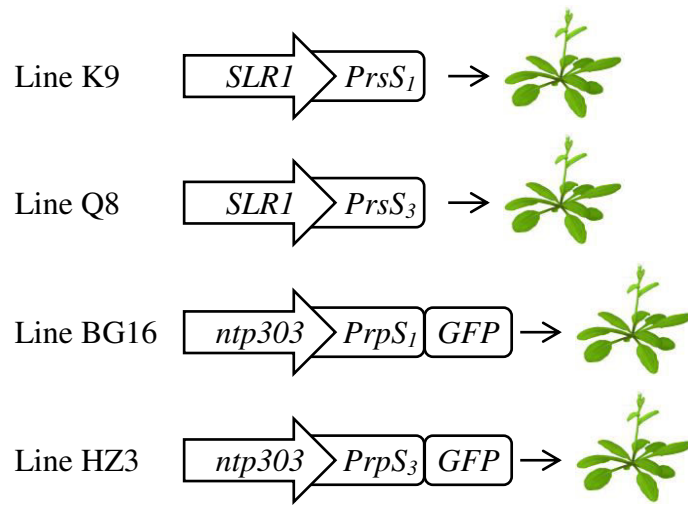


Figure 5-14 Cartoon of the *At-SLR1::PrpS* and *At-ntp303::PrpS:GFP* transgenic lines

Semi-in-vivo pollination assays were carried out in which PrpS₁ expressing stigma (K9) was pollinated with *At-PrpS₃:GFP* pollen and PrpS₃ expressing stigma (Q8) was pollinated with *At-PrpS₁:GFP* pollen. Pollen was allowed to grow under optimized conditions for 130 minutes before fixation and aniline blue staining. As shown in Figure 5-15, the growth of *At-PrpS₁:GFP* and *At-PrpS₃:GFP* pollen tubes in the Col-0 pistils was indistinguishable with the growth of self-pollinated Col-0 pollen (Figure 5-15 A-C), demonstrating the expression of PrpS_{1/3}:GFP did not affect the germination and growth of *A. thaliana* pollen. The growth of *At-PrpS₁:GFP* pollen was inhibited in the K9 pistil, whereas Col-0 pollen grew normally (Figure 5-15 D and E). However, the growth of *At-PrpS₃:GFP* pollen in the K9 pistil was comparable with that of Col-0 pollen and no inhibition was observed (Figure 5-15-F), demonstrating that *A. thaliana* expressed PrpS₁

protein inhibited the growth of *At-PrpS₁:GFP* pollen, but not *At-PrpS₃:GFP* pollen.

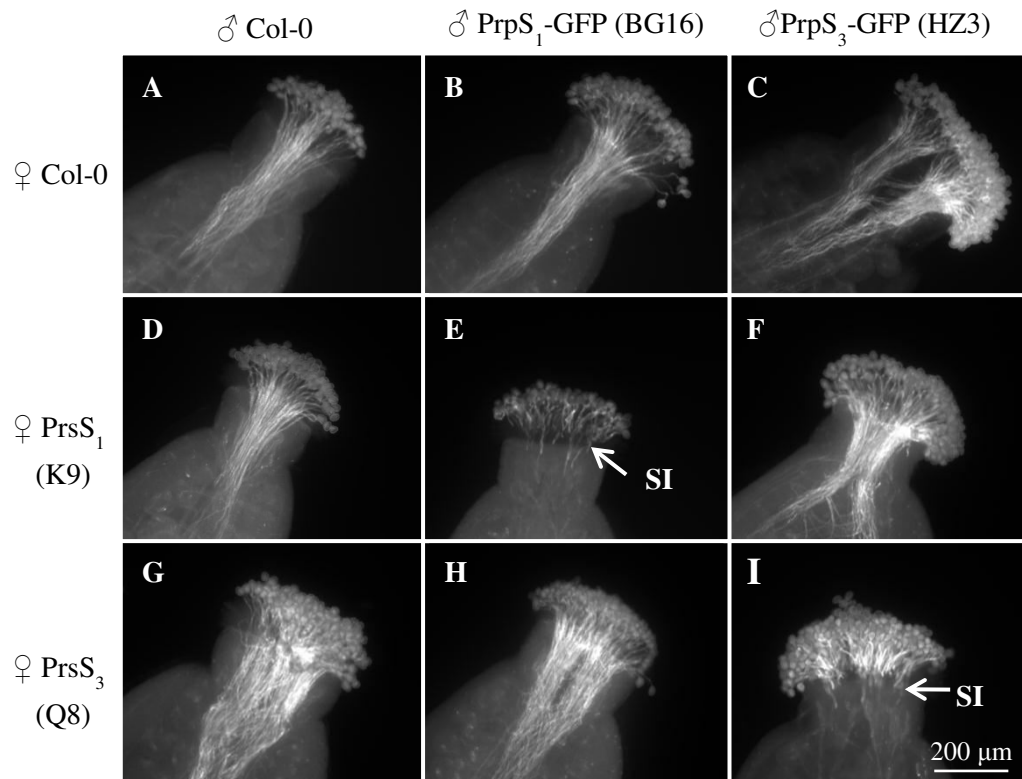


Figure 5-15 PrpS-PrsS triggered pollen tube growth inhibition in *A. thaliana* is S-allele specific

K9 and Q8 pistils were subjected to *semi-in-vivo* pollination assays, in which they were pollinated with *At-PrpS₃:GFP* and *At-PrpS₁:GFP* pollen respectively. Other pollination combinations were also carried out as the controls. A-C: the growths of BG16 and HZ3 pollen in the Col-0 stigmas were indistinguishable with the growth of Col-0 pollen self-pollinated. D, E: the growth of BG16 pollen was inhibited in the K9 stigma, whereas Col-0 pollen grew normally. F: the growth of HZ3 pollen in the K9 stigma was comparable with that of Col-0 pollen. G, I: Q8 inhibited the growth of HZ3 pollen, but not the Col-0 pollen. H: the growth of BG16 pollen in the Q8 stigma was comparable with that of Col-0 pollen. White bar indicates 200 μm , n=4.

For the pollen germination and pollen tube growth in the Q8 pistil, only the growth of *At-PrpS₃:GFP* pollen was inhibited (Figure 5-15-I), while Col-0 pollen and *At-PrpS₁:GFP* pollen grew normally and the total growths were comparable with each

other (Figure 5-15 G and H), demonstrating that *A. thaliana* expressed PrsS₃ protein inhibited the growth of *At-PrpS₃:GFP* pollen, but not *At-PrpS₁:GFP* pollen. Figure 5-15 clearly shows that the cognate stigma and pollen alleles in combination led to inhibition of pollen tube growth through the pistil, whereas the heterologous combination was compatible and pollen tube growth was unaffected, which demonstrated that *S*-allele specificity was maintained in the *A. thaliana* transgenic lines.

5.2.5.6 PrpS-PrsS triggered SI responses in transgenic *A. thaliana* results in shorter siliques and no seeds

One of the key features of SI response is that pollination between cognate pollen and stigma *S*-alleles results in no seed production. It has been demonstrated by the *semi-in-vivo* pollination assays that the expression of PrsS protein in the stigma inhibited the growth of *At-PrpS:GFP* pollen. However, it was still not known yet whether the inhibition of pollen tube growth would affect seed production. Therefore, *At-PrsS₁* and *At-PrsS₃* stigmas were emasculated and pollinated with *At-PrpS₁:GFP* and *At-PrpS₃:GFP* pollen respectively, *in planta*, and seed set analysis was carried out (Figure 5-16; Table 5-2).

In planta pollination of Col-0 stigma with Col-0, *At-PrpS₁:GFP* or *At-PrpS₃:GFP* pollen resulted in the siliques lengths of 16.4±0.7 mm, 16.6±1.0 mm, 16.6±0.8 mm respectively (Figure 5-16 A-C; Table 6-2), which were statistically indistinguishable from each other (p=0.871, one-way ANOVA). The seed yields of ♀Col-0×♂Col-0,

♀Col-0×♂PrpS₁:GFP and ♀Col-0×♂PrpS₃:GFP were around 47-50 per silique (Table 6-2), and no significant difference was observed between these pollinations (p=0.303, one-way ANOVA).

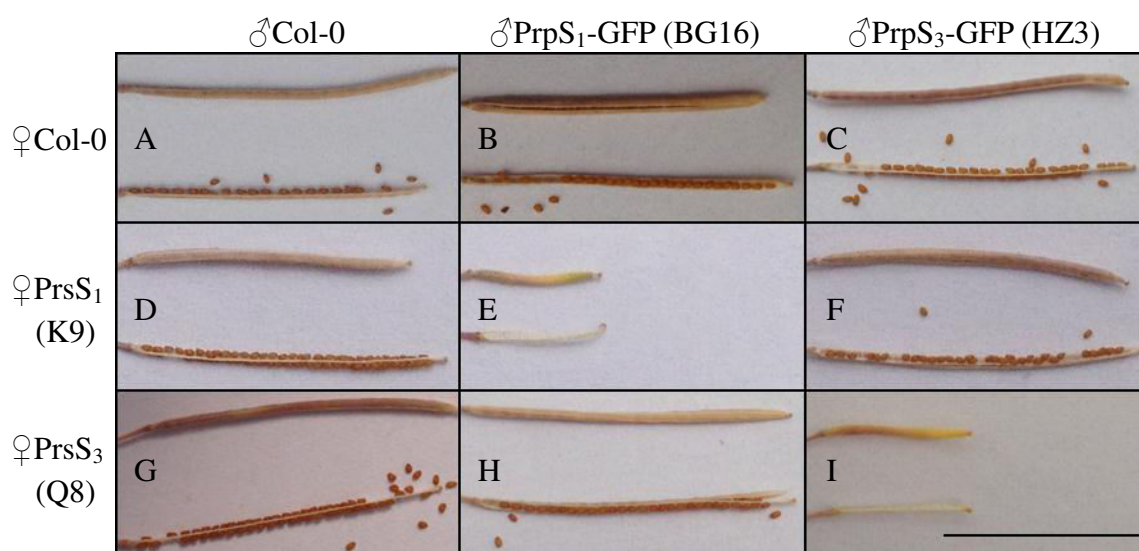


Figure 5-16 PrpS-PrsS triggered SI response in *A. thaliana* results in shorter siliques and no seed

K9 and Q8 pistils were emasculated and pollinated with BG16 and HZ3 pollen respectively in planta. Seed set analysis was carried out when the siliques were dry by measuring the siliques lengths and seeds number. Other pollination combinations as indicated in the figure were also carried out as the controls. A-C: pollination of Col-0 stigmas with Col-0, BG16 and HZ3 pollen resulted in the normal silique development and seeds number. D-F: shorter silique and no seed was observed when K9 was pollinated with BG16 pollen, while pollination of K9 stigmas with Col-0 and HZ3 pollen resulted in normal silique and seed number. G-I: shorter silique and no seed were observed when Q8 was pollinated with HZ3 pollen, while pollination of Q8 stigmas with Col-0 and BG16 pollen resulted in normal silique and seed number. The lengths of siliques and number of seeds were summarized in Table 5-2. Black bar indicates 1 cm, n=10.

These data demonstrate that expression of the PrpS:GFP protein in the *A. thaliana* pollen did not affect normal fertilization, silique development or seed formation. *In planta* pollination of Col-0, *At-PrsS₁* and *At-PrsS₃* stigmas with Col-0 pollen resulted in

the siliques lengths of 16.4 ± 0.7 mm, 16.4 ± 0.7 mm, and 16.5 ± 0.5 mm respectively (Figure 5-16 A, D, G; Table 6-2), in which no statistical difference was observed ($p=0.919$, one-way ANOVA). The seed numbers they yielded were also comparable with each other ($p=0.538$, one-way ANOVA; Table 5-2). These demonstrated that the expression of PrsS protein in the stigmas did not affect the stigmas to accept pollen for fertilization.

Table 5-2 Summary of the lengths of siliques and the number of seeds

♀ \ ♂		<i>Col-0</i>	<i>PrpS₁-GFP</i> (BG16)	<i>PrpS₃-GFP</i> (HZ3)
		<i>Col-0</i>	<i>Silique lengths (mm)</i>	16.4 ± 0.7
	<i>Seeds per silique</i>	47.7 ± 3.6	49.9 ± 3.7	47.6 ± 3.7
<i>PrsS₁</i> (K9)	<i>Silique lengths (mm)</i>	16.4 ± 0.7	6.2 ± 1.4	16.1 ± 0.8
	<i>Seeds per silique</i>	49.3 ± 5.3	0.5 ± 1.0	50.6 ± 5.1
<i>PrsS₃</i> (Q8)	<i>Silique lengths (mm)</i>	16.5 ± 0.5	16.4 ± 0.8	6.3 ± 1.7
	<i>Seeds per silique</i>	50.0 ± 3.2	50.0 ± 3.9	1.2 ± 1.8

Result= mean \pm SD, n=10

However, in the pollinations where *At-PrsS₁* stigmas were pollinated with *At-PrpS₁:GFP* pollen and *At-PrsS₃* stigmas were pollinated with *At-PrpS₃:GFP* pollen, the lengths of the siliques were significantly shortened (Figure 5-16 E and I). The mean lengths of siliques in ♀*PrsS₁* × ♂*PrpS₁:GFP* and ♀*PrsS₃* × ♂*PrpS₃:GFP* pollinations only

were 6.2 mm and 6.3 mm respectively (Table 5-2), which was less than 40% of the lengths of normal siliques. The reduction of the seeds number per silique was even more obvious. Only 0.5 and 1.2 seeds were observed per silique on average (Table 5-2), and some of the siliques were even completely empty (7/10 in ♀PrsS₁×♂PrpS₁:GFP and 6/10 in ♀PrsS₃×♂PrpS₃:GFP). This clearly demonstrates that PrsS expressed in *A. thaliana* stigmas triggers SI response in the *At-PrpS:GFP* pollen, resulting in the failure of fertilization, with shorter siliques and remarkably reduced seed formation. Moreover, ♀PrsS₁×♂PrpS₃:GFP and ♀PrsS₃×♂PrpS₁:GFP pollinations resulted in the normal siliques and seeds number (Figure 5-16 F and H; Table 5-2), indicating that heterologous combination was compatible and silique development and seed formation was unaffected. The results of the *in planta* pollinations presented here (Figure 5-16 and Table 5-2) was consistent with what were observed in the *semi-in-vivo* pollination assays described previously (section 5.2.5.5) that the growth of *At-PrpS:GFP* pollen tube was inhibited in *At-PrsS* stigma, and the inhibition was *S*-allele specific. This demonstrates that the *Papaver* SI system is functional in these transgenic *A. thaliana* plants.

5.2.6 Generation of self-incompatible *A. thaliana* by co-transformation of *PrpS* and *PrsS*

Analysis of the independent *At-ntp303::PrpS:GFP* and *At-SLRI::PrsS* transgenic lines has demonstrated that PrsS expressed in the stigmas of *A. thaliana* was functional and

could trigger SI response in cognate *At-PrpS::GFP* pollen, resulting in the failure of fertilization and seed formation. However, so far this was characterised using transgenic plants carrying either PrpS:GFP or PrsS in separate plants. It was still unknown that whether the whole poppy SI system could be put into a single plant to make self-compatible *A. thaliana* plants self-incompatible.

Experimental attempts to generate self-incompatible *A. thaliana* using *Papaver* SI system was carried out. The approach used was to transform homozygous *At-ntp303::PrpS₁::GFP* transgenic lines with a Ti vector containing *SLR1::PrsS₁* (pORE O3-*SLR1::PrsS₁*) through floral-dipping (section 2.3.7). Transgenic seeds were screened on selective MS plates containing BASTA, and surviving seedlings were transplanted to soil pots in the greenhouse. Genotyping was carried out to confirm the integration of both *PrpS* and *PrsS* in the *A. thaliana* genome.

Co-transformation of *PrpS₁::GFP* and *PrsS₁* did not affect the normal growth of *A. thaliana* plants (Figure 5-17-A). There was no significant difference observed in the size and flowering time between Col-0 and transgenic plants. When plants co-transformed with *PrpS₁::GFP* and *PrsS₁* were left to set seeds naturally, significantly smaller siliques were observed and there was no seed formation (Figure 5-17-B, n=60; Figure 5-18 A and B). Normal phenotypes were observed in other controls including the transformation of *PrpS₁::GFP* or *PrsS₁* alone (Figure 5-17 C-E; Figure 5-18 C and D).

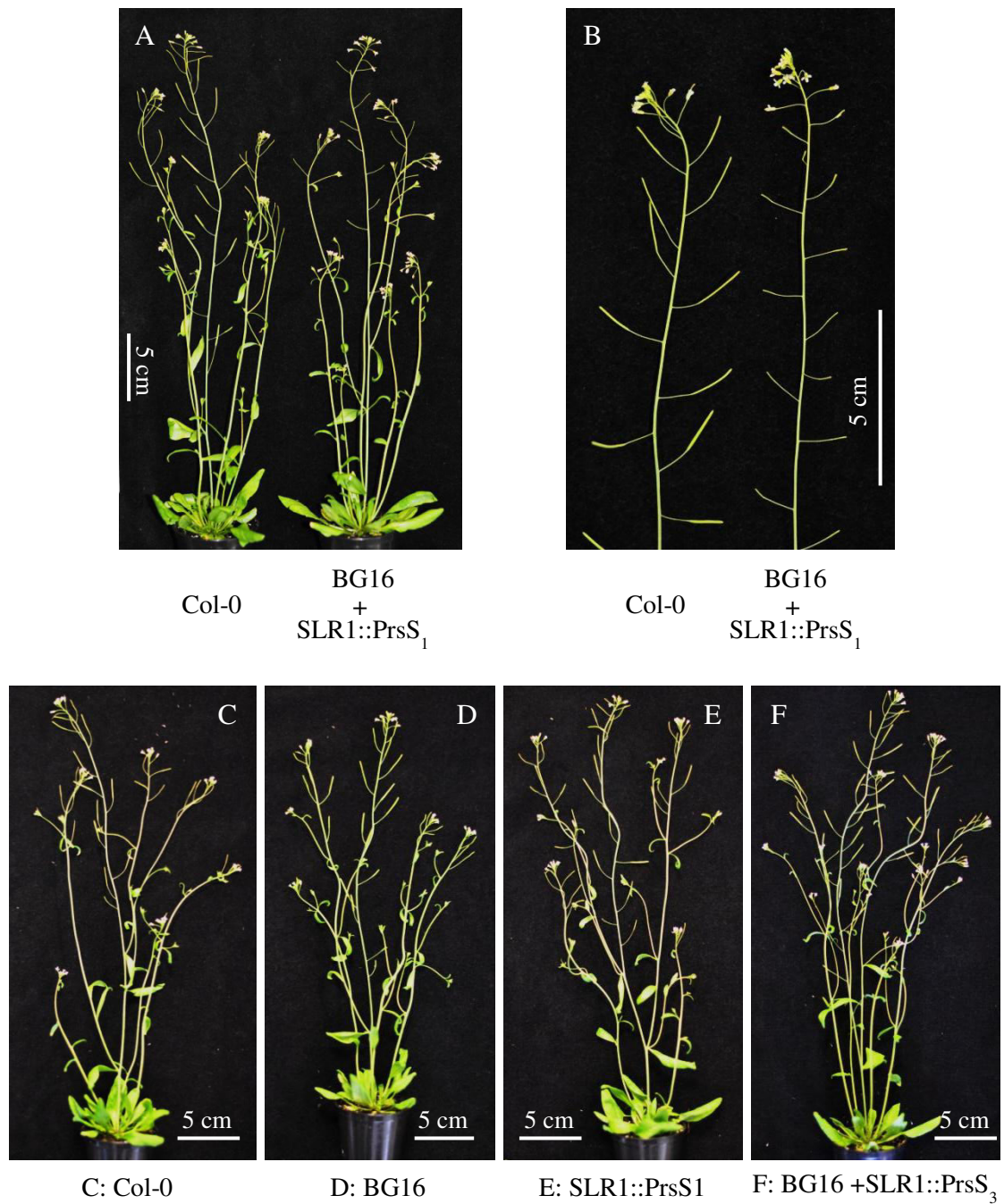


Figure 5-17 Self-incompatible *A. thaliana* is generated through transforming BG16 with *PrsS*₁

A: wild type and self-incompatible *A. thaliana*. B: significantly smaller siliques were observed in self-incompatible *A. thaliana*. Transformation of *PrpS*₁ (D) or *PrsS*₁ (E) alone did not affect the growth and siliques formation of *A. thaliana* compared with Col-0 wild type (C). F: co-transformation of *PrpS*₁ and *PrsS*₃ resulted in self-compatible *A. thaliana*. Bars indicate 5 cm. Eight-week-old plants are shown above.

These data demonstrated that *Papaver* pollen and stigma *S*-determinants were functional in *A. thaliana in vivo* to make self-compatible *A. thaliana* self-incompatible. In addition, *S*-allele specificity was also maintained in transgenic *A. thaliana*. Co-transformation of *A. thaliana* with *PrpS₁* and *PrsS₃* resulted in normal phenotypes (Figure 5-17-F, n=24; Figure 5-18-E), which was self-compatible. It was also observed that pollination of Col-0 or *At-PrpS₃:GFP* pollen on the *At-PrpS₁:GFP-PrsS₁* stigma resulted in normal seed set. This demonstrated that transgenic *At-PrpS₁:GFP-PrsS₁* plants were cross fertile, and the SI of these plants was not due to a general fertility problem.

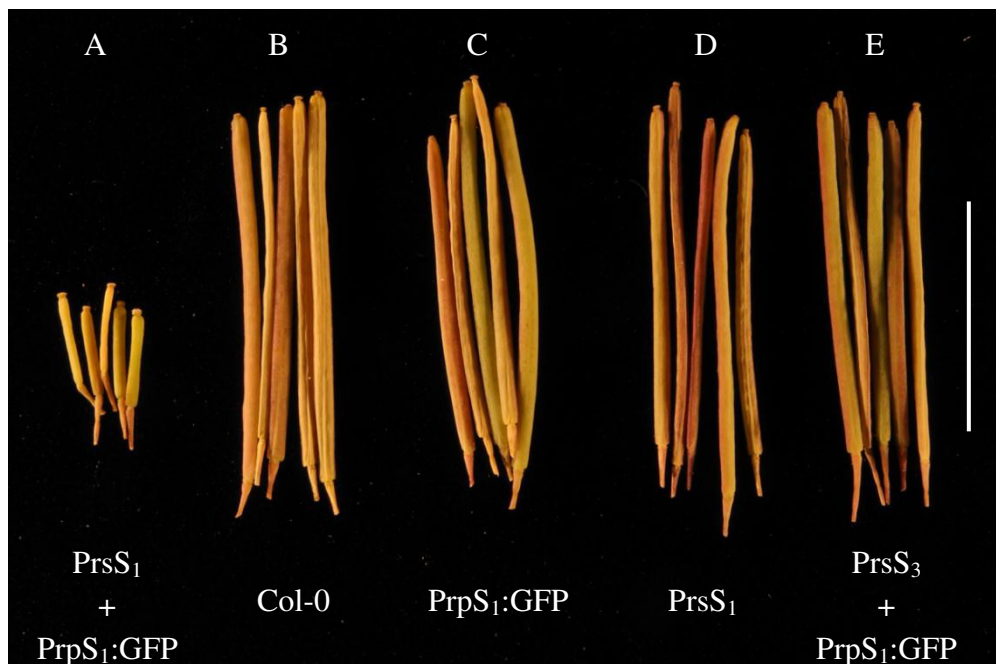


Figure 5-18 Self-incompatible *A. thaliana* forms shorter siliques and sets no seed

A: co-transformation of *PrpS₁:GFP* and *PrsS₁* resulted in the formation of significantly shorter siliques with no seeds. B-E: all the control plants set normal siliques and seeds. B: Col-0; C: BG16; D: K9; E: BG16+*SLR1::PrsS₃*. White bar indicates 1 cm.

This is the ultimate evidence that the *Papaver* SI system can be successfully transferred into *A. thaliana* to make it self-incompatible. This is the first demonstration that an SI system can be functionally transferred into a distantly related species, implicating an important step towards the utilisation of *Papaver* SI system in plant breeding.

5.3 Discussion

Transgenic *A. thaliana* lines in which *PrsS/PrsS:GFP* was driven by a *Brassica* stigma-specific promoter, *SLR1*, could express *PrsS/PrsS:GFP* in the stigma in a developmentally regulated and tissue-specific manner. *Semi-in-vivo* and *in planta* pollination assays demonstrated although the PrsS:GFP protein was not functional, PrsS protein without GFP tag was able to induce the SI response in *At-PrpS:GFP* pollen, resulting in the pollen tube growth inhibition, shorter siliques and production of few seeds. Further analysis demonstrated that other key features of SI, such as S-allele specific inhibition and developmentally controlled inhibition were also achieved in the transgenic *A. thaliana*. In summary, the work in this chapter has demonstrated that the *Papaver* stigma S-determinant, *PrsS*, is functional in *A. thaliana*. Moreover, the *Papaver* SI system comprising *PrpS* and *PrsS* can be successfully transferred into *A. thaliana* to make it self-incompatible. Self-incompatible *A. thaliana* plants were generated by transforming homozygous *At-ntp303::PrpS₁:GFP* plants with cognate *SLR1::PrsS*. Leaving these plants to self-pollinate naturally resulted in no seed set, unlike controls, which had full seed set, demonstrating that *Papaver* SI system could be

fully functional in *A. thaliana*. In the following sections, various aspects regarding the expression and functional analysis of PrsS/PrsS:GFP in *A. thaliana* will be discussed, as well as the transfer of SI system between different species.

5.3.1 PrsS protein expressed in different organisms

PrsS is a small, secreted protein produced in the stigmatic papillae cells of *P. rhoeas*. Both glycosylated and un-glycosylated isoforms of PrsS proteins are identified in *P. rhoeas*. The significance of glycosylation is still unclear. *E. coli* has been well established for the production of a variety of recombinant proteins due to its short life cycle, easy genetic manipulation and low cost (Gopal and Kumar, 2013). It has been successfully employed for the production of recombinant PrsS proteins for many years. It has been demonstrated by the *in vitro* SI assays that *E. coli* produced recombinant PrsS proteins are biologically active in inhibiting the growth of poppy pollen (Foote et al., 1994; Kurup et al., 1998; Walker et al., 1996), demonstrating that glycosylation of PrsS proteins is not essential for their biological activities. However, relatively high concentrations of *E. coli* expressed PrsS proteins ($\sim 8\text{-}10 \mu\text{g mL}^{-1}$) are needed to trigger a fully incompatible response in poppy pollen, indicating that glycosylation might play a role in bringing the activities of PrsS proteins to a higher level, perhaps by improving solubility and preventing aggregation. In addition to *E. coli*, studies using *Drosophila* cell culture system have also been employed, attempting to produce recombinant PrsS proteins with higher activities, as there are only minor differences regarding to the

post-translational modification between plants and animals, compared with that between plants and bacterial (Ma et al., 2003). However, it turned out that even higher concentration of *Drosophila* expressed PrsS protein ($\sim 30\text{-}50 \mu\text{g mL}^{-1}$) was needed for poppy pollen SI induction (Lin et al., unpublished). Overall, both bacterial and animal produced recombinant PrsS proteins have been demonstrated to be biologically active. Thus, it is considered unlikely that *A. thaliana*, which is evolutionarily closer to *P. rhoeas* than *E. coli* or *Drosophila*, produced PrsS protein is not functional, if PrsS could be expressed in *A. thaliana*. Studies here, using western blot analysis have shown that PrsS can be expressed in transgenic *A. thaliana* and that it appears to be subject to post-translational modifications (glycosylation) similar to what is observed in *P. rhoeas* as several bands were detected (Figure 5-9). Moreover, *semi-in-vivo* and *in planta* pollination assays have demonstrated that PrsS is functional in *A. thaliana* in triggering SI response in incompatible pollen. Failure to detect PrsS activities during *in vitro* SI assays using extracts derived from *At-35S::PrsS* transgenic seedlings (Chapter 4) are thought to possibly be due to the low abundance of PrsS proteins in the extracts.

In summary, it has been demonstrated that PrsS proteins expressed in bacteria, animal cell and plant are all biologically active in SI response induction, although they are subject to different post-translational modifications. The significance of glycosylation of PrsS protein remains to be further investigated.

5.3.2 GFP fusion might affect the proper function of PrsS

Fluorescent proteins, especially GFP, have been established as a remarkably useful tool in cellular and molecular biology, and have unprecedentedly increased our knowledge of protein localization and interaction, as well as cellular organization by facilitating the immunolocalization, affinity purification and immunoprecipitation. For example, the successful application of GFP labelled actin-binding proteins has revealed the structure and dynamic of actin cytoskeleton in pollen tubes (Cheung et al., 2008). Transgenic *P. inflata* plants expressing GFP-fused SLF in the pollen have been successfully employed to elucidate the relationship between the SLF and its non-self *S*-RNase (Sun and Kao, 2013). In addition, this also facilitated the identification of SLF-containing protein complex in *P. inflata* pollen (Li et al., 2014). In order to make it easier for the analysis of *PrsS* expression in *A. thaliana*, GFP fused transgenic lines, *At-SLR1::PrsS:GFP*, were also constructed. It has been demonstrated that both PrsS and PrsS:GFP proteins could be successfully expressed in the transgenic *A. thaliana* stigmas. However, functional analysis showed that PrsS:GFP failed to induce SI response in *At-PrpS:GFP* pollen, while PrsS was functional. This indicates that GFP fusion at the C-terminus of PrsS might affect the proper function of PrsS.

The GFP fusion protein is probably one of the most common biotechnological application of GFP in scientific research, as in principle, the resultant chimera does not affect the activity and localization of tagged protein in most cases (Zimmer, 2002).

However, it has been pointed out by many studies that GFP alters the expression, proper localization and function of some target proteins which were tagged (Rappoport and Simon, 2008). For example, RAD51 has been demonstrated to be involved in both meiosis and mitosis, but the GFP fusion protein is impaired. Although a RAD51:GFP fusion protein retained the capacity to assemble at DNA breaks during meiosis, it had lost the DNA break repair ability in mitosis (Da Ines et al., 2013). In yeast, it has been reported that GFP tagged actin cannot function properly as the sole actin source (Doyle and Botstein, 1996). High throughput analysis using reverse transfection microarrays indicated that for native protein localization analysis, GFP tagging at the C-terminus is generally better than fusion at the N-terminus in preserving the correct targeting and intracellular localization (Palmer and Freeman, 2004). See Rappoport and Simon (2008) for more examples of problems caused by GFP tagging.

With this information in mind, it is possible that the GFP fusion at the C-terminus of PrsS in this study might affect its function, although no solid evidence regarding to the molecular mechanisms of how GFP fusion affected PrsS function has been obtained. A simple working model is proposed here to explain why PrsS, but not PrsS:GFP, inhibited the growth of *At-PrpS:GFP* pollen. In the poppy SI response, the interaction of cognate PrpS-PrsS interaction triggered a Ca²⁺-dependent signalling network in incompatible pollen, resulting in the PCD. The mechanisms of PrpS-PrsS recognition and interaction are still not clear. However, it is known that several residues located in a

small hydrophilic loop of PrsS are crucial to in the recognition of incompatible pollen, as mutations of these residues result in the completely lost of PrsS activities (Kakeda et al., 1998). As GFP (~27 kD) is nearly twice the size of PrsS protein (~14 kD), GFP fusion of PrsS could quite possibly have the GFP moiety masking the active sites such as those resided in the hydrophilic loop mentioned above. As they are key to the PrsS-PrpS recognition, masking them might result in the loss of interaction between PrpS and PrsS, so that SI response in incompatible pollen triggered by the interaction between cognate PrpS and PrsS is not possible.

5.3.3 Functional transfer of *Papaver* SI system into *A. thaliana*

It has been demonstrated in previous research and this chapter that *Papaver* pollen and stigma *S*-determinants, *PrpS* and *PrsS*, could be functionally transferred into *A. thaliana* independently. PrpS:GFP could be successfully expressed in *A. thaliana* pollen and when *At-PrpS:GFP* pollen was treated with cognate PrsS protein, several key hallmarks of *Papaver* SI response including pollen tube growth inhibition, actin-foci formation and DEVDase activation were observed. This suggested that by the introduction of *PrpS*, endogenous components of *Arabidopsis* pollen could be recruited to form a new signalling network for the *Papaver* SI response. See de Graaf et al. (2012) and Eaves et al. (2014) for a review. For the functional transfer of the stigma *S*-determinant *PrsS*, PrsS proteins expressed in different organisms across three different kingdoms were all biologically active (section 5.3.1). However, for *in planta* analysis, a suitable promoter

was crucial for the *PrsS* being functional. Previously, *Stig1*, which is a stigma specific and developmentally regulated promoter, was employed to drive the expression of *PrsS* in *A. thaliana* (Vatovec, 2011). Although *PrsS* could be expressed in the stigma of *A. thaliana* driven by the *Stig1* promoter, *semi-in-vivo* and *in planta* pollination assays showed that *At-PrpS:GFP* pollen grew and fertilized ovules to produce normal seed sets (Vatovec, 2011). One reason why this might be the case is that although *Stig1* is stigma-specific, the expression of *Stig1* promoter peaks when the stigma is young, and decreases during the stigma maturation (Goldman et al., 1994; Verhoeven et al., 2005). This was forgotten when the constructs were made. As pollination assays are carried out using mature stigmas, and at this stage there would be hardly any expression under the control of *Stig1*. This is an obvious possible explanation for why there was no inhibition of *At-PrpS:GFP* pollen tube growth when *At-Stig1::PrsS* stigmas were pollinated. In the current studies, changing the promoter used to drive *PrsS* expression in *A. thaliana* from *Stig1* to *SLR1*, which shows peak expression in mature stigmas, successfully conferred the transgenic *A. thaliana* stigmas with the ability to inhibit *At-PrpS:GFP* pollen tube growth, resulting in almost no seed formation when pollinated with cognate *At-PrpS:GFP* pollen.

Instead of expressing *PrpS* and *PrsS* in two independent transgenic lines, *PrpS* and *PrsS* have also been co-transformed into *A. thaliana*, which resulted in self-incompatible *A. thaliana* plants. The evolutionary distance between *P. rhoeas* and *A. thaliana* is around

144 MYA (Bell et al., 2010), representing almost the furthest evolutionary distance within the dicot class. The successful transfer of *Papaver* SI system from *P. rhoeas* into *A. thaliana* suggests that *Papaver* SI system may potentially be transferred into other self-compatible species. This provides the hope that the plant breeders might have an alternative method for the production of F1 hybrid seeds.

Being able to transfer a SI system into normally self-compatible species to achieve an alternative method for the production of F1 hybrid seeds has been one of the long-term goals of SI research. Despite being conceptually simple and considerable effort invested over 30 years since the first *S*-determinants were cloned, it had not yet been realised prior to this study. SCR/SRK-based SI, *S*-RNase-based SI and *Papaver* SI represent the three SI systems whose molecular mechanisms that have been most intensively characterized. As described in Chapter 1, attempts to confer *A. thaliana* SI using *Brassica* *S*-gene pairs failed (Bi et al., 2000; Boggs et al., 2009b). Although inter-species transfer of *S*-RNase-based SI system has not been reported yet, it is considered that this is unlikely to be achieved, due to some unique cellular components required in the *S*-RNase-based SI signalling pathway. Unlike SCR/SRK-based SI and *S*-RNase-based SI systems, besides the pollen and stigma *S*-determinants, all the cellular components identified in the *Papaver* SI response so far have been demonstrated to be ubiquitous, such as Ca²⁺ (Franklin-Tong et al., 1993), F-actin (Geitmann et al., 2000; Thomas et al., 2006), microtubules (Poulter et al., 2008), MAPK (Li et al., 2007; Rudd

et al., 2003), sPPases (de Graaf et al., 2006; Rudd et al., 1996), DEVDase (Bosch and Franklin-Tong, 2007; Thomas and Franklin-Tong, 2004). This suggests that the introduction of *PrpS* and *PrsS* into a self-compatible species could quite possibly form the poppy SI signalling cascade by recruiting the existing universal cellular components. As a result, it might be predicted that self-compatible species which are transformed with *PrpS* and *PrsS* could become self-incompatible. It can be argued that as the *Papaver* SI signalling network is still not fully understood, and it is possible that there is involvement of some *Papaver* SI-specific components which are not characterized yet, but this does not matter. The successful establishment that *Papaver* SI system is functional in *A. thaliana* demonstrated that all cellular components involved in the poppy SI signalling network are conserved between *A. thaliana* and *P. rhoeas*, despite around 144 MYA evolutionary distances between them. This marks a very important step towards the production of F1 hybrid seeds in the normally self-compatible crops using *Papaver* SI systems. Some more aspects related to application of *Papaver* SI system will be discussed further in the General Discussion (Chapter 7).

**CHAPTER 6 INVESTIGATING THE ROLE
OF THE PROTEASOME IN THE *PAPAVER
RHOEAS* SI RESPONSE**

6.1 Introduction

It has been demonstrated that the ubiquitin-proteasome system (UPS) is involved in the regulation of both Brassicaceae SI and S-RNase-based SI (see Chapter 1 for more details). However, it is still unclear whether the UPS plays a role in the *Papaver* SI response. Preliminary investigations of the role of proteasome in *Papaver* SI response were carried out by Dr. Sabina Vatovec. To study whether the proteasome is involved in the SI-induced PCD in *Papaver* pollen, the poppy SI response was characterized in the presence of the proteasome inhibitor MG132. Preliminary data showed that inhibition of proteasome activities by MG132 before SI induction had virtually no effects on the SI-induced pollen tube growth inhibition, but significantly rescued pollen from SI-triggered death (Vatovec, 2011). A potential link between proteasomal degradation and SI-induced DEVDase activities has also been observed, and it was suggested that the proteasome might act upstream or in parallel with DEVDase activity during the poppy SI response (Vatovec, 2011). Also, in a pull down experiment performed by Dr. Maurice Bosch, in which DEVD-biotin probes were used to pull down DEVDase and DEVDase interacting proteins in SI-induced pollen extracts, a peptide corresponding to the proteasome alpha subunit of maize (the genome sequence of *P. rhoeas* is not available) was identified by mass-spectrometry. This suggested that poppy proteasome might also be responsible for the DEVDase activity. As mentioned in section 1.3.3 that proteasome has been identified conferring DEVDase activities during xylem

development and HR response. Thus, it is possible that the proteasome might play a role in the *Papaver* SI response, but the exact role is still unknown. Therefore, in this study, we further examined the involvement of the proteasome in the *Papaver* SI response, and the identity of DEVDase during the *Papaver* SI-induced PCD. Proteasome-specific inhibitors and probes were employed in this study to measure the proteasomal activity and define the role of the proteasome. Therefore, we introduce proteasome-specific inhibitors and probes below.

6.1.1 Tools to study the proteasome: proteasome-specific inhibitors

The most widely used are peptide aldehydes, typified by carbobenzoxy-leucinyl-leucinyl-leucinal-H (Z-LLL-al; MG132). MG132 is a proteasome substrate analogue which has been found to form a reversible covalent bond primarily with the proteasome subunit which confers chymotrypsin-like activities (Rock et al., 1994). Lysosomal proteases and calpains are also found to be blocked by MG132 (Lee and Goldberg, 1998). Other proteasome inhibitors include peptides containing a vinyl sulfone (VS) moiety at the C-terminus, such as Z-LLL-VS. Unlike MG132, Z-LLL-VS blocks proteasome activities by irreversibly modifying the N-terminal threonine of proteasome β -subunits (Bogyo et al., 1997). Similarly, these VS-based compounds have also been reported to non-specifically bind and inhibit other proteases, for example, cathepsin S (Bogyo et al., 1997; Lee and Goldberg, 1998). Recently, VS-based proteasome inhibitors have been further modified by adding a fluorophore to

enable monitoring of the proteasome activities (Berkers et al., 2007; Gu et al., 2010; Verdoes et al., 2006). Natural products, represented by lactacystin and epoxomicin, are another class of structurally distinct proteasome inhibitors, which are more specific but expensive. Lactacystin was originally isolated from *Actinomycetes* based on its ability to promote neurite outgrowth (Omura et al., 1991). β -lactone, which is the lactacystin derivate in aqueous solution, is the actual active form the inhibitor. Like VS-based inhibitor, β -lactone functions as a pseudo-substrate and covalently links to the active site threonine of all the proteasome β catalytic subunits (Fenteany et al., 1995). β -lactone shows a much higher inhibition specificity than MG132 and VS-based inhibitors do, but non-specific inhibition of cathepsin A can still be observed (Fenteany and Schreiber, 1998). Epoxomicin was also initially isolated from *Actinomycetes* based on its antitumor activity (Konishi, 1992), representing a novel class of cell permeable and irreversible inhibitors with its unique specificity and potency. In contrast to all the other proteasome inhibitors mentioned above, epoxomicin does not block non-proteasomal proteases such as cathepsin, calpain and papain at concentrations of up to 50 μ M (Meng et al., 1999). Like MG132, epoxomicin preferentially inhibits proteasome chymotrypsin-like activities, and trypsin-like and caspase-like activities are inhibited at 100-fold lower rate (Meng et al., 1999).

6.1.2 Measuring proteasome activities

Fluorogenic peptide substrates are one of the most commonly used tools to profile

proteasome activities. They are short peptides equipped with a fluorophore at the C-terminus. The fluorescence is initially quenched while they joined as an intact molecule, and only released when cleaved between the amino acid and the fluorophore by specific proteasome active site (Kisselev and Goldberg, 2005). Of all the different fluorogenic reporter groups, 7-amino-4-methylcoumarin (AMC) is most often used. Quite a few fluorogenic peptides have been developed to measure the activities of the three different proteasome catalytic subunits (Table 6-1).

Table 6-1 Fluorogenic substrates to assay proteasome activities

Proteasome subunit target	Fluorogenic peptide substrate
Caspase-like, PBA1	Z-LLE-amc
	Ac-nLPnLD-amc
	Ac-GPLD-amc
Trypsin-like, PBB	Ac-RLR-amc
	Z-ARR-amc
	Boc-LSTR-amc
Chymotrypsin-like, PBE	Suc-LLVY-amc
	Z-GGL-amc

Table adapted from Liggett et al. (2010)

Fluorogenic peptide substrates are suitable to measure catalytic activities of purified proteasome or crude cell extracts. However, non-specific cleavages from other proteases in the crude extracts can lead to the uncertainties of measurement results. Recently, a new method, activity-based protein profiling (ABPP), has been developed to enable the

profiling of proteasome activities more precisely, in both crude extracts or living tissues (Cravatt et al., 2008; Ovaa, 2007). ABPP is based on the use of irreversible covalent inhibitors, which can react with the active site residue of the proteasome in a mechanism-dependent manner (Cravatt et al., 2008). Equipping the small molecule inhibitors with reporter groups, such as bodipy or biotin, allows the detection and identification of proteasome catalytic activities in their active states. MV151 (BodipyTMR-Ahx₃L₃VS; Figure 6-1), which was employed as the proteasome activities probe in this study, will be introduced as a representative of ABPP probes. MV151 is a cell permeable, fluorescent and activity based probe for the proteasome, developed by Verdoes et al. (2006). During proteasome labelling, binding peptides (Leu × 3) act as the pseudo-substrates for proteasome catalytic subunits, and VS forms covalent bonds with the active threonine residues irreversibly. Followed by protein separation using SDS-PAGE, modified proteasome subunits (PBA1, PBB and PBE, see Chapter 1 for more details of these three active sites of proteasome) can be immediately identified and visualized through in-gel fluorescent read-out based on the molecular weight difference (Berkers et al., 2007; Verdoes et al., 2006). The cell-permeable and fluorescent nature of MV151 also makes it compatible with live-cell imaging techniques. MV151 has been demonstrated to be a robust probe for both proteasome and papain-like cysteine protease (PLCP) activities profiling in plants, both *in vitro* and *in vivo* (Gu et al., 2010). The disadvantage is that MV151 labels the proteasome and PLCP simultaneously,

which make it not so useful in live-cell imaging (van der Hoorn and Kaiser, 2012).

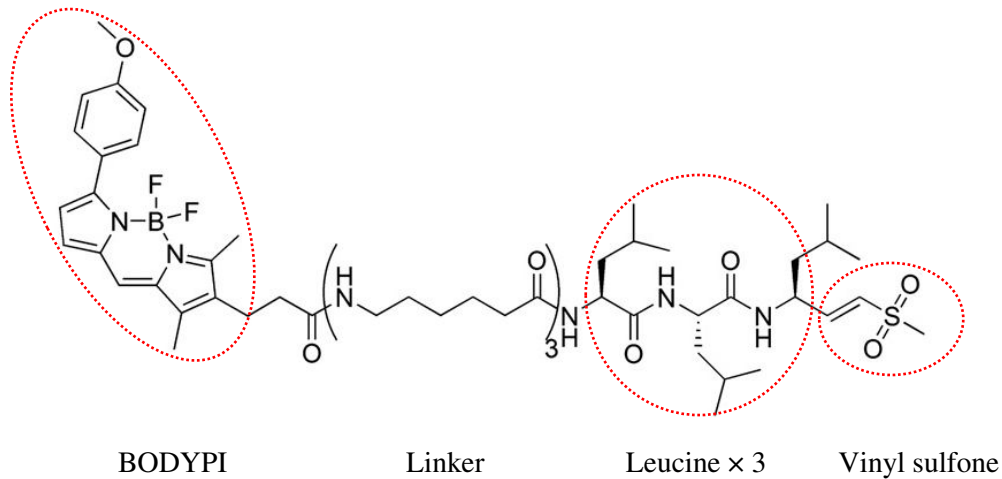


Figure 6-1 Structure of MV151

MV151 is an activity based probe for proteasome. It contains a fluorescent reporter group (BODIPY), a linker (Ahx × 3), a binding peptide (Leucine × 3) and a reactive group (VS).

6.1.3 Project aims

In this study, we investigated the possible involvement of the proteasome in the poppy SI response, as a first step, by characterizing the proteasomal activity during the poppy SI response. To examine the role of the proteasome in SI-induced PCD, proteasome specific inhibitors were applied to investigate the effects of proteasome inhibition on the poppy SI response, including SI-triggered pollen tube growth inhibition, pollen viability decrease and DNA fragmentation. As we have demonstrated that the *Papaver* SI response triggers a DEVDase-mediated PCD in incompatible pollen and identified a proteasome subunit peptide in the DEVD-pull-down assay, in the light of the finding that the proteasome is emerging to play a prominent role in plant PCD by conferring

DEVDase activities (Han et al., 2012; Hatsugai et al., 2009; section 1.3.3), we wondered if the poppy proteasome is also responsible for DEVDase activity during the *Papaver* SI-induced PCD. Therefore, in this study, we also investigated the relationship between proteasome activities and DEVDase activities in *Papaver* pollen by biochemical characterization of both activities with proteasome inhibitors, DEVDase inhibitors and gradient pH buffers.

6.2 Results

6.2.1 Characterization of proteasomal activities during the poppy SI response

In order to investigate the role of proteasome during poppy SI response, proteasomal activity was profiled using fluorogenic peptide substrates in pollen protein extracts, to see if there was any proteasomal activity change during SI response. Of the three active sites in the proteasome (see Chapter 1 for more details), PBE has been suggested to be rate-limiting in protein degradation by a variety of studies (Lee and Goldberg, 1998), and PBA1 recently has attracted lots of attention because it has been suggested to be the DEVDase candidate in plants (Hatsugai et al., 2009). Therefore, PBA1 and PBE activities of poppy proteasome were investigated in this study, using Ac-nLPnLD-amc and Z-GGL-amc as the substrates, respectively.

The proteasomal activity in the early phase (first 1h) of poppy pollen SI response was firstly characterized (sections 2.4.1-2.4.3). Poppy pollen proteins [both untreated (UT)

and SI] were extracted at different time points (0 min, 10 min, 30 min, 60 min after SI induction) and were subjected to proteasomal activity measurement (Figure 6-2).

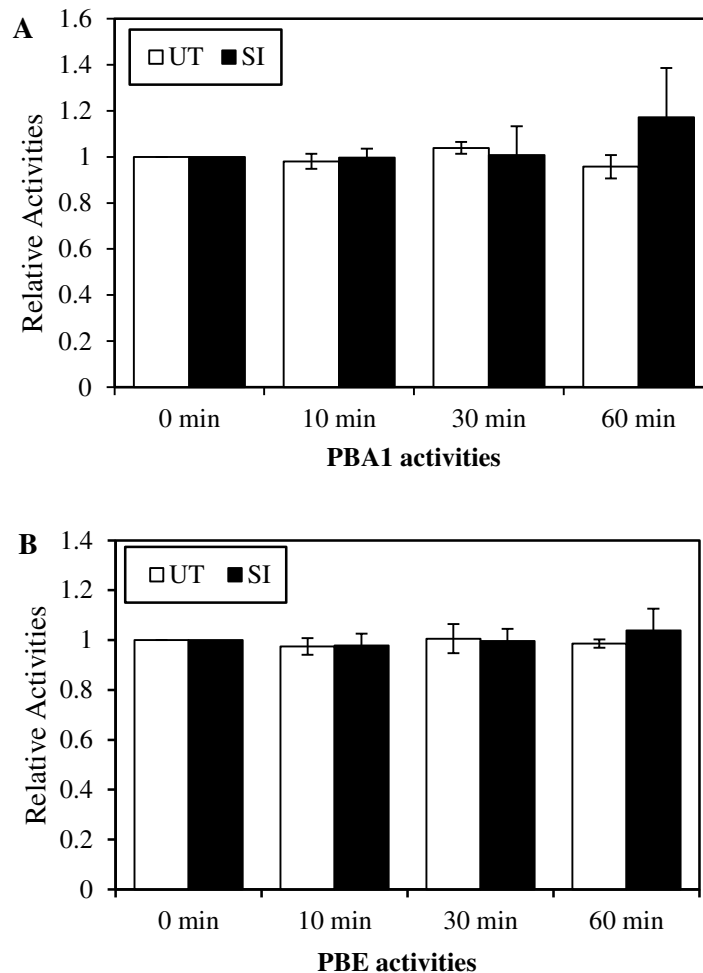


Figure 6-2 No significant alteration in proteasomal activity is observed in the early phase of poppy SI response

The proteasomal activities in the early phase of poppy SI response were investigated using fluorogenic peptide substrates in pollen extracts. No statistically significant changes in proteasome activities were observed during the first 1h after SI induction. A: time course of PBA1 activities during the early phase of poppy SI response. B: time course of PBE activities during the early phase of poppy SI response. UT: untreated control. Result =mean \pm SD, n=3.

Both PBA1 and PBE activities were detected throughout the first 1h of pollen tube growth (Figure 6-2). There was no statistically significant change of poppy pollen

proteasomal activity during the first 1h of pollen tube growth ($p=0.079$ for PBA1; $p=0.704$ for PBE; One-way ANOVA). The detection of stable PBA1 and PBE activities during poppy pollen tube growth suggested a constitutive role for the proteasome in the growth of poppy pollen tubes. This is consistent with several other studies concluded that the proteasome plays an important role during the pollen germination and tube elongation (Scoccianti et al., 2003; Sheng et al., 2006; Speranza et al., 2001).

Proteasomal activity after recombinant PrsS proteins treatment was also investigated (Figure 6-2). However, no statistically significant changes in either PBA1 or PBE activities were observed comparing SI with UT samples. This suggested that the SI response in incompatible poppy pollen did not trigger significant alterations in proteasomal activity in the early phase (1h) of poppy SI response.

Several independent studies have suggested a role of the proteasome as a DEVDase (Han et al., 2012; Hatsugai et al., 2009) or an interaction between the proteasome and DEVDase (Wang et al., 2014) in plant PCD. As activation of DEVDase activities is a key hallmark of poppy SI response and peak DEVDase activities were detected 5 h after SI induction (Bosch and Franklin-Tong, 2007; Thomas and Franklin-Tong, 2004), proteasomal activities were profiled 5 h after SI induction. Pollen protein extracts obtained 5 h after SI induction were subjected to DEVDase, PBA1 and PBE activity measurements using Ac-DEVD-amc, Ac-nLPnLD-amc and Z-GGL-amc, respectively.

Dramatic increases in DEVDase activity were observed in SI samples 5 h after SI induction (Figure 6-3, $p=0.002$, Student's t -test). DEVDase activity measurement was employed as the positive control, indicating that the UT and SI samples for proteasomal activity measurements were properly prepared.

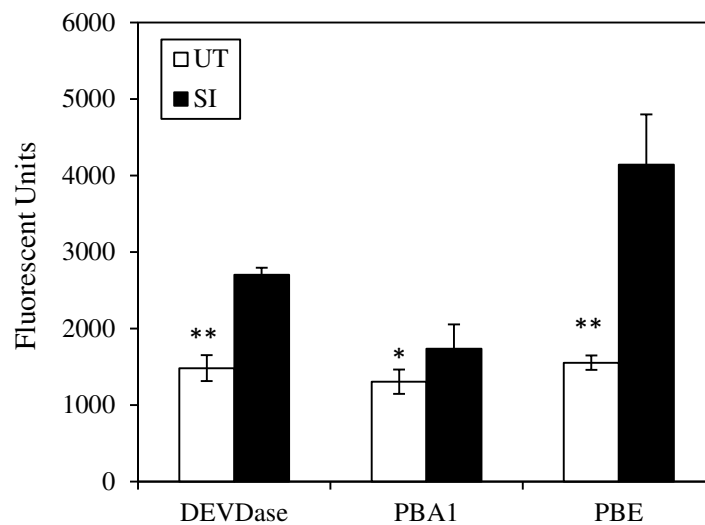


Figure 6-3 Poppy SI response triggers an increase of proteasomal activity 5h after SI induction in the incompatible pollen

The proteasomal activities in poppy SI response were investigated using fluorogenic peptide substrates in pollen extracts 5h after SI induction. DEVDase activity was measured as control. Significant increases of DEVDase, PBA1 and PBE activities were observed in the SI extracts. Note that values of DEVDase, PBA1 and PBE activities were not comparable, because different probes were used. Result =mean \pm SD, $n=4$. *, $p<0.05$; **, $p<0.01$.

SI induction for 5h triggered significant increases in PBA1 (Figure 6-3; $p=0.027$, Student t -test) and PBE (Figure 6-3; $p=0.005$, Student t -test) activity. This provided evidence that the proteasome was targeted by the poppy SI response, and might play a role. Interestingly, the increases of PBA1 and PBE activities were unsynchronized, even though both PBA1 and PBE are subunits of the proteasome. Comparing the proteasomal

activity detected in SI sample with that in UT, PBA1 activity increased by 33.3%, while PBE activity increased by 166.7% (Figure 6-3). This might indicate different roles of PBA1 and PBE, and possible multiple roles of the proteasome during the poppy SI response.

6.2.2 Investigating the effects of proteasomal inhibition on pollen tube growth

The observation of constitutive stable proteasomal activity during poppy pollen tube growth suggested that the proteasome might play an important role in pollen tube growth. However it was still unclear what the roles of proteasome are during the growth of poppy pollen tubes. Therefore, the significance of proteasome activity during poppy pollen tube growth was investigated by studying the effects of MG132, which is a proteasome inhibitor, on pollen. Various aspects, including pollen grain germination, pollen tube elongation, pollen morphology alteration and pollen viability, were evaluated.

6.2.2.1 MG132 inhibits poppy proteasome activity *in vitro*

MG132 is a potent, cell-permeable, and reversible inhibitor, which has long been involved in a variety of studies (Palombella et al., 1994; Rock et al., 1994; Sheng et al., 2006; Speranza et al., 2001). We therefore tested the ability of this compound to inhibit the poppy proteasome activity both *in vitro* and *in vivo*. MV151 labelling is a newly developed, robust and versatile method for both *in vitro* and *in vivo* proteasome

activities profiling (Gu et al., 2010). So, MV151 labelling was also employed in our study to test the ability of MG132 to inhibit poppy proteasome activities in pollen extracts (section 2.4.5; Figure 6-4).

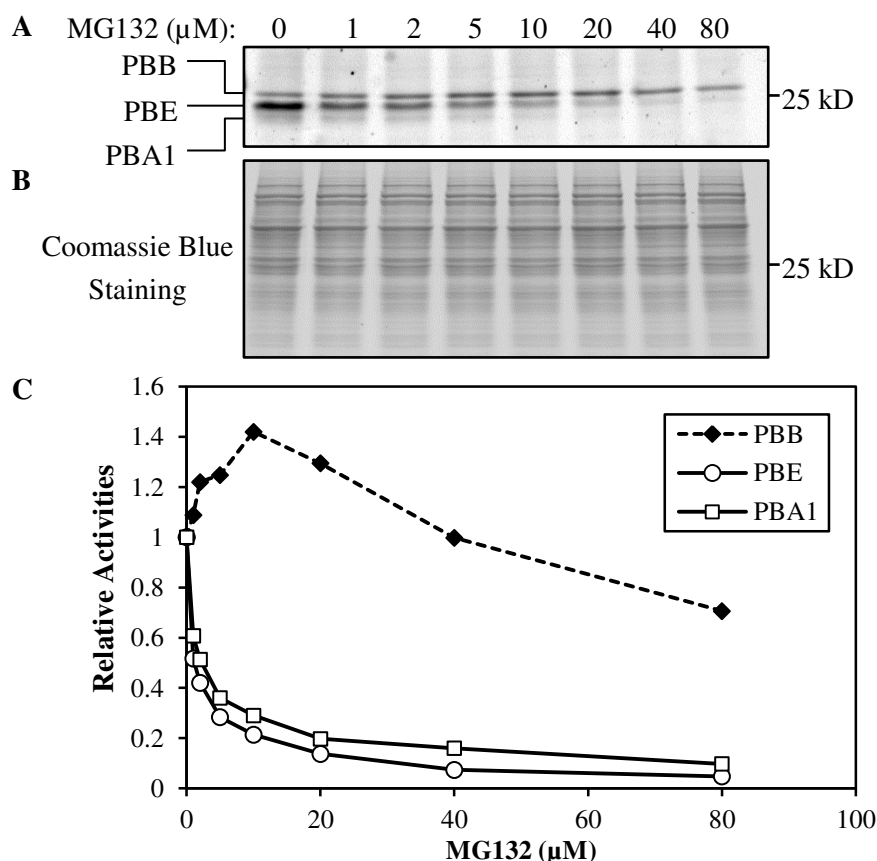


Figure 6-4 MG132 inhibits proteasome activity *in vitro* revealed by MV151 labelling

Poppy pollen extract was subjected to MV151 labelling in the presence of different concentrations of MG132. A: MV151 was able to label poppy proteasome subunits PBA1, PBB, and PBE, and MG132 affected proteasome activities in a concentration dependent manner. B: coomassie blue staining showed equal loading. C: fluorescent bands detected in A were quantified and plotted against inhibitor concentrations. N=2.

Three fluorescent bands corresponding to the three proteasome subunits were detected (Figure 6-4-A), demonstrating that MV151 was able to target poppy proteasome

subunits *in vitro*. Pre-treatment of pollen extracts with a dilution series of MG132 clearly showed that MG132 influenced the fluorescent bands intensities (Figure 6-4-A); the equal loading was verified by coomassie blue staining (Figure 6-4-B). This suggested that proteasome activity was affected by MG132. Quantification of the fluorescent bands intensities allowed a better understanding of the influence of MG132 on proteasome activities (Figure 6-4-C). As shown in Figure 6-4-C, different proteasomal subunits had different sensitivities to MG132. Of the three subunits, PBE was preferentially inhibited by MG132. A dramatic reduction of PBE activity was observed when as low as 1 μM of MG132 was added, and more than 80% of PBE activity could be abolished by 20 μM MG132. Further increases in MG132 resulted in almost complete inhibition of PBE activity. PBA1 shared a similar inhibition profile with PBE. Two μM MG132 reduced PBE activity by nearly 50%, and 20 μM MG132 was sufficient enough to reduce PBA1 activity by 80%. Interestingly, a completely different activity profile was observed for PBB. PBB activity increased when pollen extracts were treated with low concentration of MG132. Ten μM MG132 brought PBB to its peak activity, with an increase of ~40% of activity observed. Higher concentrations of MG132 inhibited PBB activity; 40 μM MG132 reduced PBB activity to below the original level. Further reduction of PBB activity was observed when higher concentrations of MG132 were added. At 80 μM , PBB activity was reduced by 30%.

These data showed that poppy proteasome subunits could be targeted by MV151,

demonstrating that MV151 was a suitable probe for poppy proteasome activities profiling. In addition, MV151 labelling demonstrated that MG132 inhibited poppy proteasome activity by preferentially inhibiting PBA1 and PBE.

6.2.2.2 MG132 inhibits poppy proteasome activity *in vivo*

In vivo inhibition of the poppy proteasome by MG132 was also examined, using MV151 as the proteasome activities profiling probe. Poppy pollen was grown in the presence of different concentrations of MG132 before MV151 labelling, protein extraction and SDS-PAGE analysis. Three fluorescent bands corresponding to the three subunits of proteasome were detected, demonstrating that MV151 was able to target poppy proteasome *in vivo* (Figure 6-5-A). The alterations of band intensities after MG132 treatment indicated that MG132 affected proteasome activities. This was further confirmed by the quantitative analysis of the fluorescent bands intensities (Figure 6-5-C). As shown in Figure 6-5-C, MG132 affected different proteasome subunits. PBA1 and PBE shared a similar inhibition pattern from MG132, while MG132 increased PBB activities. For both PBA1 and PBE, 5 μ M MG132 dramatically decreased their activities by 50%. Twenty μ M MG132 resulted in the reduction of PBA1 and PBE activities by ~80%, demonstrating MG132 as a potent inhibitor for *in vivo* inhibition of poppy proteasome. However, in contrast to PBA1 and PBE, PBB activities were increased by MG132 treatment. Peak activity of PBB was observed at 40 μ M MG132 (increased >60%). Further increased concentrations of MG132 brought

PBB activity down gradually. Figure 6-5-B shows equal loading.

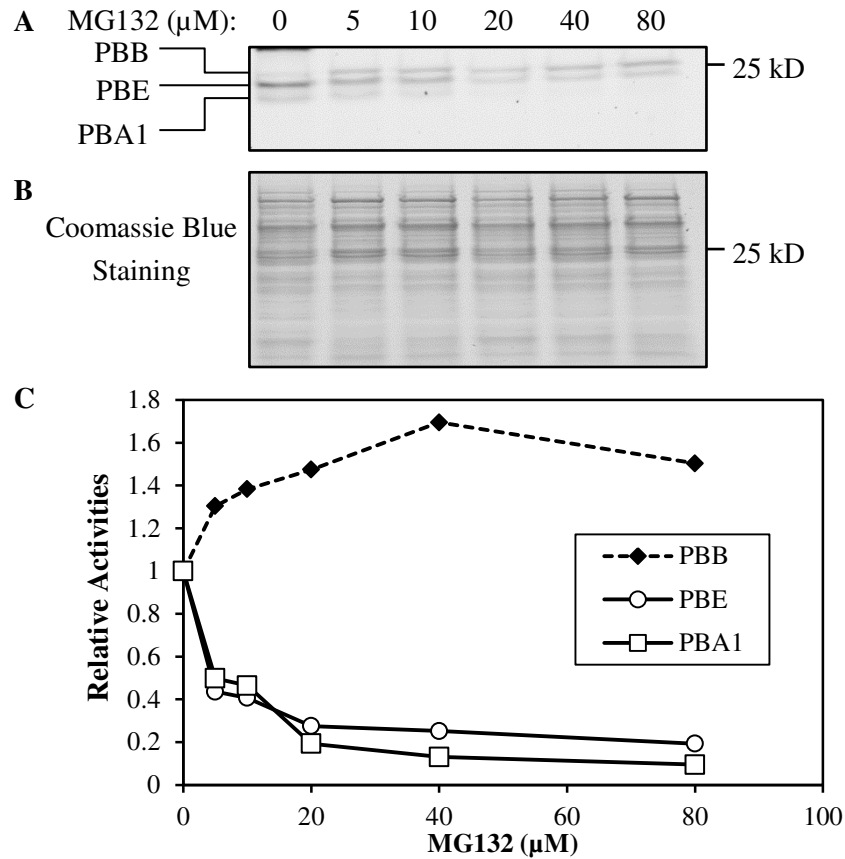


Figure 6-5 MV151 labelling revealed MG132 inhibited proteasome activities *in vivo*

Poppy pollen was grown with or without increasing concentrations of MG132 for 1h before MV151 was added. Pollen was allowed to grow for a further 2 h after adding MV151, followed by protein extraction, SDS-PAGE and fluorescent gel imaging. A: MV151 was able to label poppy proteasome subunits PBA1, PBB, as well as PBE *in vivo*, and MG132 affected proteasome activities in a concentration dependent manner. B: coomassie blue staining showed equal loading. C: fluorescent bands detected in A were quantified and plotted against the inhibitor concentrations.

In summary, MV151 labelling revealed that MG132 was able to inhibit poppy proteasome activities both *in vitro* and *in vivo* by completely blocking PBA1 and PBE activities, whilst slightly increasing PBB activities. Since the proteasome works as an

intact unit *in vivo*, and PBE has been suggested to be rate-limiting in protein degradation by a variety of studies (Lee and Goldberg, 1998), complete blocking of two of the three subunits (PBA1 and PBE) should abolish the proper function of proteasome. Therefore, MG132 was employed to investigate the effects of proteasome inhibition on poppy pollen tube growth and poppy SI response.

6.2.2.3 Proteasome inhibition affected the germination and elongation of poppy pollen tubes

As MG132 can inhibit poppy pollen proteasome *in vivo*, we examined the effects of proteasome inhibition on poppy pollen germination and pollen tube elongation by growing poppy pollen in the presence of MG132. MG132 slightly reduced poppy pollen grain germination rate by ~10% (Figure 6-6). This suggested that the proteasome was involved in poppy pollen germination.

We investigated whether the proteasome played a role in pollen tube elongation by growing poppy pollen in the presence of MG132 followed by pollen tube length measurement. We found that MG132 significantly affected pollen tube growth rate, strongly reducing it from 295 $\mu\text{m h}^{-1}$ to less than 100 $\mu\text{m h}^{-1}$ (Figure 6-7). This suggested that proteasome was involved in the poppy pollen tube growth.

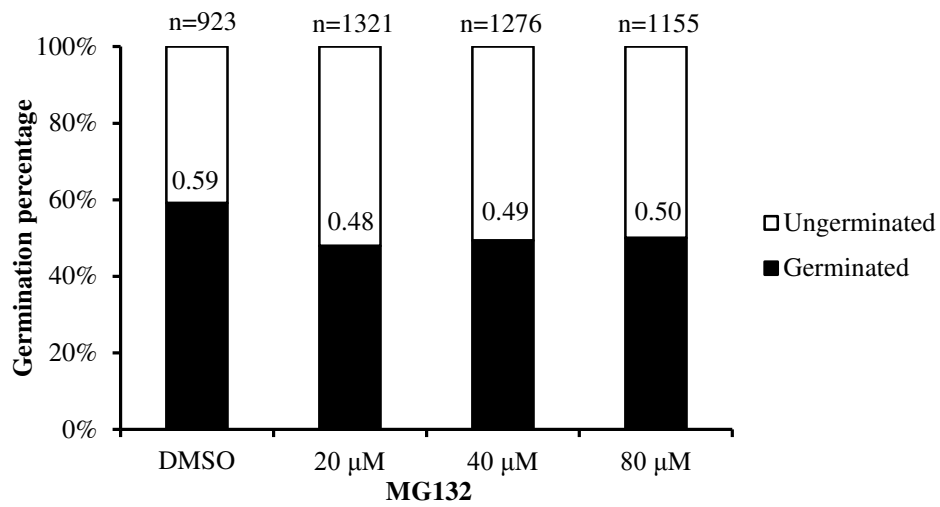


Figure 6-6 Proteasome inhibition slightly reduces poppy pollen germination

Poppy pollen was hydrated and then treated with DMSO or increasing concentrations of MG132. Pollen was allowed to grow at 27 °C for 3h before germination was checked using microscopy. N indicated the total pollen grains counted in each sample.

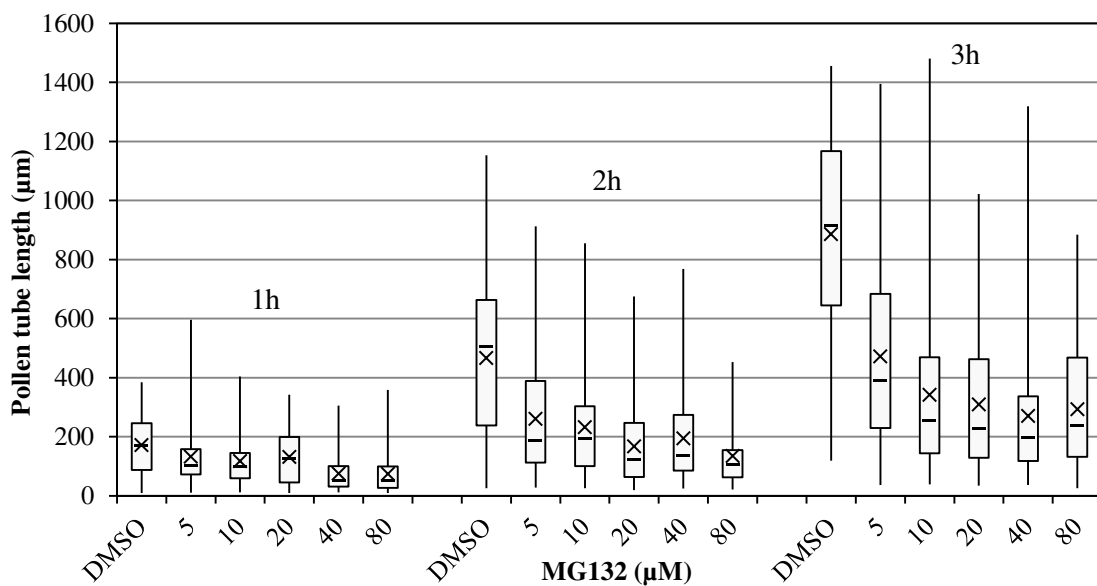


Figure 6-7 Effects of proteasome inhibition on poppy pollen tube elongation

Poppy pollen was hydrated and treated with DMSO or different concentrations of MG132. Pollen tube lengths were measured using Nikon Elements software every one hour. The distribution of pollen tube lengths in each treatment were shown in the form of quarter-boxplot. Cross indicated mean values of pollen tube lengths, and short horizontal lines indicated median values. 100-150 pollen tube lengths were measured in each sample.

Together with the observation that MG132 treatment caused significant changes in pollen tube morphology, including tip swelling, tube leakage, tube branching (data not shown), we have provided strong evidence that the proteasome is an important regulator involved in the regulation of poppy pollen germination, pollen tube growth and morphology.

6.2.3 Investigating the effects of proteasome inhibition on poppy SI response

So far, we have demonstrated that poppy SI triggered proteasome activities increase 5 h after SI induction (Figure 6-3), and investigations have demonstrated that the proteasome is involved in pollen grain germination (Figure 6-6), pollen tube elongation (Figure 6-7) and maintaining normal poppy tube shape. However, it is still unknown what the role of proteasome is during the poppy SI response.

6.2.3.1 Effects of proteasome inhibition on SI-triggered pollen growth inhibition

Pollen tube growth inhibition is one of the most rapid responses observed after SI induction in incompatible poppy pollen (Franklin-Tong et al., 1993; Geitmann et al., 2000). It has been shown that DEVDase activities play a crucial role in the arrest of incompatible pollen tube growth (Thomas and Franklin-Tong, 2004). To gain an insight into whether the proteasome was also involved in pollen tube growth arrest triggered by poppy SI, we examined the effects of MG132 on SI-induced pollen tube inhibition. As shown in Figure 6-8, DMSO treated poppy pollen was able to grow at an average

growth rate of $192 \mu\text{m h}^{-1}$, resulting in a mean pollen tube length of $609 \mu\text{m}$ 190 min after germination. SI induction significantly blocked the growth of incompatible pollen (Figure 6-8). Before SI induction, the average length of poppy pollen tubes was $159 \mu\text{m}$. However, 130 min after SI induction, the average length of poppy pollen tubes was observed to be $164 \mu\text{m}$ (Figure 6-8). Almost no pollen tube elongation after SI induction was observed compared with the pollen tube growth in the control.

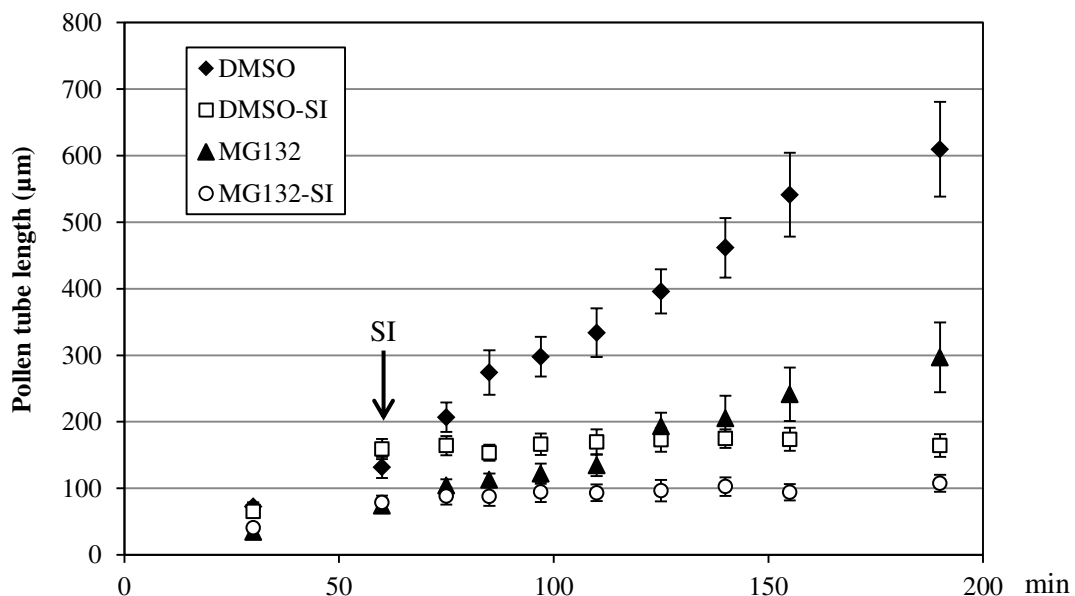


Figure 6-8 Proteasome inhibition does not alleviate SI-induced poppy pollen tube growth inhibition

Poppy pollen was pre-germinated with DMSO or MG132 ($40 \mu\text{M}$). SI responses were triggered 1 h after pre-germination. Pollen tube lengths were continuously measured within the first 200 min of incubation. Diamond, DMSO treatment only; square, DMSO treatment before SI induction; triangle, MG132 treatment only; circle, MG132 treatment before SI induction. Result = mean \pm SE, $n=30$.

MG132 ($40 \mu\text{M}$) significantly inhibited the growth rate of poppy pollen tube growth (Figure 6-8). Pre-treatment with MG132 for 1 h resulted in a mean pollen tube length of

79 μm , which was significantly shorter than that of DMSO control ($p < 0.01$), which was 132 μm . Monitoring the lengths of pollen tubes which had been pre-treated with MG132 prior to SI induction showed that pre-treatment with MG132 had no alleviation of SI-induced pollen tube growth inhibition (Figure 6-8). This provided evidence that the proteasome was not involved in the rapid inhibition of pollen tube growth induced by SI response in incompatible poppy pollen.

6.2.3.2 Effects of proteasome inhibition on SI stimulated viability decrease

It has been well established that poppy SI response stimulated the loss of viability of incompatible pollen tubes (Jordan et al., 2000). Pre-treatment with DEVDase inhibitor, Ac-DEVD-CHO, or MAPK inhibitor U0126 rescued pollen tubes viability after SI induction, demonstrating both DEVDase and MAPK played central roles in pollen tube viability inhibition during poppy SI response (de Graaf et al., 2012; Li et al., 2007). In order to investigate whether proteasome might be involved in the SI stimulated loss of pollen tube viability, we examined the viabilities of pollen tubes which had been pre-treated with MG132 before SI induction using FDA staining (Heslop-Harrison et al., 1984).

As shown in Figure 6-9, a slightly decrease in pollen viability was observed, from 68.6% at $t=0\text{h}$ to 52.3% at $t=8\text{h}$. There was no significant difference between the pollen tube viabilities at $t=0, 1, 3, 5,$ or 8h ($p=0.111$, One-way ANOVA), demonstrating that

untreated pollen retained their viability over the 8-h experimental period. SI induction triggered a dramatic decrease in pollen tube viability (Figure 6-9). Pollen viability decreased significantly from 67.9% to 42.0% 1h after SI induction. At t=3h, pollen viability was observed to further reduced to 14.5%, and retained below 10% at t=5h and t=8h.

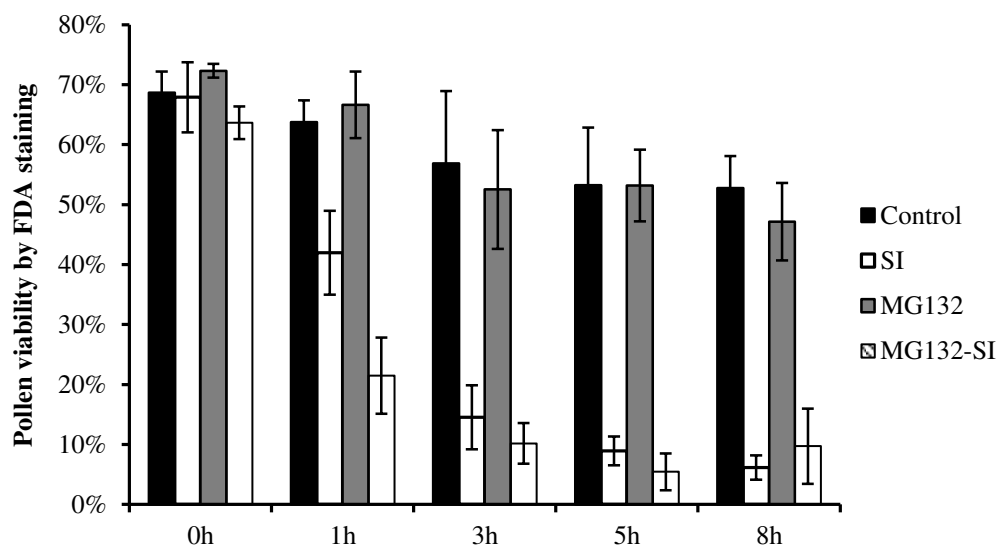


Figure 6-9 Proteasome inhibition does not alleviate SI-induced poppy pollen viability decrease

Poppy pollen was pre-treated with DMSO or MG132 (40 μ M) for 1h, followed by recombinant PrsS proteins treatments. The moment of SI induction was set as t=0h. Pollen viability was checked by measuring esterase activity using FDA staining. Black bars, DMSO only; white bars, DMSO followed by PrsS proteins treatment; grey bars, MG132 only; dashed bars, MG132 pre-treatment before SI induction. Result =mean \pm SD, n=3. One hundred pollen tubes were counted for each sample at each repeat.

MG132 treatment did not cause significant alteration in pollen viability over the 8h time period with respect to untreated pollen samples (Figure 6-9). This demonstrated that proteasome inhibition did not change the viability of normal growing poppy pollen.

Analysis of the viability over the 8-h experimental period after SI induction revealed that MG132 pre-treatment significantly accelerated pollen viability decrease in the first 1 h after SI induction ($p=0.033$). For SI treatment, pollen viability was reduced by 25.9% at $t=1h$. However, in MG132-SI, a reduction of 42.1% in pollen viability was observed at the same time point. These data suggested that proteasome inhibition enhanced SI triggered pollen viability loss, and indicated an interaction between proteasome and SI signalling cascade at the early phase of SI, which affected pollen viability. No significant increase in pollen viability was observed in SI induced pollen which had been pre-treated with MG132 (Figure 6-9) compared with SI pollen (Figure 6-9). At $t=8h$, pollen viability of SI and MG132-SI was 6.2% and 9.7%, respectively, which were not significantly different ($p=0.448$). The observation that proteasome inhibition did not alleviate SI-induced pollen loss of viability suggested that proteasome was not involved in the SI triggered pollen tube viability decrease.

6.2.3.3 Effects of proteasome inhibition on SI triggered DNA fragmentation

DNA fragmentation is well established as a hallmark of the late phase of poppy SI-PCD (Jordan et al., 2000). As SI triggered increases in proteasome activity, we wondered whether the proteasome functioned up-stream of the DNA fragmentation and might be involved in the poppy SI-induced PCD. First, it was necessary to determine whether proteasome inhibition was able to affect the DNA integrity directly in the normally growing poppy pollen, using a TUNEL assay (section 2.4.6). A TUNEL signal was

absent in most of the UT pollen, in which DNA fragmentation was only 8.2% (Figure 6-10, A, B and E). Figure 6-10 C and D show typical images of DNA fragmentation triggered by SI. A dramatic increase in the number of TUNEL positive nuclei was observed in SI pollen samples, where the DNA fragmentation was 65.3% (Figure 6-10-E).

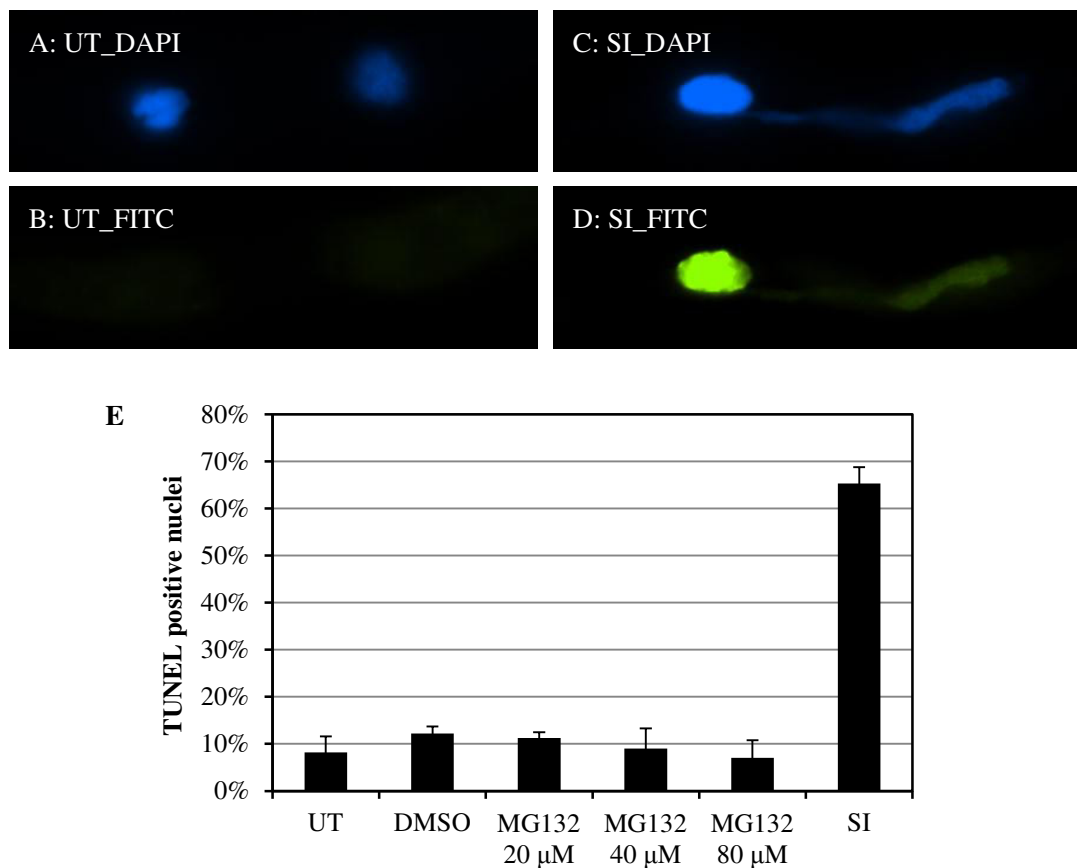


Figure 6-10 Proteasome inhibition does not trigger DNA fragmentation in poppy pollen

The effect of proteasome inhibition on DNA integrity was investigated. SI treatment was employed as a technical positive control. A and B: intact nucleus were observed in UT treated pollen. C and D: SI triggered DNA fragmentation in incompatible pollen. E: TUNEL signals from MG132 treated pollen were analysed. There was no significant alteration of the TUNEL signals compared to those of UT or DMSO control, while dramatic increase in the percentage of TUNEL positive nuclei was observed in SI. Result =mean ±SD, n=3, 100 pollen tubes were counted in each individual experiment.

In the control samples, 12.2% TUNEL positive nuclei were observed, which was statistically undistinguishable from that of UT ($p=0.202$). A slight decrease in the number of fragmented nuclei was observed in the MG132 treated pollen sample compared to the DMSO control (Figure 6-10-E). However, there was no statistical difference between the DMSO control and MG132 treatment ($p=0.228$). This suggested that inhibition of the proteasome was not able to trigger DNA degradation in poppy pollen. As DNA fragmentation is a hallmark feature of PCD, this also indicated that proteasome inhibition did not result in PCD of poppy pollen.

After confirming that proteasomal inhibition did not induce DNA fragmentation in poppy pollen, we investigated whether the proteasome was involved in the SI triggered DNA fragmentation by examining the integrity of DNA in SI induced incompatible pollen which had been pre-treated with alternative proteasome inhibitors, including MG132, epoximicin and β -lactone, which are all potent proteasome inhibitors widely used in varied proteasome-related studies. In the DMSO control, DNA fragmentation could only be found in 7.3% of the pollen sample (Figure 6-11), whereas this percentage was increased to 69.8% 8 h after SI induction ($p=0.006$; Figure 6-11). In normally growing poppy pollen, MG132 treatment did not trigger DNA fragmentation (Figure 6-10). In terms of SI induced incompatible pollen, pre-treatment with MG132 slightly raised the DNA fragmentation rate from 69.8% to 84.1% (Figure 6-11), but this was not statistically significant ($p=0.100$). These data showed that proteasome inhibition during

poppy SI response did not alleviate SI induced DNA fragmentation, suggesting that the proteasome was not involved in the SI signalling pathway resulting in the degradation of nuclear DNA.

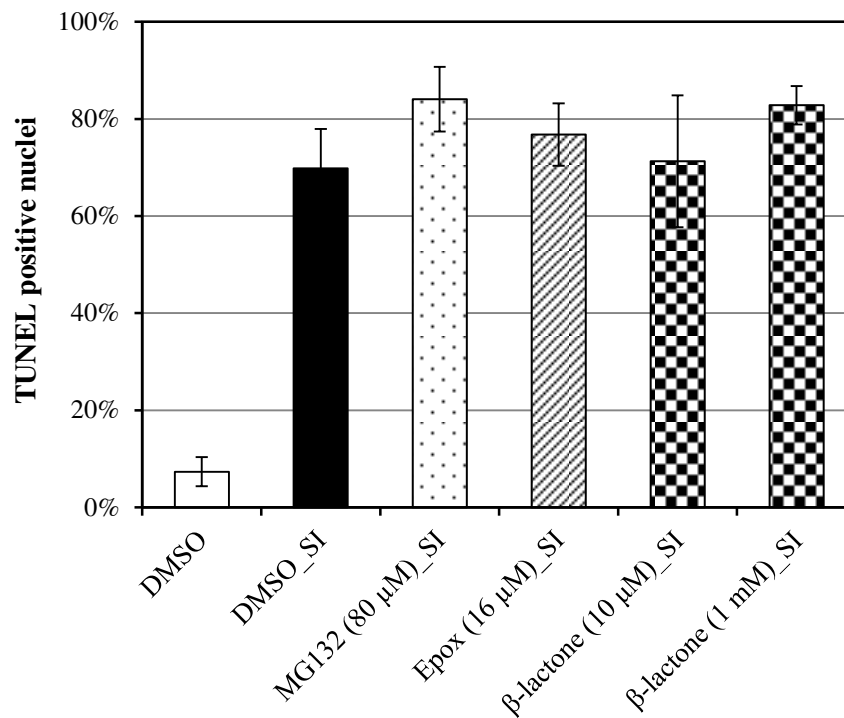


Figure 6-11 Proteasome inhibition does not alleviate SI triggered DNA fragmentation

TUNEL assays demonstrated that proteasomal inhibitions did not affect SI triggered DNA fragmentation assay. Poppy pollen were incubated with DMSO or proteasomal inhibitors MG132 (dots), or Epoximicin (dash), or β-lactone (lattice) for 1 h before SI induction. After recombinant PrsS proteins treatment, pollen samples were incubated for 8 h followed by PFA fixation and TUNEL assay. No significant alteration of SI triggered DNA fragmentation was observed by proteasomal inhibition. Result =mean ±SD, n=3.

This idea was further confirmed by pre-treatments using other proteasome inhibitors.

Incompatible pollen pre-treated with epoximicin had 76.8% DNA degradation (Figure 6-11), which was not significantly different to that in SI sample ($p=0.328$). Similarly, no DNA fragmentation alleviation was observed in incompatible pollen pre-treated with

β -lactone. Pre-treatment with 10 μ M or 1 mM β -lactone resulted in DNA fragmentation of 71.3% and 82.8%, respectively, both of which were not significantly different from SI sample ($p=0.883$, and $p=0.129$, respectively). As there was no DNA fragmentation alleviation observed in the incompatible pollen which had been pre-treated with any of the inhibitor prior to SI induction (Figure 6-11), this suggested that proteasomal inhibition did not affect SI-stimulated DNA degradation. Thus, the proteasome is unlikely to be involved in the SI signalling pathway that resulted in DNA fragmentation and PCD.

6.2.4 Characterization of SI-triggered proteasome and DEVDase activity

It has been described above that poppy SI response triggers both DEVDase and proteasome activity increases. We investigated the significance of SI-induced proteasome activity increase, and data showed that the proteasome was not involved in the SI-induced pollen tube growth inhibition, loss of pollen viability or DNA fragmentation. This suggested that the proteasome played a distinct role from DEVDase in the *Papaver* SI response. However, whether there is cross-talk between the SI-triggered proteasome and DEVDase activity remained to be elucidated. Here, we first characterized SI-induced proteasome and DEVDase activity, and their potential interaction by a biotin-DEVD pull-down assay. We then further investigated SI-induced proteasome and DEVDase activity from a biochemistry point of view by characterization of poppy pollen proteasome and DEVDase activity using DEVDase-

and proteasome-specific inhibitors, as well as in buffers with different pHs.

6.2.4.1 Identification of proteasome subunits in a biotin-DEVD pull down assay

Although the DEVDase activity was identified in poppy pollen more than a decade ago, and its significance in poppy SI response has already been demonstrated (Thomas and Franklin-Tong, 2004), the identity of the protein responsible for the DEVDase activity in poppy pollen is still unclear. Biotin-DEVD pull down assay using total protein extracts from UT/SI pollen extracts was carried out in an attempt to isolate the DEVDase in poppy pollen (section 2.4.8). DEVDase, together with DEVDase binding proteins were expected to be enriched through biotin pull down (Figure 6-12). Proteins were then separated using SDS-PAGE and identified using mass-spectrometry analysis (Figure 6-12). There were 116 and 205 peptides identified separately by mass-spectrometry obtained in the UT and SI pollen extracts respectively. Proteasome subunits were identified in both the UT and SI samples (Table 6-2). For the UT sample, 14 out of 116 peptides were identical to peptides from proteasome subunits in other green plants. For the SI sample, 23 proteasome peptides were identified. Table 6-2 shows the multiple peptides identical to 8 different proteasome subunits identified in 5 different green plant species. The complete and annotated *P. rhoeas* genome is not available, therefore, peptide hits identified in the mass-spectrometry were searched against the “whole green plant” database. This limited the identification of peptides that are identical to those available in the database.

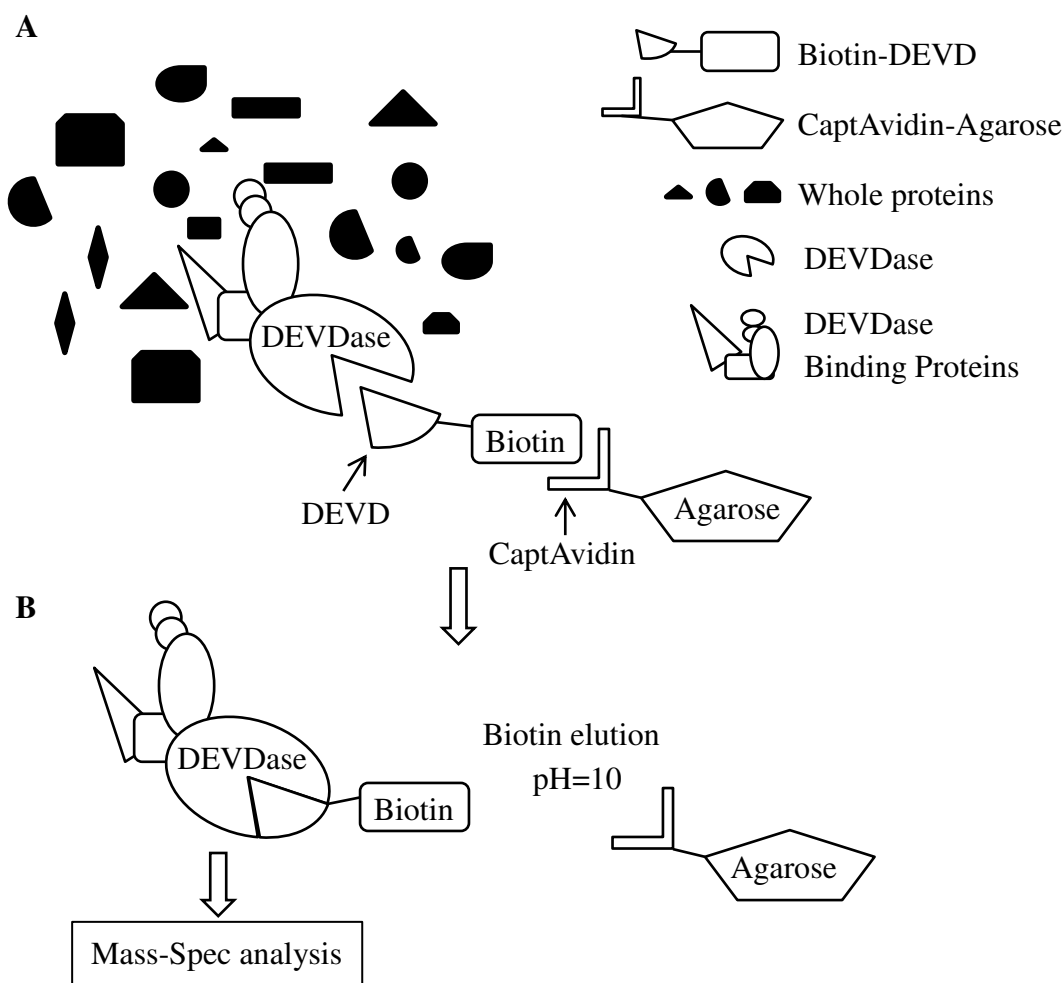


Figure 6-12 Cartoon of the biotin-DEVD pull down assay

A: UT and SI extracts (5 h after SI induction) were incubated with biotin-DEVD. CaptAvidin agarose was used to pull down biotin-DEVD conjugated proteins. B: biotin was eluted, and pull down fractionates were separated by SDS-PAGE and identified using Mass-spec analysis (see Methods and Materials for more details).

Besides the peptides shown in the Table 6-2, which were corresponding to the proteasome subunits, none of the other peptides was found to be corresponding to known protease proteins in the database. Here, only these proteasome subunits peptides will be further described.

Table 6-2 20S proteasome subunits were identified in Biotin-DEVD pull down assay

Proteasome subunit	Peptides	Protein sample	species
alpha-1 (PAA)	AAAVTSIGVR	SI	<i>Ricinus communis</i>
	AAGITSIGVR	UT	<i>Arabidopsis thaliana</i>
	ATEIEVGVVR	UT&SI	<i>Arabidopsis thaliana</i>
	ATSAGLKEQEAINFLEK	SI	<i>Ricinus communis</i>
	HITIFSPEGR	UT&SI	<i>Ricinus communis</i>
	YLGLLATGMTADAR	UT&SI	<i>Ricinus communis</i>
alpha-3 (PAC)	AAAIGANNQAAQSMLK	UT&SI	<i>Arabidopsis thaliana</i>
	DGVVLIGEK	UT&SI	<i>Arabidopsis thaliana</i>
alpha-4 (PAD)	LTVEDPVTVEYITR	UT&SI	<i>Nicotiana tabacum</i>
	IVNLDNHIALACAGLK	SI	<i>Glycine max</i>
	KIVNLDNHIALACAGLK	SI	<i>Glycine max</i>
	ALLEVVESGGK	UT&SI	<i>Nicotiana tabacum</i>
alpha-5 (PAE)	AIGSGSEGADSSLQEQFNK	UT&SI	<i>Arabidopsis thaliana</i>
	ITSPLEPSSVEK	UT&SI	<i>Arabidopsis thaliana</i>
	LFQVEYAIEAIK	UT&SI	<i>Arabidopsis thaliana</i>
alpha-6 (PAF)	NQYDTDVTTWSPAGR	SI	<i>Glycine max</i>
	VDNHIGVAIAGLTADGR	SI	<i>Glycine max</i>
beta-5 (PBE)	ASMGGYISSQSVK	SI	<i>Nicotiana tabacum</i>
	GPGLYYVDSEGR	UT&SI	<i>Nicotiana tabacum</i>
	DAASGGVASVYYVGPNGWK	UT&SI	<i>Citrus maxima</i>
	FSVSGSPYAYGVLDNGYK	SI	<i>Arabidopsis thaliana</i>
beta-6 (PBF)	GCVYTYDAVGSYER	UT&SI	<i>Ricinus communis</i>
beta-7 (PBG)	FNPLWNSLVGGVK	SI	<i>Arabidopsis thaliana</i>
	NKFNPLWNSLVGGVK	SI	<i>Arabidopsis thaliana</i>

As shown in Table 6-2, 5 out of 7 proteasome α -subunits and 3 out of 7 proteasome β -subunits were identified. The identification of proteasome subunits in the pull-down assay using biotin-DEVD confirmed that the proteasome could either directly bind to the DEVD motif, which suggests that proteasome might be responsible for the DEVDase activity directly, or physically interact with the DEVDase in poppy pollen, indicating a cross-talk between DEVDase and proteasome during poppy pollen SI response.

6.2.4.2 Effects of DEVDase inhibitors on proteasome activities *in vitro*

As the biotin-DEVD pull-down experiments suggested that the proteasome might be responsible for the DEVDase activity. We further studied this investigating whether the DEVDase-specific inhibitor (Ac-DEVD-CHO, hereafter DEVD) affected proteasome activity, and whether proteasome-specific inhibitors (MG132, epoximicin) affected DEVDase activity.

DEVD effectively blocked the DEVDase activities in poppy pollen, and more than 80% of DEVDase activities were inhibited by 50 μ M DEVD inhibitors (Figure 6-13). However, as shown in Figure 6-13, no significant proteasome activity changes were observed when pre-treated with DEVDase inhibitor. After DEVD treatment, PBA1 activity varied between 94%-102% (Figure 6-13), which were not significantly different from that of DMSO control. PBE activity also did not change after DEVD treatment

(Figure 6-13; $p=0.972$, one-way ANOVA). Thus, the DEVDase inhibitor, Ac-DEVD-CHO, had no inhibitory effect on proteasome activities, while DEVDase could be effectively inhibited.

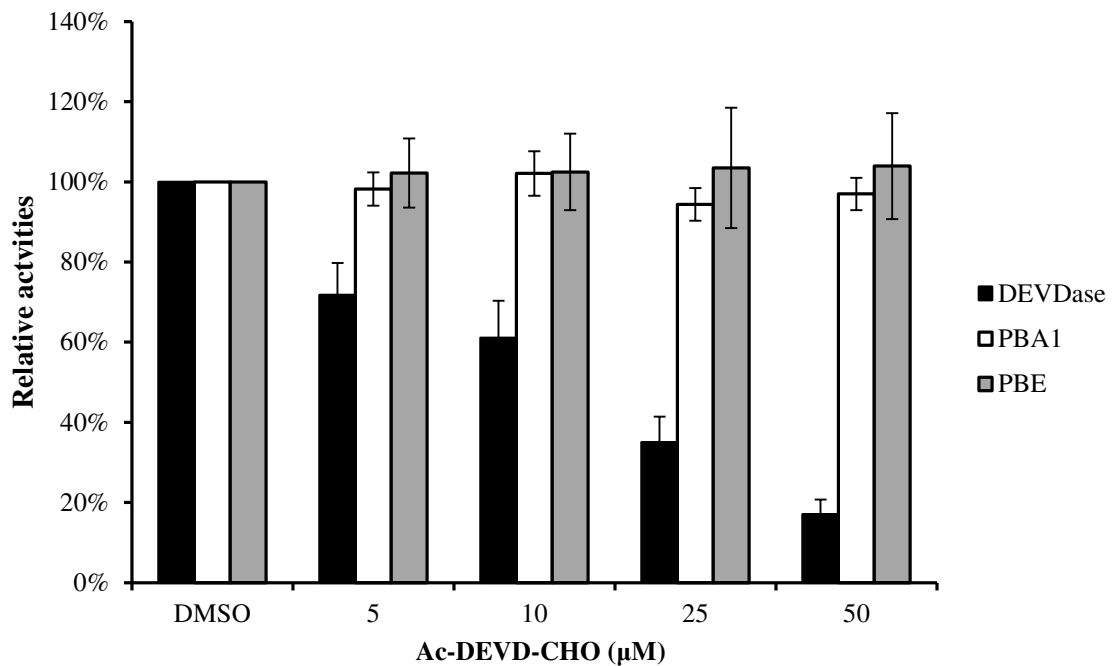


Figure 6-13 DEVDase inhibitor does not inhibit proteasome activities *in vitro*

The effects of DEVDase inhibitor, Ac-DEVD-CHO (DEVD), in inhibiting poppy pollen PBA1 and PBE activities were tested *in vitro*. Pollen protein extracts were incubated with DEVD of different concentrations (0-50 μM) for 0.5 h before being subjected to activities measurement. DEVDase activities were also measured here as controls. DEVDase (black bars), PBA1 (white bars) and PBE (grey bars) activities were measured by monitoring the hydrolysis of fluorogenic substrates Ac-DEVD-amc, Ac-nLPnLD-amc and Z-GGL-amc, respectively. DEVD did not significantly affect PBA1 or PBE activities within 50 μM , whereas dramatically inhibition of DEVDase activities was observed. Result =mean \pm SD, n=6.

6.2.4.3 Effects of proteasome inhibitors on DEVDase activities *in vitro*

Poppy pollen extracts were incubated with increasing concentrations of MG132 for 0.5 h before proteasome activity measurement. We first demonstrated that MG132 was able

to inhibit poppy proteasome activities *in vitro* (Figure 6-14).

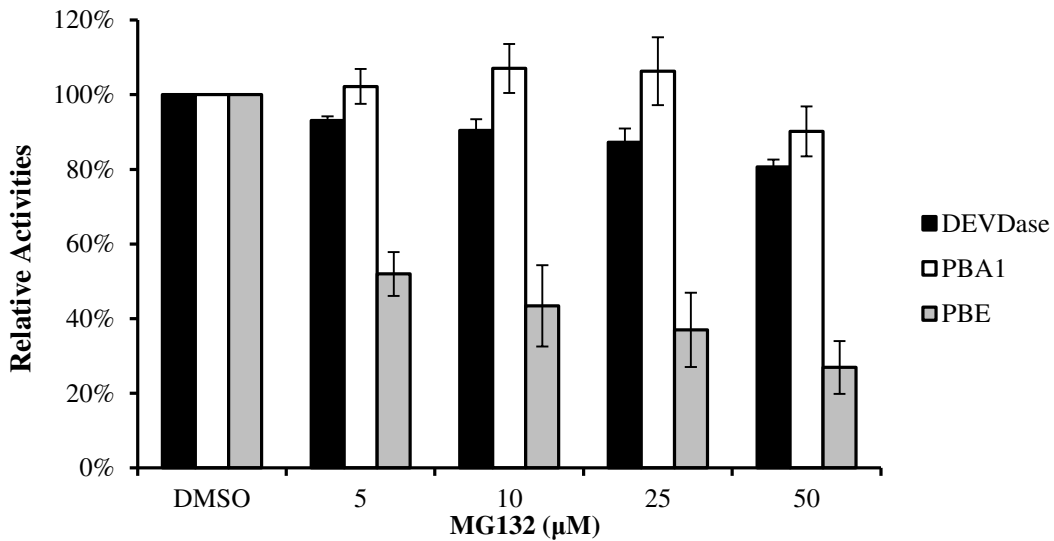


Figure 6-14 MG132 has no obvious inhibition on DEVDase activity *in vitro*

The ability of MG132 to inhibit DEVDase activity in poppy pollen extracts was tested *in vitro*. Pollen protein extracts were incubated with MG132 at different concentrations (0-50 μM) for 0.5 h before being subjected to activities measurement. DEVDase (black bars), PBA1 (white bars) and PBE (grey bars) activities were measured by monitoring the hydrolysis of fluorogenic substrates Ac-DEVD-amc, Ac-nLPnLD-amc and Z-GGL-amc, respectively. Proteasome activities were measured here as controls. MG132 slightly inhibited DEVDase activities within 50 μM *in vitro*. Result =mean ±SD, n=4.

MG132 slightly activated PBA1 activity when its concentration was below 25 μM, and 50 μM of MG132 inhibited PBA1 activity by 10% (Figure 6-14). But statistical analysis demonstrated that even though ~10% of PBA1 activity changes were observed by MG132 treatments, these activity alterations were not significantly different from controls. PBE was much more sensitive to MG132 than PBA1 (Figure 6-14). PBE activity was reduced to half by 5 μM MG132 treatments, and increasing concentrations of MG132 continued to reduce PBE activity. As shown in Figure 6-14, 50 μM MG132

significantly reduced PBE activity by nearly 75% ($p < 0.001$). Taken together, we have demonstrated that MG132 significantly inhibited poppy pollen proteasome activity by inhibiting PBE. For DEVDase, increasing concentrations of MG132 treatment resulted in the gradual decrease of DEVDase activity. Nearly 20% of DEVDase activity was inhibited by 50 μM MG132. However, this was not statistically significant ($p = 0.156$). Thus, the proteasome inhibitor MG132 had no significant inhibition on DEVDase activities, while specifically inhibited proteasome activity by targeting PBE.

MG132 has been found to effectively block papain-like cysteine protease (PLCP) in addition to proteasome inhibition. No non-specific inhibition has been reported for epoximicin to date. Therefore, in order to confirm the effect of proteasome inhibitor on DEVDase activity, epoximicin was also employed in this study. The effects of epoximicin on poppy pollen proteasome activities will be described first. Unlike MG132, epoximicin was found to preferentially inhibit PBA1 activity (Figure 6-15-A). Unexpectedly, it was also observed that PBA1 of UT and SI extracts have different sensitivities to epoximicin (Figure 6-15-A). Gradual reduction in PBA1 activity was observed when increasing concentrations of epoximicin were added. For PBA1 activity in the UT pollen extracts, no significant activity alteration was observed when they were treated with low concentration of epoximicin (4 μM), but high-dose treatment (16 μM) inhibited the PBA1 activity by nearly 30% ($p = 0.007$). However, for PBA1 activity in the SI extracts, a significant activity decrease of nearly 40% could already be observed

when 4 μM of epoximicin were added, and 16 μM of epoximicin brought the PBA1 activity further down by 70% ($p < 0.001$). When the UT and SI extracts were treated with the same concentration of epoximicin, PBA1 in the SI extracts always showed lower activity than that of UT extracts by ~40%. Thus, PBA1 activity derived from SI extracts appeared to be more sensitive to epoximicin than that of UT extracts, for which the reason is unknown.

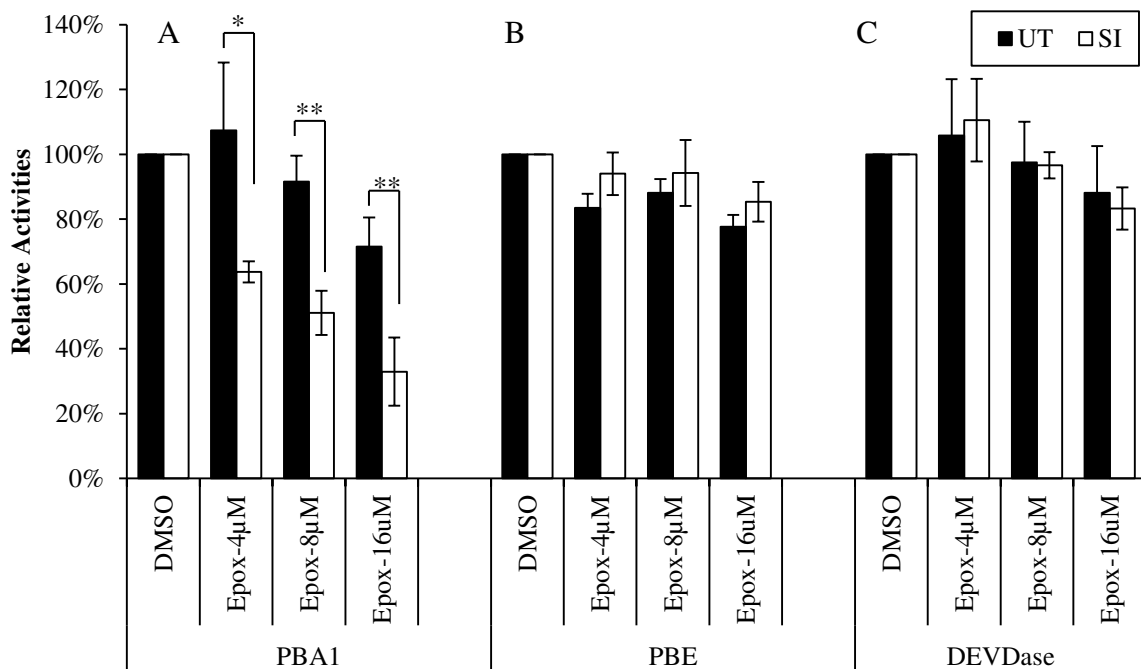


Figure 6-15 Epoximicin does not inhibit DEVDase activity *in vitro*

The effects of proteasome specific inhibitor, epoximicin, on proteasome and DEVDase activities of poppy pollen extracts, both UT (black bars) and SI (white bars), were tested *in vitro*. Pollen protein extracts were incubated with epoximicin of different concentrations (0-16 μM) for 0.5 h before being subjected to activities measurement. PBA1 (A), PBE (B) and DEVDase (C) activities were measured by monitoring the hydrolysis of fluorogenic substrates Ac-DEVD-amc, Ac-nLPnLD-amc and Z-GGL-amc, respectively. Result =mean \pm SD, n=4. *, $p < 0.05$; **, $p < 0.01$.

Epoximicin slightly inhibited PBE activity derived from both UT and SI extracts by ~20%

(Figure 6-15-B). However, there was no significant difference between the UT and SI PBE activities when they were treated with the same concentrations of epoximicin.

After confirming that epoximicin inhibited poppy pollen proteasome activity, the effects of epoximicin on poppy pollen DEVDase activity were studied (Figure 6-15-C). It could be clearly observed from Figure 6-15-C that epoximicin had similar effects on DEVDase activity derived from the UT and SI extracts, and there was no significant activity difference between them. Gradually DEVDase activity reductions could be observed when increasing concentrations of epoximicin were added. Sixteen μM of epoximicin treatment resulted in the inhibition of UT and SI DEVDase activity by 12% and 17% respectively, but this was not statistically significant ($p=0.318$).

These data demonstrated that while the inhibitors were able to block proteasome and DEVDase activity specifically, there was no cross-inhibition between the proteasome and DEVDase activity in the poppy pollen using proteasome- and DEVDase-specific inhibitors. It was observed that PBA1 activity in UT and SI extracts had different sensitivities to epoximicin. Together with the observation that PBA1 activity was increased by SI induction (Figure 6-3), a role of PBA1 in poppy SI response was suggested. However, the significance of these observations remains to be further investigated.

6.2.4.4 Characterization of proteasome and DEVDase activities in buffers with different pHs

In the last section, we demonstrated that proteasome and DEVDase inhibitors do not have the cross-inhibition capacity, suggesting that poppy pollen proteasome and DEVDase are distinct. In order to further confirm this, the relationship between SI-induced proteasome and DEVDase activities was investigated from an alternative aspect. Both DEVDase and proteasome activity have been demonstrated to be pH-dependent. However, DEVDase activity was optimal at acidic pH (Bosch and Franklin-Tong, 2007; Han et al., 2012), whereas the proteasome favoured basic pH conditions (Tanaka et al., 1988). Therefore, we decided to profile DEVDase and proteasome activity in poppy pollen in different pHs. This revealed a difference between poppy pollen DEVDase and proteasome.

As shown in Figure 6-16, both poppy pollen DEVDase and proteasome showed pH-dependent activity. The optimal pH of poppy pollen DEVDase activity was found at pH=5.0 (Figure 6-16). Sharply reduced DEVDase activity was observed at other pH levels, which agreed with what was reported by Bosch and Franklin-Tong (2007). In contrast, the poppy pollen proteasome showed a different pH-dependent activity profile. For PBA1, within the pH region measured, the highest activity was observed at pH=7.5, and its activity continued to reduce with the decrease of pH to 5.5, where the lowest PBA1 activity was observed. However, at pH=5, the PBA1 activity increased again, to a

level which was comparable to that at pH=7.0. It has been demonstrated that the PBA1 activity observed at pH=5.0 was caused by non-specific cleavage of fluorogenic substrate Ac-nLPnLD-amc by DEVDase (data not shown). Thus, the poppy pollen PBA1 activity actually increased with an increase in pH between 5.0-7.0, with peak activity at pH=7.0. In terms of PBE, no activity was detected at pH=5.0 and pH=5.5. PBE gradually reached its peak activity at pH=7.0. When pH was further increased to 7.5, an activity reduction by ~15% was observed ($p < 0.05$).

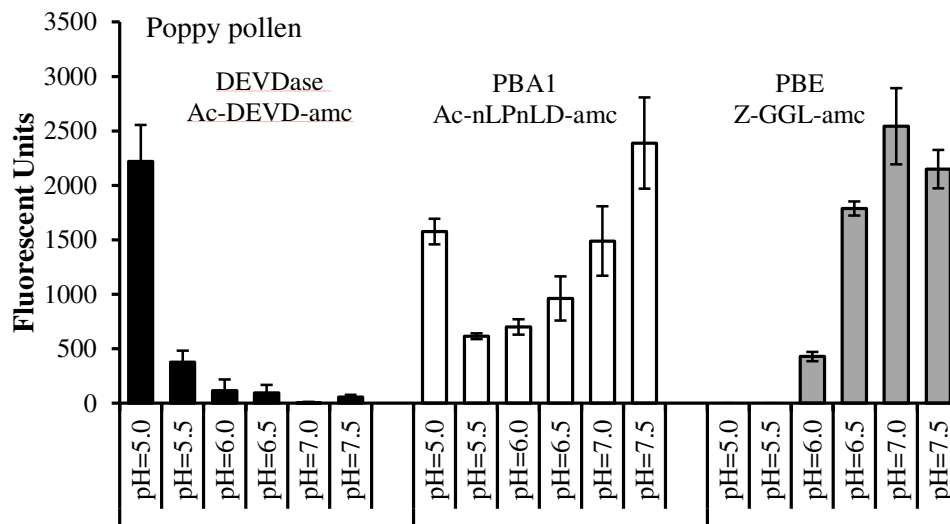


Figure 6-16 Poppy pollen proteasome and DEVDase activities are pH-dependent

Poppy pollen DEVDase and proteasome activities were profiled in different pHs using fluorogenic substrates-based activity assay. Black bars: DEVDase activities profiled using Ac-DEVD-amc. White bars: PBA1 activities using Ac-nLPnLD-amc. Grey bars: PBE activities profiled using Z-GGL-amc. Result = mean \pm SD, n=3.

In summary, the pH optima of the poppy pollen DEVDase activity were acidic, while the pH optima of the pollen proteasome activity were neutral and basic. This provided further evidence that the proteasome is distinct from the DEVDase during poppy pollen

SI response. Together with the mass-spectrometry data presented in section 6.2.4.1, this suggested that there might be interaction between the proteasome and DEVDase in incompatible poppy pollen. The significance of proteasome and DEVDase interaction remains to be further confirmed and elucidated.

6.3 Discussion

The proteasome has been demonstrated to play an important role in both SCR/SRK-based SI and S-RNase-based SI (Entani et al., 2014; Liu et al., 2014; Stone et al., 2003). Previous research also suggested a role of proteasome in *Papaver* SI-induced PCD (Vatovec, 2011). Therefore, we examined the role of proteasome during *Papaver* SI response in more detail. This chapter has described investigations aimed at identifying the proteasome as a target during the *Papaver* SI response in incompatible pollen.

As a first step, the proteasome activity during *Papaver* SI response was profiled. We demonstrated that SI induced an increase in proteasome activity in incompatible pollen compared with UT pollen in the late phase of SI response, whereas in the early phase of SI, no significant alteration in proteasome activity was observed. This demonstrates that the proteasome is one of the signalling targets of *Papaver* SI response in incompatible pollen. The next step was to investigate the role of the increase in proteasome activity in *Papaver* SI. It has been shown that proteasome inhibition by proteasomal specific

inhibitors was not able to alleviate SI-induced pollen tube growth inhibition, pollen viability decrease or DNA fragmentation. This indicates that proteasome is not involved in these SI-induced PCD signalling cascades. As the proteasome has been demonstrated to be responsible for the DEVDase activity in PCD involved in the xylem development and bacteria-induced hypersensitive response (Han et al., 2012; Hatsugai et al., 2009), we further characterized the relationship between proteasome and DEVDase activity in poppy pollen. We provide strong evidence showing that proteasome is distinct from the DEVDase in poppy pollen, suggesting that the *Papaver* SI-induced DEVDase activity, unlike DEVDase activity during xylem development and hypersensitive response (Han et al., 2012; Hatsugai et al., 2009), is not a proteasomal activity.

6.3.1 The proteasome is required for the normal poppy pollen germination and pollen tube growth

The ubiquitin-proteasome system plays a significant important role in various cellular processes through regulation of the degradation of key regulatory proteins (Smalle and Vierstra, 2004). Pollen germination and growth represents a key switch in plant reproduction procedure, defining the transition from mature dormancy pollen to active pollen for sperm delivery (Taylor and Hepler, 1997). It involves a variety of cellular proteins and the maintenance of the proteome stability during this process is of crucial importance. This is demonstrated by the observation that the disruption of proteasome activity in pollen using proteasome specific inhibitor significantly affects pollen grain

germination, pollen tube organisation, elongation and morphology, suggesting the involvement of ubiquitin-proteasome system in the pollen germination and growth as a major regulator (Scoccianti et al., 2003; Sheng et al., 2006; Speranza et al., 2001). A similar phenomenon was also observed in poppy pollen. Proteasome inhibition resulted in a reduction in both poppy pollen germination rate and elongation rate. Pollen tube morphology alterations such as tip swelling, unpolarised growth and pollen tube leakage were also observed. This demonstrates a key role of the proteasome in the normal poppy pollen germination and pollen tube growth as reported in other pollen. The detailed mechanism regarding how proteasome is involved is still unclear. Furthermore, even though proteasome inhibition strongly affected the pollen tube growth, no significant viability changes in poppy pollen was detected, and pollen DNA integrity remained intact. This suggests that the proteasome is crucial for pollen tube growth, but not directly involved in the control of pollen cell death.

6.3.2 SI induces an increase in proteasome activity in incompatible pollen

In the SCR/SRK-based SI, cognate SRK and SCR interaction activates ARC1, a novel E3 ubiquitin ligase, which leads to the ubiquitination and proteasomal turnover of Exo70A1, resulting in the failure of stigmatic factors secretion, and subsequent self-pollen rejection (Samuel et al., 2009; Zhang et al., 2009). For the *S*-RNase-based SI, in a compatible reaction, non-self *S*-RNase is recognized by SLF containing E3 ligase complex, followed by ubiquitination and subsequent proteasomal degradation, while in

an incompatible reaction, *S*-RNase is left intact, leading to the inhibition of pollen tube growth due to its cytotoxic activity (McClure et al., 2011; Zhang et al., 2009). The identification of the involvement of the proteasome in the SCR/SRK-based SI and *S*-RNase-based SI systems leads to a question that whether proteasome is also involved in the *Papaver* SI response.

We started to examine the role of proteasome in the *Papaver* SI response by profiling the proteasome activities in incompatible pollen. It was found that in the early phase of SI response, no significant change in proteasome activity was observed in incompatible pollen as compared with UT pollen. However, in the *Papaver* SI late phase, significant proteasome activity increase was detected. As the rate-limiting subunit of the proteasome, PBE activity was found to increase by nearly two fold compared to that in UT pollen. A significant increase in PBA1 activity was also detected. The detection of increases in proteasome activity in incompatible pollen suggests that proteasome is one of the signalling targets during the *Papaver* SI response. However, the role of proteasome activity increase during the *Papaver* SI response is still unknown, and remains to be elucidated.

Increases in proteasomal activity have been observed in many different biological systems. For example, human embryonic stem cells (hESCs) exhibit higher proteasome activity compared with the resulting differentiated cell lineages derived from hESCs

(Vilchez et al., 2012). It is proposed to be correlated with the maintenance of the proteome stability hESCs as passaging the daughter cells with damaged proteins might potentially result in the destruction of the differentiated cell lineages (Vilchez et al., 2012). There is also an increase in proteasome activity after myeloma cells are inoculated into the bone marrow (Edwards et al., 2009). In wheat, when the root is subjected to salt stress, a gradual increase in the activity of proteasome can be detected, with the involvement of increased oxidation levels with the cells (Shi et al., 2011). The biological significance of the increase in proteasome activity in these three very different biological systems is still unclear. We propose a possible role of the proteasome activity increase in incompatible poppy pollen. PCD in incompatible poppy pollen involves the alteration of a various signalling proteins including the depolymerisation of actin and microtubule cytoskeleton (Poulter et al., 2008; Snowman et al., 2002), rearrangement of actin binding proteins (Poulter et al., 2010), phosphorylation of p26 (Rudd et al., 1996) and activation of MAP kinase (Rudd et al., 2003). Furthermore, the involvement of ROS and NO in the PCD in incompatible poppy pollen has also been demonstrated (Wilkins et al., 2011). The increase in ROS and NO levels in incompatible pollen results in the subsequent oxidation and nitrosylation of various cellular proteins (Haque et al., unpublished). Therefore, a good understanding of how incompatible poppy pollen maintains the proteome stability is of central significance. Since failure in the degradation of certain protein might result in the

failure of PCD (Bader and Steller, 2009), our studies suggest that proteasome activity increase might be involved in regulating the proteome stability in incompatible pollen.

It is interesting to note that SI-induced proteasome activity exhibited an enhanced response to inhibition in response to epoxomicin. A lower concentration of this proteasome specific inhibitor was required to halve the proteasome activity in SI pollen extracts than that for UT extracts. A similar phenomenon has already been reported in myeloma cells. Inoculation of myeloma cells into the bone marrow *in vivo* results in the significant increase in the proteasome activity as compared with the pre-inoculation cells (Edwards et al., 2009). Moreover, myeloma cells following *in vivo* growth in the bone marrow are more sensitive to proteasome specific inhibitors than cells prior to inoculation (Edwards et al., 2009). The different sensitivities of UT and SI pollen extracts in response to proteasome inhibitor might indicate an alteration of the composition of the proteasome subunits after SI induction (Busse et al., 2008). Further experiments are still needed to characterise the role of proteasome activity increase and investigate the reason underlying the differentiation of the sensitivity between the UT and SI pollen in response to the proteasome inhibitor.

6.3.3 SI-induced proteasome activity increase and acidification

SI-induced cytosolic pH acidification has been demonstrated to be an integral and essential event for SI-induced PCD. It is proposed that SI-induced cytosolic pH

acidification triggers the activation of DEVDase, which is optimal at pH 5.5, thus committing incompatible pollen to death (Bosch and Franklin-Tong, 2007; Wilkins, 2013). The poppy pollen proteasome activity exhibits maximal substrate cleavage at neutral and low basic pH values *in vitro*, and acidic pH results in the inhibition of almost all proteasomal activity. This is consistent with what is observed for purified proteasome *in vitro* (Tanaka et al., 1988). However, it is surprising that SI induces a dramatic increase in the proteasome activity during the late phase of SI response, as the pH-dependent activity profile of proteasome predicts that SI should result in the inhibition of proteasome activity due to the SI-triggered cytosolic acidification. The reason for this is still unknown. One of the possible reasons might be that SI-induced low pH inhibits the proteasome activity, but at the same time, SI triggers the assembling of more proteasomes. As a result, an increase in proteasome activity is detected. However, this needs to be further confirmed as the amount of proteasome in UT and SI has not been investigated. Furthermore, it might be worth to confirm this finding by using MV151-based *in vivo* proteasome activity profiling, as fluorogenic substrate-based *in vitro* proteasome profiling was used to assay the proteasome activity in UT and SI pollen extracts in this study. Preliminary experiments using this *in vivo* labelling technique supports the observation described in this chapter that SI induces an increase in proteasome activity. However, further experiments are still needed to make a solid conclusion.

The contrasting between the SI-triggered proteasome activity increase and cytosolic pH decrease might suggest that there is another unknown signalling cascade which overcomes the activity inhibition brought to the proteasome by cytosolic pH acidification and triggers an increase in proteasome activity. It has been strongly suggested that the proteasome is a target of the *Papaver* SI response, but is unlikely to be directly involved in the PCD signalling. Therefore, we propose that there might be another signalling pathway, which is distinct from the cell death signalling known so far, triggered by SI to maintain the proteome stability and assist execution of the PCD in incompatible poppy pollen (see section 6.3.6 for more details).

6.3.4 Role of proteasome in SI-induced pollen tube growth inhibition, viability decrease and DNA fragmentation

In the *Papaver* SI response, interaction between cognate PrpS and PrsS triggers a Ca^{2+} -dependent signalling network, resulting in the pollen tube growth inhibition, viability decrease, and finally PCD incompatible pollen. A variety of cellular components, such as actin cytoskeleton, MAPK and DEVDase, have been identified as the signalling targets during *Papaver* SI response (Bosch and Franklin-Tong, 2007; Rudd et al., 2003; Snowman et al., 2002). Inhibition of these cellular components using corresponding inhibitors alleviates SI-induced pollen tube growth inhibition, viability decrease and DNA fragmentation, thus rescuing incompatible pollen from PCD, and demonstrating them to be involved in the commitment of PCD in incompatible pollen

(Li et al., 2007; Thomas and Franklin-Tong, 2004; Thomas et al., 2006). We examined the role of the proteasome in the *Papaver* SI response by investigating whether inhibition of proteasome was able to alleviate the SI-induced pollen tube growth inhibition, viability decrease and DNA fragmentation. We obtained evidence showing that pre-treatment of poppy pollen with proteasome specific inhibitors before SI induction does not significantly affect the pollen tube growth inhibition, viability decrease and DNA fragmentation triggered by SI. This strongly suggests that SI-induced pollen tube growth inhibition and PCD does not require proteasome activity to proceed, and the proteasome might not be directly involved in PCD in incompatible pollen during the *Papaver* SI response.

Microtubules are another example that is not directly involved in the PCD, but is a target for SI signalling. SI induction triggered rapid microtubule depolymerisation downstream of F-actin depolymerisation, demonstrating that microtubules are a target for *Papaver* SI signalling (Poulter et al., 2008). Furthermore, drug treatments causing microtubule depolymerisation in *Papaver* pollen did not trigger DEVDase activation and subsequent DNA fragmentation, suggesting microtubules alone are not able to signal to PCD (Poulter et al., 2008; Poulter et al., unpublished). However, the demonstration that stabilized microtubule prior to SI-induced F-actin depolymerisation partly alleviated SI-induced DEVDase activation suggests a functional role for the signal integration between F-actin and microtubule (Poulter et al., 2008). Actin

microfilament and DEVDase are two of the key cellular components in the *Papaver* SI signalling network, the interaction between proteasome and actin microfilaments, as well as proteasome and DEVDase still needs to be investigated to precisely address the role of proteasome as a target for SI signalling in incompatible poppy pollen.

6.3.5 Which protease is responsible for SI-induced DEVDase activity?

Many caspase-like activities have been identified in a variety of plant PCD systems as the key executioners. However, there is no animal caspase gene orthologous in the plant genome. Therefore, characterisation and isolation of these caspase-like enzymes is of considerable importance in understanding plant PCD. For caspase-3-like enzyme (DEVDase), it has been reported that the proteasome might potentially be responsible (Han et al., 2012; Hatsugai et al., 2009).

As proteasome activation was observed at 5h after SI induction when the peak SI-induced DEVDase activity was detected, we wondered whether the proteasome could also be responsible for the SI-induced DEVDase activity during the *Papaver* SI response. We provided strong evidence showing that proteasome specific inhibitors were not able to significantly inhibit the SI-induced DEVDase activity, and DEVDase inhibitor was not able to inhibit the proteasome activity neither. Moreover, poppy pollen proteasome and DEVDase showed different pH-dependent activity profiles. These data demonstrate that proteasome is distinct from the DEVDase in the *Papaver* SI response,

and does not represent the caspase-3-like enzyme. Further, the identification of proteasome subunits in the biotin-DEVD pull down suggests a physical interaction between proteasome and DEVDase. Details of the signalling interaction between proteasome and DEVDase in incompatible *Papaver* pollen remains to be investigated.

Not all plant caspase-like proteases have been identified as proteasome-related. Of those few whose identity is known, vacuolar processing enzyme (VPE) has been demonstrated to be the key executioner conferring YVADase activity during the tobacco mosaic virus induced cell death in tobacco (Hatsugai et al., 2004). However, during fungus induced cell death in oat, the executioner YVADase turned out to be a serine protease (Coffeen and Wolpert, 2004). In terms of the DEVDase, in addition to proteasome, a serine protease has also been reported to confer DEVDase activity during *P. infestans* induced PCD in potato (Fernández et al., 2012). These indicate that, unlike in animals, there are a variety of proteases responsible for the caspase-like activities in the PCD of plants. In the SI-induced PCD in incompatible *Papaver* pollen, the proteasome has been demonstrated to play a distinct role from DEVDase activity in this study. Although VPE was identified in a biotin-DEVD pull-down, and recombinant *PrVPE* exhibits DEVDase activity besides YVADase activity, it was demonstrated to be a YVADase that binds biotin-DEVD, but not DEVDase in poppy pollen (Bosch et al., 2010). Serine proteases are also unlikely to be responsible for the SI-induced DEVDase

activity, because the serine protease specific inhibitor, PMSF, is not able to inhibit SI-induced DEVDase activity (Bosch and Franklin-Tong, 2007). Therefore, the proteasome, VPE and serine protease have all been excluded as candidates for the identity of the DEVDase involved in poppy SI. Further investigation is still needed to figure out what is responsible for the SI-induced DEVDase activity in incompatible *Papaver* pollen and the identity of this protein.

6.3.6 SI signalling model and summary

Based on the data obtained here, a new SI signalling model involving the proteasome is proposed (Figure 6-17). During an incompatible SI response, PrsS interacts with cognate PrpS, triggering a rapid Ca^{2+} influx in incompatible pollen. The increase in cytosolic Ca^{2+} induces a signalling network comprising three integral cascades: (1) pollen tube growth inhibition signalling cascade, (2) programmed cell death signalling cascade and (3) helper signalling cascade (Figure 6-17). For the growth inhibition signalling cascade, the phosphorylation and inhibition of p26-sPPases decreases pollen metabolic activity and inhibits biosynthesis of the cell wall and membranes. Dramatic and rapid actin depolymerisation is also induced. As a result, pollen tube growth is inhibited (Figure 6-17). In terms of the cell death signalling cascade, increase in cytosolic Ca^{2+} triggers microtubule depolymerisation, cytosolic acidification, increase in ROS and NO levels, F-actin foci formation and activation of MAPK. These signals further activate DEVDase, the executioner protease, resulting in the subsequent DNA

fragmentation, which commits cell to death.

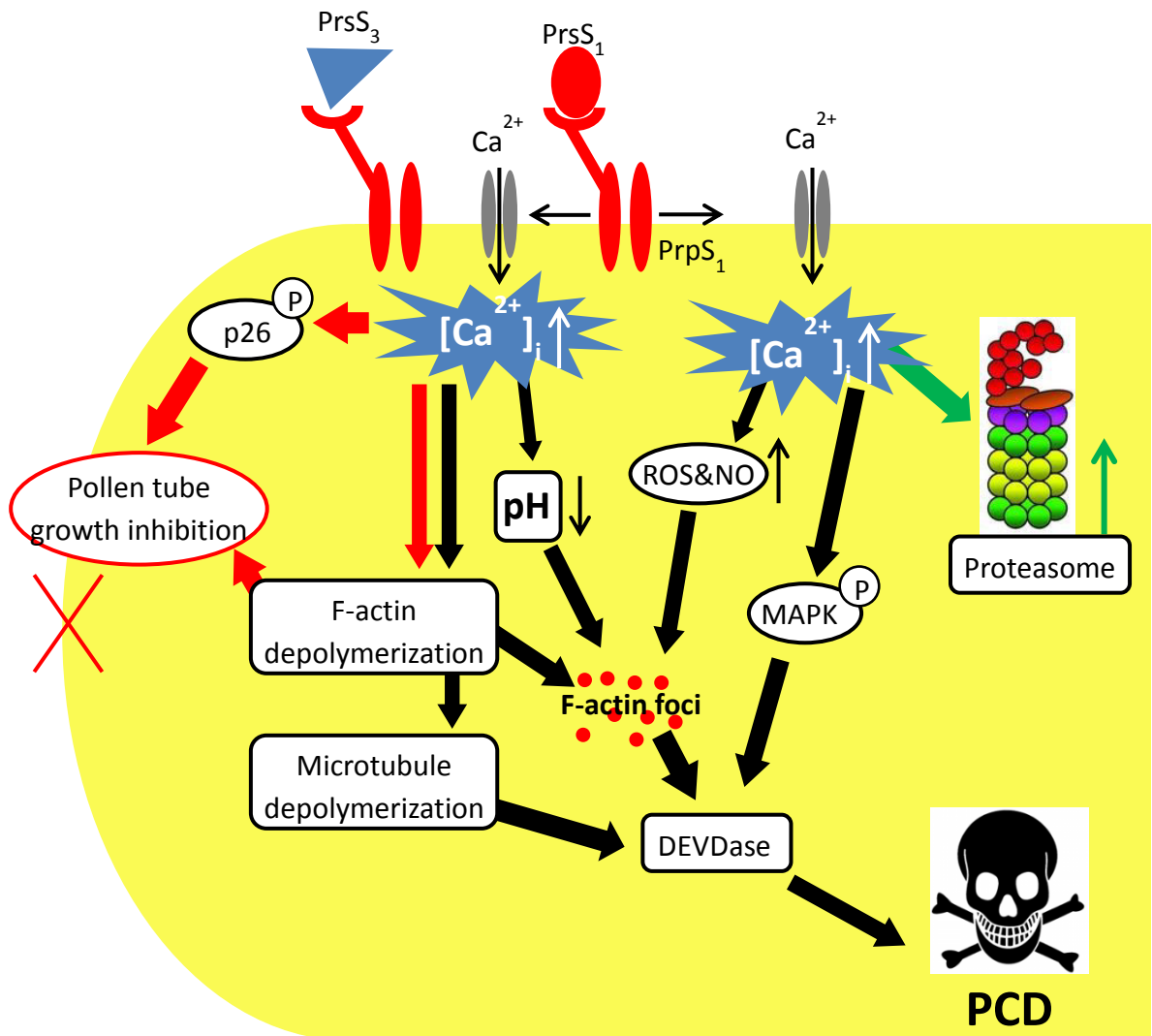


Figure 6-17 Signalling model for the *Papaver* SI response

A new SI signaling model is proposed based on the data published and presented in this chapter. Cognate PrsS and PrpS interaction triggers a Ca²⁺ dependent signaling network comprising three integral signaling cascades: pollen tube growth inhibition signaling cascade (red arrow), programmed cell death signaling cascade (black arrow) and helper signaling cascade (green arrow).

A helper signalling cascade involving the proteasome is also triggered. The increase in proteasomal activity helps to turnover the “unnecessary” proteins resulted from the

inhibition and death signalling cascades, to maintain the proteome stability in incompatible pollen. However, this signalling cascade might not be directly involved in the PCD, and the significance of this signalling cascade during the *Papaver* SI response merits further investigations.

Data presented in this chapter has shown that there is a significant increase in proteasome activity in incompatible pollen at the late phase of *Papaver* SI response, demonstrating that the proteasome is a target for SI in *Papaver* pollen, and is activated around the time DEVDase reaches peak activity (~5h). In addition, proteasome inhibition prior to SI induction has no significant effect on the SI-induced pollen tube growth inhibition, pollen viability decrease and nuclear DNA fragmentation, indicating that proteasome is not directly involved in the SI-induced PCD. Furthermore, we also demonstrate that the proteasome activity is distinct from DEVDase activity during the *Papaver* SI response. Although we still do not know the exact role of proteasome activity increase in the SI response, the studies presented in this chapter mark an important step towards understanding the role of the proteasome in *Papaver* SI response.

CHAPTER 7 GENERAL DISCUSSION

7.1 Introduction

The role of the proteasome during the *Papaver* SI response has been discussed thoroughly in Chapter 6. Here, we only focus on discussing the functional transfer of *Papaver* SI system into self-compatible *A. thaliana*. It has been previously shown that PrpS:GFP expressed in the transgenic *A. thaliana* pollen was functional in the *in vitro* pollen SI assay. In this study, we have constructed transgenic plants expressing PrsS under the direction of a stigma-specific promoter, *SLR1*, and performed pollinations with these plants. We have obtained data showing unequivocally that transgenic stigmas expressing PrsS inhibit transgenic *A. thaliana* pollen expressing PrpS:GFP in an *S*-allele specific manner. Furthermore, by co-transformation of *PrpS:GFP* and *PrsS*, we have also obtained self-incompatible *A. thaliana* plants. When these plants were left to set seed naturally, they had tiny siliques and set no seed. Here, we will discuss the transfer of *Papaver* SI system from three different points of view: (1) from an evolutionary point of view, how robust the *Papaver* SI system is, with PrpS-PrsS interaction in triggering signals in different organisms; (2) from an application point of view, how far we can go in using the *Papaver* SI system for hybrid breeding; (3) mechanistically, how the generation of self-incompatible *A. thaliana* will facilitate research investigating the molecular mechanisms underlying *Papaver* SI.

7.2 PrpS-PrsS interaction triggers signals not only in *P. rhoeas*

During the *Papaver* SI response, cognate interaction between PrpS and PrsS triggers a

Ca²⁺-dependent signalling network, featuring F-actin depolymerisation, reorganization and stabilization, and the activation of DEVDase, resulting in pollen tube growth inhibition and PCD in incompatible pollen. PCD provides a novel mechanism for the *Papaver* reproduction system to prevent selfing and promote outcrossing. Recently studies have suggested that PrpS and PrsS might be a pair of robust “ligand-receptor” partners for the induction of Ca²⁺-mediated downstream signals in a variety of cell types.

7.2.1 PrpS-PrsS interaction triggers pollen tube growth inhibition in both *A. thaliana* and *N. tabacum*-implication in the evolution of SI signalling across the higher plants?

It has been demonstrated that a functional “*Papaver*-like” SI response could be triggered in transgenic *A. thaliana* expressing both PrpS:GFP and PrsS (de Graaf et al., 2012; Chapter 5). When pollen expressing PrpS:GFP lands on a PrsS expressing stigma, rapid pollen tube growth inhibition could be observed, resulting in an SI response in these transgenic plants. *In vitro* SI assays have demonstrated that the involvement of F-actin and DEVDase, which are the two most important hallmarks of the *Papaver* SI response, are exhibited in transgenic *A. thaliana* pollen during an “SI” response *in vitro*. *At-PrpS:GFP* pollen exhibited F-actin alterations in an *S*-specific manner after addition of recombinant PrsS protein (de Graaf et al., 2012). Moreover, pre-treatment of *At-PrpS:GFP* pollen with DEVDase inhibitor significantly alleviated the SI-induced

pollen viability (de Graaf et al., 2012). These data suggest that interaction of PrpS and PrsS triggers PCD in transgenic *A. thaliana* pollen. As *A. thaliana* does not normally exhibit features of poppy SI, it appears that this is achieved by recruiting the existing cellular components to form a “*Papaver*-like” SI signalling network, which does not usually operate in *A. thaliana* pollen, despite that *P. rhoeas* and *A. thaliana* have an evolutionary distance more than 140 MYA and share distinctly different SI ancestors.

Besides *A. thaliana* pollen, functional analysis of PrpS and PrsS in *N. tabacum* pollen has also been carried out. Preliminary *semi-in-vivo* studies have shown that *N. tabacum* pollen expressing PrpS:GFP can be inhibited in the pistil transmitting tract expressing cognate PrsS (de Graaf et al., unpublished). This suggests that PrpS and PrsS might also be functional to make *N. tabacum* self-incompatible, although whether it triggers PCD in *N. tabacum* pollen has yet to be tested.

The observation that interaction of PrpS and PrsS triggers pollen tube growth inhibition in both *A. thaliana* pollen and *N. tabacum* pollen, suggests that *Papaver* SI system might be a potential robust system capable of making highly diverged self-compatible plants self-incompatible. This might also have an important implication for our perspectives of the evolution of different SI systems in flowering plants.

There is already a good example of solving evolutionary questions by using transfer of SI trait between different species. Transgenic self-incompatible *A. thaliana* has already

been established as a good model for the investigation of evolutionary switch from SI to SC (Boggs et al., 2009a). Upon transformation with SCR-SRK, different *A. thaliana* ecotypes differed in their ability to express the SI trait due to their *S*-locus polymorphisms (Nasrallah et al., 2004). Further analysis identified the loci which are targets of natural selection for self-fertility, and demonstrated that independent mutation of *S*-locus genes is a major mechanism which contributes to the switch to self-fertility in *A. thaliana* (Boggs et al., 2009a; Liu et al., 2007). This is consistent with that reported by Chantha et al. (2013) and Tang et al. (2007). However, the transfer of SCR-SRK is restricted within the *Arabidopsis* genus. Attempts to generate self-incompatible *A. thaliana* using the *Brassica* SI gene pairs failed. Therefore, this self-incompatible *A. thaliana* model cannot provide us with further information regarding to the evolution of different SI systems. However, successful transfer of SI system from *P. rhoeas* into *A. thaliana*, which are distinctly evolved from each other and belong to two different SI systems, has an important implication for the evolution of SI signalling across the higher plants.

7.2.2 PrpS-PrsS might function in *A. thaliana* protoplasts and mammalian cells, which has implication in elucidating mechanisms involved in the PrpS-PrsS interaction

PrpS and PrsS have not only shown their functionality in reproductive tissues, but also in the plant somatic cells. When *A. thaliana* protoplasts which have been transfected

with Ti vectors containing 35S::PrpS:GFP were treated with recombinant PrsS protein, a significant decrease in the protoplast viability was observed (Beacham et al., unpublished). In addition, this viability reduction was prevented through pre-treatment with DEVDase inhibitor (Beacham et al., unpublished), indicating the involvement of DEVDase. Despite this being not very reproducible, and it still needs further confirmation by using stable transformed lines, this suggests that the functionality of PrpS-PrsS interaction is not pollen-specific.

Moreover, other investigations in the Franklin-Tong's lab have shown that PrpS and PrsS might function in mammalian cells. Stable HeLa cell lines expressing PrpS:mCherry have been established (Flores-Ortiz et al., unpublished). Treatment of these cells with PrsS elicits rapid increases in the cytosolic Ca²⁺ level, and subsequent cell morphological changes, coupled with F-actin alterations (Flores-Ortiz et al., unpublished). This suggests the functionality of PrpS and PrsS in HeLa cells, despite the fact that *P. rhoeas* and *H. sapiens* come from two distinct biological kingdoms. The signalling network triggered by PrpS in HeLa cells has not been fully investigated. This also provides potentially a very good model system for studying the nature of PrpS protein and the mechanism involved in the PrpS-PrsS interaction. PrpS is a novel, small transmembrane protein, with no homologues in the database (Wheeler et al., 2009). It has been observed that PrpS forms a dimer (Hadjiosif, 2007). Also, based on the predicted structure of PrpS, it was also noticed that PrpS has similar structural

hallmarks with FLOWER and CRACM1, which are transmembrane channel proteins (Vig et al., 2006; Yao et al., 2009; Juarez-Diaz et al., unpublished). This suggests that PrpS might function as a channel protein through multimerization. However, this needs to be confirmed by further investigations. The establishment of the functionality of PrpS in HeLa cells provides a good platform for the investigation of the nature of PrpS protein and PrpS-PrsS interaction, by making use of the research tools available for HeLa cells, such as patch clamp and live cell imaging.

Taken together, we have provided good evidence that PrpS is able to trigger a Ca^{2+} -mediated signalling network in a variety of cell types spanning from plant reproduction cells, plant somatic cells and animal cells. Whether this signalling networks in different organisms are all “*Papaver* SI-like” remains unclear. The establishment of self-incompatible *A. thaliana* using the *Papaver* SI system has an important implication for understanding the evolution of different SI systems and SI signalling across the flowering plants. Furthermore, establishment that the PrpS-PrsS is functional in a variety of cell types might provide a good system for investigating the mechanisms involved in the PrpS-PrsS interaction.

7.3 How far can we go? Possible application of *Papaver* SI system in F1 hybrids breeding

With the increase in the world population and food demands, in the meantime, shrinkage in environmental resources and changes in the climate, a substantial increase

in agriculture production is under urgent requirement (Whitford et al., 2013). Hybrid breeding represents one of the most superior and popular technologies in increasing crop yields by systematically exploiting heterosis. In an effective F1 hybrid breeding system, a robust system is required to block inbreeding and force outcrossing. This can be accomplished by hand emasculation, or by making use of the cytoplasmic male sterility (CMS) or SI system.

The first F1 hybrid breeding system was developed in maize through a combination of hand emasculation and hand pollination in the 1920s in USA; this provided a very easy and straightforward way to avoid selfing. Even nowadays, hybrid seeds produced in Solanaceae and Cucurbitaceae crops, such as eggplant, cucumber and water melon, still benefit from this traditional system (Watanabe et al., 2008; Yamagishi and Bhat, 2014). Due to the nature of the flower and fruit structure of these crops, many hundreds or even thousands of hybrid seeds can be produced from a single flower through hand emasculation and pollination, which makes hand emasculation a practical way in hybrid seeds production in these plants. However, it is time consuming and labour intensive, and it is impossible to use hand emasculation and manual pollination to produce hybrid seeds in most of the crops for commercial purpose because of the small number of seeds derived from the pollination of one flower. Therefore, alternative methods, such as SI and CMS are chosen for the production of hybrid seed production.

7.3.1 Brassicaceae SI and *Papaver* SI in F1 hybrid breeding

We will focus on discussion about SI in this section; see the following section for discussion of CMS. SI has long been an important agricultural trait for hybrid breeding in Brassicaceae vegetable crops. For plants, such as turnip and cabbage, which are self-incompatible, a combination of pollination by honey bees and breakdown SI by CO₂ treatment (for the maintenance of SI lines) has been well established as a practical hybrid breeding system for commercial F1-hybrid seed production (Watanabe et al., 2008). This demonstrates that SI is a feasible system for hybrid breeding. However, other Brassicaceae crops such as *B. napus* and *B. juncea*, which are the most important oilseed crops in the world, do not express SI. A lot of effort has been devoted in the oilseed hybrid breeding by utilising the Brassicaceae SI trait. However, two major problems remained to be solved: the introduction of SI into oilseed rape, and choosing appropriate restorer lines.

For the introduction of SI into the Brassicaceae oilseed crops, there are two possible choices: (1) transfer of the *S*-locus from related SI species and (2) interspecific hybridization. Although it has been demonstrated that the *S*-locus derived from *A. lyrata* and *C. grandiflora* are able to restore SI in *A. thaliana*, attempts to confer SI into *A. thaliana* using the *Brassica* *S*-locus have failed (Bi et al., 2000; Boggs et al., 2009b; Nasrallah et al., 2002). This indicates that despite being conceptually simple, expressing SI in the self-compatible Brassicaceae species by transformation of the *SCR/SRK* gene

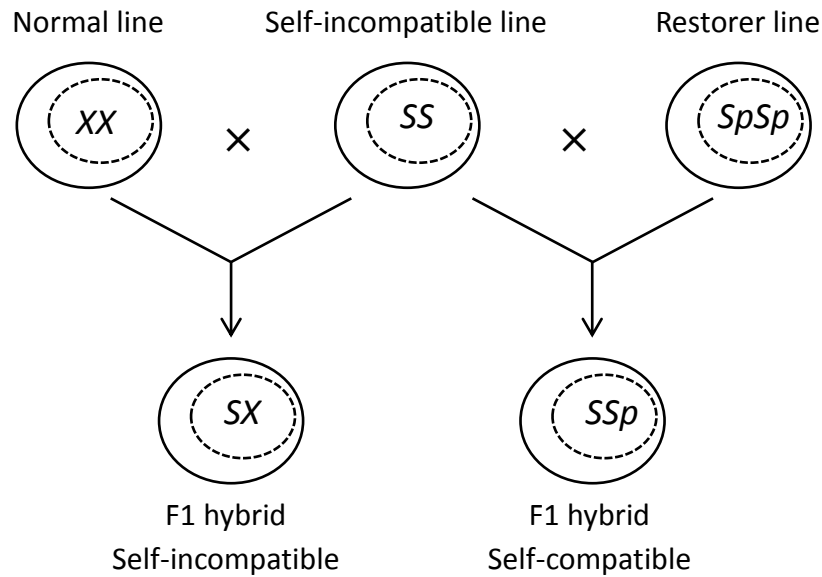
pair is not as straightforward as previously thought. Although, it has not been reported yet whether it is possible to generate self-incompatible oilseed rape by transformation of the *S*-locus, we can infer from previous studies that it might only be accomplished using an *S*-locus derived from species which are closely related to *B. napus* or *B. juncea*. In terms of interspecific hybridization, self-incompatible *B. napus* has been generated through interspecific hybridization by introgressing a *B. rapa* *S* haplotype into *B. napus* (Ma et al., 2009). However, as the molecular mechanisms underlying interspecific hybridization is still not clear, a lot of work is needed for the screening of SI plants in the F1 offspring after interspecific hybridization, during which fortune plays an important role in most cases. The establishment that *Papaver* SI can be functionally transferred into *A. thaliana*, which belongs to the Brassicaceae family, suggests that *Papaver* SI might also be functional in other Brassicaceae members, such as *B. napus* and *B. juncea*, and that it might be possible to utilise the *Papaver* SI system to produce F1 hybrids in these species.

Even if the Brassicaceae SI can be successfully transferred into oilseed rape, choosing an appropriate restorer line for the construction of an intact F1-hybrid breeding system represents a further big challenge. As Brassicaceae SI has sporophytic SI, a cross between a homozygous self-incompatible line and a normal (self-compatible) line will result in self-incompatible offspring (Figure 7-1-A). This makes Brassicaceae SI useless in F1 hybrid breeding for seed-crops like *B. napus* and *B. juncea*, because seeds are the

main products of these crops, but F1 hybrid offspring are self-incompatible, which produce no seed through selfing. So if plant breeders want to utilise Brassicaceae SI in hybrid breeding, a specific restorer line with a suppressor of the *S*-locus, which is able to restore the self-fertility phenotype in the F1 hybrid offspring, is required (Yang et al., 2001). Thus additional work is needed for plant breeders to identify a suitable and specific restorer line (Figure 7-1-A). However, in the F1-hybrid breeding system utilising the *Papaver* SI, this kind of issue potentially does not exist. Crosses between a homozygous SI line and a normal restorer line (self-compatible) will result in offspring which are *S*-heterozygous (Figure 7-1-B). As *Papaver* has gametophytic SI, plants which are *S*-heterozygous are still able to set full seed through selfing. Therefore, in a *Papaver* SI-based hybrid breeding system, a special restorer line is not necessary, and any elite line can be used to cross with the SI line to produce F1 hybrid seeds.

Taken together, there is the possibility that, in theory, even in the breeding of Brassicaceae crop hybrid seeds, *Papaver* SI may be potentially better than the Brassicaceae SI, by allowing the generation of self-incompatible lines, and production of F1 hybrid seeds more easily.

A: Theoretical utilisation of Brassicaceae SI for hybrid breeding



B: Theoretical utilisation of *Papaver* SI for hybrid breeding

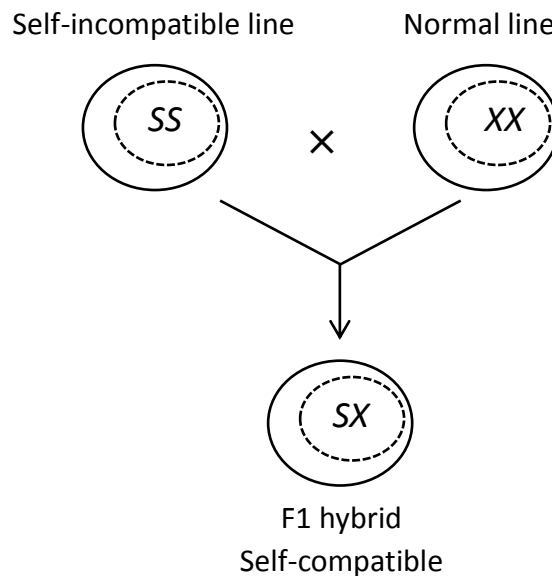


Figure 7-1 Comparison between the Brassicaceae SI and *Papaver* SI in hybrid breeding

A: in a Brassicaceae SI-based hybrid breeding system, cross between the self-incompatible line and a normal line results in the SI of the F1 hybrid offspring. A specific restorer line containing a specific *S*-locus suppressor gene (*Sp*) is needed to restore the self-fertility in the F1 hybrid offspring. B: in a *Papaver* SI-based hybrid breeding system, no specific restorer line is needed. Cross between the self-incompatible line and a random line will result in *S*-heterozygous offspring, which can set seeds normally.

7.3.2 Comparison between CMS and the *Papaver* SI in hybrids breeding

CMS is a maternal inherited trait resulting from the incompatible interaction between mitochondrial and nuclear proteins (Luo et al., 2013); see review by Chen and Liu, (2014) for more details. It is the most popular and practical system adopted world-wide by the F1-hybrid seed breeders to avoid self-pollination and promote hybridization. It has already been successfully utilised for the commercial production of hybrid seeds of many crops such as rice, maize and oilseed rape.

As mentioned in the previous section, to construct a functional and practical hybrid breeding system, it is vital to identify an appropriate restorer line, so that the self-fertility phenotype can be restored in the F1 generation. The restoration of fertility ensures that plants of the F1 generation produces seeds, which are the agricultural products we need, normally. However, it is not easy to identify a suitable restorer line. This usually constrains the application of CMS in hybrid breeding for many crops, such as wheat, one of the most important cereal crops in the world. A CMS wheat line was identified in the 1960s, and huge amounts of money and effort have been devoted to hybrid wheat programmes since then. However, the wheat hybrid system turns out to be quite impractical and difficult to use because of the lack of an effective fertility restoration line (Whitford et al., 2013). If the *Papaver* SI can be functionally transferred into wheat, it could potentially facilitate the production of hybrid wheat seeds because in a *Papaver* SI-based hybrid breeding system, no specific line is required to restore

self-fertility in the F1 hybrid offspring (Figure 7-2).

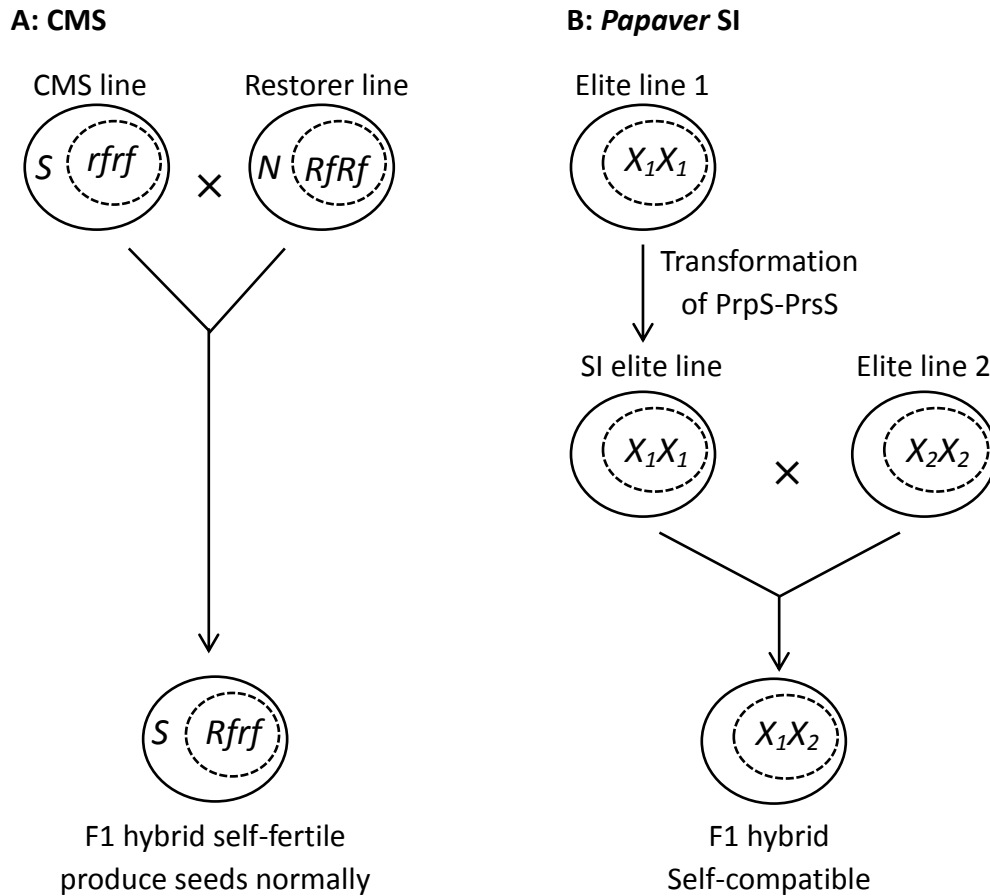


Figure 7-2 Comparison between CMS and the *Papaver* SI system in hybrid breeding

A: in a CMS-based hybrid breeding system, a specific restorer line containing restorer of fertility gene (*Rf*) is needed to restore the self-fertility in the F1 hybrid offspring. This narrows the range of elites which can be selected as the parent lines in this hybrid breeding system. B: in a *Papaver* SI-based hybrid breeding system, no specific line is needed to restore the self-fertility in the F1 offspring. Therefore, any two elite lines can be utilised as the parent lines in the *Papaver* SI-based hybrid breeding system. This facilitates a further increase in the crop production by allowing the incorporation of other breeding technologies to breed the best possible elite lines as the parent lines.

Furthermore, the *Papaver* SI system has another very obvious advantage over the CMS in the hybrid breeding. Hybrid breeding provides a potential way to lift crop yields by

exploiting heterosis, which is a biological phenomenon that the hybrid offspring shows an improved biological functionality over its parents. In a CMS-based hybrid breeding system, the F1 hybrid seeds are derived from the cross between the CMS line and restorer line (Figure 7-2). As it has been described above, not every normal line can be used as the restorer line in a CMS-based hybrid breeding system. This limits the application of elite lines being used as the parent lines in the CMS-based hybrid breeding system. However, there is no such constraint using the *Papaver* SI-based hybrid breeding system. F1 hybrid seeds can be produced through the cross between any two elite lines (Figure 7-2). This could allow a further increase in the crop yields by using the best possible lines, which can be elite lines derived from tolerance breeding and disease resistant breeding, as the parent lines.

However, there are still many steps to go through to construct a practical F1 hybrid breeding system using *Papaver* SI. Besides establishment of self-incompatible plants by transformation of the *Papaver* *S*-determinants, maintenance of the transgenic SI lines represents one of the greatest challenges. This might be solved by using inducible or environmentally sensitive promoter to drive the expression of *Papaver* *S*-determinants when generating transgenic SI lines, so that the expression of SI in the transgenic SI lines can be manually controlled. Thus, the SI in the transgenic SI lines can be “switched on” when crossing with another parental line to produce hybrid seeds, and “switched off” when plant breeders need to bulk up SI lines. Further investigations are

still needed to establish this.

In summary, the *Papaver* SI system might be potentially applied in hybrid breeding. It has an advantage over the CMS-based hybrid breeding system, in theory, by allowing the construction of a hybrid breeding system more easily and the incorporation of other breeding technologies. Despite being theoretically applicable, it is still not known yet whether this can be successfully translated into a robust and practical outcome.

7.4 Functional transfer of the *Papaver* SI system into *A. thaliana*: implications in the SI molecular mechanism research

A. thaliana has been the model plant for analysis of a large variety of physiological, developmental and evolutionary processes due to the availability of its large arsenal of genetic and molecular resources (Bergelson and Roux, 2010; Liepman et al., 2010). However, limitations in making full use of *A. thaliana* are also found because of the absence of some biological phenomena, for example, SI. Understanding the evolutionary, genetic and molecular mechanisms of SI has been an enduring source of curiosity since its discovery by Darwin in the nineteenth century. However, it is difficult to carry out molecular genetic studies in non-model self-incompatible species. The successful development of self-incompatible *A. thaliana* through the transfer of the SI trait facilitates molecular research underlying different SI systems by using the genetic and molecular tools available in *A. thaliana*.

It has been demonstrated that the SI trait isolated from the self-incompatible *A. lyrata* or *C. grandiflora* is sufficient to impart the SI phenotype in self-compatible *A. thaliana*, demonstrating that the signalling cascade leading to the self-pollen rejection is maintained in *A. thaliana*, establishing the transgenic self-incompatible *A. thaliana* a good model for mechanistic studies of Brassicaceae SI (Boggs et al., 2009b; Nasrallah et al., 2002, 2004; Rea et al., 2010). The role of ARC1 in Brassicaceae SI was examined using self-incompatible *A. thaliana* as the model plant. ARC1 has been demonstrated to be the positive regulators in the SI of *B. napus*, because the down-regulation of ARC1 is associated with the breakdown of SI (Stone et al., 1999). In Col-0 *A. thaliana*, *ARC1* is absent in the genome (Indriolo et al., 2012; Kitashiba et al., 2011). However, transformation of *ARC1* confers a stronger SI phenotype in the transgenic Col-0::SCR/SRK *A. thaliana* plants, demonstrating *ARC1* promotes a strong and stable SI expression, further confirming the role of *ARC1* as a positive regulator in Brassicaceae SI (Indriolo et al., 2014). This demonstrates that transgenic self-incompatible *A. thaliana* is a good model for understanding Brassicaceae SI molecular mechanisms. See Goring et al. (2014), Kitashiba et al. (2011) and Nasrallah and Nasrallah (2014) for more about the Brassicaceae SI molecular mechanism research in *A. thaliana*.

7.4.1 Experimental design and preliminary work in investigating the *Papaver* SI molecular mechanism using transgenic *A. thaliana*

P. rhoeas is not a model organism for plant research, and gene manipulation in *P. rhoeas* is still unavailable. This makes it difficult to perform investigations into the *Papaver* SI molecular mechanism *in vivo*. All the knowledge about the *Papaver* SI response is accumulated through *in vitro* SI assays. Moreover, the *P. rhoeas* whole genome sequence is not available yet, which makes it difficult to carry out *Papaver* SI mechanism research using transcriptomics/proteomics-based approaches (Deshmukh et al., 2014). Development of self-incompatible *A. thaliana* expressing the *Papaver* SI-like phenotype provides a very good model system for studying and elucidating the mechanisms involved in the *Papaver* SI response *in vivo*, by making use of the wealth of *A. thaliana* resources, such as whole genome/RNA sequences, T-DNA insertion lines, RNAi lines and CRISPR/Cas9-mediated transgenic lines (Kumar and Jain, 2014; Sessions et al., 2002; The *Arabidopsis* Genome Initiative, 2000). Investigation of *Papaver* SI in *A. thaliana* focus mainly on two aspects: (1) genes/pathways identification using transcriptomics/proteomics-based approaches (Figure 7-3); (2) characterising the role of target genes using *in vivo* SI pollination (Figure 7-4).

Figure 7-3 outlines the procedures for the identification of genes/pathways involved in the *Papaver* SI response using transcriptomics/proteomics-based approaches. As the genome of *P. rhoeas* has not been sequenced, this makes it difficult to explain the

microarray and mass-spectrometry data obtained from *Papaver* pollen using databases derived from other plants. The availability of annotated *A. thaliana* genome and transcriptome facilitates the identification of genes/pathways involved in the *Papaver* SI response using omics-based approaches. This also provides insights into the candidate genes/pathways which might be involved in the SI for further detailed characterization.

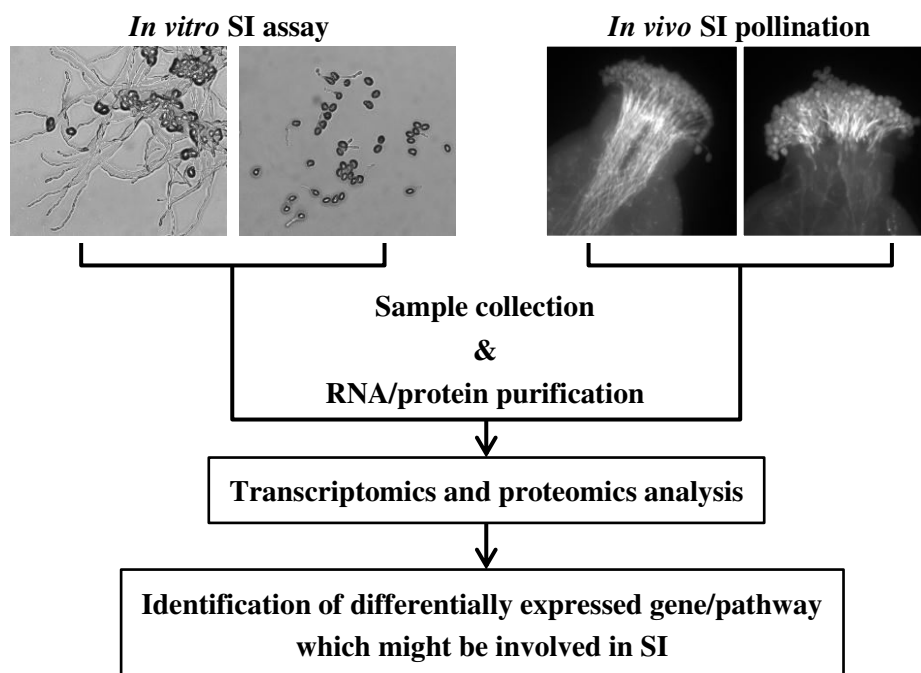


Figure 7-3 Investigating the *Papaver* SI response using omics-based approaches in *A. thaliana*

Incompatible/compatible pollen samples are collected through *in vitro/vivo* SI assays. RNA and protein are purified from the pollen and subjected to transcriptomics and proteomics analysis, respectively. Differentially expressed genes/pathways identified between the incompatible and compatible pollen are the candidates which might be involved in the regulation of SI.

Figure 7-4 details the experimental design in which the transgenic *A. thaliana* is used for the investigation of a target gene in *Papaver* SI. A cross between line BG16 (*At-ntp303::PrpS₁:GFP*) and transgenic RNAi line in which a gene of interest (GOI) is

specifically down-regulated in the pollen will result in a new transgenic line (hereafter crossed-line) expressing both PrpS₁:GFP and the down-regulated GOI. Pollination between this new transgenic line and line K (*At-SLR1::PrsS₁*) followed by aniline blue staining and seed set analysis will allow us to characterize the role of GOI in the *Papaver* SI response. If the GOI is involved in the *Papaver* SI, we would expect that pollen derived from crossed-line grows normally in the transgenic stigma expressing PrsS₁, and that cross between line K and crossed-line results in normal seed set. For example, we have attempted to investigate the role of proteasome during the *Papaver* SI response using this strategy. BG16 line was crossed with transgenic *ipba1* line, in which the *PBA1* gene is specifically suppressed by RNAi, resulting in the reduction of proteasome activity as a whole (Hatsugai et al., 2009). Homozygous plants expressing both PrpS₁:GFP and down-regulated PBA1 had already been obtained. Unfortunately, the transgenic *ipba1* line was constructed using the 35S promoter, which does not express in the *A. thaliana* pollen. Therefore, no further investigation was carried out. Although this project had met with failure, it still retains the possibility of using the strategy mentioned in Figure 7-4 to investigate the role of proteasome during the *Papaver* SI response if an alternative promoter that functions in pollen is used.

Besides the proteasome, there are still many other genes/proteins, such as p26-sPPases and p56-MAPK, or any other candidate identified in the omics-based studies, whose roles during the *Papaver* SI response can be investigated using the strategy outlined in

Figure 7-4.

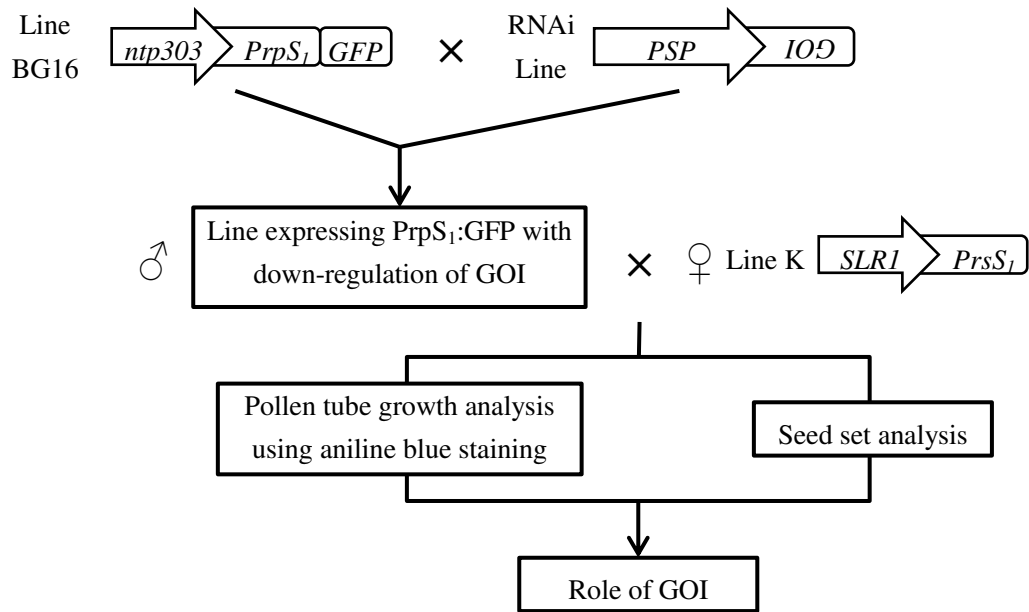


Figure 7-4 Characterizing the role of a target gene during the *Papaver* SI response in *A. thaliana*

Transgenic RNAi line with down-regulation of gene of interest (GOI) is constructed using pollen specific promoter (PSP). Cross BG16 line with transgenic RNAi line to obtain the line pollen-specifically expressing both PrpS₁:GFP and down-regulated GOI. Carry out pollination assay to investigate the effects of GOI down-regulation on SI-induced pollen tube growth inhibition and abnormal seed set, through aniline blue staining and seed set analysis.

7.5 Summary

Our studies have demonstrated that the *Papaver* female *S*-determinant, PrsS, is functional in *A. thaliana in vivo*, allowing inhibition of the growth of *At-PrpS:GFP* pollen in an *S*-allele specific manner. We have also shown that the *Papaver* SI system is functional in *A. thaliana* to make the plant self-incompatible. This is the first demonstration that SI system can be functionally transferred into another self-compatible species which has an evolutionarily distinct SI ancestor. Our work has

important implications for understanding the evolution of different SI systems in higher plants, as well as the relationship between the plant and animal PCD. The establishment of self-incompatible *A. thaliana* using the *Papaver* SI system facilitates the *Papaver* SI mechanism research by using *A. thaliana* as the model plant, and also mark an important step towards solving the food security issues, by potentially enabling easier F1 hybrid breeding in agricultural crops.

REFERENCE LIST

- Acarcan, A., Rossberg, M., Koch, M., and Schmidt, R. (2000). Comparative genome analysis reveals extensive conservation of genome organisation for *Arabidopsis thaliana* and *Capsella rubella*. *Plant J.* *23*, 55–62.
- Ai, Y., Singh, A., Coleman, C.E., Ioerger, T.R., Kheyr-Pour, A., and Kao, T. (1990). Self-incompatibility in *Petunia inflata*: isolation and characterization of cDNAs encoding three *S*-allele-associated proteins. *Sex. Plant Reprod.* *3*, 130–138.
- Allen, A.M., and Hiscock, S.J. (2008). Evolution and phylogeny of self-incompatibility systems in angiosperms. In: Franklin-Tong, V.E. ed. *Self-Incompatibility in Flowering Plants*, pp. 73–95.
- Alnemri, E.S., Livingston, D.J., Nicholson, D.W., Salvesen, G., Thornberry, N.A., Wong, W.W., and Yuan, J. (1996). Human ICE/CED-3 protease nomenclature. *Cell* *87*, 171.
- Bader, M., and Steller, H. (2009). Regulation of cell death by the ubiquitin-proteasome system. *Curr. Opin. Cell Biol.* *21*, 878–884.
- Beers, E.P., Woffenden, B.J., and Zhao, C. (2000). Plant proteolytic enzymes: possible roles during programmed cell death. *Plant Mol. Biol.* *44*, 399–415.
- Bell, C.D., Soltis, D.E., and Soltis, P.S. (2010). The age and diversification of the angiosperms re-revisited. *Am. J. Bot.* *97*, 1296–1303.
- Bergelson, J., and Roux, F. (2010). Towards identifying genes underlying ecologically relevant traits in *Arabidopsis thaliana*. *Nat. Rev. Genet.* *11*, 867–879.
- Berkers, C.R., van Leeuwen, F.W.B., Groothuis, T.A., Peperzak, V., van Tilburg, E.W., Borst, J., Neefjes, J.J., and Ovaas, H. (2007). Profiling proteasome activity in tissue with fluorescent probes. *Mol. Pharm.* *4*, 739–748.
- Bi, Y.M., Brugière, N., Cui, Y., Goring, D.R., and Rothstein, S.J. (2000). Transformation of *Arabidopsis* with a *Brassica SLG/SRK* region and *ARC1* gene is not sufficient to transfer the self-incompatibility phenotype. *Mol. Gen. Genet.* *263*, 648–654.
- Bibikova, T.N., Zhigilei, A., and Gilroy, S. (1997). Root hair growth in *Arabidopsis thaliana* is directed by calcium and an endogenous polarity. *Planta* *203*, 495–505.
- Bleecker, A.B., and Patterson, S.E. (1997). Last exit: senescence, abscission, and meristem arrest in *Arabidopsis*. *Plant Cell* *9*, 1169–1179.

- Boavida, L.C., and McCormick, S. (2007). Temperature as a determinant factor for increased and reproducible *in vitro* pollen germination in *Arabidopsis thaliana*. *Plant J.* 52, 570–582.
- Boggs, N.A, Dwyer, K.G., Shah, P., McCulloch, A.A, Bechsgaard, J., Schierup, M.H., Nasrallah, M.E., and Nasrallah, J.B. (2009b). Expression of distinct self-incompatibility specificities in *Arabidopsis thaliana*. *Genetics* 182, 1313–1321.
- Boggs, N.A, Nasrallah, J.B., and Nasrallah, M.E. (2009a). Independent *S*-locus mutations caused self-fertility in *Arabidopsis thaliana*. *PLoS Genet.* 5, e1000426.
- Bogyo, M., McMaster, J.S., Gaczynska, M., Tortorella, D., Goldberg, A.L., and Ploegh, H. (1997). Covalent modification of the active site threonine of proteasomal β subunits and the *Escherichia coli* homolog HslV by a new class of inhibitors. *Proc. Natl. Acad. Sci.* 94, 6629–6634.
- Boivin, N., Morse, D., and Cappadocia, M. (2014). Degradation of *S*-RNase in compatible pollen tubes of *Solanum chacoense* inferred by immunogold labeling. *J. Cell Sci.* In press.
- Borén, M., Höglund, A.S., Bozhkov, P., and Jansson, C. (2006). Developmental regulation of a VEIDase caspase-like proteolytic activity in barley caryopsis. *J. Exp. Bot.* 57, 3747–3753.
- Bosch, M., and Franklin-Tong, V.E. (2008). Self-incompatibility in *Papaver*: signalling to trigger PCD in incompatible pollen. *J. Exp. Bot.* 59, 481–490.
- Bosch, M., and Franklin-Tong, V.E. (2007). Temporal and spatial activation of caspase-like enzymes induced by self-incompatibility in *Papaver* pollen. *Proc. Natl. Acad. Sci.* 104, 18327–18332.
- Bosch, M., Poulter, N.S., Perry, R.M., Wilkins, K.A, and Franklin-Tong, V.E. (2010). Characterization of a legumain/vacuolar processing enzyme and YVADase activity in *Papaver* pollen. *Plant Mol. Biol.* 74, 381–393.
- Bower, M.S., Matias, D.D., Fernandes-Carvalho, E., Mazzurco, M., Gu, T., Rothstein, S.J., and Goring, D.R. (1996). Two members of the thioredoxin-h family interact with the kinase domain of a *Brassica S* locus receptor kinase. *Plant Cell* 8, 1641–1650.
- Bredemeijer, G.M., and Blaas, J. (1981). *S*-specific proteins in styles of self-incompatible *Nicotiana glauca*. *Theor. Appl. Genet.* 59, 185–190.

- Broemer, M., and Meier, P. (2009). Ubiquitin-mediated regulation of apoptosis. *Trends Cell Biol.* *19*, 130–140.
- Busse, A., Kraus, M., Na, I.K., Rietz, A., Scheibenbogen, C., Driessen, C., Blau, I.W., Thiel, E., and Keilholz, U. (2008). Sensitivity of tumor cells to proteasome inhibitors is associated with expression levels and composition of proteasome subunits. *Cancer* *112*, 659–670.
- Cai, G., Moscatelli, A., and Cresti, M. (1997). Cytoskeletal organization and pollen tube growth. *Trends Plant Sci.* *2*, 86–91.
- Capron, A., Gourgues, M., Neiva, L.S., Faure, J.E., Berger, F., Pagnussat, G., Krishnan, A., Alvarez-Mejia, C., Vielle-Calzada, J.P., Lee, Y.R., et al. (2008). Maternal control of male-gamete delivery in *Arabidopsis* involves a putative GPI-anchored protein encoded by the *LORELEI* gene. *Plant Cell* *20*, 3038–3049.
- Cardozo, T., and Pagano, M. (2004). The SCF ubiquitin ligase: insights into a molecular machine. *Nat. Rev. Mol. Cell Biol.* *5*, 739–751.
- Cerretti, D.P., Kozlosky, C.J., Mosley, B., Nelson, N., van Ness, K., Greenstreet, T.A., March, C.J., Kronheim, S.R., Druck, T., and Cannizzaro, L.A (1992). Molecular cloning of the interleukin-1 β converting enzyme. *Science* *256*, 97–100.
- Chantha, S.C., Herman, A.C., Platts, A.E., Vekemans, X., and Schoen, D.J. (2013). Secondary evolution of a self-incompatibility locus in the Brassicaceae genus *Leavenworthia*. *PLoS Biol.* *11*, e1001560.
- Chen, L., and Liu, Y.G. (2014). Male sterility and fertility restoration in crops. *Annu. Rev. Plant Biol.* *65*, 579–606.
- Cheung, A.Y., Duan, Q., Costa, S.S., de Graaf, B.H.J., Di Stilio, V.S., Feijo, J., and Wu, H.M. (2008). The dynamic pollen tube cytoskeleton: live cell studies using actin-binding and microtubule-binding reporter proteins. *Mol. Plant* *1*, 686–702.
- Coffeen, W.C., and Wolpert, T.J. (2004). Purification and characterization of serine proteases that exhibit caspase-like activity and are associated with programmed cell death in *Avena sativa*. *Plant Cell* *16*, 857–873.
- Cooperman, B.S., Baykov, A.A, and Lahti, R. (1992). Evolutionary conservation of the active site of soluble inorganic pyrophosphatase. *Trends Biochem. Sci.* *17*, 262–266.

- Coutu, C., Brandle, J., Brown, D., Brown, K., Miki, B., Simmonds, J., and Hegedus, D.D. (2007). pORE: a modular binary vector series suited for both monocot and dicot plant transformation. *Transgenic Res.* *16*, 771–781.
- Cravatt, B.F., Wright, A.T., and Kozarich, J.W. (2008). Activity-based protein profiling: from enzyme chemistry to proteomic chemistry. *Annu. Rev. Biochem.* *77*, 383–414.
- Cucinotta, M., Colombo, L., and Roig-Villanova, I. (2014). Ovule development, a new model for lateral organ formation. *Front. Plant Sci.* *5*, 117.
- Davis, A.M., Hall, A., Millar, A.J., Darrah, C., and Davis, S.J. (2009). Protocol: streamlined sub-protocols for floral-dip transformation and selection of transformants in *Arabidopsis thaliana*. *Plant Methods* *5*, 3.
- Deshaies, R. (1999). SCF and Cullin/Ring H2-based ubiquitin ligases. *Annu. Rev. Cell Dev. Biol.* *15*, 435–467.
- Deshmukh, R., Sonah, H., Patil, G., Chen, W., Prince, S., Mutava, R., Vuong, T., Valliyodan, B., and Nguyen, H.T. (2014). Integrating omic approaches for abiotic stress tolerance in soybean. *Front. Plant Sci.* *5*, 244.
- Van Doorn, W.G., Beers, E.P., Dangl, J.L., Franklin-Tong, V.E., Gallois, P., Hara-Nishimura, I., Jones, A.M., Kawai-Yamada, M., Lam, E., Mundy, J., et al. (2011). Morphological classification of plant cell deaths. *Cell Death Differ.* *18*, 1241–1246.
- Doughty, J., Dixon, S., Hiscock, S.J., Willis, A.C., Parkin, I.A.P., and Dickinson, H.G. (1998). PCP-A1, a defensin-like *brassica* pollen coat protein that binds the *S* locus glycoprotein, is the product of gametophytic gene expression. *Plant Cell* *10*, 1333–1347.
- Doughty, J., Aljabri, M., and Scott, R.J. (2014). Flavonoids and the regulation of seed size in *Arabidopsis*. *Biochem. Soc. Trans.* *42*, 364–369.
- Doyle, T., and Botstein, D. (1996). Movement of yeast cortical actin cytoskeleton visualized *in vivo*. *Proc. Natl. Acad. Sci.* *93*, 3886–3891.
- Dresselhaus, T., and Franklin-Tong, V.E. (2013). Male-female crosstalk during pollen germination, tube growth and guidance, and double fertilization. *Mol. Plant* *6*, 1018–1036.
- Drews, G., Lee, D., and Christensen, C. (1998). Genetic analysis of female gametophyte development and function. *Plant Cell* *10*, 5–17.

- Earley, K.W., Haag, J.R., Pontes, O., Opper, K., Juehne, T., Song, K., and Pikaard, C.S. (2006). Gateway-compatible vectors for plant functional genomics and proteomics. *Plant J.* 45, 616–629.
- Eaves, D.J., Flores-Ortiz, C., Haque, T., Lin, Z., Teng, N., and Franklin-Tong, V.E. (2014). Self-incompatibility in *Papaver*: advances in integrating the signalling network. *Biochem. Soc. Trans.* 42, 370-376.
- Edwards, C.M., Lwin, S.T., Fowler, J.A., Oyajobi, B.O., Bates, A.L., and Mundy, G.R. (2009). Myeloma cells exhibit an increase in proteasome activity and an enhanced response to proteasome inhibition in the bone marrow microenvironment *in vivo*. *Am J Hematol* 84, 268–272.
- Entani, T., Iwano, M., Shiba, H., Che, F.S., Isogai, A., and Takayama, S. (2003). Comparative analysis of the self-incompatibility (*S*-) locus region of *Prunus mume*: identification of a pollen-expressed F-box gene with allelic diversity. *Genes to Cells* 8, 203–213.
- Entani, T., Kubo, K., Isogai, S., Fukao, Y., Shirakawa, M., Isogai, A., and Takayama, S. (2014). Ubiquitin-proteasome-mediated degradation of *S*-RNase in a solanaceous cross-compatibility reaction. *Plant J.* 78, 1014–1021.
- Escobar-Restrepo, J.M., Huck, N., Kessler, S., Gagliardini, V., Gheyselinck, J., Yang, W.C., and Grossniklaus, U. (2007). The FERONIA receptor-like kinase mediates male-female interactions during pollen tube reception. *Science* 317, 656–660.
- Fan, L.M., Wang, Y.F., Wang, H., and Wu, W.H. (2001). *In vitro Arabidopsis* pollen germination and characterization of the inward potassium currents in *Arabidopsis* pollen grain protoplasts. *J. Exp. Bot.* 52, 1603–1614.
- Fenteany, G., and Schreiber, S. (1998). Lactacystin, proteasome function, and cell fate. *J. Biol. Chem.* 273, 8545–8548.
- Fenteany, G., Standaert, R.F., Lane, W.S., Choi, S., Corey, E.J., and Schreiber, S.L. (1995). Inhibition of proteasome activities and subunit-specific amino-terminal threonine modification by lactacystin. *Science* 268, 726–731.
- Fernández, M.B., Daleo, G.R., and Guevara, M.G. (2012). DEVDase activity is induced in potato leaves during *Phytophthora infestans* infection. *Plant Physiol. Biochem.* 61, 197–203.
- Figueiredo, D.D., and Köhler, C. (2014). Signalling events regulating seed coat development. *Biochem. Soc. Trans.* 42, 358–363.

Finkelstein, R., Gampala, S., and Rock, C. (2002). Abscisic acid signaling in seeds and seedlings. *Plant Cell* 14, S15–S46.

Finkelstein, R., Lynch, T., Reeves, W., Petitfils, M., and Mostachetti, M. (2011). Accumulation of the transcription factor ABA-insensitive (ABI)4 is tightly regulated post-transcriptionally. *J. Exp. Bot.* 62, 3971–3979.

Foote, H.C.C. (1993). The cloning and characterisation of the stigmatic self-incompatibility (*S*-) gene from *Papaver rhoeas* L. PhD thesis, University of Birmingham.

Foote, H.C.C., Ride, J.P., Franklin-Tong, V.E., Walker, E.A., Lawrence, M.J., and Franklin, F.C.H. (1994). Cloning and expression of a distinctive class of self-incompatibility (*S*) gene from *Papaver rhoeas* L. *Proc. Natl. Acad. Sci.* 91, 2265–2269.

Franklin, T., Oldknow, J., and Trick, M. (1996). SLR1 function is dispensable for both self-incompatible rejection and self-compatible pollination processes in *Brassica*. *Sex. Plant Reprod.* 9, 203–208.

Franklin-Tong, V.E., and Franklin, F.C.H. (2000). Self-incompatibility in *Brassica*: the elusive pollen *S* gene is identified! *Plant Cell* 12, 305–308.

Franklin-Tong, V.E., and Gourlay, C. (2008). A role for actin in regulating apoptosis/programmed cell death: evidence spanning yeast, plants and animals. *Biochem. J.* 413, 389–404.

Franklin-Tong, V.E., Lawrence, M., and Franklin, C. (1988). An *in vitro* bioassay for the stigmatic product of the self-incompatibility gene in *Papaver rhoeas* L. *New Phytol.* 110, 109–118.

Franklin-Tong, V.E., Ruuth, E., Marmey, P., Lawrence, M.J., and Franklin, F.C.H. (1989). Characterization of a stigmatic component from *Papaver rhoeas* L. which exhibits the specific activity of a self-incompatibility (*S*-) gene product. *New Phytol.* 112, 307–315.

Franklin-Tong, V.E., Ride, J.P., Read, N.D., Trewavas, A.J., and Franklin, F.C.H. (1993). The self-incompatibility response in *Papaver rhoeas* is mediated by cytosolic free calcium. *Plant J.* 4, 163–177.

Franklin-Tong, V.E., Ride, J.P., and Franklin, F.C.H. (1995). Recombinant stigmatic self-incompatibility (*S*-) protein elicits a Ca²⁺ transient in pollen of *Papaver rhoeas*. *Plant J.* 8, 299–307.

- Franklin-Tong, V.E., Hackett, G., and Hepler, P. (1997). Ratio-imaging of Ca^{2+}_i in the self-incompatibility response in pollen tubes of *Papaver rhoeas*. *Plant J.* *12*, 1375–1386.
- Fukuda, H. (1996). Xylogenesis: initiation, progression, and cell death. *Annu. Rev. Plant Physiol. Plant Mol. Biol.* *47*, 299–325.
- Fukuda, H., and Komamine, A. (1983). Changes in the synthesis of RNA and protein during tracheary element differentiation in single cells isolated from the mesophyll of *Zinnia elegans*. *Plant Cell Physiol.* *24*, 603–614.
- Gagne, J.M., Downes, B.P., Shiu, S.H., Durski, A.M., and Vierstra, R.D. (2002). The F-box subunit of the SCF E3 complex is encoded by a diverse superfamily of genes in *Arabidopsis*. *Proc. Natl. Acad. Sci.* *99*, 11519–11524.
- Gavrieli, Y., Sherman, Y., and Ben-Sasson, S. (1992). Identification of programmed cell death *in situ* via specific labeling of nuclear DNA fragmentation. *J. Cell Biol.* *119*, 493–501.
- Geitmann, A, Snowman, B.N., Emons, A.M., and Franklin-Tong, V.E. (2000). Alterations in the actin cytoskeleton of pollen tubes are induced by the self-incompatibility reaction in *Papaver rhoeas*. *Plant Cell* *12*, 1239–1251.
- Godfray, H.C.J., Beddington, J.R., Crute, I.R., Haddad, L., Lawrence, D., Muir, J.F., Pretty, J., Robinson, S., Thomas, S.M., and Toulmin, C. (2010). Food security: the challenge of feeding 9 billion people. *Science* *327*, 812–818.
- Goldman, M., Goldberg, R., and Mariani, C. (1994). Female sterile tobacco plants are produced by stigma-specific cell ablation. *EMBO J.* *13*, 2976–2984.
- Goldraij, A., Kondo, K., Lee, C.B., Hancock, C.N., Sivaguru, M., Vazquez-Santana, S., Kim, S., Phillips, T.E., Cruz-Garcia, F., and McClure, B. (2006). Compartmentalization of S-RNase and HT-B degradation in self-incompatible *Nicotiana*. *Nature* *439*, 805–810.
- Gopal, G.J., and Kumar, A. (2013). Strategies for the production of recombinant protein in *Escherichia coli*. *Protein J.* *32*, 419–425.
- Goring, D.R., and Rothstein, S.J. (1992). The S-locus receptor kinase gene in a self-incompatible *Brassica napus* line encodes a functional serine/threonine kinase. *Plant Cell* *4*, 1273–1281.
- Goring, D.R., Glavin, T.L., Schafer, U., and Rothstein, S.J. (1993). An S receptor kinase gene in self-compatible *Brassica napus* has a 1-bp deletion. *Plant Cell* *5*, 531–539.

- Goring, D.R., Indriolo, E., and Samuel, M.A (2014). The ARC1 E3 ligase promotes a strong and stable self-incompatibility response in *Arabidopsis* species: response to the Nasrallah and Nasrallah commentary. *Plant Cell* In press.
- De Graaf, B.H.J., Rudd, J.J., Wheeler, M.J., Perry, R.M., Bell, E.M., Osman, K., Franklin, F.C.H., and Franklin-Tong, V.E. (2006). Self-incompatibility in *Papaver* targets soluble inorganic pyrophosphatases in pollen. *Nature* 444, 490–493.
- De Graaf, B.H.J., Vatovec, S., Juárez-Díaz, J.A., Chai, L., Kooblall, K., Wilkins, K. a, Zou, H., Forbes, T., Franklin, F.C.H., and Franklin-Tong, V.E. (2012). The *Papaver* self-incompatibility pollen *S*-determinant, PrpS, functions in *Arabidopsis thaliana*. *Curr. Biol.* 22, 154–159.
- Greenberg, J. (1997). Programmed cell death in plant-pathogen interactions. *Annu. Rev. Plant Biol.* 48, 525–545.
- Groll, M., Ditzel, L., Löwe, J., Stock, D., Bochtler, M., Bartunik, H.D., and Huber, R. (1997). Structure of 20S proteasome from yeast at 2.4 Å resolution. *Nature* 386, 463–471.
- Gu, C., Kolodziejek, I., Misas-Villamil, J., Shindo, T., Colby, T., Verdoes, M., Richau, K.H., Schmidt, J., Overkleeft, H.S., and van der Hoorn, R.A.L. (2010). Proteasome activity profiling: a simple, robust and versatile method revealing subunit-selective inhibitors and cytoplasmic, defense-induced proteasome activities. *Plant J.* 62, 160–170.
- Gu, T., Mazzurco, M., Sulaman, W., Matias, D.D., and Goring, D.R. (1998). Binding of an arm repeat protein to the kinase domain of the *S*-locus receptor kinase. *Proc. Natl. Acad. Sci.* 95, 382.
- Guilley, H., Dudley, R.K., Jonard, G., Balazs, E., and Richards, K.E. (1982). Transcription of Cauliflower mosaic virus DNA: detection of promoter sequences, and characterization of transcripts. *Cell* 30, 763–773.
- Hackett, R., Cadwallader, G., and Franklin, F. (1996). Functional analysis of a *Brassica oleracea* *SLR1* gene promoter. *Plant Physiol.* 112, 1601–1607.
- Hackett, R.M., Lawrence, M.J., and Franklin, F.C.H. (1992). A *Brassica* *S*-locus related gene promoter directs expression in both pollen and pistil of tobacco. *Plant J.* 2, 613–617.
- Hadjiosif, N. (2007). Functional characterization of *PrpS*, a pollen *S* locus specific gene that is required for the self-incompatibility reaction in *Papaver rhoeas*. PhD thesis, University of Birmingham.

- Han, J.J., Lin, W., Oda, Y., Cui, K.M., Fukuda, H., and He, X.Q. (2012). The proteasome is responsible for caspase-3-like activity during xylem development. *Plant J.* 72, 129–141.
- Hanna, J., and Finley, D. (2007). A proteasome for all occasions. *FEBS Lett.* 581, 2854–2861.
- Hara-Nishimura, I., and Hatsugai, N. (2011). The role of vacuole in plant cell death. *Cell Death Differ.* 18, 1298–1304.
- Hatsugai, N., Kuroyanagi, M., Yamada, K., Meshi, T., Tsuda, S., Kondo, M., Nishimura, M., and Hara-Nishimura, I. (2004). A plant vacuolar protease, VPE, mediates virus-induced hypersensitive cell death. *Science* 305, 855–858.
- Hatsugai, N., Iwasaki, S., Tamura, K., Kondo, M., Fuji, K., Ogasawara, K., Nishimura, M., and Hara-Nishimura, I. (2009). A novel membrane fusion-mediated plant immunity against bacterial pathogens. *Genes Dev.* 23, 2496–2506.
- Heslop-Harrison, J., Heslop-Harrison, Y., and Shivanna, K.R. (1984). The evaluation of pollen quality, and a further appraisal of the fluorochromatic (FCR) test procedure. *Theor. Appl. Genet.* 67, 367–375.
- Hicke, L. (2001). Protein regulation by monoubiquitin. *Nat. Rev. Mol. Cell Biol.* 2, 195–201.
- Van der Hoorn, R.A.L., and Kaiser, M. (2012). Probes for activity-based profiling of plant proteases. *Physiol. Plant.* 145, 18–27.
- Hsu, S.C., TerBush, D., Abraham, M., and Guo, W. (2004). The exocyst complex in polarized exocytosis. *Int. Rev. Cytol.* 233, 243–265.
- Hua, Z., and Kao, T. (2006). Identification and characterization of components of a putative *Petunia* S-locus F-box-containing E3 ligase complex involved in S-RNase-based self-incompatibility. *Plant Cell* 18, 2531–2553.
- Hua, Z., and Kao, T. (2008). Identification of major lysine residues of S₃-RNase of *Petunia inflata* involved in ubiquitin-26S proteasome-mediated degradation *in vitro*. *Plant J.* 54, 1094–1104.
- Hua, Z., and Vierstra, R.D. (2011). The cullin-RING ubiquitin-protein ligases. *Annu. Rev. Plant Biol.* 62, 299–334.
- Huang, J., Zhao, L., Yang, Q., and Xue, Y. (2006). AhSSK1, a novel SKP1-like protein that interacts with the S-locus F-box protein SLF. *Plant J.* 46, 780–793.

- Indriolo, E., Tharmapalan, P., Wright, S.I., and Goring, D.R. (2012). The ARC1 E3 ligase gene is frequently deleted in self-compatible Brassicaceae species and has a conserved role in *Arabidopsis lyrata* self-pollen rejection. *Plant Cell* 24, 4607–4620.
- Indriolo, E., Safavian, D., and Goring, D.R. (2014). The ARC1 E3 ligase promotes two different self-pollen avoidance traits in *Arabidopsis*. *Plant Cell* 26, 1525–1543.
- Da Ines, O., Degroote, F., Goubely, C., Amiard, S., Gallego, M.E., and White, C.I. (2013). Meiotic recombination in *Arabidopsis* is catalysed by DMC1, with RAD51 playing a supporting role. *PLoS Genet.* 9, e1003787.
- Ivanov, R., Fobis-Loisy, I., and Gaude, T. (2010). When no means no: guide to Brassicaceae self-incompatibility. *Trends Plant Sci.* 15, 387–394.
- Iwano, M., and Takayama, S. (2012). Self/non-self discrimination in angiosperm self-incompatibility. *Curr. Opin. Plant Biol.* 15, 78–83.
- Iwano, M., Shiba, H., Matoba, K., Miwa, T., Funato, M., Entani, T., Nakayama, P., Shimosato, H., Takaoka, A., and Isogai, A. (2007). Actin dynamics in papilla cells of *Brassica rapa* during self- and cross-pollination. *Plant Physiol.* 144, 72–81.
- Jacobson, M., Weil, M., and Raff, M. (1997). Programmed cell death in animal development. *Cell* 88, 347–354.
- De Jong, A., Schuurman, K.G., Rodenko, B., Ovaa, H., and Berkers, C.R. (2012). Fluorescence-based proteasome activity profiling. *Methods Mol. Biol.* 803, 183–204.
- Jordan, N.D., Franklin, F.C.H., and Franklin-Tong, V.E. (2000). Evidence for DNA fragmentation triggered in the self-incompatibility response in pollen of *Papaver rhoeas*. *Plant J.* 23, 471–479.
- Kachroo, A., Schopfer, C.R., Nasrallah, M.E., and Nasrallah, J.B. (2001). Allele-specific receptor-ligand interactions in *Brassica* self-incompatibility. *Science* 293, 1824–1826.
- Kakeda, K., Jordan, N.D., Conner, A., Ride, J.P., Franklin-Tong, V.E., and Franklin, F.C.H. (1998). Identification of residues in a hydrophilic loop of the *Papaver rhoeas* S protein that play a crucial role in recognition of incompatible pollen. *Plant Cell* 10, 1723–1732.
- Kao, T., and Tsukamoto, T. (2004). The molecular and genetic bases of S-RNase-based self-incompatibility. *Plant Cell* 16, S72–S83.
- Kessler, S.A., and Grossniklaus, U. (2011). She's the boss: signaling in pollen tube reception. *Curr. Opin. Plant Biol.* 14, 622–627.

- Kim, M., Ahn, J.W., Jin, U.H., Choi, D., Paek, K.H., and Pai, H.S. (2003). Activation of the programmed cell death pathway by inhibition of proteasome function in plants. *J. Biol. Chem.* *278*, 19406–19415.
- Kisselev, A.F., and Goldberg, A.L. (2005). Monitoring activity and inhibition of 26S proteasomes with fluorogenic peptide substrates. *Methods Enzymol.* *398*, 364–378.
- Kitashiba, H., Liu, P., Nishio, T., Nasrallah, J.B., and Nasrallah, M.E. (2011). Functional test of *Brassica* self-incompatibility modifiers in *Arabidopsis thaliana*. *Proc. Natl. Acad. Sci.* *108*, 18173–18178.
- Klaas, M., Yang, B., Bosch, M., Thorogood, D., Manzanares, C., Armstead, I.P., Franklin, F.C.H., and Barth, S. (2011). Progress towards elucidating the mechanisms of self-incompatibility in the grasses: further insights from studies in *Lolium*. *Ann. Bot.* *108*, 677–685.
- Koch, M.A., Haubold, B., and Mitchell-Olds, T. (2000). Comparative evolutionary analysis of chalcone synthase and alcohol dehydrogenase loci in *Arabidopsis*, *Arabis*, and related genera (Brassicaceae). *Mol. Biol. Evol.* *17*, 1483–1498.
- Konishi, M. (1992). Epoxomicin, a new antitumor agent of microbial origin. *J. Antibiot.* *45*, 1746–1752.
- Korthout, H.A, Berecki, G., Bruin, W., van Duijn, B., and Wang, M. (2000). The presence and subcellular localization of caspase 3-like proteinases in plant cells. *FEBS Lett.* *475*, 139–144.
- Kraft, E., Stone, S.L., Ma, L., Su, N., Gao, Y., Lau, O.S., Deng, X.W., and Callis, J. (2005). Genome analysis and functional characterization of the E2 and RING-type E3 ligase ubiquitination enzymes of *Arabidopsis*. *Plant Physiol.* *139*, 1597–1611.
- Kubo, K., Entani, T., Takara, A., Wang, N., Fields, A.M., Hua, Z., Toyoda, M., Kawashima, S., Ando, T., Isogai, A., et al. (2010). Collaborative non-self recognition system in S-RNase-based self-incompatibility. *Science* *330*, 796–799.
- Kumar, V., and Jain, M. (2014). The CRISPR-Cas system for plant genome editing: advances and opportunities. *J. Exp. Bot.* In press.
- Kurepa, J., and Smalle, J.A. (2008). Structure, function and regulation of plant proteasomes. *Biochimie* *90*, 324–335.

- Kurup, S., Ride, J., Jordan, N., Fletcher, G., Franklin-Tong, V.E., and Franklin, F.C.H. (1998). Identification and cloning of related self-incompatibility *S*-genes in *Papaver rhoeas* and *Papaver nudicaule*. *Sex. Plant Reprod.* *11*, 192–198.
- Kusaba, M., Dwyer, K., Hendershot, J., Vrebalov, J., Nasrallah, J.B., and Nasrallah, M.E. (2001). Self-incompatibility in the genus *Arabidopsis*: characterization of the *S* locus in the outcrossing *A. lyrata* and its autogamous relative *A. thaliana*. *Plant Cell* *13*, 627–643.
- Lai, Z., Ma, W., Han, B., Liang, L., Zhang, Y., Hong, G., and Xue, Y. (2002). An F-box gene linked to the self-incompatibility (*S*) locus of *Antirrhinum* is expressed specifically in pollen and tapetum. *Plant Mol. Biol.* *50*, 29–41.
- Lalonde, B.A., Nasrallah, M.E., Dwyer, K.G., Chen, C.H., Barlow, B., and Nasrallah, J.B. (1989). A highly conserved *Brassica* gene with homology to the *S*-locus-specific glycoprotein structural gene. *Plant Cell* *1*, 249–258.
- Lee, D.H., and Goldberg, L. (1998). Proteasome inhibitors: valuable new tools for cell biologists. *Trends Cell Biol.* *8*, 397–403.
- Lee, H.S., Huang, S., and Kao, T. (1994). *S* proteins control rejection of incompatible pollen in *Petunia inflata*. *Nature* *367*, 560–563.
- Leydon, A.R., Chaibang, A., and Johnson, M.A. (2014). Interactions between pollen tube and pistil control pollen tube identity and sperm release in the *Arabidopsis* female gametophyte. *Biochem. Soc. Trans.* *42*, 340–345.
- Li, S., and Franklin-Tong, V.E. (2008). Self-incompatibility in *Papaver*: A MAP kinase signals to trigger programmed cell death. *Plant Signal. Behav.* *3*, 243–245.
- Li, W., and Chetelat, R.T. (2014). The role of a pollen-expressed Cullin1 protein in gametophytic self-incompatibility in *Solanum*. *Genetics* *196*, 439–442.
- Li, H., Lin, Y., Heath, R.M., Zhu, M.X., and Yang, Z. (1999). Control of pollen tube tip growth by a Rop GTPase-dependent pathway that leads to tip-localized calcium influx. *Plant Cell* *11*, 1731–1742.
- Li, S., Šamaj, J., and Franklin-Tong, V.E. (2007). A mitogen-activated protein kinase signals to programmed cell death induced by self-incompatibility in *Papaver* pollen. *Plant Physiol.* *145*, 236–245.
- Li, S., Sun, P., Williams, J.S., and Kao, T. (2014). Identification of the self-incompatibility locus F-box protein-containing complex in *Petunia inflata*. *Plant Reprod.* *27*, 31–45.

- Liepman, A.H., Wightman, R., Geshi, N., Turner, S.R., and Scheller, H.V. (2010). *Arabidopsis* - a powerful model system for plant cell wall research. *Plant J.* *61*, 1107–1121.
- Liggett, a, Crawford, L.J., Walker, B., Morris, T.C.M., and Irvine, a E. (2010). Methods for measuring proteasome activity: current limitations and future developments. *Leuk. Res.* *34*, 1403–1409.
- Liu, P., Sherman-Broyles, S., Nasrallah, M.E., and Nasrallah, J.B. (2007). A cryptic modifier causing transient self-incompatibility in *Arabidopsis thaliana*. *Curr. Biol.* *17*, 734–740.
- Liu, W., Fan, J., Li, J., Song, Y., Li, Q., Zhang, Y., and Xue, Y. (2014). SCF(SLF)-mediated cytosolic degradation of *S*-RNase is required for cross-pollen compatibility in *S*-RNase-based self-incompatibility in *Petunia hybrida*. *Front. Genet.* *5*, 228.
- Luo, D., Xu, H., Liu, Z., Guo, J., Li, H., Chen, L., Fang, C., Zhang, Q., Bai, M., Yao, N., et al. (2013). A detrimental mitochondrial-nuclear interaction causes cytoplasmic male sterility in rice. *Nat. Genet.* *45*, 573–577.
- Luu, D., Marty-Mazars, D., Trick, M., Dumas, C., and Heizmann, P. (1999). Pollen–stigma adhesion in *Brassica* spp involves SLG and SLR1 glycoproteins. *Plant Cell* *11*, 251–262.
- Luu, D., Qin, X., Morse, D., and Cappadocia, M. (2000). *S*-RNase uptake by compatible pollen tubes in gametophytic self-incompatibility. *Nature* *407*, 649–651.
- Luu, D.T., Heizmann, P., Dumas, C., Trick, M., and Cappadocia, M. (1997). Involvement of *SLR1* genes in pollen adhesion to the stigmatic surface in Brassicaceae. *Sex. Plant Reprod.* *10*, 227–235.
- Ma, H. (2005). Molecular genetic analyses of microsporogenesis and microgametogenesis in flowering plants. *Annu. Rev. Plant Biol.* *56*, 393–434.
- Ma, C., Gao, C., Zhang, J., Li, F., Wang, X., Liu, Y., and Fu, T. (2009). A promising way to produce *B. napus* hybrid seeds by self-incompatibility pollination system. 16th Aust. Res. Assem. Brassicas.
- Ma, J.K.C., Drake, P.M.W., and Christou, P. (2003). The production of recombinant pharmaceutical proteins in plants. *Nat. Rev. Genet.* *4*, 794–805.

- Malho, R., Read, N., Pais, M., and Trewavas, A. (1994). Role of cytosolic free calcium in the reorientation of pollen tube growth. *Plant J.* 5, 331–341.
- Márton, M.L., Cordts, S., Broadhvest, J., and Dresselhaus, T. (2005). Micropylar pollen tube guidance by egg apparatus 1 of maize. *Science* 307, 573–576.
- McClure, B., Cruz-García, F., and Romero, C. (2011). Compatibility and incompatibility in *S*-RNase-based systems. *Ann. Bot.* 108, 647–658.
- McClure, B.A., Haring, V., Ebert, P.R., Anderson, M.A., Simpson, R.J., Sakiyama, F., and Clarke, A.E. (1989). Style self-incompatibility gene products of *Nicotiana alata* are ribonucleases. *Nature* 342, 955–957.
- Meng, L., Mohan, R., Kwok, B.H., Eloffsson, M., Sin, N., and Crews, C.M. (1999). Epoxomicin, a potent and selective proteasome inhibitor, exhibits *in vivo* antiinflammatory activity. *Proc. Natl. Acad. Sci.* 96, 10403–10408.
- Murase, K., Shiba, H., Iwano, M., Che, F.S., Watanabe, M., Isogai, A., and Takayama, S. (2004). A membrane-anchored protein kinase involved in *Brassica* self-incompatibility signaling. *Science* 303, 1516–1519.
- Murfett, J., Atherton, T.L., Mou, B., Gassert, C.S., and McClure, B.A. (1994). *S*-RNase expressed in transgenic *Nicotiana* causes *S*-allele-specific pollen rejection. *Nature* 367, 563–566.
- Nasrallah, J.B., and Nasrallah, M.E. (2014). Robust self-incompatibility in the absence of a functional ARC1 Gene in *Arabidopsis thaliana*. *Plant Cell* In press.
- Nasrallah, M.E., and Wallace, D.H. (1967). Immunogenetics of self-incompatibility in *Brassica oleracea* L. *Heredity* 22, 519–527.
- Nasrallah, J.B., Rundle, S.J., and Nasrallah, M.E. (1994). Genetic evidence for the requirement of the *Brassica S*-locus receptor kinase gene in the self-incompatibility response. *Plant J.* 5, 373–384.
- Nasrallah, M.E., Barber, J.T., and Wallace, D.H. (1970). Self-incompatibility proteins in plants: detection, genetics, and possible mode of action. *Heredity* 25, 23–27.
- Nasrallah, M.E., Liu, P., and Nasrallah, J.B. (2002). Generation of self-incompatible *Arabidopsis thaliana* by transfer of two *S* locus genes from *A. lyrata*. *Science* 297, 247–249.

- Nasrallah, M.E., Liu, P., Sherman-Broyles, S., Boggs, N.A., and Nasrallah, J.B. (2004). Natural variation in expression of self-incompatibility in *Arabidopsis thaliana*: implications for the evolution of selfing. *Proc. Natl. Acad. Sci.* *101*, 16070–16074.
- Ngo, Q.A, Vogler, H., Lituiev, D.S., Nestorova, A., and Grossniklaus, U. (2014). A calcium dialog mediated by the FERONIA signal transduction pathway controls plant sperm delivery. *Dev. Cell* *29*, 491–500.
- Nicholson, D., and Thornberry, N. (1997). Caspases: killer proteases. *Trends Biochem. Sci.* *22*, 229–305.
- Nick, P. (1999). Signals, Motors, Morphogenesis - the Cytoskeleton in Plant Development. *Plant Biol.* *1*, 169–179.
- O'Brien, M., Major, G., Chantha, S.C., and Matton, D.P. (2004). Isolation of *S*-RNase binding proteins from *Solanum chacoense*: identification of an SBP1 (RING finger protein) orthologue. *Sex. Plant Reprod.* *17*, 81–87.
- Odell, J.T., Nagy, F., and Chua, N.H. (1985). Identification of DNA sequences required for activity of the cauliflower mosaic virus 35S promoter. *Nature* *313*, 810–812.
- Okuda, S., Tsutsui, H., Shiina, K., Sprunck, S., Takeuchi, H., Yui, R., Kasahara, R.D., Hamamura, Y., Mizukami, A., Susaki, D., et al. (2009). Defensin-like polypeptide LUREs are pollen tube attractants secreted from synergid cells. *Nature* *458*, 357–361.
- Omura, S., Fujimoto, T., Otaguro, K., Matsuzaki, K., Moriguchi, R., Tanaka, H., and Sasaki, Y. (1991). Structure of lactacystin, a new microbial metabolite which induces differentiation of neuroblastoma cells. *J. Antibiot.* *44*, 113–116.
- Van Ooijen, G., Dixon, L.E., Troein, C., and Millar, A.J. (2011). Proteasome function is required for biological timing throughout the twenty-four hour cycle. *Curr. Biol.* *21*, 869–875.
- Orlowski, M., and Wilk, S. (2003). Ubiquitin-independent proteolytic functions of the proteasome. *Arch. Biochem. Biophys.* *415*, 1–5.
- Ovaa, H. (2007). Active-site directed probes to report enzymatic action in the ubiquitin proteasome system. *Nat. Rev. Cancer* *7*, 613–620.
- Pajeroska-Mukhtar, K., and Dong, X. (2009). A kiss of death--proteasome-mediated membrane fusion and programmed cell death in plant defense against bacterial infection. *Genes Dev.* *23*, 2449–2454.

- Palmer, E., and Freeman, T. (2004). Investigation into the use of C- and N-terminal GFP fusion proteins for subcellular localization studies using reverse transfection microarrays. *Comp. Funct. Genomics* 5, 342–353.
- Palombella, V.J., Rando, O.J., Goldberg, A.L., and Maniatis, T. (1994). The ubiquitin-proteasome pathway is required for processing the NF- κ B1 precursor protein and the activation of NF- κ B. *Cell* 78, 773–785.
- Patterson, G.H., Knobel, S.M., Sharif, W.D., Kain, S.R., and Piston, D.W. (1997). Use of the green fluorescent protein and its mutants in quantitative fluorescence microscopy. *Biophys. J.* 73, 2782–2790.
- Pennell, R.I., and Lamb, C. (1997). Programmed cell death in plants. *Plant Cell* 9, 1157–1168.
- Poulter, N.S., Vatovec, S., and Franklin-Tong, V.E. (2008). Microtubules are a target for self-incompatibility signaling in *Papaver* pollen. *Plant Physiol.* 146, 1358–1367.
- Poulter, N.S., Staiger, C.J., Rappoport, J.Z., and Franklin-Tong, V.E. (2010). Actin-binding proteins implicated in the formation of the punctate actin foci stimulated by the self-incompatibility response in *Papaver*. *Plant Physiol.* 152, 1274–1283.
- Qiao, H., Wang, H., Zhao, L., Zhou, J., Huang, J., Zhang, Y., and Xue, Y. (2004). The F-box protein *AhSLF-S₂* physically interacts with *S*-RNases that may be inhibited by the ubiquitin/26S proteasome pathway of protein degradation during compatible pollination in *Antirrhinum*. *Plant Cell* 16, 582–595.
- Raff, M. (1998). Cell suicide for beginners. *Nature* 396, 119–122.
- Rappoport, J., and Simon, S. (2008). A functional GFP fusion for imaging clathrin-mediated endocytosis. *Traffic* 9, 1250–1255.
- Rea, A.C., Liu, P., and Nasrallah, J.B. (2010). A transgenic self-incompatible *Arabidopsis thaliana* model for evolutionary and mechanistic studies of crucifer self-incompatibility. *J. Exp. Bot.* 61, 1897–1906.
- Riedl, S.J., and Shi, Y. (2004). Molecular mechanisms of caspase regulation during apoptosis. *Nat. Rev. Mol. Cell Biol.* 5, 897–907.
- Rock, K.L., Gramm, C., Rothstein, L., Clark, K., Stein, R., Dick, L., Hwang, D., and Goldberg, A.L. (1994). Inhibitors of the proteasome block the degradation of most cell proteins and the generation of peptides presented on MHC class I molecules. *Cell* 78, 761–771.

- Rodriguez-Enriquez, M.J., Mehdi, S., Dickinson, H.G., and Grant-Downton, R.T. (2013). A novel method for efficient *in vitro* germination and tube growth of *Arabidopsis thaliana* pollen. *New Phytol.* *197*, 668–679.
- Royo, J., Kunz, C., Kowyama, Y., Anderson, M., Clarke, A.E., and Newbigin, E. (1994). Loss of a histidine residue at the active site of *S*-locus ribonuclease is associated with self-compatibility in *Lycopersicon peruvianum*. *Proc. Natl. Acad. Sci.* *91*, 6511–6514.
- Rudd, J.J., Franklin, F., Lord, J.M., and Franklin-Tong, V.E. (1996). Increased phosphorylation of a 26-kD pollen protein is induced by the self-incompatibility response in *Papaver rhoeas*. *Plant Cell* *8*, 713–724.
- Rudd, J.J., Osman, K., Franklin, F.C.H., and Franklin-Tong, V.E. (2003). Activation of a putative MAP kinase in pollen is stimulated by the self-incompatibility (SI) response. *FEBS Lett.* *547*, 223–227.
- Safavian, D., and Goring, D.R. (2013). Secretory activity is rapidly induced in stigmatic papillae by compatible pollen, but inhibited for self-incompatible pollen in the Brassicaceae. *PLoS One* *8*, e84286.
- Samuel, M.A., Chong, Y.T., Haasen, K.E., Aldea-Brydges, M.G., Stone, S.L., and Goring, D.R. (2009). Cellular pathways regulating responses to compatible and self-incompatible pollen in *Brassica* and *Arabidopsis* stigmas intersect at Exo70A1, a putative component of the exocyst complex. *Plant Cell* *21*, 2655–2671.
- Sassa, H., Hirano, H., and Ikehashi, H. (1993). Identification and characterization of stylar glycoproteins associated with self-incompatibility genes of Japanese pear, *Pyrus serotina* Rehd. *Mol Gen Genet* *241*, 17–25.
- Sawada, H., Morita, M., and Iwano, M. (2014). Self/non-self recognition mechanisms in sexual reproduction: new insight into the self-incompatibility system shared by flowering plants and hermaphroditic animals. *Biochem. Biophys. Res. Commun.* *450*, 1142–1148.
- Schopfer, C.R., Nasrallah, M.E., and Nasrallah, J.B. (1999). The male determinant of self-incompatibility in *Brassica*. *Science* *286*, 1697–1700.
- Scoccianti, V., Ovidi, E., Taddei, A.R., Tiezzi, A., Crinelli, R., Gentilini, L., and Speranza, A. (2003). Involvement of the ubiquitin/proteasome pathway in the organisation and polarised growth of kiwifruit pollen tubes. *Sex. Plant Reprod.* *16*, 123–133.
- Sessions, A., Burke, E., and Presting, G. (2002). A high-throughput *Arabidopsis* reverse genetics system. *Plant Cell* *14*, 2985–2994.

- Sheng, X., Hu, Z., Lü, H., Wang, X., Baluska, F., Samaj, J., and Lin, J. (2006). Roles of the ubiquitin/proteasome pathway in pollen tube growth with emphasis on MG132-induced alterations in ultrastructure, cytoskeleton, and cell wall components. *Plant Physiol.* *141*, 1578–1590.
- Sherman-Broyles, S., and Nasrallah, J.B. (2008). Self-incompatibility and evolution of mating systems in the Brassicaceae. In: Franklin-Tong, V.E. ed. *Self-Incompatibility in Flowering Plants*, pp. 123–147.
- Shi, Y. (2002). Mechanisms of caspase activation and inhibition during apoptosis. *Mol. Cell* *9*, 459–470.
- Shi, C., Zhang, Y., Bian, K., and Xu, L. (2011). Amount and activity changes of 20S proteasome modified by oxidation in salt-treated wheat root tips. *Acta Physiol. Plant.* *33*, 1227–1237.
- Shiba, H., Takayama, S., Iwano, M., Shimosato, H., Funato, M., Nakagawa, T., Che, F.S., Suzuki, G., Watanabe, M., and Hinata, K. (2001). A pollen coat protein, SP11/SCR, determines the pollen *S*-specificity in the self-incompatibility of *Brassica* species. *Plant Physiol.* *125*, 2095–2103.
- Sijacic, P., Wang, X., Skirpan, A.L., Wang, Y., Dowd, P.E., McCubbin, A.G., Huang, S., and Kao, T. (2004). Identification of the pollen determinant of *S*-RNase-mediated self-incompatibility. *Nature* *429*, 302–305.
- Sims, T.L., and Ordanic, M. (2001). Identification of a *S*-ribonuclease-binding protein in *Petunia hybrida*. *Plant Mol. Biol.* *47*, 771–783.
- Smalle, J., and Vierstra, R.D. (2004). The ubiquitin 26S proteasome proteolytic pathway. *Annu. Rev. Plant Biol.* *55*, 555–590.
- Smyth, D., Bowman, J., and Meyerowitz, E. (1990). Early flower development in *Arabidopsis*. *Plant Cell* *2*, 755–767.
- Snowman, B., Kovar, D., Shevchenko, G., Franklin-Tong, V.E., and Staiger, C. (2002). Signal-mediated depolymerization of actin in pollen during the self-incompatibility response. *Plant Cell* *14*, 2613–2626.
- Speranza, a, Scoccianti, V., Crinelli, R., Calzoni, G.L., and Magnani, M. (2001). Inhibition of proteasome activity strongly affects kiwifruit pollen germination. Involvement of the ubiquitin/proteasome pathway as a major regulator. *Plant Physiol.* *126*, 1150–1161.

- Sprunck, S., Rademacher, S., Vogler, F., Gheyselinck, J., Grossniklaus, U., and Dresselhaus, T. (2012). Egg cell-secreted EC1 triggers sperm cell activation during double fertilization. *Science* 338, 1093–1097.
- Staiger, C.J. (2000). Signaling to the actin cytoskeleton in plants. *Annu. Rev. Plant Physiol Plant Mol Biol.* 51, 257–288.
- Stein, J.C., Howlett, B., Boyes, D.C., Nasrallah, M.E., and Nasrallah, J.B. (1991). Molecular cloning of a putative receptor protein kinase gene encoded at the self-incompatibility locus of *Brassica oleracea*. *Proc. Natl. Acad. Sci.* 88, 8816–8820.
- Steller, H. (1995). Mechanisms and genes of cellular suicide. *Science* 267, 1445–1449.
- Stone, S.L., Arnoldo, M.A., and Goring, D.R. (1999). A breakdown of *Brassica* self-incompatibility in ARC1 antisense transgenic plants. *Science* 286, 1729–1731.
- Stone, S.L., Anderson, E.M., Mullen, R.T., and Goring, D.R. (2003). ARC1 is an E3 ubiquitin ligase and promotes the ubiquitination of proteins during the rejection of self-incompatible *Brassica* pollen. *Plant Cell* 15, 885–898.
- Stone, S.L., Hauksdóttir, H., Troy, A., Herschleb, J., Kraft, E., and Callis, J. (2005). Functional analysis of the RING-type ubiquitin ligase family of *Arabidopsis*. *Plant Physiol.* 137, 13–30.
- Sun, P., and Kao, T. (2013). Self-incompatibility in *Petunia inflata*: the relationship between a self-incompatibility locus F-box protein and its non-self *S*-RNases. *Plant Cell* 25, 470–485.
- Suzuki, G., Kai, N., Hirose, T., Fukui, K., Nishio, T., Takayama, S., Isogai, A., Watanabe, M., and Hinata, K. (1999). Genomic organization of the *S* locus: identification and characterization of genes in SLG/SRK region of *S*₉ haplotype of *Brassica campestris* (syn. *rapa*). *Genetics* 153, 391–400.
- Takasaki, T., Hatakeyama, K., Suzuki, G., Watanabe, M., Isogai, A., and Hinata, K. (2000). The *S* receptor kinase determines self-incompatibility in *Brassica* stigma. *Nature* 403, 913–916.
- Takayama, S., Shiba, H., Iwano, M., Shimosato, H., Che, F.S., Kai, N., Watanabe, M., Suzuki, G., Hinata, K., and Isogai, A. (2000). The pollen determinant of self-incompatibility in *Brassica campestris*. *Proc. Natl. Acad. Sci.* 97, 1920–1925.

- Takayama, S., Shimosato, H., Shiba, H., Funato, M., Che, F.S., Watanabe, M., Iwano, M., and Isogai, A. (2001). Direct ligand–receptor complex interaction controls *Brassica* self-incompatibility. *Nature* 413, 534–538.
- Takeuchi, H., and Higashiyama, T. (2011). Attraction of tip-growing pollen tubes by the female gametophyte. *Curr. Opin. Plant Biol.* 14, 614–621.
- Tanaka, K., Yoshimura, T., Kumatori, a, Ichihara, a, Ikai, a, Nishigai, M., Kameyama, K., and Takagi, T. (1988). Proteasomes (multi-protease complexes) as 20S ring-shaped particles in a variety of eukaryotic cells. *J. Biol. Chem.* 263, 16209–16217.
- Tang, C., Toomajian, C., Sherman-Broyles, S., Plagnol, V., Guo, Y.L., Hu, T.T., Clark, R.M., Nasrallah, J.B., Weigel, D., and Nordborg, M. (2007). The evolution of selfing in *Arabidopsis thaliana*. *Science* 317, 1070–1072.
- Tantikanjana, T., Nasrallah, M.E., and Nasrallah, J.B. (2010). Complex networks of self-incompatibility signaling in the Brassicaceae. *Curr. Opin. Plant Biol.* 13, 520–526.
- Taylor, L.P., and Hepler, P.K. (1997). Pollen Germination and Tube Growth. *Annu. Rev. Plant Physiol. Plant Mol. Biol.* 48, 461–491.
- Tester, M., and Langridge, P. (2010). Breeding technologies to increase crop production in a changing world. *Science* 327, 818–822.
- The *Arabidopsis* Genome Initiative (2000). Analysis of the genome sequence of the flowering plant *Arabidopsis thaliana*. *Nature* 408, 796–815.
- Thomas, S.G., and Franklin-Tong, V.E. (2004). Self-incompatibility triggers programmed cell death in *Papaver* pollen. *Nature* 429, 305–309.
- Thomas, S., Huang, S., Li, S., Staiger, C.J., and Franklin-Tong, V.E. (2006). Actin depolymerization is sufficient to induce programmed cell death in self-incompatible pollen. *J. Cell Biol.* 174, 221–229.
- Tochigi, T., Udagawa, H., Li, F., Kitashiba, H., and Nishio, T. (2011). The self-compatibility mechanism in *Brassica napus* L. is applicable to F1 hybrid breeding. *Theor. Appl. Genet.* 123, 475–482.
- Trick, M. (1990). Genomic sequence of a *Brassica S* locus-related gene. *Plant Mol. Biol.* 15, 203–205.
- Trick, M., and Flavell, R.B. (1989). A homozygous *S* genotype of *Brassica oleracea* expresses two *S*-like genes. *Mol. Gen. Genet.* 218, 112–117.

Unno, M., Mizushima, T., Morimoto, Y., Tomisugi, Y., Tanaka, K., Yasuoka, N., and Tsukihara, T. (2002). The structure of the mammalian 20S proteasome at 2.75 Å resolution. *Structure* 10, 609–618.

Ushijima, K., Sassa, H., Dandekar, A., Gradziel, T., Tao, R., and Hirano, H. (2003). Structural and transcriptional analysis of the self-incompatibility locus of almond: identification of a pollen-expressed F-box gene with haplotype-specific polymorphism. *Plant Cell* 15, 771–781.

Vacca, R.A., Valenti, D., Bobba, A., de Pinto, M.C., Merafina, R.S., De Gara, L., Passarella, S., and Marra, E. (2007). Proteasome function is required for activation of programmed cell death in heat shocked tobacco Bright-Yellow 2 cells. *FEBS Lett.* 581, 917–922.

Valenti, D., Vacca, R.A., Guaragnella, N., Passarella, S., Marra, E., and Giannattasio, S. (2008). A transient proteasome activation is needed for acetic acid-induced programmed cell death to occur in *Saccharomyces cerevisiae*. *FEMS Yeast Res.* 8, 400–404.

Vatovec, S. (2011). Investigating the mechanism of self-incompatibility in *Papaver rhoeas* and functional transfer of *Papaver* S-determinants to *Arabidopsis thaliana*. PhD thesis, University of Birmingham.

Verdoes, M., Florea, B.I., Menendez-Benito, V., Maynard, C.J., Witte, M.D., van der Linden, W.A., van den Nieuwendijk, A.M.C.H., Hofmann, T., Berkers, C.R., van Leeuwen, F.W.B., et al. (2006). A fluorescent broad-spectrum proteasome inhibitor for labeling proteasomes *in vitro* and *in vivo*. *Chem. Biol.* 13, 1217–1226.

Verhoeven, T., Feron, R., Wolters-Arts, M., Edqvist, J., Gerats, T., Derksen, J., and Mariani, C. (2005). STIG1 controls exudate secretion in the pistil of petunia and tobacco. *Plant Physiol.* 138, 153–160.

Vig, M., Beck, A., Billingsley, J.M., Lis, A., Parvez, S., Peinelt, C., Koomoa, D.L., Soboloff, J., Gill, D.L., Fleig, A., et al. (2006). CRACM1 multimers form the ion-selective pore of the CRAC channel. *Curr. Biol.* 16, 2073–2079.

Vilchez, D., Boyer, L., Morante, I., Lutz, M., Merkwirth, C., Joyce, D., Spencer, B., Page, L., Masliah, E., Berggren, W.T., et al. (2012). Increased proteasome activity in human embryonic stem cells is regulated by PSMD11. *Nature* 489, 304–308.

Walker, E. a, Ride, J.P., Kurup, S., Franklin-Tong, V.E., Lawrence, M.J., and Franklin, F.C. (1996). Molecular analysis of two functional homologues of the *S*₃ allele of the *Papaver rhoeas* self-incompatibility gene isolated from different populations. *Plant Mol. Biol.* 30, 983–994.

- Walsh, C.T., Garneau-Tsodikova, S., and Gatto, G.J. (2005). Protein posttranslational modifications: the chemistry of proteome diversifications. *Angew. Chemie* 44, 7342–7372.
- Wang, N., and Kao, T.H. (2012). Self-incompatibility in *Petunia*: a self/nonself-recognition mechanism employing *S*-locus F-box proteins and *S*-RNase to prevent inbreeding. *Wiley Interdiscip. Rev. Dev. Biol.* 1, 267–275.
- Wang, H., Zhu, X., Li, H., Cui, J., Liu, C., Chen, X., and Zhang, W. (2014). Induction of Caspase-3-like activity in rice following release of cytochrome-*f* from the chloroplast and subsequent interaction with the ubiquitin-proteasome system. *Sci. Rep.* 4, 5989.
- Wang, K., Peng, X., Ji, Y., Yang, P., Zhu, Y., and Li, S. (2013). Gene, protein, and network of male sterility in rice. *Front. Plant Sci.* 4, 92.
- Watanabe, M., Takasaki, T., Toriyama, K., Yamakawa, S., Isogai, A., Suzuki, A., and Hinata, K. (1994). A high degree of homology exists between the protein encoded by SLG and the *S* receptor domain encoded by SRK in self-incompatible *Brassica campestris* L. *Plant Cell Physiol.* 35, 1221–1229.
- Watanabe, M., Suzuki, G., and Takayama, S. (2008). Milestones identifying self-incompatibility genes in *Brassica* species: from old stories to new findings. In: Franklin-Tong, V.E. ed. *Self-Incompatibility in Flowering Plants*, pp. 151–172.
- Weterings, K., Schrauwen, J., Wullems, G., and Twell, D. (1995). Functional dissection of the promoter of the pollen-specific gene *NTP303* reveals a novel pollen-specific, and conserved *cis*-regulatory element. *Plant J.* 8, 55–63.
- Wheeler, M.J., de Graaf, B.H.J., Hadjiosif, N., Perry, R.M., Poulter, N.S., Osman, K., Vatovec, S., Harper, A., Franklin, F.C.H., and Franklin-Tong, V.E. (2009). Identification of the pollen self-incompatibility determinant in *Papaver rhoeas*. *Nature* 459, 992–995.
- Wheeler, M.J., Vatovec, S., and Franklin-Tong, V.E. (2010). The pollen *S*-determinant in *Papaver*: comparisons with known plant receptors and protein ligand partners. *J. Exp. Bot.* 61, 2015–2025.
- Whitford, R., Fleury, D., Reif, J.C., Garcia, M., Okada, T., Korzun, V., and Langridge, P. (2013). Hybrid breeding in wheat: technologies to improve hybrid wheat seed production. *J. Exp. Bot.* 64, 5411–5428.
- Widmann, C., Gibson, S., Jarpe, M.B., and Johnson, G.L. (1999). Mitogen-activated protein kinase: conservation of a three-kinase module from yeast to human. *Physiol. Rev.* 79, 143–180.

- Wilkins, K.A. (2013). Investigating pollen signalling networks triggered by the self-incompatibility response in *Papaver rhoeas*. PhD thesis, University of Birmingham.
- Wilkins, K.A., Bancroft, J., Bosch, M., Ings, J., Smirnoff, N., and Franklin-Tong, V.E. (2011). Reactive oxygen species and nitric oxide mediate actin reorganization and programmed cell death in the self-incompatibility response of *Papaver*. *Plant Physiol.* *156*, 404–416.
- Williams, J.S., Der, J.P., de Pamphilis, C.W., and Kao, T.H. (2014a). Transcriptome analysis reveals the same 17 *S*-Locus F-Box genes in two haplotypes of the self-incompatibility locus of *Petunia inflata*. *Plant Cell* *26*, 2873–2888.
- Williams, J.S., Natale, C.A, Wang, N., Li, S., Brubaker, T.R., Sun, P., and Kao, T.H. (2014b). Four previously identified *Petunia inflata* *S*-locus F-box genes are involved in pollen specificity in self-incompatibility. *Mol. Plant* *7*, 567–569.
- Xu, C., Li, M., Wu, J., Guo, H., Li, Q., Zhang, Y., Chai, J., Li, T., and Xue, Y. (2013). Identification of a canonical SCF(SLF) complex involved in *S*-RNase-based self-incompatibility of *Pyrus* (Rosaceae). *Plant Mol. Biol.* *81*, 245–257.
- Xue, Y., Carpenter, R., Dickinson, H.G., and Coen, E.S. (1996). Origin of allelic diversity in antirrhinum *S* locus RNases. *Plant Cell* *8*, 805–814.
- Yamagishi, H., and Bhat, S.R. (2014). Cytoplasmic male sterility in Brassicaceae crops. *Breed. Sci.* *64*, 38–47.
- Yang, G., Chen, C., Zhou, G., Geng, C., Ma, C., Tu, J., and Fu, T. (2001). Genetic analysis of four self-incompatible lines in *Brassica napus*. *Plant Breed.* *120*, 57–61.
- Yao, C.K., Lin, Y.Q., Ly, C. V, Ohyama, T., Haueter, C.M., Moiseenkova-Bell, V.Y., Wensel, T.G., and Bellen, H.J. (2009). A synaptic vesicle-associated Ca²⁺ channel promotes endocytosis and couples exocytosis to endocytosis. *Cell* *138*, 947–960.
- Zhang, D., and Yang, L. (2014). Specification of tapetum and microsporocyte cells within the anther. *Curr. Opin. Plant Biol.* *17*, 49–55.
- Zhang, Z., and Galileo, D.S. (1997). Direct *in situ* end-labeling for detection of apoptotic cells in tissue sections. *Biotechniques* *22*, 834–836.
- Zhang, X., Henriques, R., Lin, S., Niu, Q., and Chua, N. (2006). *Agrobacterium*-mediated transformation of *Arabidopsis thaliana* using the floral dip method. *Nat. Protoc.* *1*, 641–646.

Zhang, Y., Zhao, Z., and Xue, Y. (2009). Roles of proteolysis in plant self-incompatibility. *Annu. Rev. Plant Biol.* *60*, 21–42.

Zhao, L., Huang, J., Zhao, Z., Li, Q., Sims, T.L., and Xue, Y. (2010). The Skp1-like protein SSK1 is required for cross-pollen compatibility in *S*-RNase-based self-incompatibility. *Plant J.* *62*, 52–63.

Zheng, N., Schulman, B.A, Song, L., Miller, J.J., Jeffrey, P.D., Wang, P., Chu, C., Koepp, D.M., Elledge, S.J., Pagano, M., et al. (2002). Structure of the Cul1-Rbx1-Skp1-F boxSkp2 SCF ubiquitin ligase complex. *Nature* *416*, 703–709.

Zimmer, M. (2002). Green fluorescent protein (GFP): applications, structure, and related photophysical behavior. *Chem. Rev.* *102*, 759–781.

APPENDIX I-PUBLISHED PAPER

Eaves, D.J., Flores-Ortiz, C., Haque, T., Lin, Z., Teng, N., and Franklin-Tong, V.E. (2014). Self-incompatibility in *Papaver*: advances in integrating the signalling network. *Biochem. Soc. Trans.* 42, 370-376.

DOI:10.1042/BST20130248

This article is redacted from the thesis for copyright reasons. Please consult the journal.

A pre-publication version of this article is available via Research at Birmingham:

<http://rab.bham.ac.uk/>.

My contribution: I wrote the last two sections of this review together with Franklin-Tong, V.E.. I also proof-read the manuscript before submission.